AD-A131 402 DEVELOPMENT AND FLIGHT TEST OF AN ACTIVE FLUTTER SUPPRESSION SYSTEM FOR T..(U) AIR FORCE WRIGHT AERONAUTICAL LABS WRIGHT-PATTERSON AFB OH

1/2

UNCLASSIFIED H HOENLINGER ET AL. APR 83 F/G 20/4 NL

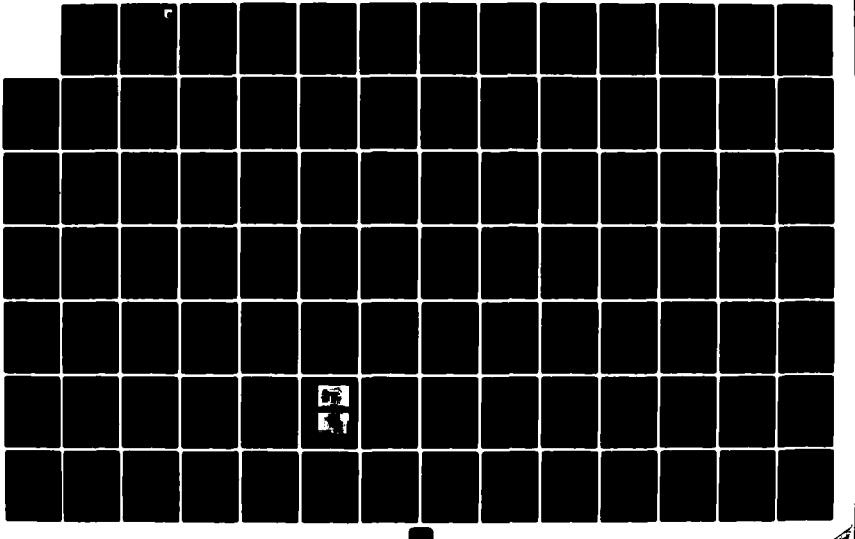

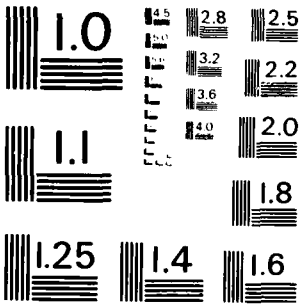

AFWAL-TR-82-3040
Part II



# DEVELOPMENT AND FLIGHT TEST OF AN ACTIVE FLUTTER SUPPRESSION SYSTEM FOR THE F-4F WITH STORES

## PART II. GROUND TESTS AND SUBCRITICAL FLIGHT TESTS

H. Könlinger
D. Mussman
R. Manser
Messerschmitt-Bölkow-Blohm GmbH
Ottobrunn, Federal Republic of Germany

and

T. J. Huttsell
Air Force Wright Aeronautical Laboratories
Wright-Patterson Air Force Base, Ohio 45433

April 1983

Final Report for Period March 1973 - March 1980





FLIGHT DYNAMICS LABORATORY
AIR FORCE WRIGHT AERONAUTICAL LABORATORIES
AIR FORCE SYSTEMS COMMAND
WRIGHT-PATTERSON AIR FORCE BASE, OHIO 45433

NOTICE

When Government drawings, specifications, or other data are used for any purpose other than in connection with a definitely related Government procurement operation, the United States Government thereby incurs no responsibility nor any obligation whatsoever; and the fact that the government may have formulated, furnished, or in any way supplied the said drawings, specifications, or other data, is not to be regarded by implication or otherwise as in any manner licensing the holder or any other person or corporation, or conveying any rights or permission to manufacture use, or sell any patented invention that may in any way be related thereto.

This report has been reviewed by the Office of Public Affairs (ASD/PA) and is releasable to the National Technical Information Service (NTIS). At NTIS, it will be available to the general public, including foreign nations.

This technical report has been reviewed and is approved for publication.

LAWRENCE J. HUTTSELL
Aerospace Engineer
Aeroelastic Group

FREDERICK A. PICCHIONI, LT COL, USAF
Chief, Analysis & Optimization Branch
Structures & Dynamics Division

FOR THE COMMANDER

RALPH L. MEYER, JR., Colonel, USAF
Chief, Structures & Dynamics Division

"If your address has changed, if you wish to be removed from our mailing list, or if the addressee is no longer employed by your organization please notify AFWAL/FIBAA, W-PAFB, OH 45433 to help us maintain a current mailing list".

Copies of this report should not be returned unless return is required by security considerations, contractual obligations, or notice on a specific document.

UNCLASSIFIED

SECURITY CLASSIFICATION OF THIS PAGE (When Data Entered)

| REPORT DOCUMENTATION PAGE | | READ INSTRUCTIONS BEFORE COMPLETING FORM |
|---|---|---|
| 1. REPORT NUMBER<br>AFWAL-TR-82-3040, Part II | 2. GOVT ACCESSION NO.<br>AD A131 403 | 3. RECIPIENT'S CATALOG NUMBER |
| 4. TITLE (and Subtitle)<br>DEVELOPMENT AND FLIGHT TEST OF AN ACTIVE FLUTTER SUPPRESSION SYSTEM FOR THE F-4F WITH STORES, PART II. GROUND TESTS AND SUBCRITICAL FLIGHT TESTS | | 5. TYPE OF REPORT & PERIOD COVERED<br>Final Report<br>March 1978 - March 1980<br>6. PERFORMING ORG. REPORT NUMBER |
| 7. AUTHOR(s)<br>H. Hönlinger, D. Mussman, R. Manser, and L. Huttsell | | 8. CONTRACT OR GRANT NUMBER(s)<br>Memorandum of Understanding |
| 9. PERFORMING ORGANIZATION NAME AND ADDRESS<br>Messerschmitt-Bolkow-Blohm GmbH. (MBB)<br>Ottobrunn, Federal Republic of Germany | | 10. PROGRAM ELEMENT, PROJECT, TASK AREA & WORK UNIT NUMBERS<br>PE 62201F<br>2401/02/23 |
| 11. CONTROLLING OFFICE NAME AND ADDRESS<br>Flight Dynamics Laboratory (AFWAL/FIBR)<br>Air Force Wright Aeronautical Laboratories, AFSC<br>Wright-Patterson Air Force Base, Ohio 45433 | | 12. REPORT DATE<br>April 1983<br>13. NUMBER OF PAGES<br>156 |
| 14. MONITORING AGENCY NAME & ADDRESS(if different from Controlling Office) | | 15. SECURITY CLASS (of this report)<br>Unclassified<br>15a. DECLASSIFICATION/DOWNGRADING SCHEDULE |

16. DISTRIBUTION STATEMENT (of this Report)

Approved for public release; distribution unlimited.

17. DISTRIBUTION STATEMENT (of the abstract entered in Block 20, if different from Report)

18. SUPPLEMENTARY NOTES

19. KEY WORDS (Continue on reverse side if necessary and identify by block number)

Active Controls
Aeroservoelasticity
Flutter
Flutter Suppression
Wing/Store Flutter

20. ABSTRACT (Continue on reverse side if necessary and identify by block number)

Extensive research programs have been conducted at MBB and at AFWAL to investigate the application of active controls for the suppression of wing/store flutter. A flutter suppression system was developed and flight tested on an F-4F aircraft. The control law was designed by MBB using optimal control theory to minimize the control surface motion and to provide the required stability margins. During the test it was found that the dynamic behavior of the wing-pylon-store changed considerably with excitation amplitude due to free

DD FORM 1 JAN 73 1473 EDITION OF 1 NOV 65 IS OBSOLETE

UNCLASSIFIED

SECURITY CLASSIFICATION OF THIS PAGE (When Data Entered)

play and preload. The active flutter suppression system worked well and provided an increase in flutter speed.

# FOREWORD

The research described in this report was conducted by Messerschmitt-Bolkow-Blohm GmbH. (MBB) under a joint U.S. Air Force/German Ministry of Defense Memorandum of Understanding. The Air Force Project Engineers for this effort (work unit 24010223) were Thomas E. Noll and Lawrence J. Huttsell of the Structures and Dynamics Division, Flight Dynamics Laboratory, Air Force Wright Aeronautical Laboratories. The MBB Project Engineer Was H. Hönlinger.

The authors wish to acknowledge the cooperation and support of the OTC E-61 of the Federal Armed Forces in Manching and DFVLR, Institute for Aeroelastics, in Gottingen.

This report (Part II) documents the ground vibration tests, the ground tests on the flutter suppression system, and the initial sub-critical flight tests. Part I documents the design of the active flutter suppression system and Part III documents the flight test demonstration.

This report covers work conducted from March 1978 to March 1980.

TABLE OF CONTENTS

# LIST OF ILLUSTRATIONS

LIST OF ILLUSTRATIONS (Cont'd)

## LIST OF ILLUSTRATIONS (Cont'd)

LIST OF ILLUSTRATIONS (Cont'd)

LIST OF ILLUSTRATIONS (Cont'd)

LIST OF ILLUSTRATIONS (Concluded)

# LIST OF TABLES

# SECTION I

## INTRODUCTION

During the last several years, considerable interest has emerged in the U.S. and European community for the application of active control technology to suppress flutter. Both the U.S. Air Force and MBB have performed extensive research programs accompanied by wind tunnel tests in the field of active flutter and elastic mode suppression.

In 1975, MBB conducted a successful wind tunnel test which also led to a flight demonstration. This research demonstrated suppression of wing store flutter with store mounted vanes (Reference 1). On another program, flutter speed was increased on a fin-tailplane-aft fuselage with a hydraulically driven rudder (References 2, 3). Miniature model actuators and new wind tunnel test techniques were developed to investigate Flutter Suppression Systems (FSS) with flutter models. Special computer programs - utilizing optimal control theory - were adapted to find suitable control laws for flutter suppression (Reference 4). A very successful application of these programs is described in Reference 5. Analytical development of systems to reduce buffet induced pilot vibrations was presented in Reference 6. A system to improve ride comfort of a low wing loaded fighter was laid out recently (Reference 7).

Two full scale airplanes were equipped and flight tested to prove the feasibility of active flutter suppression. The first flight test was performed with a Fiat G 91/T3 which used additional control surfaces (vanes) to produce aerodynamic forces which counteract the store motion (Reference 8). In 1977, a much more challenging flight test program was launched in cooperation with the Bundesamt fur Wehrtechnik and Beschaffung (BWB) and the U.S. Air Force Flight Dynamics Laboratory (FDL). The objective of this program was to design and flight test a system for flutter suppression on an F-4F aircraft with stores. As flying test bed for this program, an F-4F aircraft of the German Air Force test center at Manching (Erprobungsstelle 61 der Bundeswehr) was chosen. This airplane was already equipped to perform flight flutter tests with stores. To generate the necessary unsteady aerodynamic control forces, existing control surfaces (ailerons) were used. Accelerometers located on the

wing provided the signals which were fed back through the existing stability augmentation system of the airplane.

This report (Part II) documents the ground vibration tests, the ground tests on the flutter suppression system, and the initial sub-critical flight tests. Part I documents the analysis and design of the active flutter suppression system for the F-4F aircraft with stores (Reference 9). Part III documents the flight test demonstration of the active flutter suppression system.

# SECTION II

# GROUND TEST RESULTS

## 1. GROUND VIBRATION TEST AND COMPARISON WITH ANALYSES

A ground vibration test was conducted with the LBFK external stores on the F-4F before flight test with an active flutter suppression system. The purpose of the test was to check the mathematical structural model of the F-4F wing with the critical external stores, as indicated by the aircraft manufacturer (References 10, 11). Special emphasis was placed on the measurement of the vibration modes critical for flutter and to study nonlinearities of the wing-pylon external store combination (Reference 12).

### a. Description of the Ground Vibration Test

The ground vibration test was performed with the aircraft on the landing gear. To simulate free-free conditions, the tires were deflated to 50% of the required pressure. The excitation of the modes was performed by electrodynamic shakers with harmonic force input. The exciter locations and the applied force amplitudes are noted on the graphic representations of the measured mode shapes (Figure 8). For the measurement of the mode shapes a sufficient number of accelerometers were fixed on the surfaces, stores, and fuselage as shown on Figure 8.

Since practically all actual reasonant frequencies of elastic structures depend more or less on the vibration amplitude and thus on the exciter forces, so-called linearity checks were recorded together with each measured mode, i.e. the frequency and the amplitudes at some chosen measurement points versus exciter force.

Additionally a dimensionless nonlinearity number (NN) was defined and plotted to have a quick look at the degree of nonlinearity for each resonant vibration mode. NN is defined by:

$NN = \frac{\Delta f}{\Delta a} \cdot \frac{a}{f}$ where f = frequency (Hz)

a = an amplitude of the vibration mode.

$\frac{\Delta f}{\Delta a}$ = frequency increase divided by the corresponding increase of amplitude

For linear vibration NN = 0 and for nonlinear vibration NN $\lesssim$ 0. The magnitude of /NN/ is a measure for the degree of nonlinearity.

Two methods have been applied for evaluation of the damping values g (%): First decay curves were recorded and used for the evaluation of the logarithmic decrement D. Where $D = \frac{1}{m} \ln \frac{a_1}{a_{m+1}}$ and where $a_1, a_2, \ldots, a_m$ are consecutive amplitudes. The damping value g is approximately = $\frac{D}{\pi}$, if the damping is small. In the second method a "complex power" method was applied yielding the damping value g as well as the generalized masses, which were transformed (normalized) to the vibration amplitude of 1 m at a chosen reference point.

b. Comparison of Calculated and Measured Results

The first four calculated vibration modes were compared with those measured on the aircraft in order to check the mathematical structural model. The mass data of the external store configurations used for comparison of vibration modes are compiled in Table 1. Figures 1 through 8 present the first four measured modes and Figures 9 through 15 present the first four calculated modes for both the flutter critical and the safe store configuration. The vibration modes for wing bending, store yaw, and store roll are presented in Figures 9, 10, 12, 13, and 14. The external store pitching mode calculated as critical for flutter, however, demonstrates deviations from the experiment both in mode shape and in frequency. The nodal line of the measured mode (Figure 3) curves to the front (in the direction of flight). This shift of the nodal line in the pitching mode would indicate that a higher flutter speed may be

expected than was calculated. The nodal line of the vibration mode for the flutter stopper with the weights in the "safe" position (Figure 7), however, turns to the rear, indicating a lower flutter speed than calculated. This test result is opposite to the calculations with the mathematical model given by MDC (Figures 11 and 15).

Before it was possible to begin flight tests, this serious difference between calculation and experiment had to be explained and the mathematical model modified in such a manner that it correctly reflected the behavior of the real aircraft. Section III will discuss these modifications to the analysis.

## 2. COMPONENT TEST RESULTS

### a. Impedance Test of the Aileron Actuator

The stiffness of the hydraulic actuator must be known in order to estimate the effect of aileron stiffness on flutter speed. Hydraulic actuators have a stiffness dependence on frequency (impedance), which cannot yet be satisfactorily determined by analysis. The DFVLR in Gottingen has developed an experimental analytical procedure to determine the actuator impedance. The DFVLR Gottingen, Institute for Aeroelastics, therefore carried out the impedance test with the Weston Power aileron actuator. The experimental results are compiled in a separate report (Reference 13). The resulting impedance of the aileron actuator did not lead to any great changes in the flutter speed calculated with real actuator stiffness.

### b. Measurement of the Transfer Function of the Aileron

In Reference 14, the transfer function of the modified National Waterlift aileron actuator employed in flight tests was compared with that of the standard and the modified Weston Power actuator. The calculations of the control law for the flutter suppression system are based partially on these results. Since the flight tests were performed with the modified National Waterlift actuator for reasons of durability, it was necessary to measure the transfer function of the aileron control system with the National Waterlift actuator again for both wings, and to compare this with the calculated results. Figure 16 shows a block diagram

for the measurement of the aileron actuator transfer function. Figures 17 and 18 show the transfer functions of the left and right aileron control system for different electrical input signals.

The nonlinear behavior is clearly noticeable from the deviating amplitude and phase paths for various input signals. It was assumed for the interpretation of the control law that the actuator becomes even more nonlinear under the effect of the air load. Therefore the effect of the air load on the transfer function of the actuator was estimated in calculating the control law.

c. Modification and Testing of the Flutter Stopper

Because of the major differences between the calculated and measured vibration results, the flutter stopper had to be modified. The radius of gyration of the external store had to be increased to obtain a low flutter point on the basis of the measured vibration data. The mechanism to shift the mass in the flutter stopper had to be changed by $180^{0}$ in order to increase flutter speed, as can be seen in Figure 19. The diagram of the altered flutter stopper is presented in Figure 20.

The necessary radius of gyration ($\rho$ = 1.40 m) could be achieved without major changes in construction by increasing the total weight. Additional weights were installed for this purpose in the front and rear section of the external store, as can be seen in Figure 20. Figures 21 and 22 show the construction in detail.

Changing the shift mechanism for the trimming weights was also possible without large structural changes, because only individual components were shifted internally. Figure 23 shows the altered mounts of the guide rods for the trimming weights and the new position of the buffers for the trimming weights. The new location of holding mechanisms for the trimming weights and the installation of the solenoid switch can be seen in Figures 21 and 22.

The flutter stopper was equipped with accelerometers and terminal switches for controlling the position of the trimming weights as shown in Figure 20. The connection to the aircraft was established via a magnetic plug in the rear third of the external store. The cabling plan

for the external store can be seen in Figure 24 with details of the electrical equipment.

After completing the modification of the external stores with the built-in flutter stopper, the operation of the shift mechanism for the trimming weights was then checked in the laboratory. The springs employed shift both trimming weights of 150 kg each within 0.5 sec from the position critical for flutter to the safe position. The switching forces of the solenoid switch first proved to be insufficient and an additional spring had to be installed, as can be seen in Figures 21 and 22. With this modification, the flutter stopper functioned faultlessly. The inertial radius of gyration of the flutter stopper with the weights in "safe" and "critical" position were determined for the pitch axis with the standard pendulum test. This mass data are shown on Figure 25.

## 3. FUNCTIONAL TESTS ON THE FLUTTER SUPPRESSION SYSTEM

The detailed design of the flutter suppression system and the associated test equipment is given in Reference 9. Only the circuit diagram for the electronic control system is given in this report (Figure 26). The entire circuit for an aircraft wing with aileron was accommodated on one circuit board. The electronic control box together with the MBB limit value switch-off was mounted on an instrument carrier (Figure 27). The instrument carrier was constructed especially for accommodating the two instruments and achieving the installation weight prescribed by the aircraft manufacturer. A simple redundant switching logic was developed for the combination of the limit value cut-off and the emergency switch-off, installed in control panel 2 in the rear of the cockpit (Figure 28).

The following functional tests were performed, after the installation of the flutter suppression system, the switch-off devices, and the flutter stopper in the aircraft:

- checking the individual test programs which are possible with the electronic control and setting the aileron bias.

- checking the switch-off devices and adjusting the limit value cut-off.
- checking the operation of the flutter stopper.

During the function tests the test pilots also became acquainted with the flutter suppression system.

4. STRUCTURAL COUPLING TESTS

In contrast to the pure functional tests as described in previous paragraphs, the structural coupling test has special significance. The purpose of this test is to prove that the active suppression system is stable on the ground. Only after successful completion of this test was the control circuit of the active flutter suppression system closed.

For these tests, the air pressure in the tires was reduced to half the pressure in order to simulate the free-free aircraft not subject to the air forces. Two configurations were examined:

- Configuration 1 with critical external store.
- Configuration 2 with safe external store (flutter stopper released, trim weights in safe position).

The structure coupling test had to be conducted twice; once for the Weston Power actuator, with which the flight tests were begun and the second time after reequipping with the National Waterlift actuators. In order to gain information on the nonlinearities in the flutter suppression system, the tests were conducted with three different electrical input quantities, corresponding to three different amplitudes.

The structure coupling test was conducted in a frequency range of 2-25 Hz. At frequencies above 25 Hz, the actuator is too weak to excite the aircraft above the inertial force of the aileron. As a test signal, a sine wave was fed into the control electronics as an open loop circuit, as shown in the block diagram of Figure 16. The returning signal was set up as a ratio to the input signal and plotted for all frequencies as a Nyquist diagram. Figures 29 through 36 show the measured Nyquist diagrams for the critical external store configuration in each case for the three different input parameters Xi. Figures 37 through 40 show the

Nyquist diagrams for the safe external store configurations. The critical point is situated at -1 for all Nyquist diagrams. Since none of the curves passes to the left of the critical point with increasing frequency, the system is stable on the ground both for the "critical" and for the "safe" external store configuration. In the frequency range under study, the amplitude boundary amounts to at least 6 dB. It was only possible to attain these values, however, after the transfer function of the control electronics was modified by an additional filter (Figure 41). This is presented in the Nichols diagrams (Figure 42) for the cases with and without filters. The Nichols diagram for the wing bending mode is shown on Figure 43. The ratio of output to input versus the input signal for the flutter frequency was plotted in Figure 44 to demonstrate the nonlinear behavior of the flutter suppression system. At the same time, the corresponding phases for the generator signal are given. This diagram (Figure 44) shows that in the area of very small amplitudes a strongly nonlinear behavior may be expected, while the nonlinear behavior is acceptable at normal amplitudes.

# SECTION III

## THEORETICAL RESULTS BASED ON TEST DATA

### 1. MODIFICATION OF THE ANALYTICAL PYLON PITCH STIFFNESS

The calculations for the wing alone (without external stores) with MDC stiffness data (Reference 15) demonstrate good agreement with the vibration test (References 12, 15). The main differences must therefore stem from the pylon being incorrectly included in the calculations, the weapon lock, or the nonlinearities in the pylon-external store combination. The pylon bending stiffness in the pylon stiffness matrix provided by MDC was varied to make the frequency and vibration mode of the first four modes agree with the experimental results. The different variations carried out for bending stiffness are compiled in Table 2. The effect of this change in stiffness on the nodal position in the external store pitching mode is shown in Figure 45. The best correlation with the vibration tests was attained with an increase in bending stiffness by a factor of 1.8. New vibration calculations were conducted for the "safe" and "critical" external store configuration with the mathematical model modified in this manner (Figures 46-54). The external store pitching modes (Figures 48, 52) then agreed relatively well with the modes measured in the experiment (Figures 3, 7).

### 2. FLUTTER TRENDS FOR DETERMINING FLUTTER CRITICAL CONFIGURATION

With the adjusted pylon bending stiffness, the calculated flutter speed with LBFK external stores increased to more than 650 kts. Since the demonstration of flutter suppression can only be carried out at flight speeds of less than or equal 0.98 Mach because of flight limitations at the flight test center in Manching, an attempt had to be made to find a low flutter speed by changing the mass data of the LBFK external stores to flutter at the desired speed of about 450-500 kts. Vibration calculations with the LBFK external store configuration 1 M (1500 kg mass and 1.45 radius of gyration) finally demonstrated a favorable nodal position for the external store pitching mode (Figure 56), permitting expectation of a low flutter speed. The yawing mode (Figure 54) thus had a lower frequency than the wing bending (Figure 55), while there was

no great change for the external store roll mode (Figure 57). The results of the trend study are compiled in Figures 19, 58, and 59. All three diagrams explain the connection between flutter speed, mass of the external store, and radius of gyration in different ways. All diagrams show that a low flutter speed can only be achieved by increasing mass and radius of gyration of the external store. Furthermore, the diagrams show that the flutter speed can be increased significantly with constant external store mass by reducing the radius of gyration from the range $r_y$ = 1.42 m.

In the original concept of the flutter stopper, it was assumed that the flutter speed could be increased by expanding the radius of gyration. It became necessary to restructure the flutter stopper on the basis of these facts as presented in Section II.

Several other pertinent flutter calculations are provided in Figures 60 through 64, demonstrating that these are all "mild" cases of flutter and are suitable for demonstrating a flutter suppression system. All flutter calculations were made without structural damping.

## 3. EFFECT OF CENTER OF GRAVITY ON FLUTTER SPEED

In addition to the variation in mass and radius of gyration of the LBFK external store, the effect of the center of gravity of the external store on flutter was also examined. Flutter calculations were conducted for this purpose with a shift in center of gravity by $\pm$ 38 cm. In both cases the shift in center of gravity resulted in higher flutter speed (Figures 65, 66). The lowest flutter speeds were attained when the center of gravity was situated between the suspension hooks, as in the study in the previous paragraphs. These results are opposite to those values provided by MDC in Reference 10.

## 4. INFLUENCE OF STORE AERODYNAMICS AND MACH NUMBER ON FLUTTER

The unsteady air forces were calculated at Ma = 0.9 with both wing theory and doublet lattice procedures (Reference 16). Both procedures predicted approximately the same flutter speed. Unsteady aerodynamics were calculated for external stores using slender body theory and were

included in the flutter calculations. As expected, this led to a negligible change in the flutter speed (Figure 67).

Flutter calculations were performed to study the effect of Mach number (Figure 68). A comparison of Figure 60 with Figure 68 shows a slight reduction in flutter speed at Ma = 0.95 compared to Ma = 0.9.

## 5. CALCULATION OF THE FLUTTER SUPPRESSION CONTROL LAW BASED ON TEST DATA

The control law for active flutter suppression was altered based on the updated mathematical structural model. Figures 69 and 70 contain calculated Nyquist diagrams for the updated control law to be tested in the flight trials. In the desired speed range, a calculated increase in flutter speed of about 100 kts was achieved (Figure 71). Another optimization of the control law was carried out (Control Law 1112) after the completion of the initial flight tests. In this calculation, the transfer function of the actuators under air loads and the optimal sensor locations ascertained in the experiment were taken into consideration.

Figure 72 shows the flutter calcuation and Figures 73 and 74 show the Nyquist diagrams with this control law. As can be seen from the flutter calculation, Control Law 1112 is even more effective than that studied in the flight trials. It was possible to increase the calculated flutter speed by another 40 kts.

# SECTION IV

# INITIAL FLIGHT TESTS

## 1. FLIGHT TEST PROGRAM

The flight program for testing the active flutter suppression system involved a three step approach:

- Flight tests to determine the flutter point of the "critical" and "safe" external store configuration
- Open loop measurements for checking the phase positions of the suppression system and for optimizing the location of the sensors
- Flight tests with closed loop control in the subcritical and supercritical flight range

In the course of the flight tests, however, the program had to be expanded to study the effects of nonlinearities in the wing-pylon-external store combination on the flutter speed. This nonlinear problem will be examined more closely in Subsection 3.

Another important point for conducting the flight tests was the definition of the test area and the flight course. Since the expected flutter speeds were accompanied by relatively high dynamic pressures, the flights had to be conducted at low altitudes. In addition, a faultless telemetry reception had to be ensured. The flights had to be conducted over the least populated area possible. The test area and flight course drawn in Figure 75 was chosen for the flight tests in cooperation with the telemetry experts at the test center.

It was difficult to obtain a flight permit for the F-4F with active flutter suppression system and the safety equipment, since no comparable active systems had been permitted in West Germany. Even the MIL specifications normally employed for flight permits of military aircraft

had no provisions for qualifications of active flutter suppression systems. Three steps were undertaken to obtain the flight permit:

- The control electronics and switching logic for the switch-off devices were subjected to the following qualification tests:
  - vibration
  - temperature
  - electromagnetic compatibility
  - high voltage spikes

  It had to be proven that the flutter stopper and the switch-off devices of the suppression system function faultlessly both in ground tests and in flight tests.
- The permit for the entire system was granted on the basis of the safety concept developed by MBB in agreement with the other partners of the program and on the basis of the qualifcation of the indivdual components of the active flutter suppression system.

Twenty test flights were conducted with the F-4F, W. No. 1126, from March 21 to August 14, 1979 within the framework of the joint F-4F flutter suppression program. The flight tests were conducted by E-61 Flight Test Center in Manching.

The flight tests were conducted with the modified LBFK dummies. The mass data, especially the radius of gyration, were increased in order to obtain the lowest possible flutter speed. It was possible to alter the radius of gyration during the flight by shifting the trim weights in the flutter stopper (Section II). The external stores were suspended on the outer pylon station (13.250) with the load lock MAU-12 C/A. The mass data for the configuration critical to flutter and the safe configuration can be seen in Figure 25. Since the wing-pylon-external store combination is a very nonlinear system, the tightening torque of the mounting elements from the pylon to the wing and pylon to external store must be known precisely as reference quantities. The individual tightening torques during the flight tests are compiled on Figure 76.

The first through the sixth flights were conducted with Weston Power High Gain aileron actuators. From the seventh flight on, the aircraft

was equipped with National Waterlift High Gain aileron actuators. Table 3 presents a list of the flight and configuration data.

An extensive measurement program was carried out in 18 flights with external stores. One-hundred-forty test points were included in the flights with the eight test programs built into the suppression system (Table 4). The following specific studies were conducted:

- Determination of damping and frequency as a function of speed for the critical external store configuration.

- Determination of the damping and frequency as a function of speed with disengaged flutter stopper.

- Study of the effect of nonlinearities of the wing-pylon-external store combination on the flutter speed.

- Flights with high dynamic pressures for more precise determination of the flutter point.

- Determination of optimal sensor combinations for the suppression system.

- Measurements with open loop and closed loop control circuits during the flights.

- Tests for finding the optimal phase positions for the suppression systems.

- Tests with an unstable damping system for automatic generation of vibration modes.

- Tests for determining the effectiveness of the suppression system in the subcritical velocity range.

It was not possible to demonstrate the effectiveness of the suppression system in the supercritical range because of flight speed limitations at the flight test center in Manching.

## 2. FLIGHT TEST RESULTS

Stability as a function of flight speed was determined for both external store configurations with the standard methods of flight testing. A frequency sweep (frequency range of 4-16 Hz, rise time of 30 sec/octave) was employed for exciting the individual vibration modes via the aileron. Stability was determined by means of filter correlation methods with an HP 5451 B Fourier analyzer. Figure 77 shows the damping trend and Figure 78 shows the frequency versus airspeed for the critical external store configuration. It can be seen from both diagrams that stability is zero at 600 KIAS; i.e., the flutter point is reached. However, flutter begins at higher speeds than expected on the basis of the nonlinearities in the wing-pylon-external store combination. This problem is examined more closely in the next paragraph. Figures 79 and 80 show damping and frequency trends for the flutter stopper. A comparison of Figure 79 with 77 shows that the flutter stopper is very effective. When the damping is extrapolated in Figure 79, the flutter point is around 750 KIAS for the flutter stopper (compare also Figure 58). There is good agreement with the calculations.

### a. Effect of Nonlinearities in the Wing-Pylon-Store Combination on Flutter Speed

In the evaluation of frequency variation of the external store roll mode, a jump in frequency was discovered, as can be seen in Figure 81, leading to the conclusion of reduced roll stiffness of the external store or the pylon. A computation with reduced roll stiffness showed that this effect drastically increases flutter speed, so that it is above the flight range. In order to reduce these effects of nonlinearity, the tightening torque on the swaybrace, the adjustment screw, and the attachment bolt (Figure 76, Configuration A) was first increased to Configuration B. After a flight with the torques given in Configuration B for the swaybrace, it was discovered that the load lock was displaced. For this reason, all further flight tests were conducted with the torques of Configuration C. Increasing the torque of the adjustment screw, however, was not sufficient for the heavier external stores to avoid the

frequency jump in the external store mode at the high excitation levels. Therefore, either the tightening torque had to be further increased or the excitation forces (amplitude) had to be reduced. Since an increase in tightening torque was not permissible for structural reasons, the excitation forces were reduced to 25% or 17% of the maximum level. As can be seen in Figure 82, the frequency for the external store roll mode remains constant for all measured speeds with the reduced excitation forces. The effects of nonlinearity on the external store pitch mode and the wing bending mode were also examined. As can be seen from the compilation in Figure 83, the effect remains within the framework of measuring accuracy with the low excitation force. The elastic system may therefore be considered linear for small excitation forces or amplitudes. This also confirms the damping trend (Figure 84) of the critical external store configuration found with small excitation forces at high dynamic pressures, compared to small excitation calculated results.

b. Optimizing Sensor Locations

Figure 85 shows the location of the sensors and pick-ups for this program. In order to achieve a more precise experimental determination of the flutter point (shifted to higher speeds by the nonlinearities), two flights at less than Mach 1 but with high dynamic pressures were carried out at $V_{max}$ = 610 KIAS. The time response record in Figures 86 through 90 show that the external stores vibrate harmonically at V = 600 KIAS (Figure 87). At V = 580 KIAS (Figure 86), however, the external store vibration is not yet harmonic. Especially when Figure 86 is compared With Figure 90, it can be seen that the amplitude of the harmonic vibration becomes larger with increasing speed.

The control law optimized for the flutter suppression system refers to the generalized coordinates as state variables (Reference 9). In order to employ the control law in the suppression system, the coefficients of the control law must therefore be converted with a transformation matrix to the individual sensor combinations, measuring the quantities corresponding to the generalized coordinates. The coefficients converted for three different sensor combinations I - III are compiled

in Table 5. Figures 91 through 93 show the geometrical position of the sensor combinations in the wing and the control law. In order to evaluate the individual sensor combinations, all representing the same control law, the Nyquist diagrams at V = 520 or V = 500 KIAS of the suppression system were compared with the three different sensor combinations in Figure 94 (critical point in the Nyquist diagram is -1). It must also be noted on the Nyquist diagram with the sensor combination III, that the entire phase was rotated by $80^{o}$ (counter clockwise).

The comparison shows that the sensor combination III is the most favorable, since it essentially accommodates only the external store modes and suppresses the outer wing mode at about 11 Hz. The sensor location, FBL(R)4, had to be subsequently altered because of disturbing aerodynamic effects, as can be seen in Figure 93.

c. Open Loop Tests

Very extensive open loop measurements were made in flight and the results were plotted as Nyquist diagrams (critical point -1) with the aim of checking the calculations (stability and phase position) and for correcting the phase experimentally. This procedure is necessary, since phase shifts occurring because of Mach number effects and nonlinearities in the actuator which were not accounted for in the analysis.

A review of the results, (Figures 95 through 98) indicates that:

- It was possible to identify the flutter modes clearly with the chosen sensor combinations. (Amplification of the external store pitch mode at high speeds, Figure 96).
- The entire phase position was not yet optimal for all three sensor combinations. A rotation of the entire phase of about $90^{o}$ counter clockwise was still required, because the control law was calculated using an actuator transfer function exhibiting a lag of about $80^{o}$ instead of the $140^{o}$ measured.
- The entire amplification was in the correct range, but it also had be optimized.

- The symmetry was good between the left and right wings, as can be seen in the Figures 96, 97, and 98.

d. Tests with Unstable System for Automatic Excitation

One point of the flight test program was to test the procedure developed by MBB for automatic mode excitation which can be used to introduce an artificial flutter. This provides a determination of the suppression capability in the flight vibration experiments with an unstable system exciting one wing while the other wing is suppressing this flutter. The calculations in Figures 99 through 102 show that an automatic generation of the external store pitching mode should be possible with the unstable suppression system. At one point in the flight test, the outer wing mode was excited at 11 Hz and at another point the wing bending mode was excited at 5.2 Hz (Figure 103). It was not possible, however, to generate the external store pitching mode. The cause can be easily seen in comparisons of the Nyquist diagrams in Figure 94. The 11 Hz mode was generated when the suppression mode was tested with sensor combination I. The 5.2 Hz mode was generated with sensor combination III. In both cases the phase position was unfavorable for generating the external store pitch mode (5.7 Hz). The experiments showed that automatic generation of an unstable mode is possible with correct phase position.

e. Effectiveness of the Flutter Suppression System in the Subcritical Flight Range

In order to estimate the effectiveness of the suppression system in the subcritical flight range, flight tests were carried out by means of test programs 2 and 3 of Table 4. One system functioned as a suppressor in these programs, while the other was generating a frequency sweep via the aileron. This is presented in detail in the time responses (Figures 104 through 109). Since it was not possible to conduct a flight test with one-sided aileron excitation to which a reduction in amplitude could be precisely related, it was assumed that at least 60% of the generator energy reached the aircraft side on which the aileron functions as a suppressor (estimations are based on structure coupling tests). With this assumption, a reduction of the vibration amplitudes at the

external store tips (ZAL/ZAR) of 6dB and 8dB is achieved. The most effective reduction is in the area of wing bending on the basis of the not yet optimal phase position; however, the external store pitching mode is also suppressed.

# SECTION VI

# CONCLUSIONS

A flutter suppression system was designed for the F-4F aircraft with external stores (Reference 9). The existing control surfaces (ailerons) were used as the active control surfaces. Accelerometers located on the wing provided signals which were compensated and fed back through the existing stability augmentation system.

During the ground vibration test, it was found that the dynamic behavior of the wing-pylon-store was different than that predicted. The analytical pylon pitch stiffness was modified to improve the agreement between analysis and test and the theoretical results were recomputed.

The flight test program was divided into three major sections: 1) classical flight flutter tests to find the passive flutter speed for both the critical and safe configurations, 2) open loop tests for substantiation and optimization of the analytically defined control law, and 3) closed loop tests to demonstrate flutter and mode suppression. The classical flight flutter tests indicated a limited amplitude flutter at 600 knots. Part III of this report documents the final flight test demonstration of the active flutter suppression system at supercritical speeds (i.e.above the passive flutter speed).

## REFERENCES

1. G. Haidl, A. Lotze, O. Sensburg, "Active Flutter Suppression on Wings with External Stores," AGARDograph No. 175, July 1975.

2. O. Sensburg, H. Hönlinger, M. Kuhn, "Active Control of Empennage Flutter," AGARD-SMP Brussels, 13-18 April 1975.

3. H. Hönlinger, O.Sensburg, "Dynamic Simulation in Wind Tunnels," AGARD Conference Proceedings, No. 187.

4. G. Oesterheld, W. Kubbat, "Entwurf von Regelungssystemen mit Hilfe von Computer Aided Design and ihre Anwedung," MBB-Report GD 8-74.

5. H. Hönlinger, O. Sensburg, M. Kuhn, "Definition of the German Flutter Suppression Control Law for the YF-17 International Wind Tunnel Program," Paper presented at the 51st SMP of AGARD, Athens 13-18 April 1980.

6. O. Sensburg, J. Becker, H. Hönlinger, "Active Control of Flutter and Vibration of an Aircraft," IUTAM Symposium, Waterloo/Canada June 4-7, 1979, MBB-Report No. S/PUB/8.

7. J. Becker, W. Schmidts, "TKF-Boenbelastung," International MBB-Report TKF.

8. H. Hönlinger and A. Lotze, "Active Flutter Suppression of Aircraft Flutter," 11th ICAS-Congress, Lisbon/Portugal, 10-16 Sept. 1978.

9. H. Hönlinger, D. Mussman, R. Manser, and L. Huttsell, "Development and Flight Test of an Active Flutter Suppression System for the F-4F with Stores, Part I, Design of the Active Flutter Suppression System", AFWAL-TR-82-3040, Part I, September 1982.

10. H.R. Gongloff and J.W. Walker, "Model F-4E (Slat) Aircraft Wing Flutter Analysis with External Stores", MDC Report A 2560, November 30, 1973.

11. J.W. Walker and C.J. Moore, "Model F-4E (Slat) Thick Wing Flutter Analysis With and Without External Stores", MDC Report A 2770, June 15, 1974.

12. W. Gatter, "F-4F Flatterdämpfungsprogramm - Standschwingungsversuch am Flugzeug F-4F mit Flatter LBFK", MBB-Bericht UF1472, 1977.

13. R. Freymann and H. Giese, "Experimentell-rechnerische Ermittlung der dynamischen Obertragungsfunktionen des in einer F-4F Phantom zur Flatterunterdrucküng eigesetzten Querruderaktuators", DFVLR-interner Bericht Nr. IB 253-78 J 05, 1978.

REFERENCES (Concluded)

14. H. Hönlinger, "Versuche zur Flatterunterdruckung and Schwingungsdampfung mittels Querrunder an einer F-4F mit AuBenlasten", MBB-Bericht UF1391, 1977.

15. G. Schneider, "Flatteruntersuchungen am Flugel der MDC-F-4F mit LBFK-Tragflugkorpern am auBeren Flugelpylon", MBB-Bericht Nr. UFE 1280, Sept 1976.

16. H. Hönlinger, "F-4F Flutter Suppression Program - Flutter Analysis of F-4F with LBFK Stores Using an Adjusted Structural Model (Derived from Ground Resonance Tests)", MBB-Bericht UF 1473, 1978.

TABLE 1

MASS DATA FOR THE STORE CONFIGURATIONS

| | CALCULATION | | GROUND VIBRATION TEST | |
|---|---|---|---|---|
| LBFK STORE CONFIGURATION | MASS [kg] | RADIUS OF GYRATION $\rho_y$ [m] | MASS [kg] | RADIUS OF GYRATION $\rho_y$ [m] |
| 1 CRITICAL | 1500 | 1.28 | 1525 | 1.29 |
| 2 SAFE | 1500 | 1.34 | 1525 | 1.36 |
| MODIFIED STORE MASS DATA | | | | |
| 1M CRITICAL | 1500 | 1.45 | | |
| 2M SAFE | 1500 | 1.38 | | |

TABLE 2

VARIATIONS OF THE STORE PITCH STIFFNESS TO MATCH THE MATHEMATICAL MODEL

| LBFK 15 CRITICAL | TEST | VARIATIONS OF THE PYLON PITCH STIFFNESS TO MATCH THE MATHEMATICAL MODEL | | | | |
|---|---|---|---|---|---|---|
| MODE | FREQ. (HZ) | MDC DATA x 1.0 | PYLON PITCH x 1.4 | PYLON PITCH RIGID | x 1.4 FL x1.1 | PYLON PITCH x 1.8 |
| WING BENDING | 5.63 | 5.33 | 5.43 | 5.52 | 5.43 | 5.46 |
| STORE YAW | 5.93 | 5.70 | 5.70 | 5.70 | 5.70 | 5.70 |
| STORE PITCH | 6.67 | 5.97 | 6.29 | 7.28 | 6.29 | 6.52 |
| STORE ROLL | 8.54 | 8.31 | 8.40 | 9.44 | 8.40 | 8.48 |
| LBFK 1S (SAFE CONFIGURATION) | | | | | | |
| WING BENDING | 5.54 | 5.22 | | | | 5.41 |
| STORE YAW | 5.62 | 5.46 | | | | 5.47 |
| STORE PITCH | 6.48 | 5.87 | | | | 6.36 |
| STORE ROLL | 8.53 | 8.30 | | | | 8.45 |

TABLE 3
MEASURED TEST POINTS

| | FLIGHT DATA | | | CONFIGURATION | | | | FLIGHT TESTS | |
|---|---|---|---|---|---|---|---|---|---|
| FLIGHT | ALT.[ft] | SPEED [KIAS] | Ma-NO. | STORE | ACTUAT. | SENSOR COMB. | PYLON T.MOM. | TEST PROGR. | REMARKS |
| 175/1 | 6,000 - 10,000 | 300-500 | | clean | W.P. H.G. | I | A | 1(50 ) | Freq. sweep 2.8-11.2 [Hz] |
| 176/2 | -"- | -"- | | -"- | -"- | -"- | -"- | 1(50 ) | |
| 177/3 | 15,000 | 300 | 0.59 | critical | -"- | -"- | -"- | 1(100 ) | |
| -"- | -"- | 350 | 0.68 | -"- | -"- | -"- | -"- | -"- | |
| -"- | -"- | 375 | 0.73 | -"- | -"- | -"- | -"- | -"- | |
| -"- | -"- | 400 | 0.78 | -"- | -"- | -"- | -"- | -"- | |
| 178/4 | 8,000 | 380 | 0.66 | -"- | -"- | -"- | -"- | -"- | |
| -"- | -"- | 400 | 0.69 | -"- | -"- | -"- | -"- | -"- | |
| -"- | -"- | 425 | 0.73 | -"- | -"- | -"- | -"- | -"- | |
| -"- | -"- | 450 | 0.78 | -"- | -"- | -"- | -"- | -"- | |
| -"- | -"- | 475 | 0.82 | -"- | -"- | -"- | -"- | -"- | |
| -"- | -"- | 500 | 0.86 | -"- | -"- | -"- | -"- | -"- | |
| 179/5 | 14,000 | 450 | 0.85 | -"- | -"- | -"- | -"- | -"- | |
| -"- | -"- | 475 | 0.90 | -"- | -"- | -"- | -"- | -"- | |
| -"- | 6,000 | 475 | 0.79 | -"- | -"- | -"- | -"- | -"- | |
| -"- | -"- | 500 | 0.83 | -"- | -"- | -"- | -"- | -"- | |
| -"- | -"- | 510 | 0.85 | -"- | -"- | -"- | -"- | -"- | |
| -"- | -"- | 300 | 0.51 | safe | -"- | -"- | -"- | -"- | |
| -"- | -"- | 350 | 0.58 | -"- | -"- | -"- | -"- | -"- | |
| -"- | -"- | 400 | 0.67 | -"- | -"- | -"- | -"- | -"- | |

TABLE 3 (Cont'd)

| | FLIGHT DATA | | | CONFIGURATION | | | | FLIGHT TESTS | |
|---|---|---|---|---|---|---|---|---|---|
| FLIGHT | ALT.[ft] | SPEED [KIAS] | Ma-NO. | STORE | ACTUAT. | SENSOR COMB. | PYLON T.MOM. | TEST PROGR. | REMARKS |
| 179/5 | 6,000 | 425 | 0.71 | safe | W.P.HG. | I | A | 1(100 ) | Freq. Sweep 2.8-11.2[Hz] |
| -"- | -"- | 450 | 0.75 | -"- | -"- | -"- | -"- | -"- | |
| -"- | -"- | 475 | 0.79 | -"- | -"- | -"- | -"- | -"- | |
| -"- | -"- | 500 | 0.83 | -"- | -"- | -"- | -"- | -"- | |
| 181/7 | 7,000 | 400 | 0.68 | critical | N.W.H.G. | -"- | -"- | -"- | Freq. Sweep 4-11.2[Hz] |
| -"- | -"- | 450 | 0.76 | -"- | -"- | -"- | -"- | -"- | |
| -"- | -"- | 500 | 0.85 | -"- | -"- | -"- | -"- | -"- | |
| -"- | -"- | 400 | 0.68 | safe | -"- | -"- | -"- | -"- | |
| -"- | -"- | 450 | 0.76 | -"- | -"- | -"- | -"- | -"- | |
| -"- | -"- | 500 | 0.85 | -"- | -"- | -"- | -"- | -"- | |
| -"- | -"- | 520 | 0.88 | -"- | -"- | -"- | -"- | -"- | |
| -"- | -"- | 540 | 0.91 | -"- | -"- | -"- | -"- | -"- | |
| 182/8 | 7,000 | 500 | 0.85 | critical | -"- | -"- | -"- | 1(70%) | |
| -"- | -"- | 500 | 0.85 | -"- | -"- | -"- | -"- | 1(100%) | |
| -"- | -"- | 520 | 0.88 | -"- | -"- | -"- | -"- | 1(100 ) | |
| -"- | -"- | 540 | 0.91 | safe | -"- | -"- | -"- | 1(100 ) | |
| -"- | -"- | 550 | 0.92 | -"- | -"- | -"- | -"- | 1(100%) | |
| -"- | -"- | 560 | 0.93 | -"- | -"- | -"- | -"- | 1(100%) | |
| 183/9 | 7,000 | 520 | 0.87 | critical | -"- | -"- | -"- | 1(70%) | |
| -"- | -"- | 520 | 0.87 | -"- | -"- | -"- | -"- | 1(100%) | |

TABLE 3 (Cont'd)

| | FLIGHT DATA | | | CONFIGURATION | | | | FLIGHT TESTS | |
|---|---|---|---|---|---|---|---|---|---|
| FLIGHT | ALT.[ft] | SPEED [KIAS] | Ma-NO. | STORE | ACTUAT. | SENSOR COMB. | PYLON T.MOM. | TEST PROGR. | REMARKS |
| 1-3/9 | 7,000 | 540 | 0.91 | critical | N.W.H.G. | I | A | 1(100 ) | Freq. Sweep 4-11.2[Hz] |
| -"- | -"- | 550 | 0.9[illegible] | -"- | -"- | -"- | -"- | 1(100 ) | |
| -"- | -"- | 550 | 0.92 | -"- | -"- | -"- | -"- | 1(70 ) | |
| -"- | -"- | 560 | 0.94 | -"- | -"- | -"- | -"- | 1(70 ) | |
| -"- | -"- | 560 | 0.94 | -"- | -"- | -"- | -"- | 1(100 ) | |
| -"- | -"- | 400 | 0.69 | -"- | -"- | -"- | -"- | 1(100 ) | Slats extended |
| -"- | -"- | 450 | 0.76 | -"- | -"- | -"- | -"- | 1(100 ) | -"- -"- |
| -"- | -"- | 500 | 0.85 | -"- | -"- | -"- | -"- | 1(100 ) | -"- -"- |
| -"- | -"- | 530 | 0.90 | -"- | -"- | -"- | -"- | 1(100 ) | -"- -"- |
| 1-3/10 | 8,000 | 400 | 0.69 | -"- | -"- | -"- | -"- | 1(25 ) | |
| -"- | -"- | 400 | 0.69 | -"- | -"- | -"- | -"- | 1(50 ) | |
| -"- | -"- | 400 | 0.69 | -"- | -"- | -"- | -"- | 4 | |
| -"- | -"- | 450 | 0.77 | -"- | -"- | -"- | -"- | 1(25 ) | Freq. Sweep 4-11.2[Hz] |
| -"- | -"- | 450 | 0.77 | -"- | -"- | -"- | -"- | 1(50 ) | -"- -"- -"- -"- |
| -"- | -"- | 450 | 0.77 | -"- | -"- | -"- | -"- | 4 | |
| -"- | -"- | 500 | 0.86 | -"- | -"- | -"- | -"- | 1(25 ) | Freq. Sweep 4-11.2[Hz] |
| -"- | -"- | 500 | 0.86 | -"- | -"- | -"- | -"- | 1(50 ) | -"- -"- -"- -"- |
| -"- | -"- | 500 | 0.86 | -"- | -"- | -"- | -"- | 3 | -"- -"- -"- -"- |
| -"- | -"- | 500 | 0.86 | -"- | -"- | -"- | -"- | 4 | |
| -"- | -"- | 500 | 0.86 | -"- | -"- | -"- | -"- | 2 | Freq. Sweep 4-11.2[Hz] |

TABLE 3 (Cont'd)

| | FLIGHT DATA | | | CONFIGURATION | | | | FLIGHT TESTS | |
|---|---|---|---|---|---|---|---|---|---|
| FLIGHT | ALT.[ft] | SPEED [KIAS] | Ma-NC. | STORE | ACTUAT. | SENSOR COMB. | PYLON T.MOM. | TEST PROGR. | REMARKS |
| 184/10 | 3,000 | 500 | 0.86 | critical | N.W.H.G. | I | A | 3 | Freq. Sweep 4-11.2[Hz] |
| -"- | -"- | 520 | 0.89 | -"- | -"- | -"- | -"- | 1(25%) | -"- -"- -"- |
| -"- | -"- | 500 | 0.86 | -"- | -"- | -"- | -"- | 4 | |
| -"- | -"- | 510 | 0.87 | -"- | -"- | -"- | -"- | 4 | |
| -"- | -"- | 540 | 0.93 | -"- | -"- | -"- | -"- | 4 | |
| 185/11 | 10,000 | 450 | 0.84 | -"- | -"- | -"- | B | 1(25%) | Freq. Sweep 4-16[Hz] |
| -"- | -"- | 450 | 0.84 | -"- | -"- | -"- | -"- | 1(12%) | |
| -"- | -"- | 500 | 0.90 | -"- | -"- | -"- | -"- | 1(25%) | |
| -"- | 10,500 | 500 | 0.90 | -"- | -"- | -"- | -"- | 1(17%) | |
| -"- | 10,300 | 520 | 0.92 | -"- | -"- | -"- | -"- | 1(17%) | |
| -"- | -"- | 520 | 0.92 | -"- | -"- | -"- | -"- | 1(25%) | |
| -"- | 10,700 | 520 | 0.92 | -"- | -"- | -"- | -"- | 1(12%) | |
| -"- | 9,300 | 550 | 0.96 | -"- | -"- | -"- | -"- | 1(12%) | |
| -"- | -"- | 550 | 0.96 | -"- | -"- | -"- | -"- | 1(17%) | |
| -"- | 9,500 | 450 | 0.85 | -"- | -"- | -"- | -"- | 1(17%) | Slats extended |
| 187/13 | 5,900 | 450 | 0.75 | -"- | -"- | II | -"- | 1(17%) | |
| -"- | -"- | 450 | 0.75 | -"- | -"- | -"- | -"- | 1(25%) | |
| -"- | -"- | 450 | 0.75 | -"- | -"- | -"- | -"- | 1(50%) | |
| -"- | -"- | 500 | 0.83 | -"- | -"- | -"- | -"- | 1(17%) | |
| -"- | -"- | 500 | 0.83 | -"- | -"- | -"- | -"- | 1(25%) | |

TABLE 3 (Cont'd)

| | FLIGHT DATA | | | CONFIGURATION | | | | FLIGHT TESTS | |
|---|---|---|---|---|---|---|---|---|---|
| FLIGHT | ALT.[ft] | SPEED [KIAS] | Ma-NO. | STORE | ACTUAT. | SENSOR COMB. | PYLON T.MOM. | TEST PROGR. | REMARKS |
| [illegible] | 5,900 | 500 | [illegible] | [illegible] | A.W.R.S. | II | B | 1(59 ) | Freq. Sweep 4-16[Hz] |
| -"- | -"- | 520 | 0.86 | -"- | -"- | -"- | -"- | 1(17 ) | |
| -"- | -"- | 520 | 0.86 | -"- | -"- | -"- | -"- | 1(25 ) | |
| -"- | -"- | 520 | 0.86 | -"- | -"- | -"- | -"- | 1(59 ) | |
| -"- | -"- | 450 | 0.73 | -"- | -"- | -"- | -"- | 1(17 ) | |
| -"- | -"- | 450 | 0.74 | -"- | -"- | -"- | -"- | 1(25 ) | |
| -"- | -"- | 520 | 0.86 | -"- | -"- | -"- | -"- | 1(17 ) | |
| -"- | -"- | 540 | 0.90 | -"- | -"- | -"- | -"- | 1(17 ) | |
| -"- | -"- | 540 | 0.90 | -"- | -"- | -"- | -"- | 1(25 ) | |
| [illegible] | 14,000 | 450 | 0.76 | -"- | -"- | -"- | B | 1(17 ) | |
| -"- | -"- | 500 | 0.94 | -"- | -"- | -"- | -"- | 1(17 ) | |
| -"- | 12,000 | 520 | 0.94 | -"- | -"- | -"- | -"- | 1(17 ) | |
| -"- | 12,100 | 520 | 0.93 | -"- | -"- | -"- | -"- | 1(25 ) | |
| -"- | 12,400 | 450 | 0.83 | -"- | -"- | -"- | -"- | 1(17 ) | Struts extended |
| -"- | 12,000 | 500 | 0.90 | -"- | -"- | -"- | -"- | 1(17 ) | -"- -"- |
| -"- | 12,500 | 520 | 0.95 | -"- | -"- | -"- | -"- | 1(17 ) | -"- -"- |
| -"- | 13,000 | 520 | 0.97 | -"- | -"- | -"- | -"- | 1(25 ) | -"- -"- |
| 189/15 | 8,650 | 500 | 0.87 | -"- | -"- | -"- | -"- | 1(17 ) | |
| -"- | 8,220 | 520 | 0.90 | -"- | -"- | -"- | -"- | 1(17 ) | |
| -"- | 7,800 | 540 | 0.92 | -"- | -"- | -"- | -"- | 1(12 ) | |

TABLE 3 (Cont'd)

| | FLIGHT DATA | | | CONFIGURATION | | | | FLIGHT TESTS | |
|---|---|---|---|---|---|---|---|---|---|
| FLIGHT | ALT.[ft] | SPEED [KIAS] | Ma-NO. | STORE | ACTUAT. | SENSOR COMB. | PYLON T.MOM. | TEST PROGR. | REMARKS |
| 189/15 | 7,650 | 540 | 0.92 | critical | N.W.H.G. | II | C | 1(25 ) | Freq. Sweep 4-16[Hz] |
| -"- | 7,400 | 540 | 0.92 | -"- | -"- | -"- | -"- | 1(17 ) | -"- -"- -"- |
| -"- | 8,550 | 540 | 0.92 | safe | -"- | -"- | -"- | - | without system |
| -"- | 8,150 | 560 | 0.94 | -"- | -"- | -"- | -"- | - | -"- -"- |
| -"- | -"- | 450 | 0.78 | -"- | -"- | -"- | -"- | - | -"- -"- |
| -"- | 8,200 | 540 | 0.92 | -"- | -"- | -"- | -"- | - | -"- -"- |
| 190/16 | 5,900 | 540 | 0.89 | critical | -"- | -"- | -"- | 1(12 ) | Freq. Sweep 4-16[Hz] |
| -"- | -"- | 560 | 0.91 | -"- | -"- | -"- | -"- | 1(12 ) | |
| -"- | -"- | 560 | 0.91 | -"- | -"- | -"- | -"- | 1(17 ) | |
| -"- | -"- | 540 | 0.89 | safe | -"- | -"- | -"- | 1(17 ) | |
| -"- | 5,400 | 560 | 0.91 | -"- | -"- | -"- | -"- | 1(17 ) | |
| -"- | 5,300 | 580 | 0.94 | -"- | -"- | -"- | -"- | 1(17 ) | |
| -"- | 4,100 | 600 | 0.96 | -"- | -"- | -"- | -"- | 1(17 ) | |
| -"- | 5,400 | 580 | 0.94 | -"- | -"- | -"- | -"- | 1(25 ) | |
| 191/17 | 5,300 | 540 | 0.88 | critical | -"- | -"- | -"- | 1(17 ) | |
| -"- | 4,800 | 580 | 0.94 | -"- | -"- | -"- | -"- | 1(12 ) | |
| -"- | -"- | 580 | 0.94 | -"- | -"- | -"- | -"- | 1(17 ) | |
| -"- | 3,800 | 600 | 0.94 | -"- | -"- | -"- | -"- | 1(12 ) | |
| -"- | -"- | 600 | 0.95 | -"- | -"- | -"- | -"- | 1(17 ) | |
| -"- | 3,500 | 610 | 0.98 | -"- | -"- | -"- | -"- | 1(17 ) | |

TABLE 3 (Cont'd)

| | FLIGHT DATA | | | CONFIGURATION | | | | FLIGHT TESTS | |
|---|---|---|---|---|---|---|---|---|---|
| FLIGHT | ALT.[ft] | SPEED [KIAS] | Ma-NO. | ST. E | A. TOAT | SENSOR COMB. | PYLON T.MOM. | TEST PROGR. | REMARKS |
| 134/1 | 4,000 | 580 | 0.91 | [illegible] | [illegible] | II | [illegible] | - | [illegible]de slipping |
| -"- | -"- | 600 | 0.9[illegible] | - | | - - | - - | - | - - - - |
| - - | 3,900 | 610 | 0.9[illegible] | - - | - - | - - | - - | - | - - -"- |
| - - | 2,2[illegible] | 6[illegible] | 0.[illegible] | - - | - | - - | -"- | - | - - - - |
| [illegible] | 5,0[illegible] | [illegible] | 0.[illegible] | - | - - | [illegible] | - - | [illegible] | [illegible]ween 4-16[Hz], phase changed |
| - - | 5,[illegible]00 | [illegible]5[illegible] | [illegible] | - - | | - - | - - | [illegible] | |
| - - | 5,600 | [illegible] 0 | [illegible] | - | - - | - | - - | [illegible] | |
| - - | 5,250 | [illegible] | [illegible] | - - | - - | - - | - - | [illegible] | |
| - - | 5,700 | 540 | [illegible] | - - | - - | - - | -"- | [illegible] | |
| - - | 5,900 | 500 | [illegible] | - - | - | - - | - - | [illegible] | Fr.Sw. 4-16[Hz], [illegible] changed |
| - - | 5,900 | 450 | 0.79 | -"- | -"- | -"- | -"- | [illegible] | |
| - - | 5,250 | 450 | 0.79 | -"- | - - | -"- | -"- | 2(50 ) | Fr.Sw. 4-16[Hz], phase changed |
| - - | 5,250 | 450 | 0.79 | -"- | - - | -"- | -"- | 3(100 ) | |
| -"- | 5,700 | 450 | 0.79 | -"- | - - | - - | -"- | 2(100 ) | |
| 134/20 | 6,750 | 450 | 0.7[illegible] | - - | -"- | - - | - - | 1(17 ) | |
| -"- | -"- | 450 | 0.7[illegible] | -"- | -"- | -"- | -"- | - | Pitch/Roll |
| -"- | 7,000 | 500 | 0.8[illegible] | -"- | -"- | -"- | -"- | 1(17 ) | Fr.Sw. 4-16[Hz], phase changed |
| -"- | -"- | 500 | 0.[illegible] | -"- | -"- | -"- | -"- | 4 | Pitch/Roll |
| -"- | -"- | 550 | 0.91 | -"- | -"- | -"- | -"- | 4 | -"- |
| -"- | -"- | 550 | 0.91 | -"- | -"- | -"- | -"- | 1(17 ) | Fr.Sw. 4-16[Hz], phase changed |

TABLE 3 (Cont'd)

| | FLIGHT DATA | | | CONFIGURATION | | | | FLIGHT TESTS | |
|---|---|---|---|---|---|---|---|---|---|
| FLIGHT | ALT.[ft] | SPEED [KIAS] | Ma-NO. | STORE | ACTUAT. | SENSOR COMB. | PYLON T.MOM. | TEST PROGR. | REMARKS |
| 194/20 | 6,600 | 550 | 0.91 | critical | N.W.H.G. | III | C | 1(50 ) | Fr.Sw. 4-16[Hz], phase changed |
| -"- | -"- | 550 | 0.91 | -"- | -"- | -"- | -"- | 8 | |
| -"- | -"- | 550 | 0.91 | -"- | -"- | -"- | -"- | 8 | Roll |
| -"- | 5,950 | 550 | 0.91 | -"- | -"- | -"- | -"- | 7(50%) | Freq. Sw. 4-16[Hz], phase changed |
| -"- | -"- | 550 | 0.91 | -"- | -"- | -"- | -"- | 7(50 ) | |
| -"- | -"- | 450 | 0.75 | -"- | -"- | -"- | -"- | 2(50 ) | |

TABLE 4

TEST PROGRAMS OF THE FLUTTER SUPPRESSION SYSTEM

| TEST PROGRAMM/TEST PROGRAM F-SF WING TEST | | |
|---|---|---|
| [illegible] | FUNKTION/FUNCTION | |
| [illegible] | RE. GE[illegible]/RIGHT WING | LI. FLÜGEL/LEFT WING |
| 1 | GESCHL. KR[illegible] M. [illegible]<br>CLOSED LOOP W. [illegible] | GESCHL. KREIS M. GLEITFREQ. SWEEP<br>CLOSED LOOP W. FREQU. SWEEP |
| 2 | GLEIT[illegible] | DÄMPFUNG/DAMPING |
| 3 | DÄMP[illegible] | GLEITFREQU./FREQUENCY SWEEP |
| 4 | AUTOMATI[illegible]<br>AUTOMATI[illegible] | AUTOMATISCHE ERREGUNG<br>AUTOMATIC EXCITATION |
| 5 | DÄMPFUNG/DAMPING | AUTOMATISCHE ERREGUNG<br>AUTOMATIC EXCITATION |
| 6 | AUTOMATISCHE ERREGUNG<br>AUTOMATIC EXCITATION | DÄMPFUNG/DAMPING |
| 7 | GESCHL. KREIS M. GLEITFREQUENZ<br>CLOSED LOOP W. FREQU. SWEEP | GESCHL. KREIS M. GLEITFREQUENZ<br>CLOSED LOOP W. FREQU. SWEEP |
| 8 | DÄMPFUNG/DAMPING | DÄMPFUNG/DAMPING |

TABLE 5

COEFFICIENTS OF THE CONTROL LAW FOR VARIOUS SENSOR COMBINATIONS

| SENSOR COMBINATION | | CONTROL LAW | | | |
|---|---|---|---|---|---|
| | | $K\varphi$ | $K\theta$ | $K\dot{\varphi}$ | $K\dot{\theta}$ |
| $\varphi = \frac{① - ③}{L_1}$ <br> $\theta = \frac{③ - ④}{L_2}$ | I <br> II | 0.41571 | 0.44105 | $-0.3195 \times 10^{-1}$ | $-0.4637 \times 10^{-1}$ |
| $\varphi = \frac{① + ④}{L_2}$ <br> $\theta = \frac{③ - ④}{L_2}$ | III | 0.1484 | 0.2148 | $-0.11403 \times 10^{-1}$ | $-0.2898 \times 10^{-1}$ |

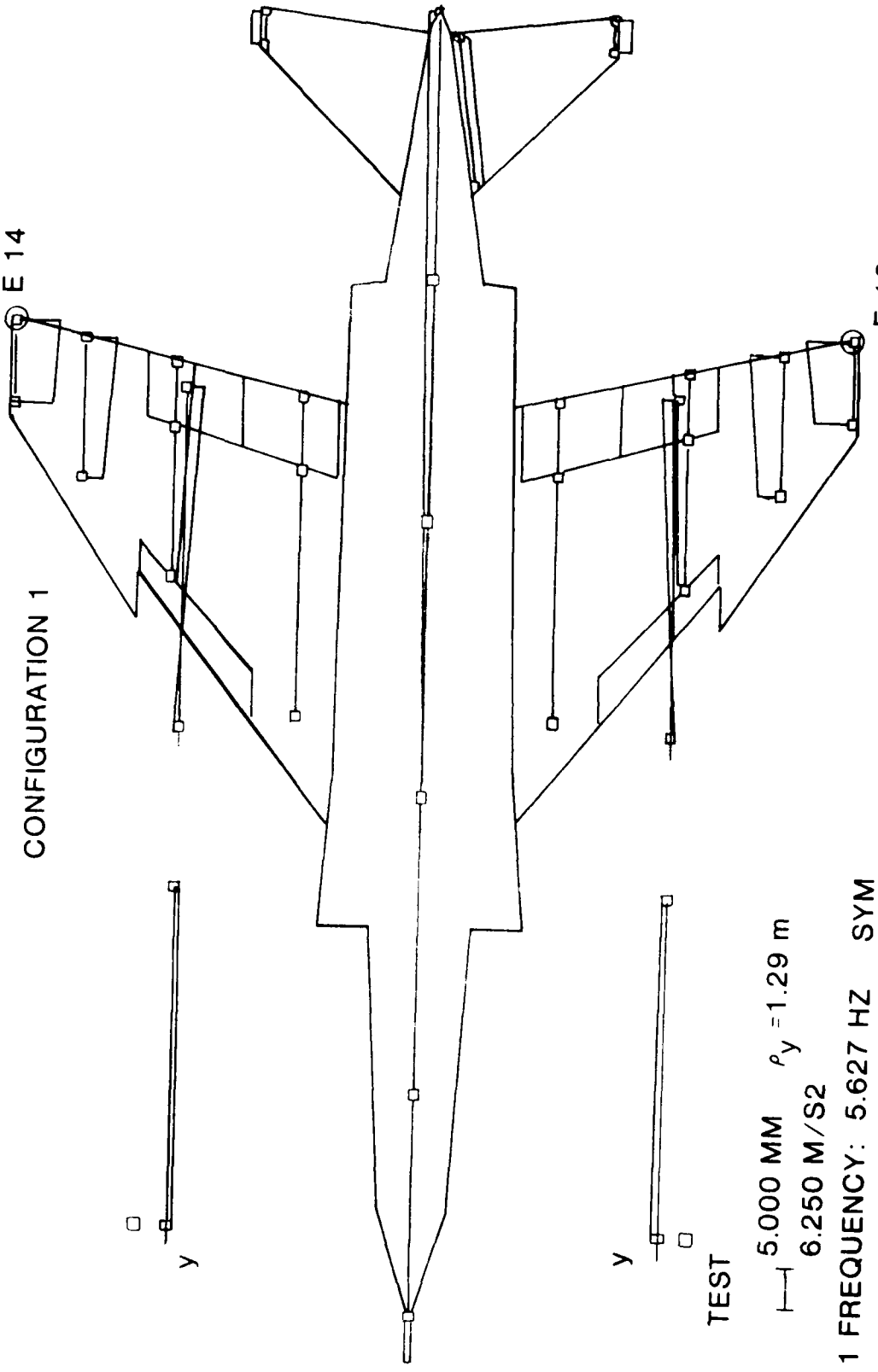


Figure 1. GVT, 1st Wing Bending, Configuration 1

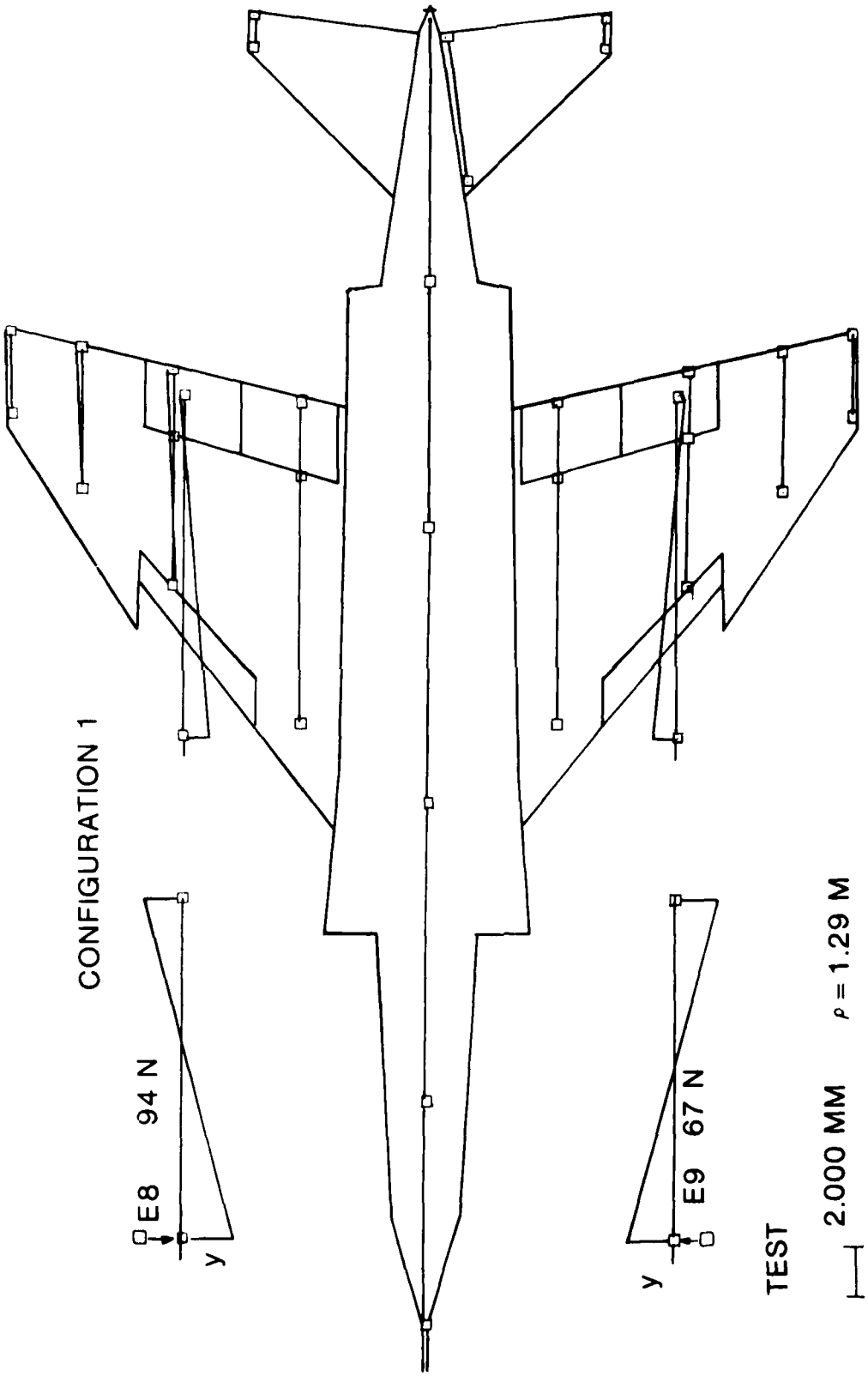


Figure 2. GVT, Store Yaw Mode, Configuration 1

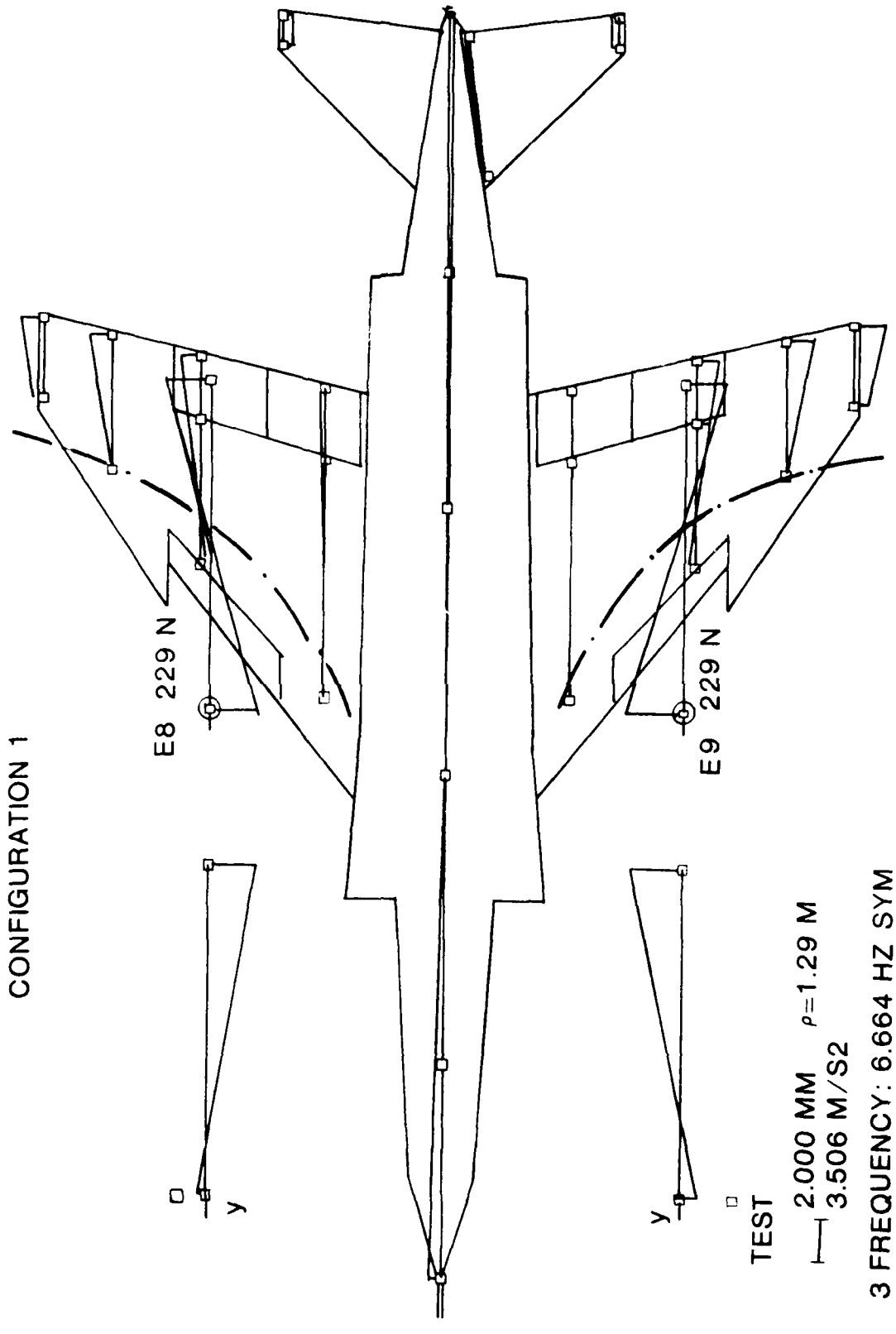


Figure 3. GVT, Store Pitch Mode, Configuration 1

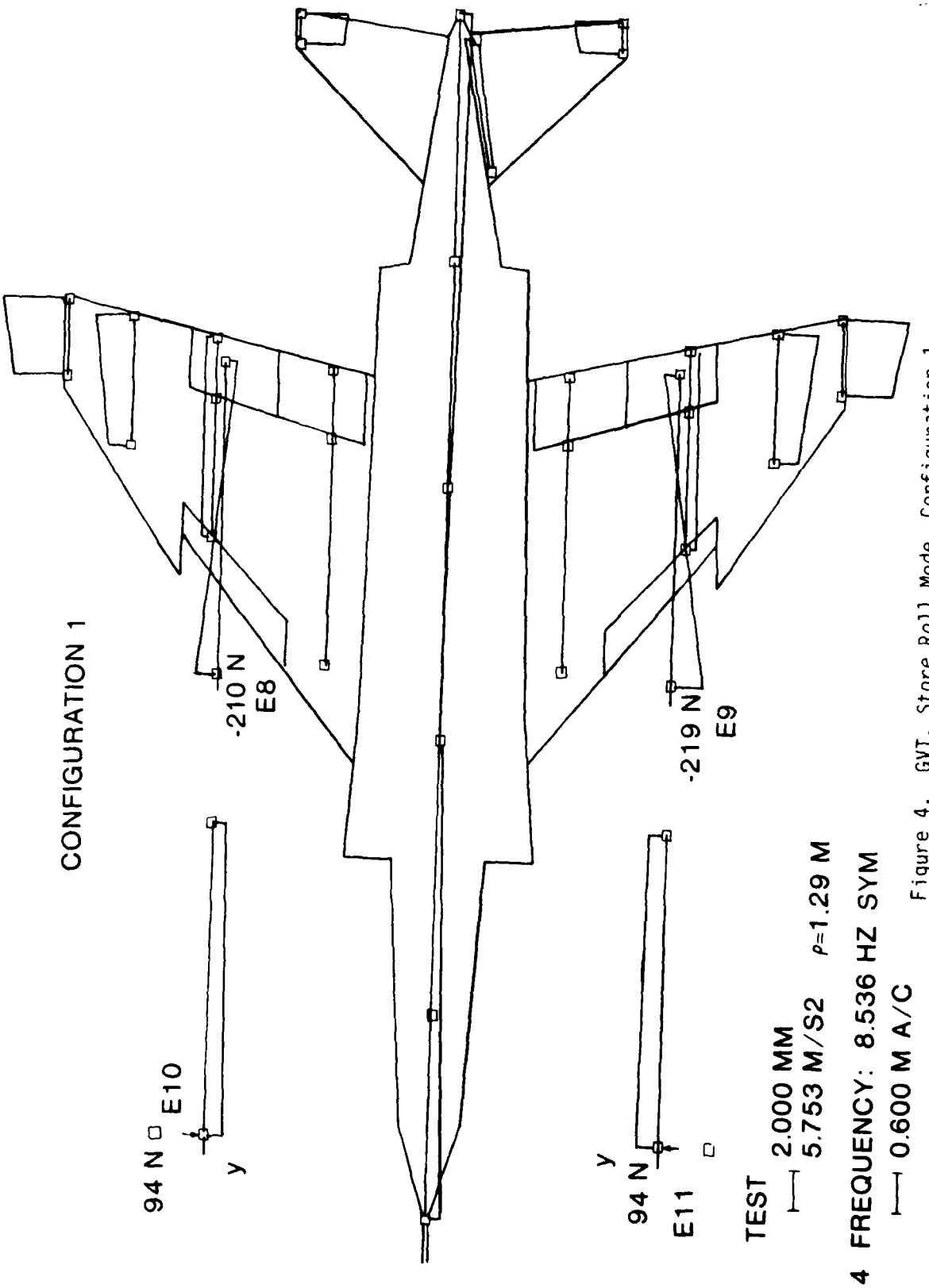


Figure 4. GVT, Store Roll Mode, Configuration 1

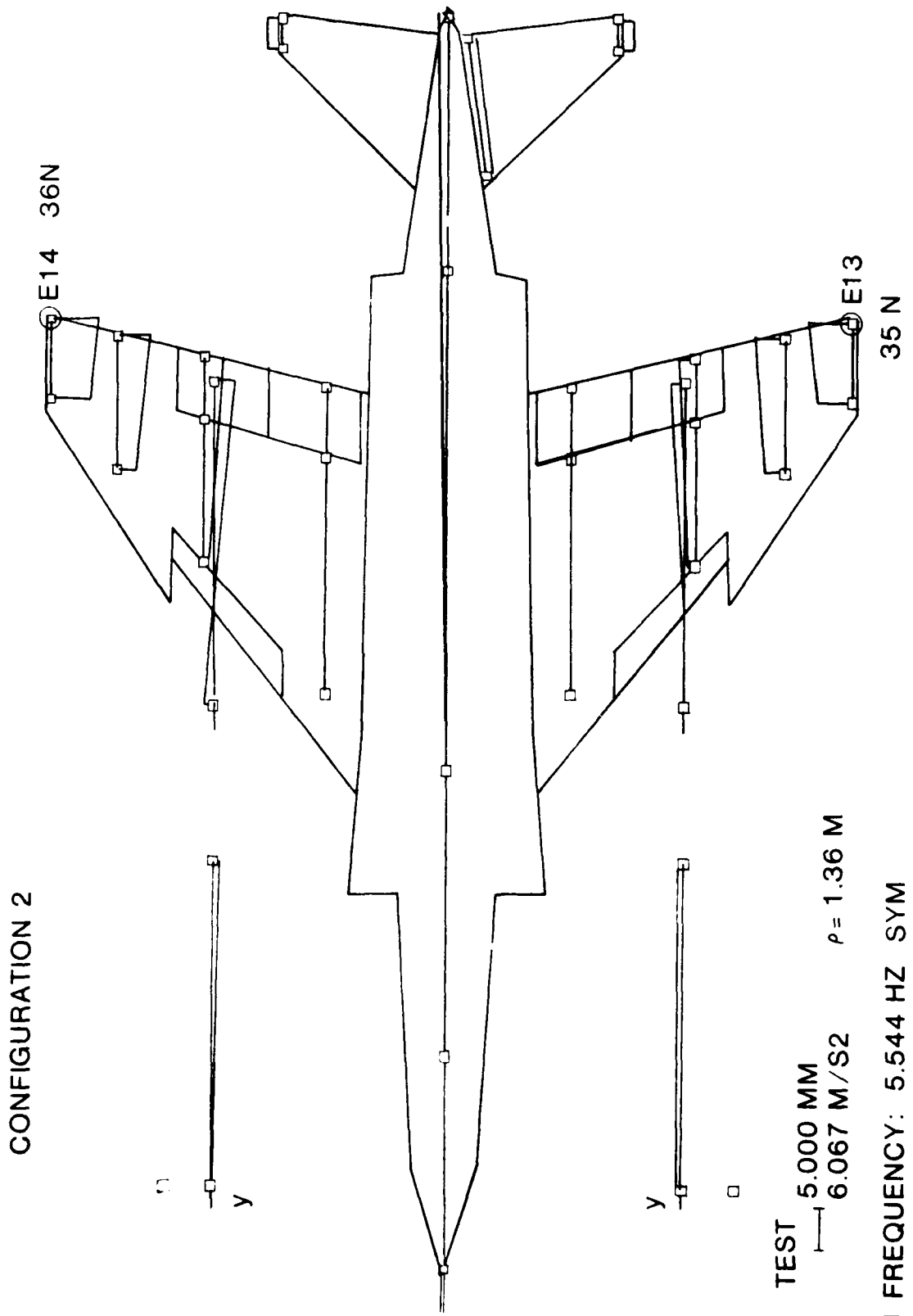


Figure 5. GVT, 1st Wing Bending, Configuration 2

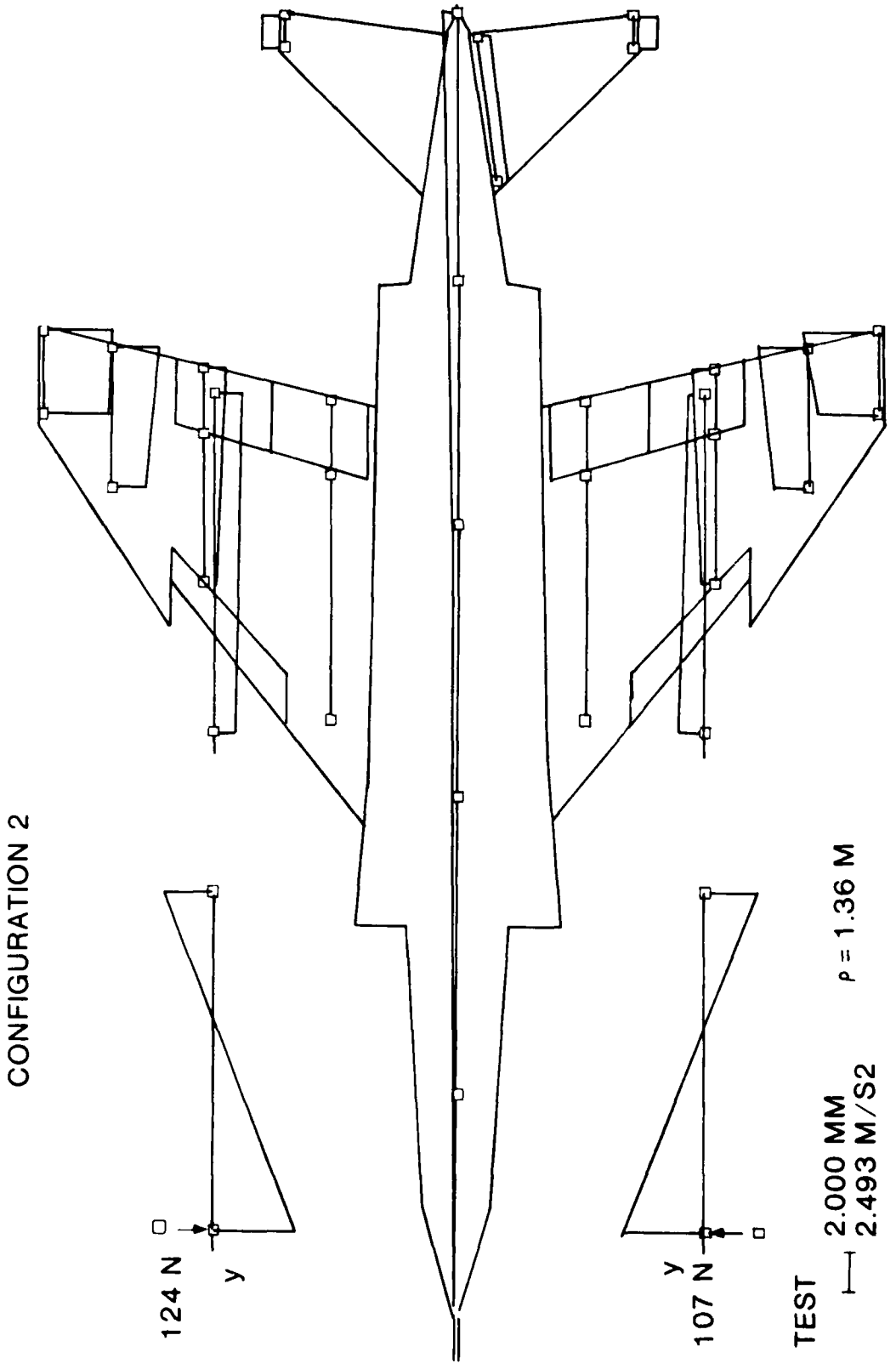


Figure 6. GVT, Store Yaw Mode, Configuration 2

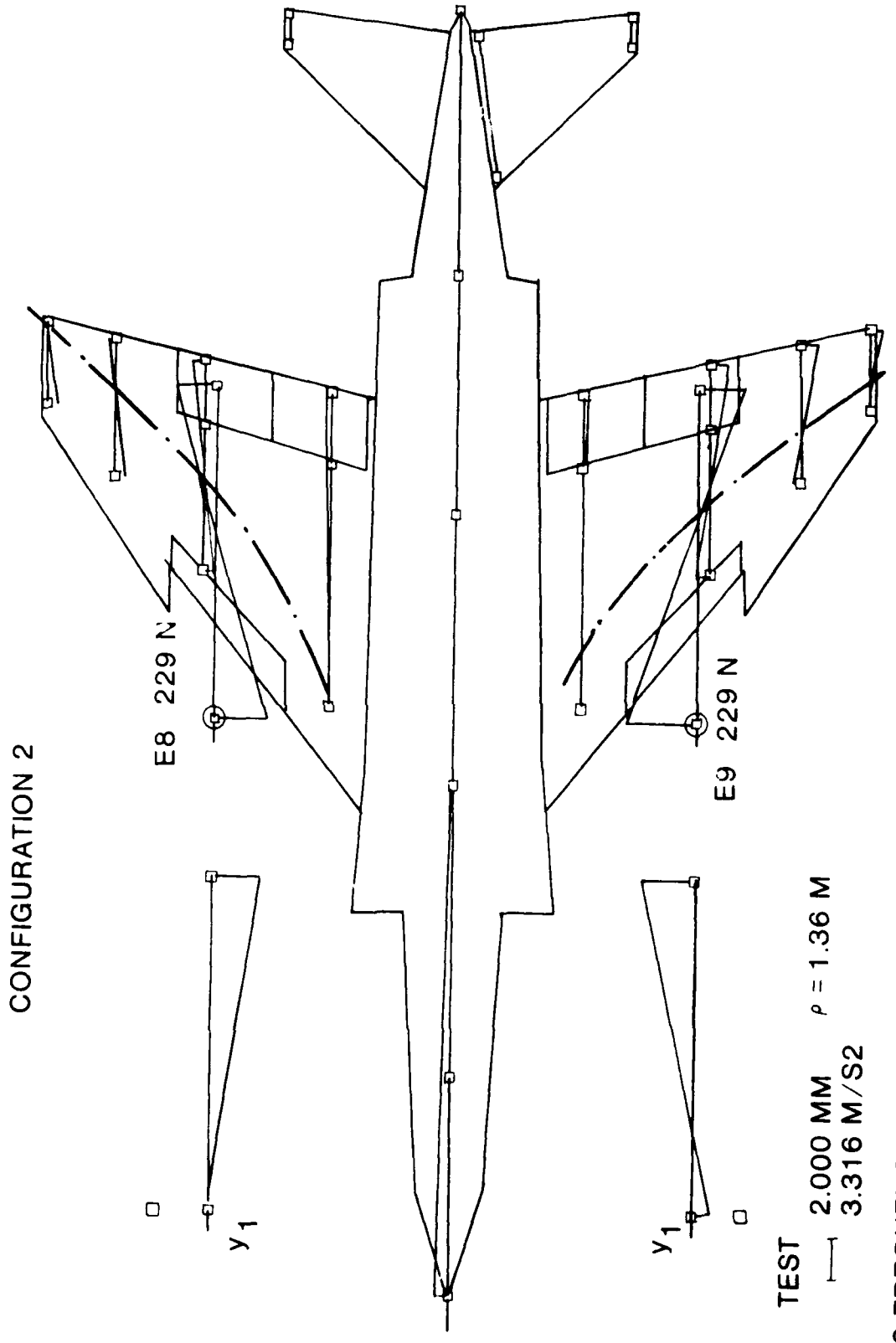


Figure 7. GVT, Store Pitch Mode, Configuration 2

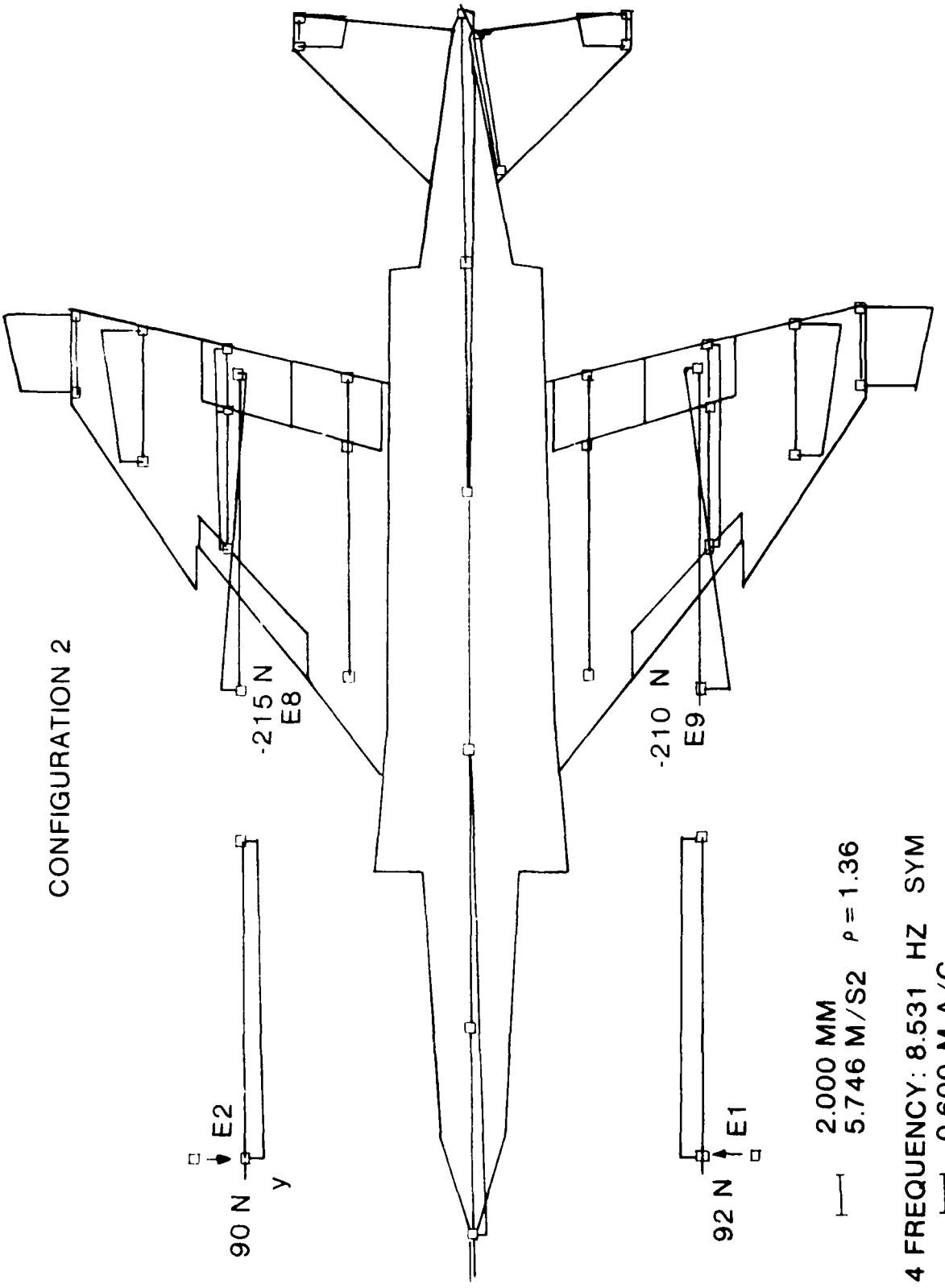


Figure 8. GVT, Store Roll Mode, Configuration 2

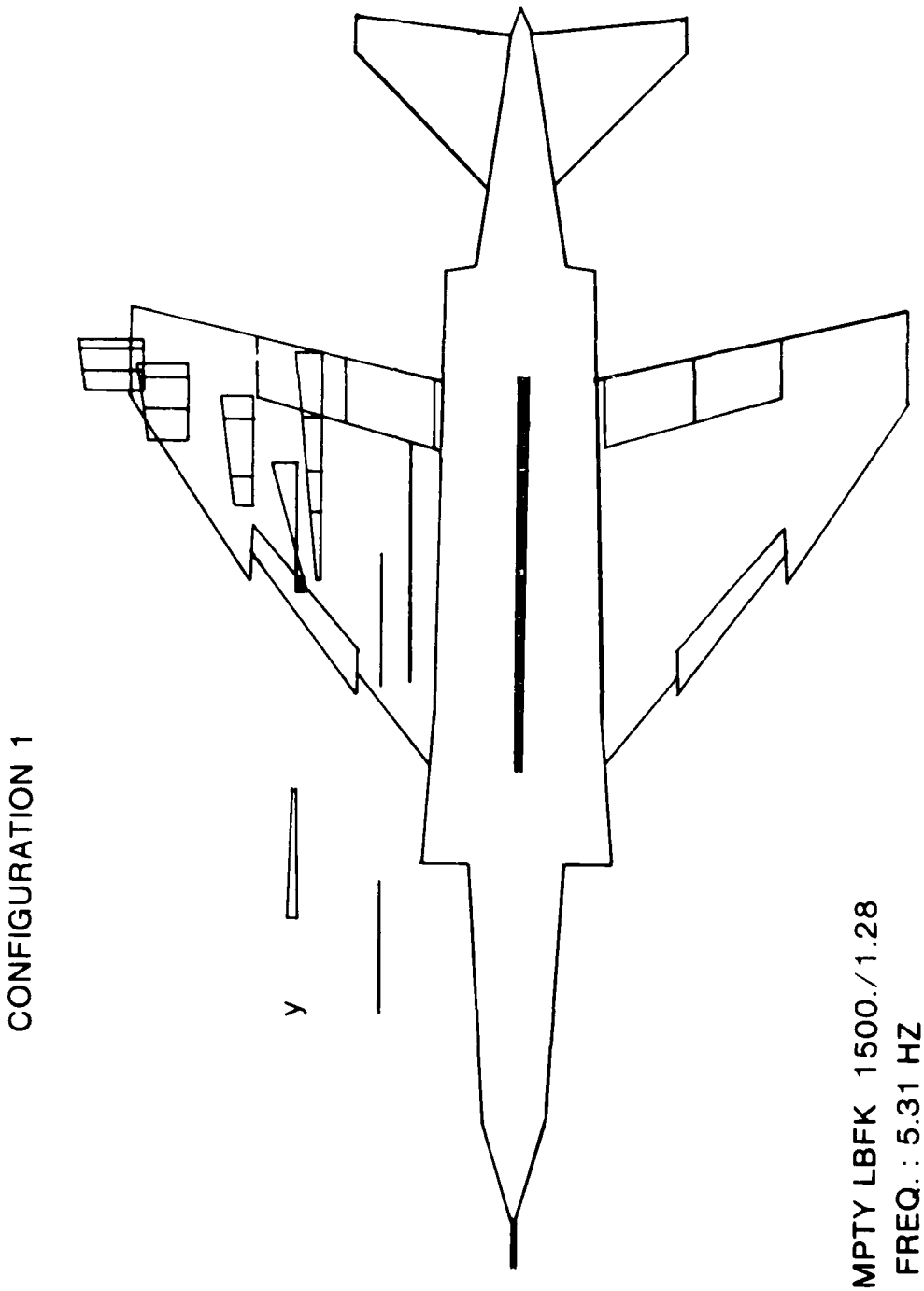


Figure 9. Calculated 1st Wing Bending, Configuration 1

CONFIGURATION 1

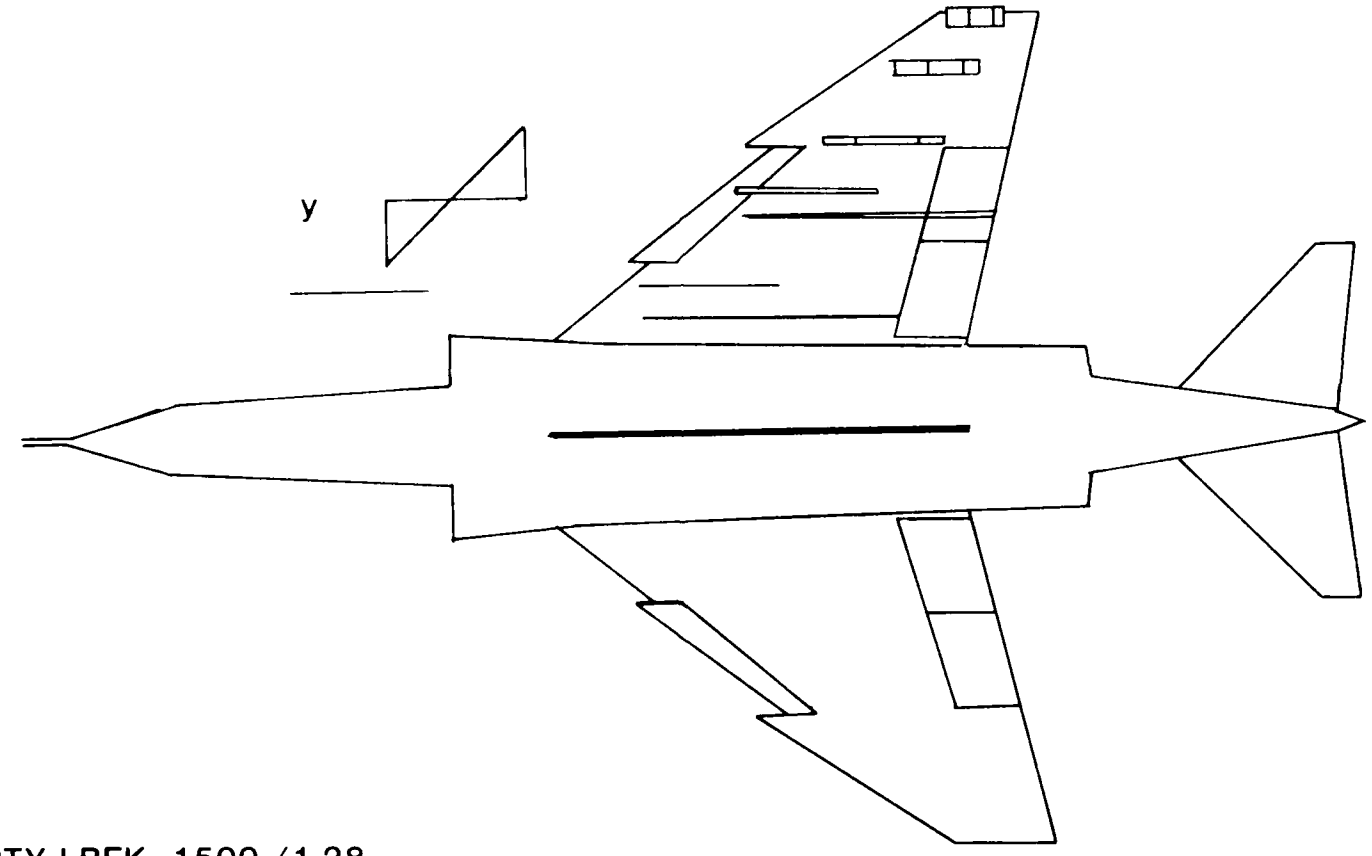


F-4 EMPTY LBFK 1500./1.28

2. SYM FREQ.: 5.70 HZ

Figure 10. Calculated Store Yaw Mode, Configuration 1

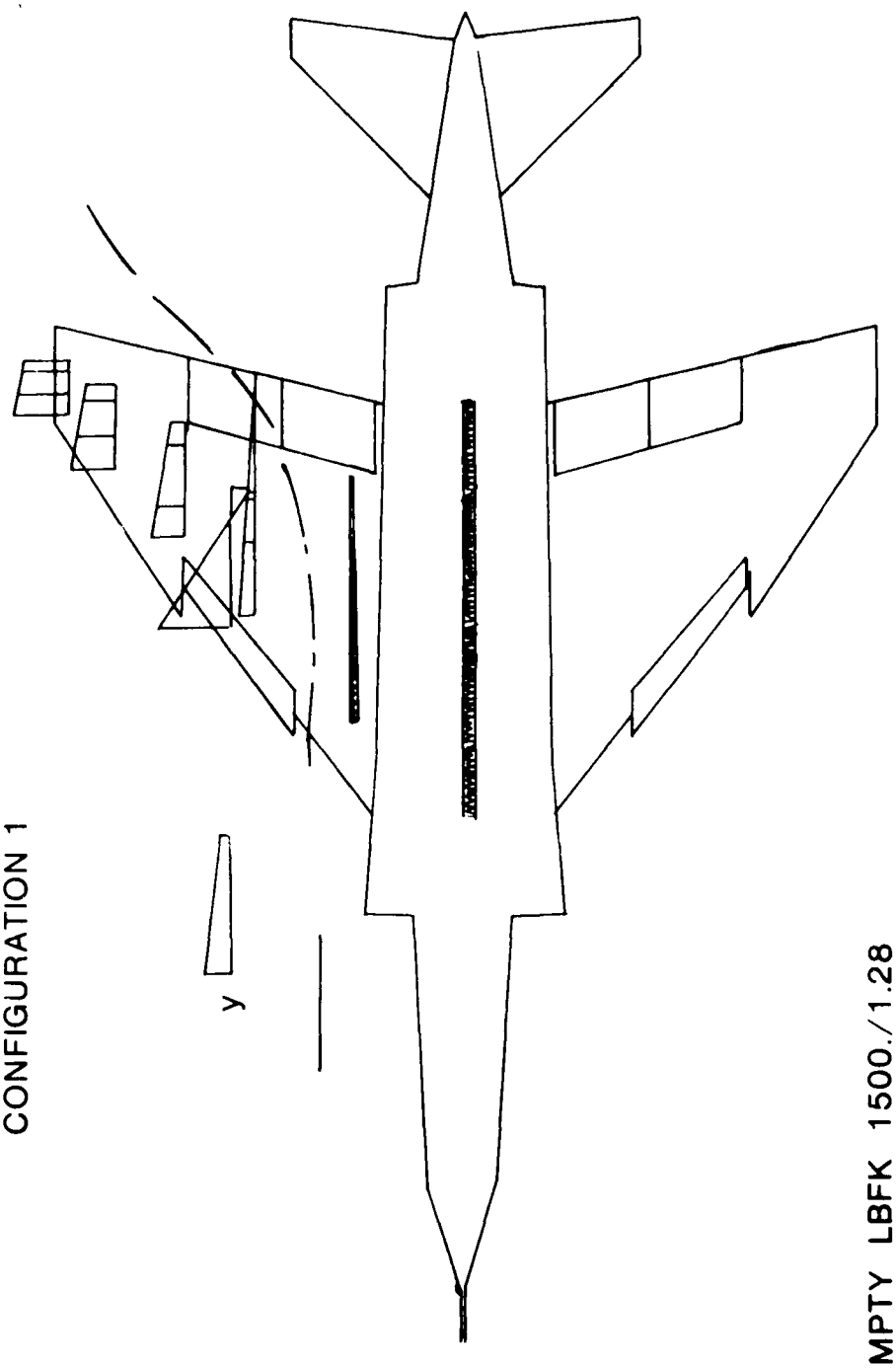


Figure 11. Calculated Store Pitch Mode, Configuration 1

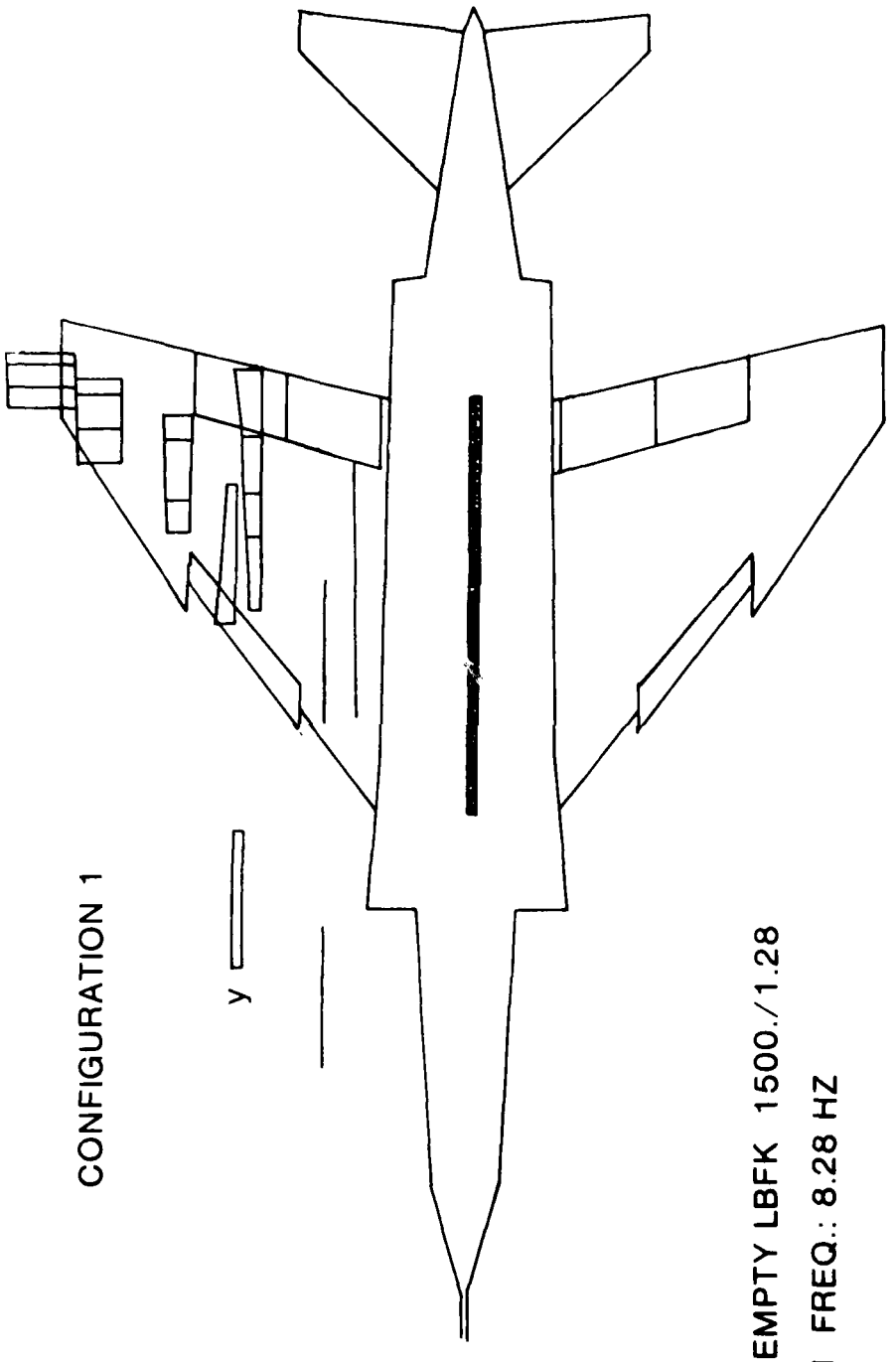


Figure 12. Calculated Store Roll Mode, Configuration 1

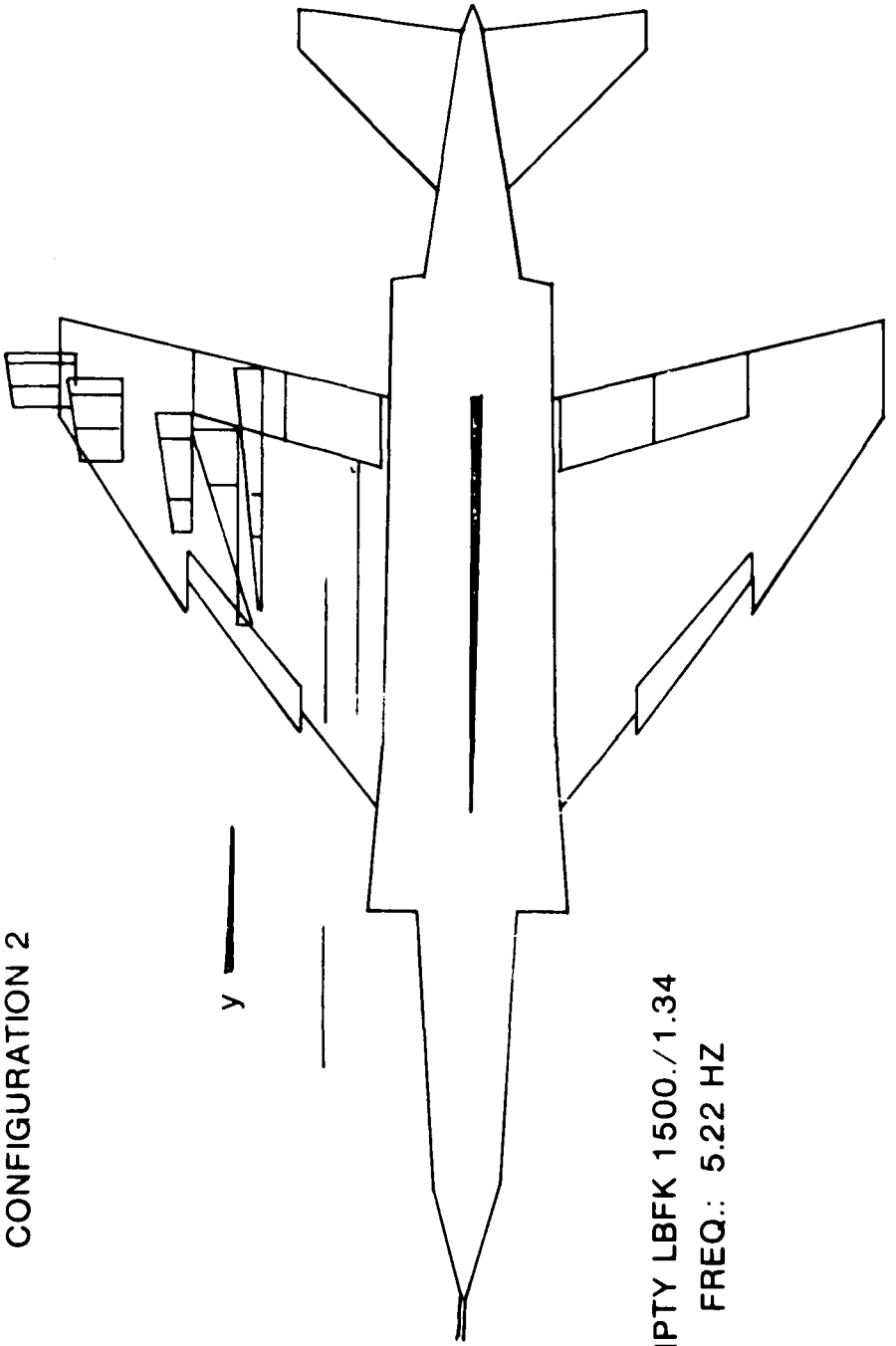


Figure 13. Calculated 1st Wing Bending, Configuration 2

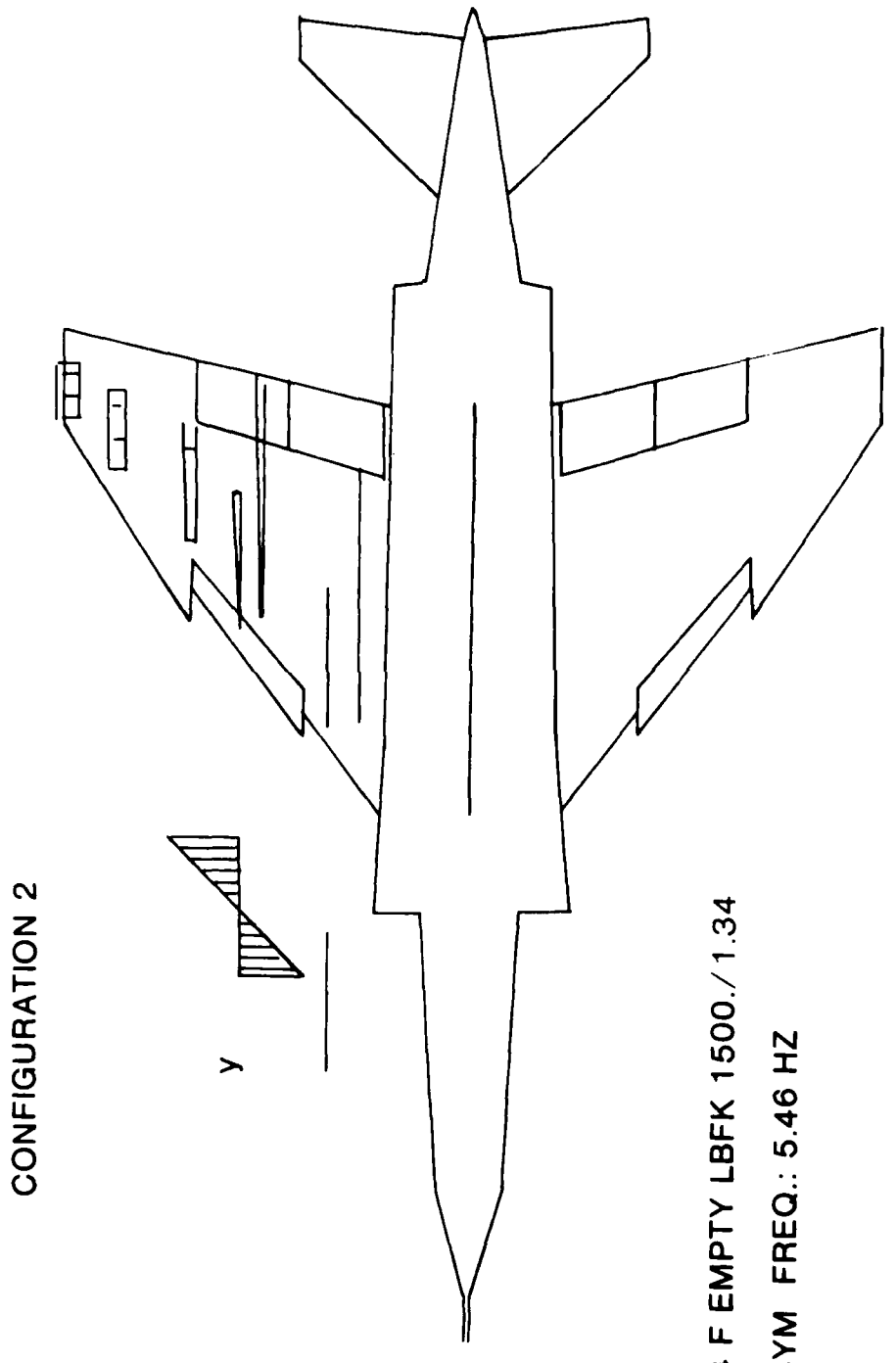


Figure 14. Calculated Store Yaw Mode, Configuration 2

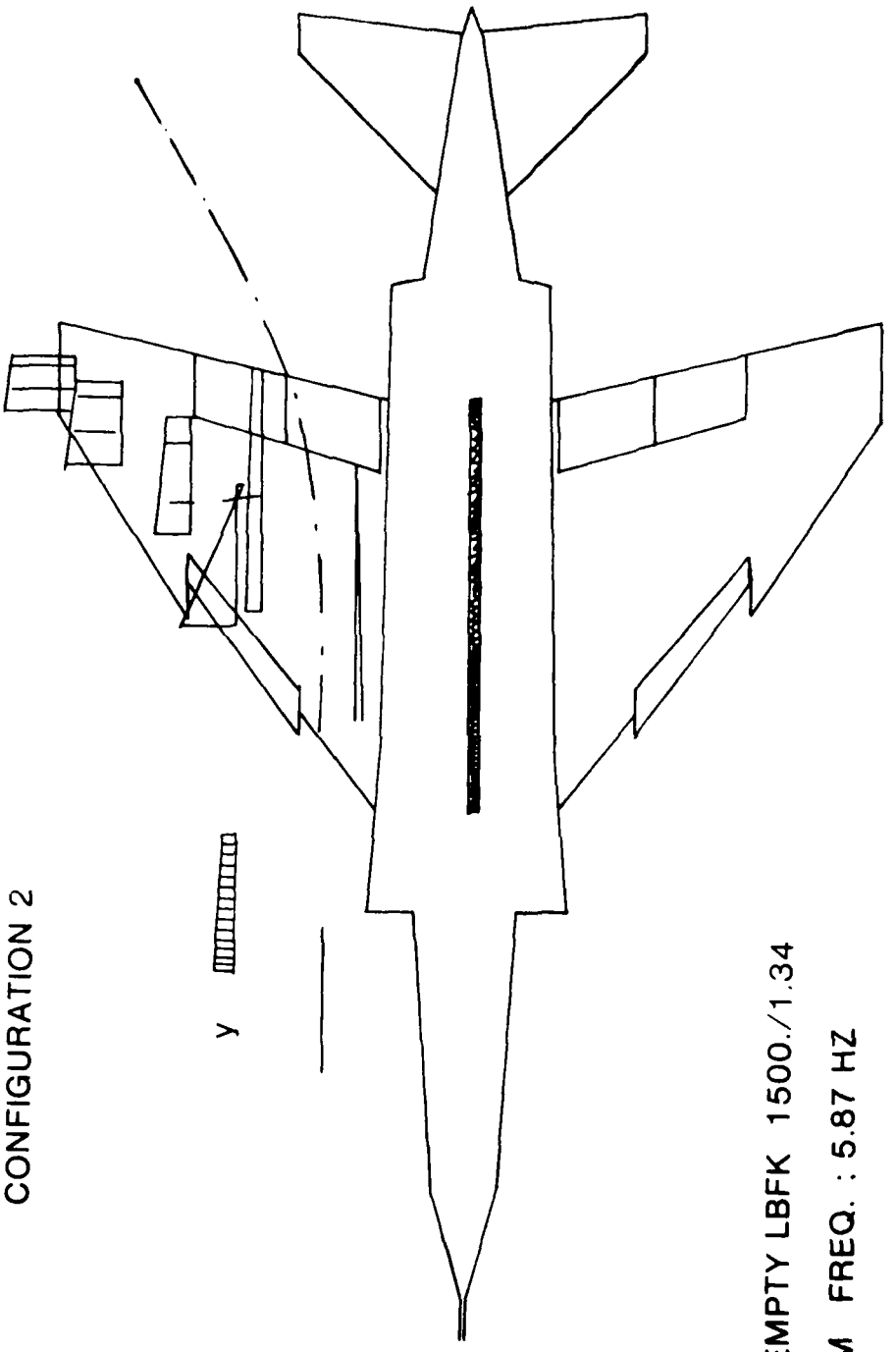


Figure 15. Calculated Store Pitch Mode, Configuration 2

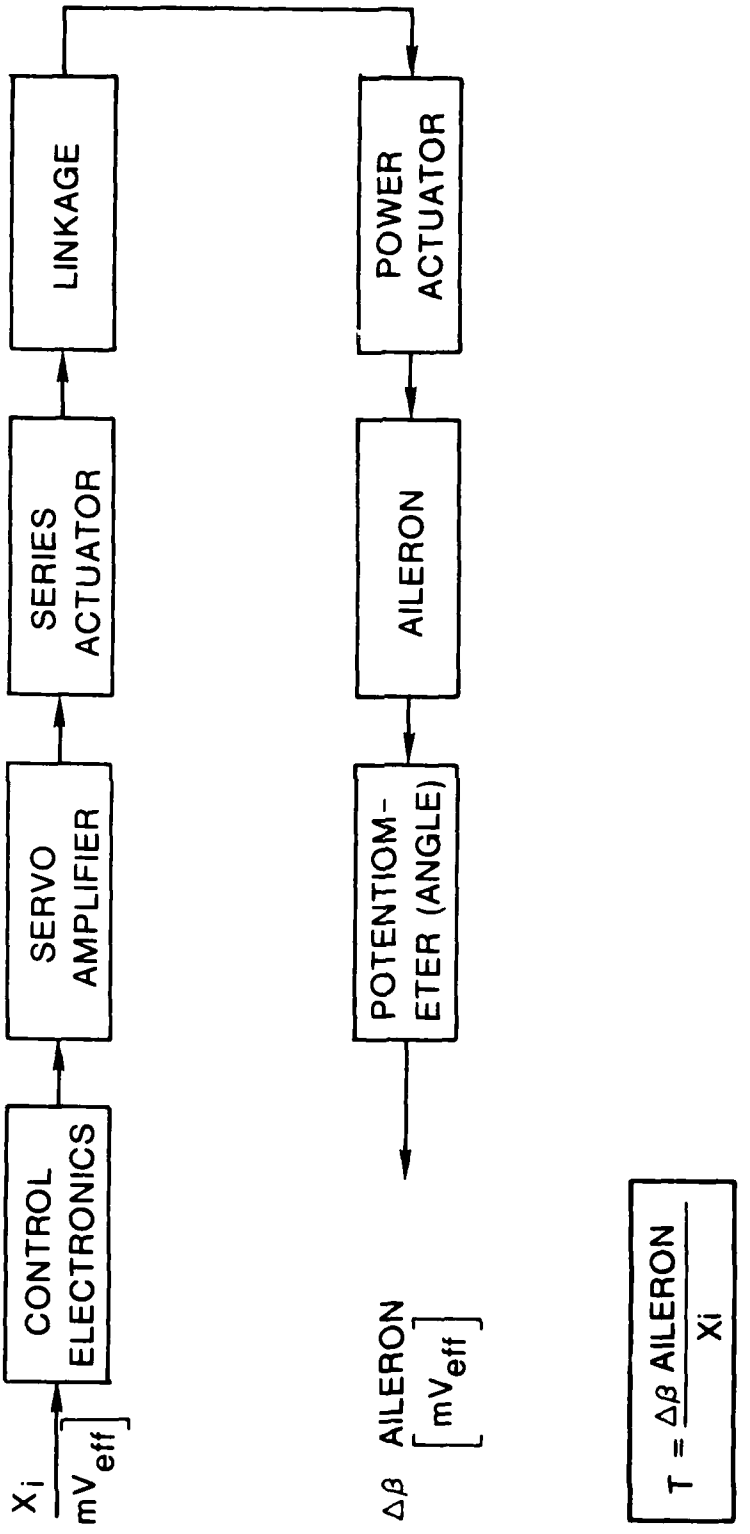


Figure 16. Block Diagram for Measurement of Aileron Actuator Transfer Function

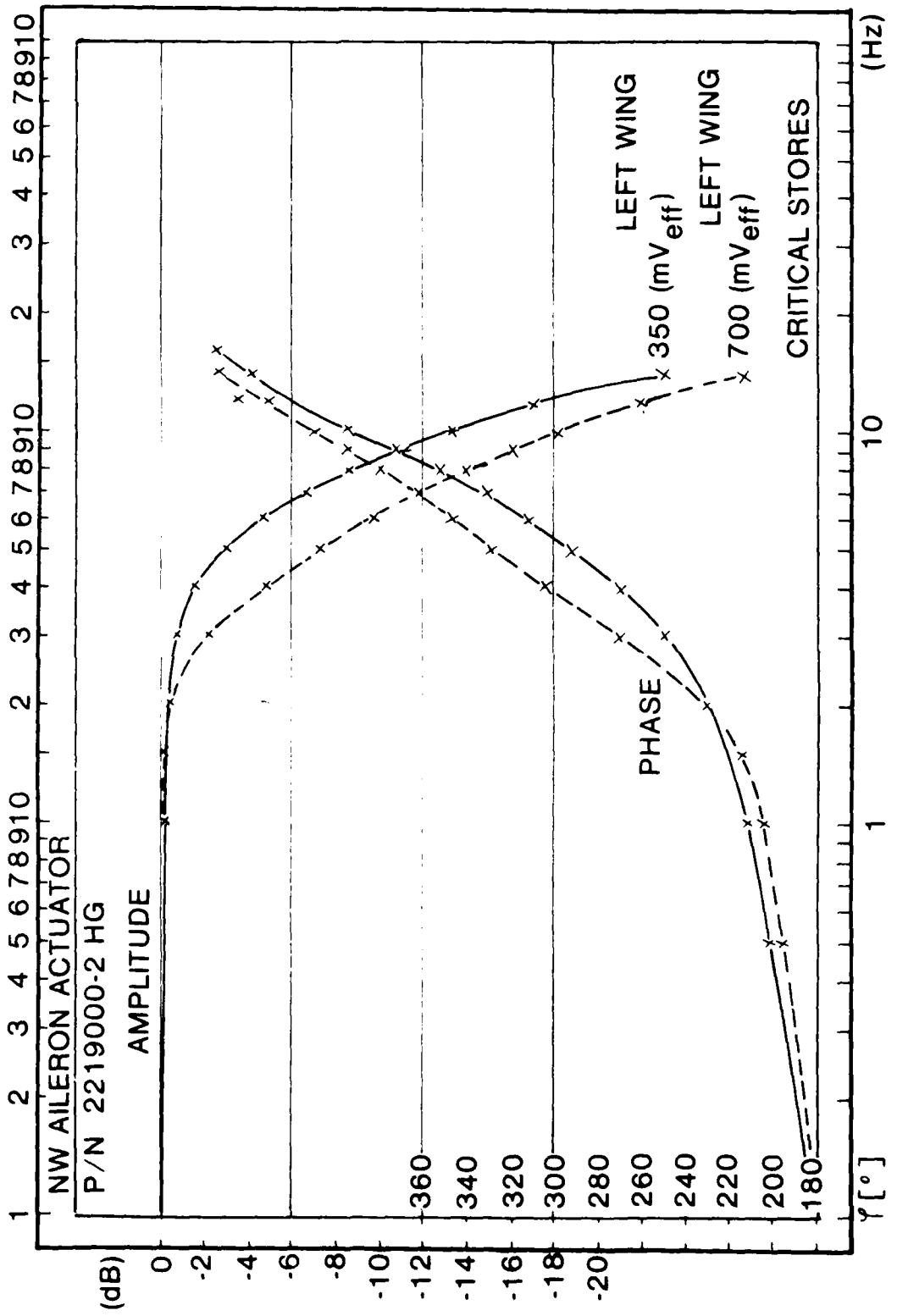


Figure 17. Measured Transfer Function of the Left Aileron

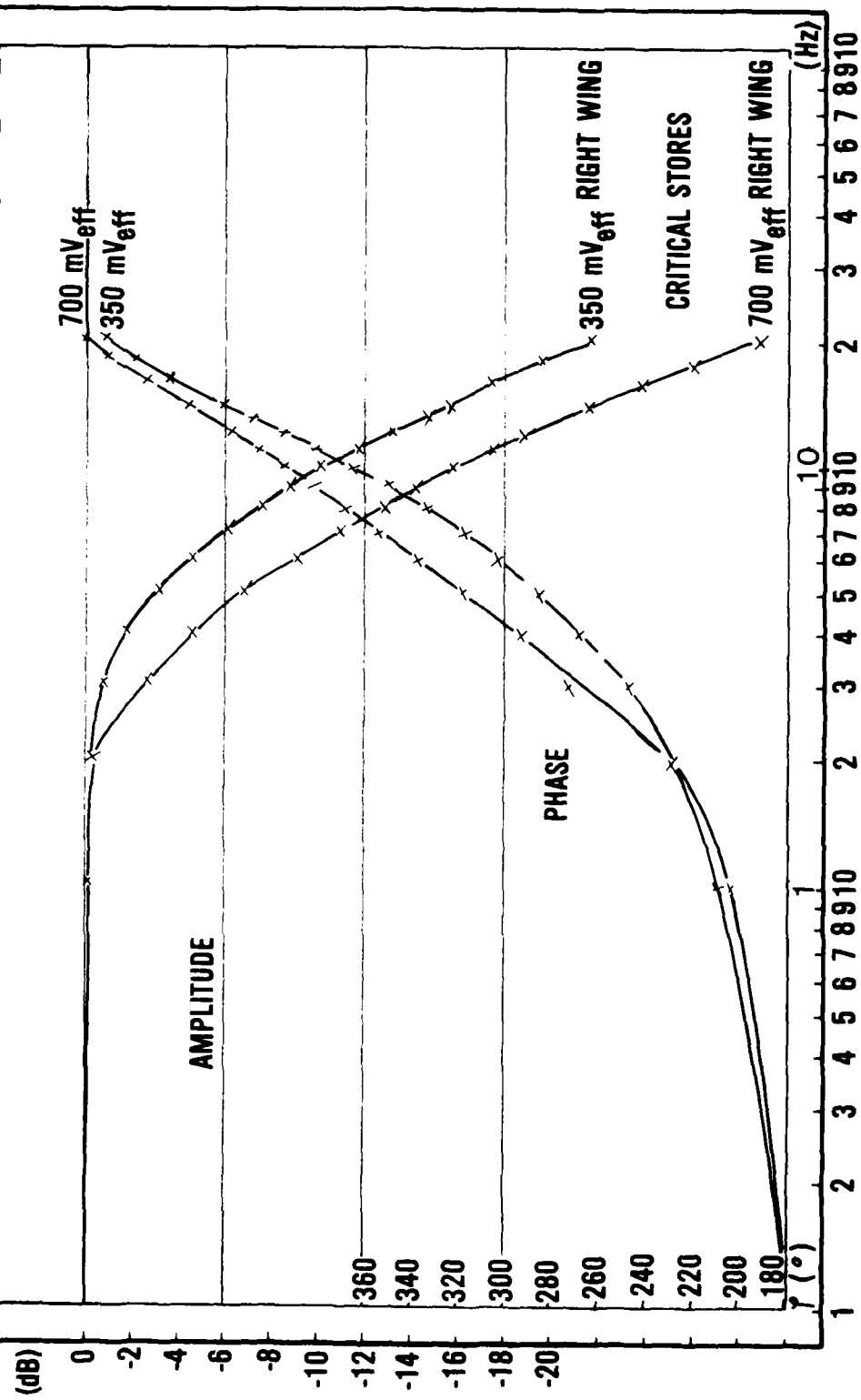


Figure 18. Measured Transfer Function of the Right Aileron

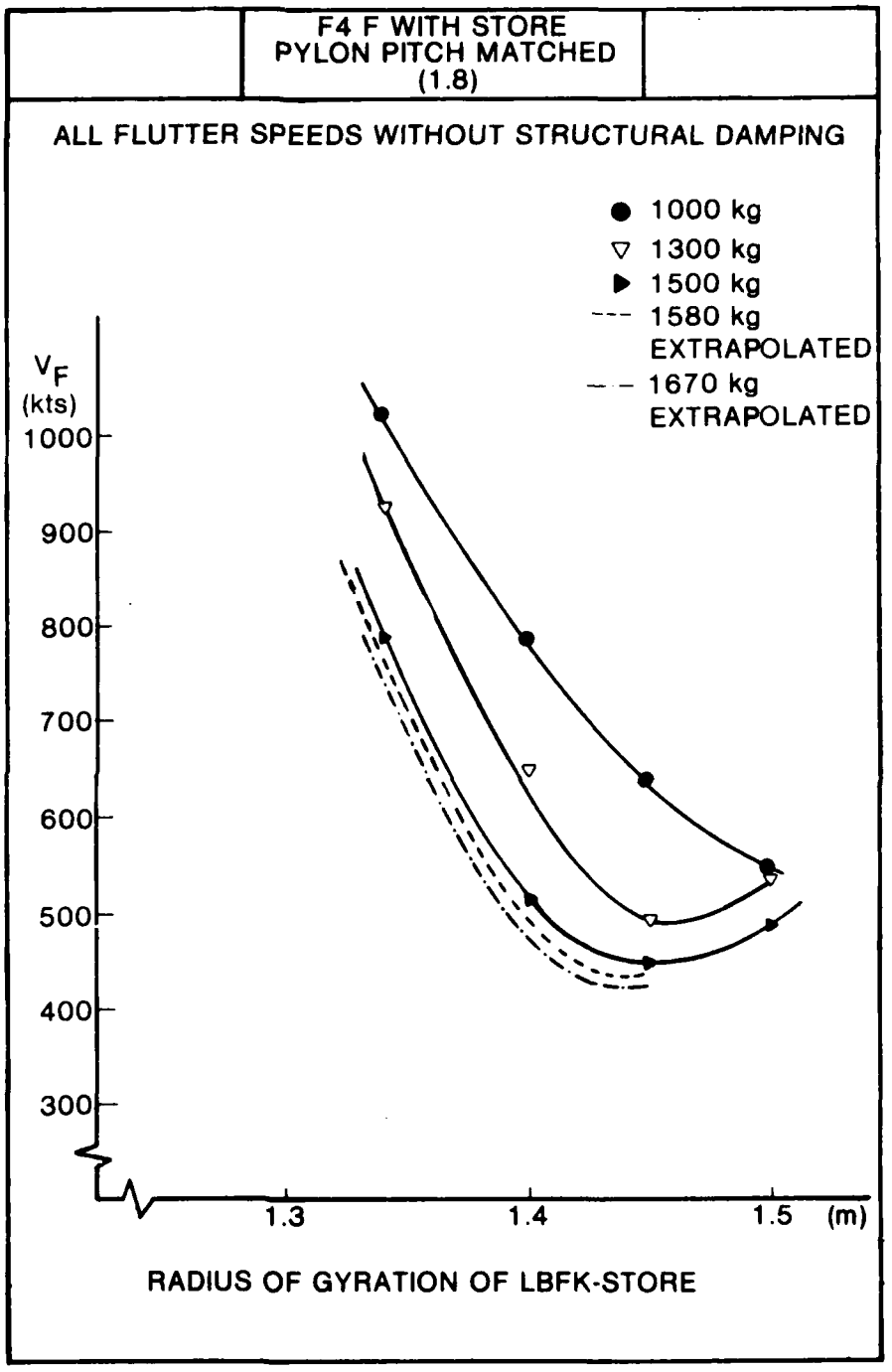


Figure 19. Flutter Speed vs Radius of Gyration of the LBFK-Store

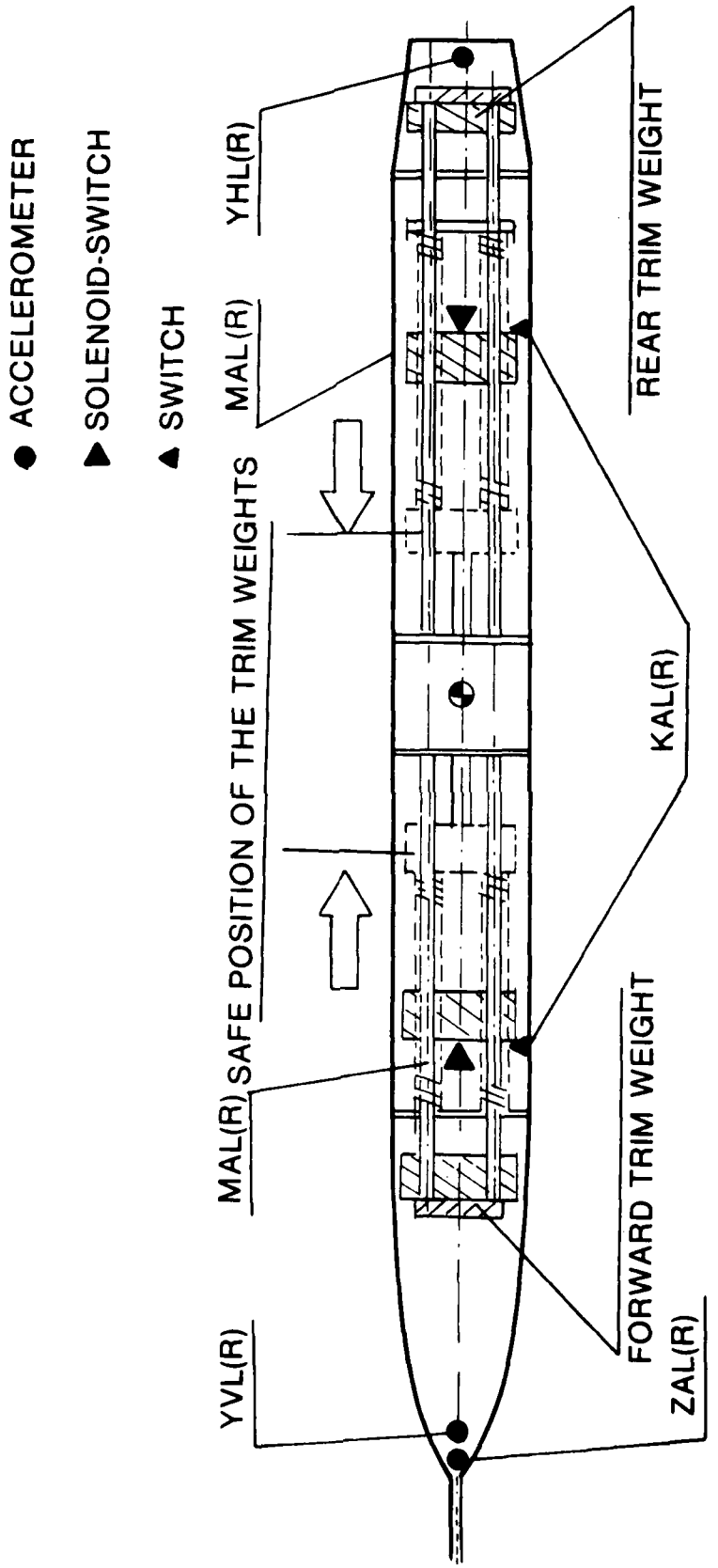


Figure 20. Scheme for the Modified Flutter Stopper

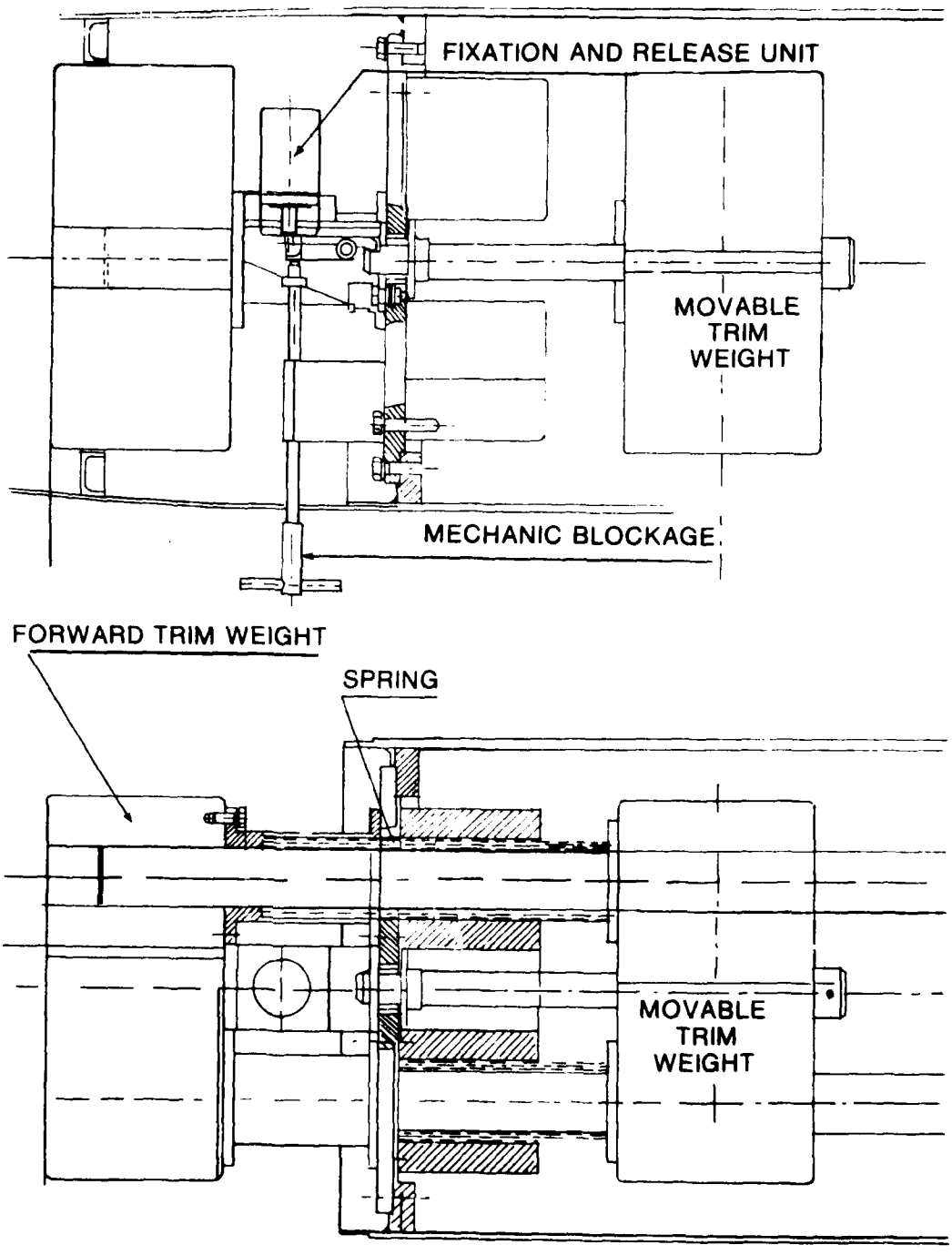


Figure 21. Forward Part of the Flutter Stopper

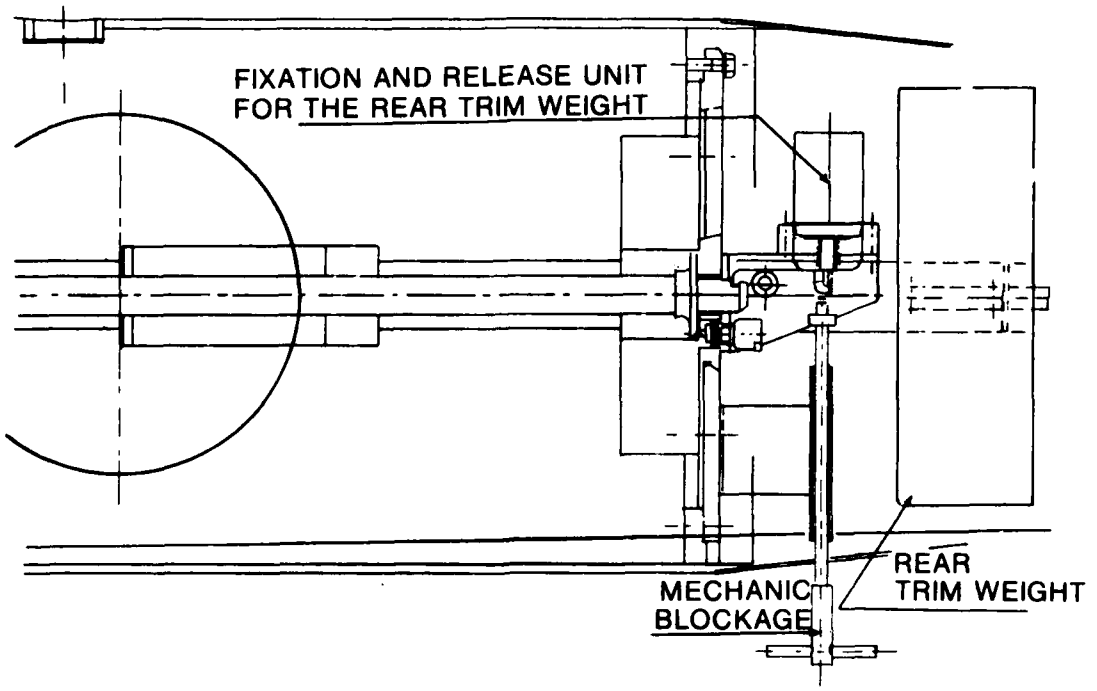


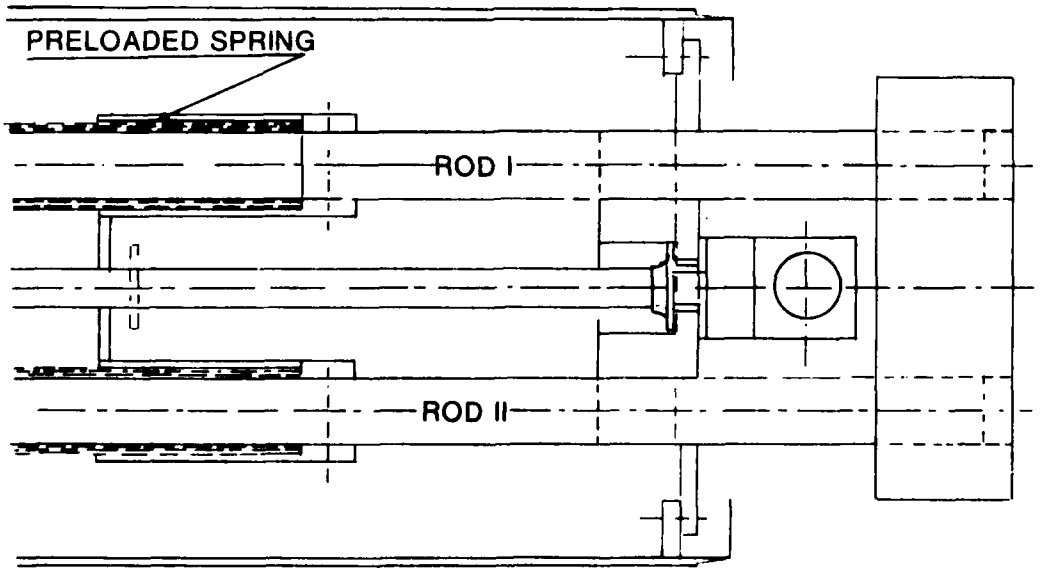


Figure 22. Rear Part of the Flutter Stopper

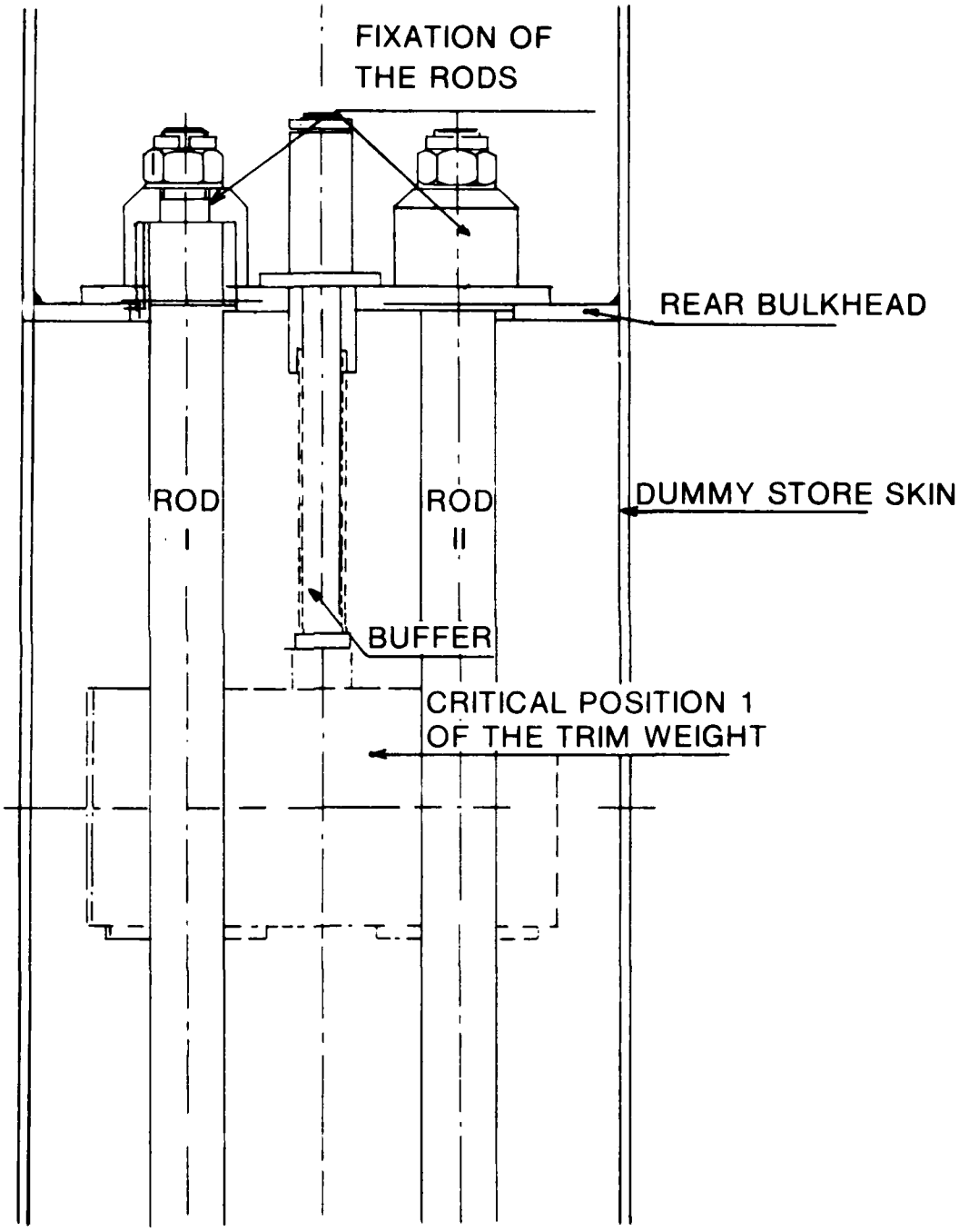


Figure 23. Fixation of the Rods in the LBFK Dummy Store

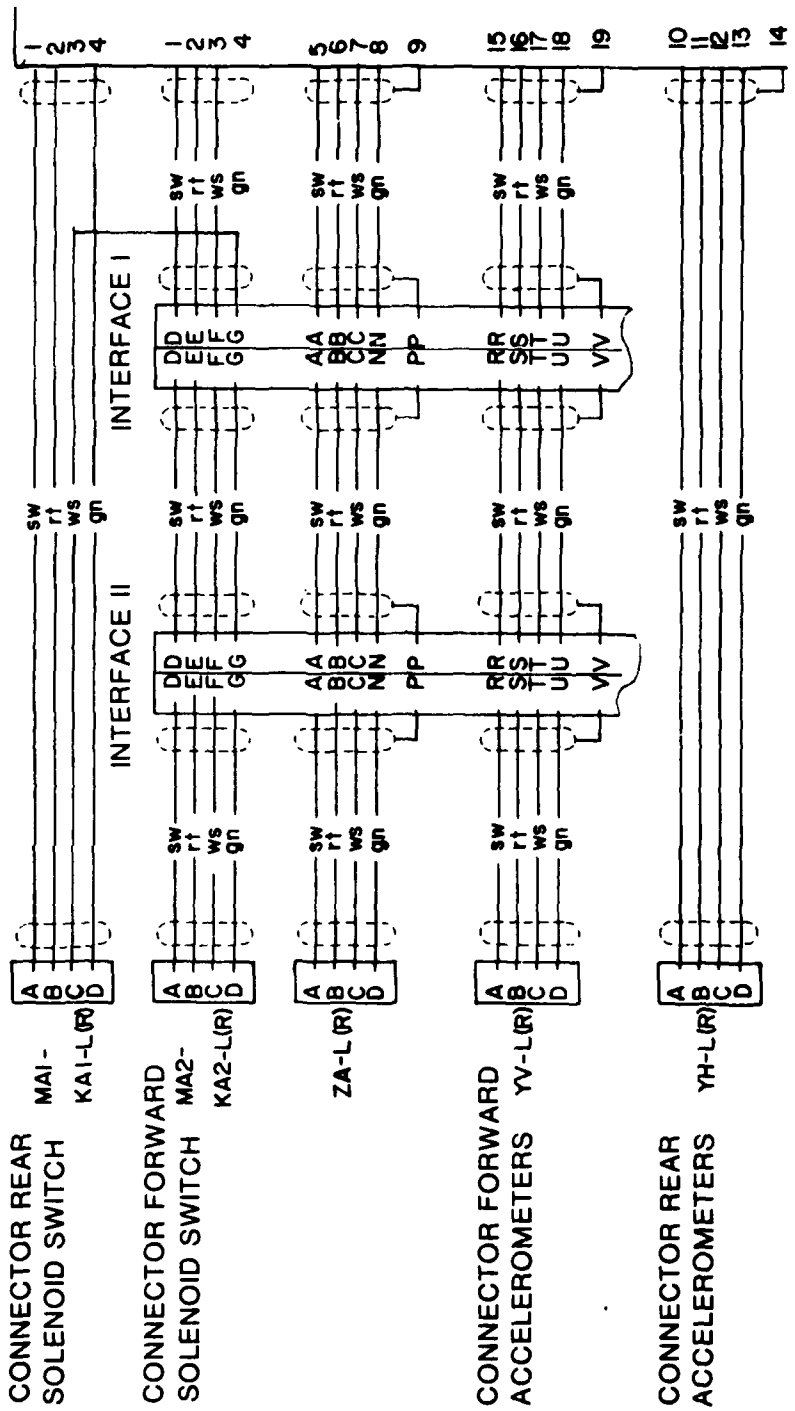


Figure 24. Wiring Plan for the Flutter Stopper

F-4F DUMMY STORE (LBFK)

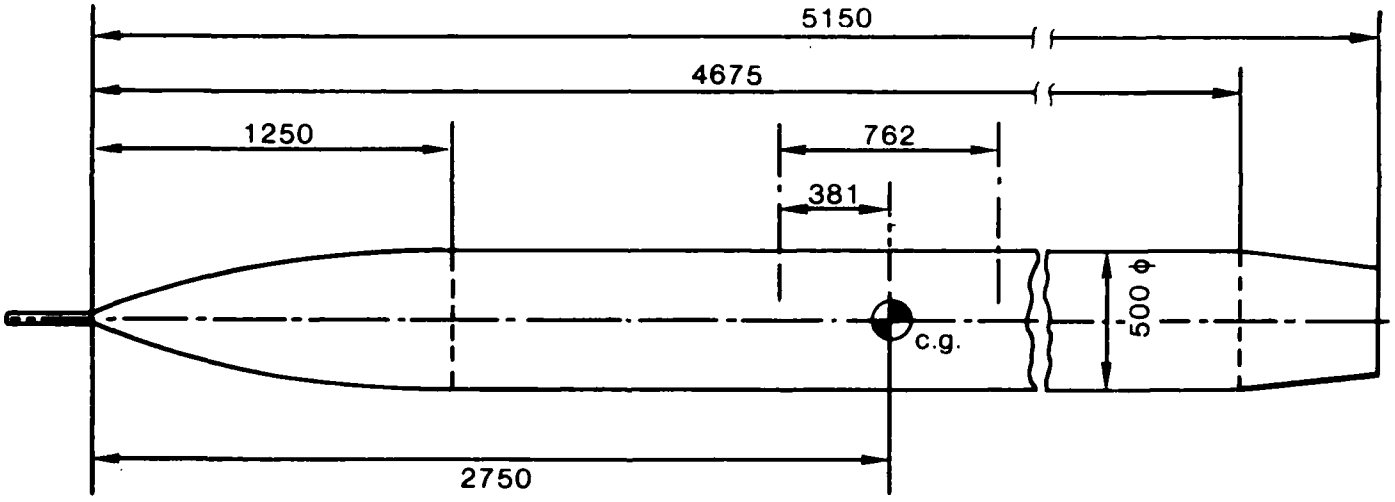


DUMMY D1 (LEFT WING)

W=1576 (kg)

$\rho_y$=1.341 (m) SAFE CONFIG.

$\rho_y$=1.409 1.341 (m) CRITICAL CONFIG

DUMMY D3: (RIGHT WING)

W=1583 (kg)

$\rho_y$=1.347 (m) SAFE CONFIG.

$\rho_y$=1.416 (m) CRITICAL CONFIG.

Figure 25. Geometry and Mass Data of the Modified Store

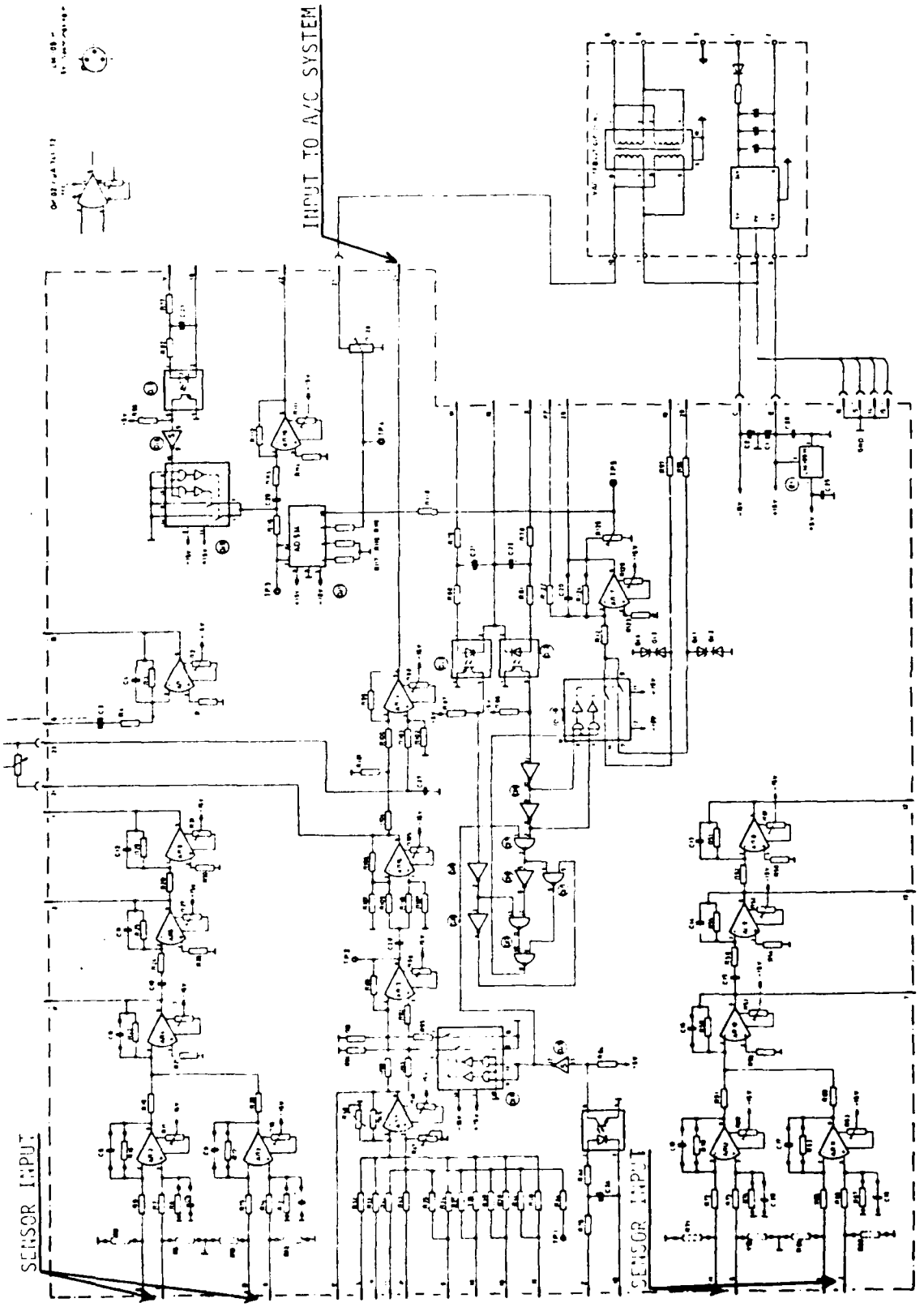


Figure 26. Design of the Control Electronics

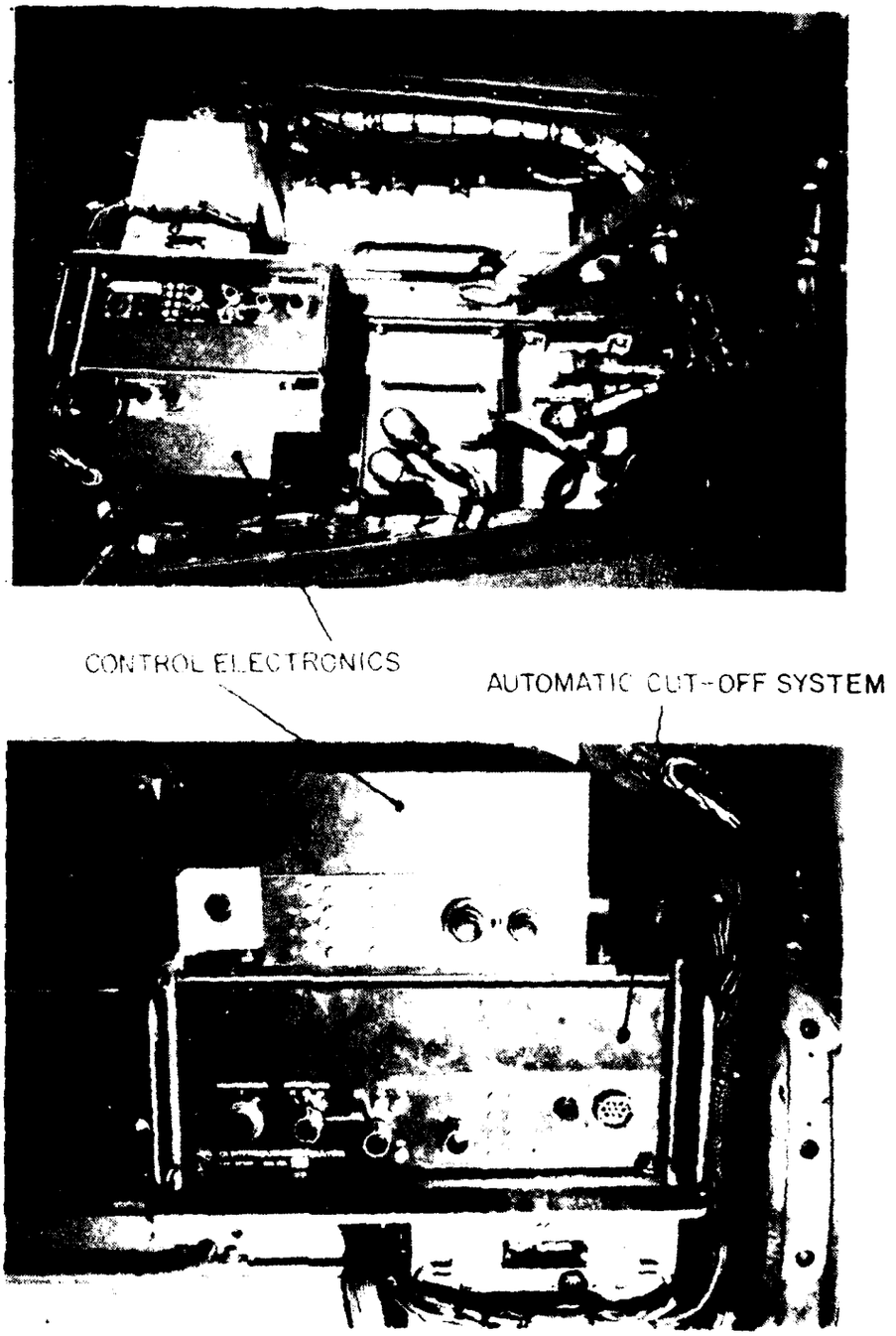


Figure 27. Installation of Control Electronics and Automatic Cut-Off System in the Aircraft

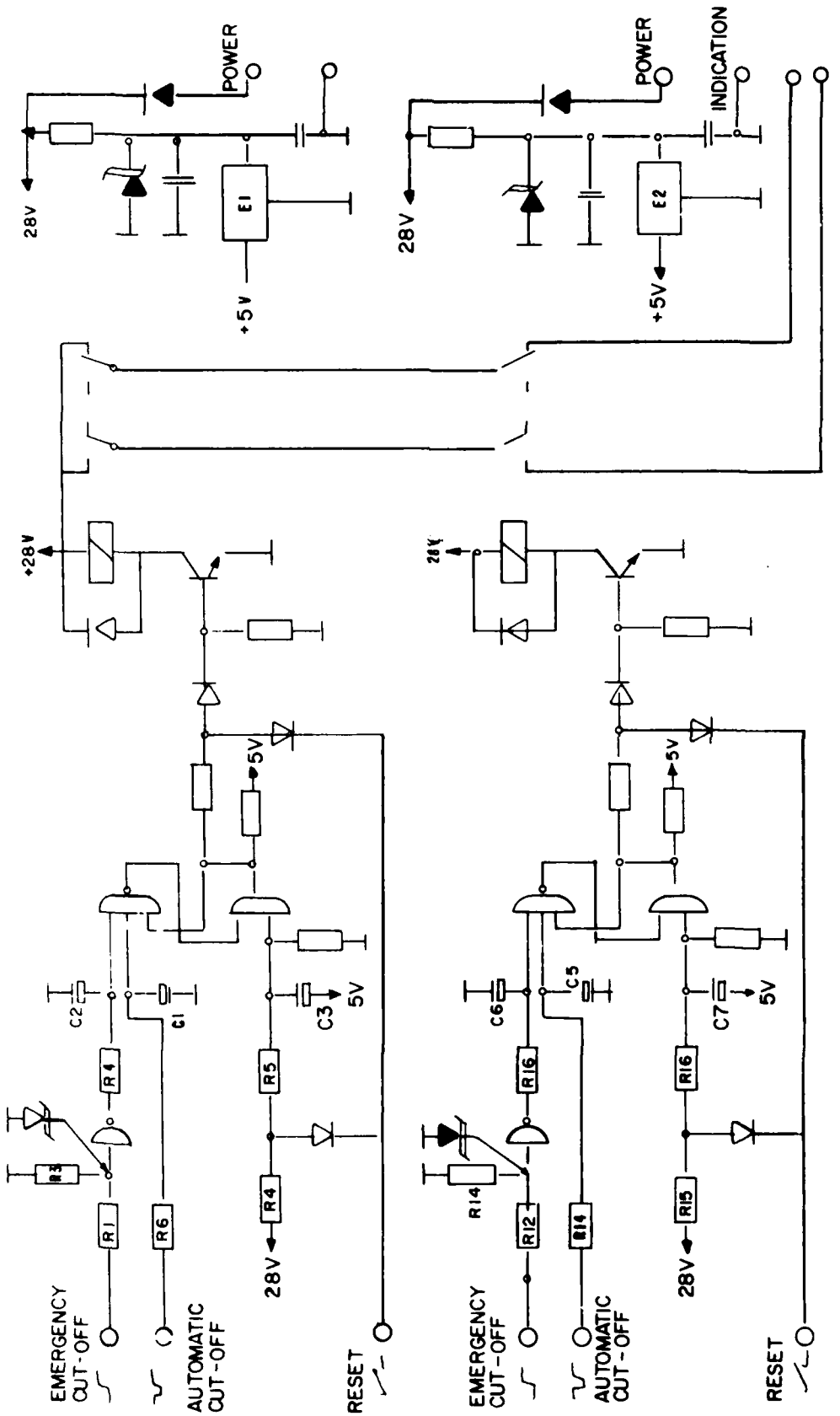


Figure 28. Design of the Cut-Off Logic

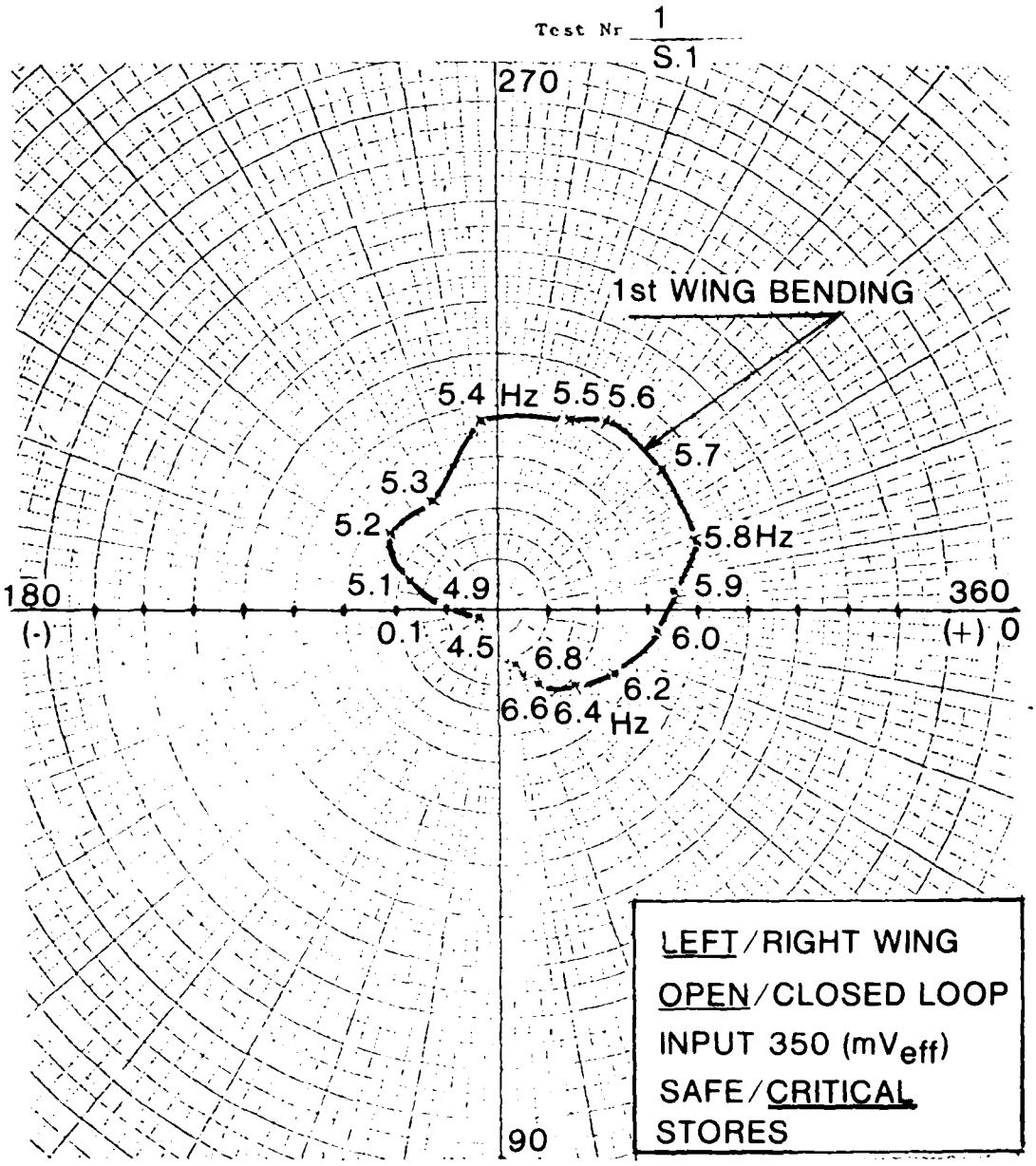


Figure 29. Nyquist Diagram, Structural Mode Coupling Test, Left Wing Bending

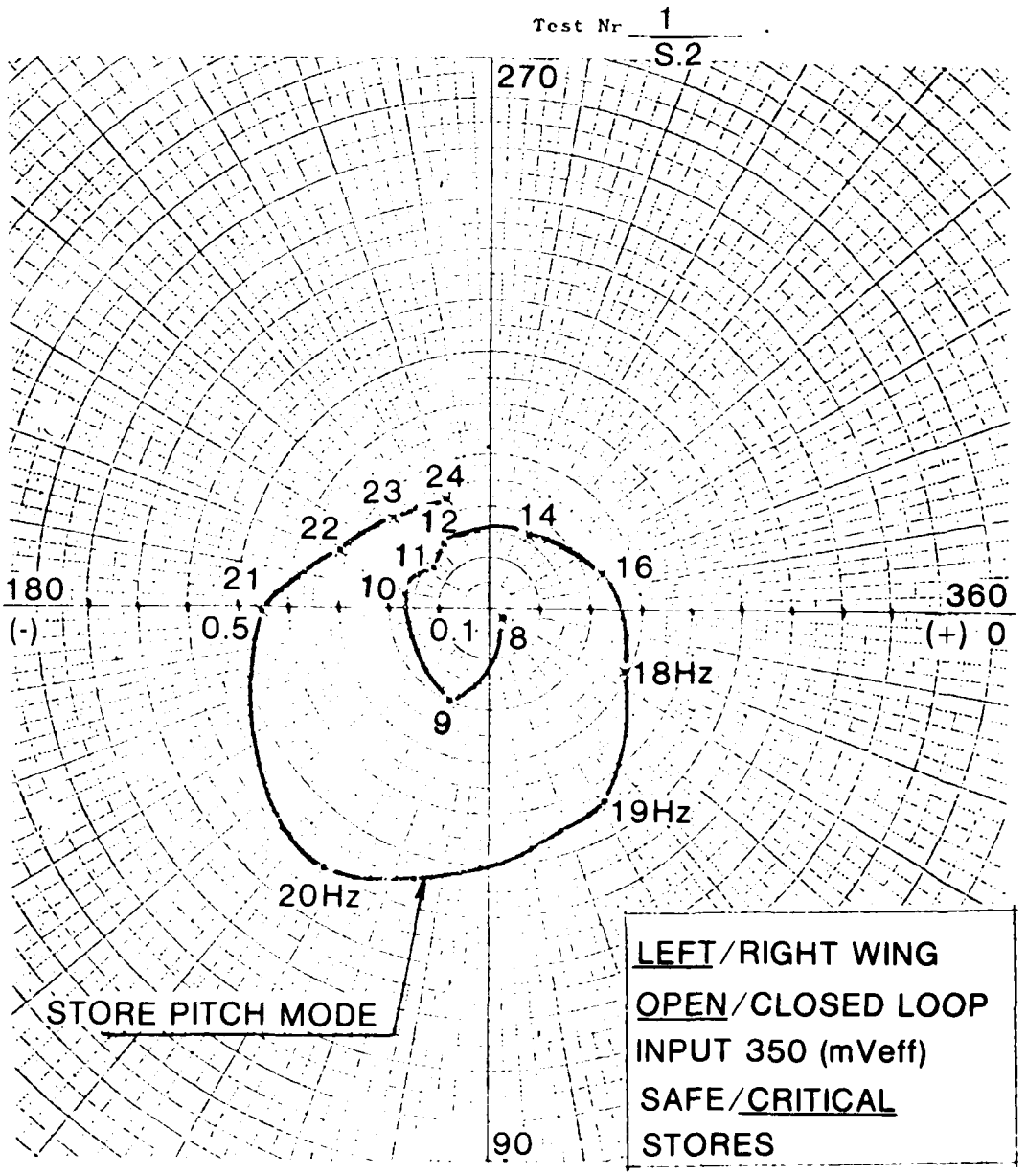


Figure 30. Nyquist Diagram, Structural Mode Coupling Test, Left Wing Store Pitch

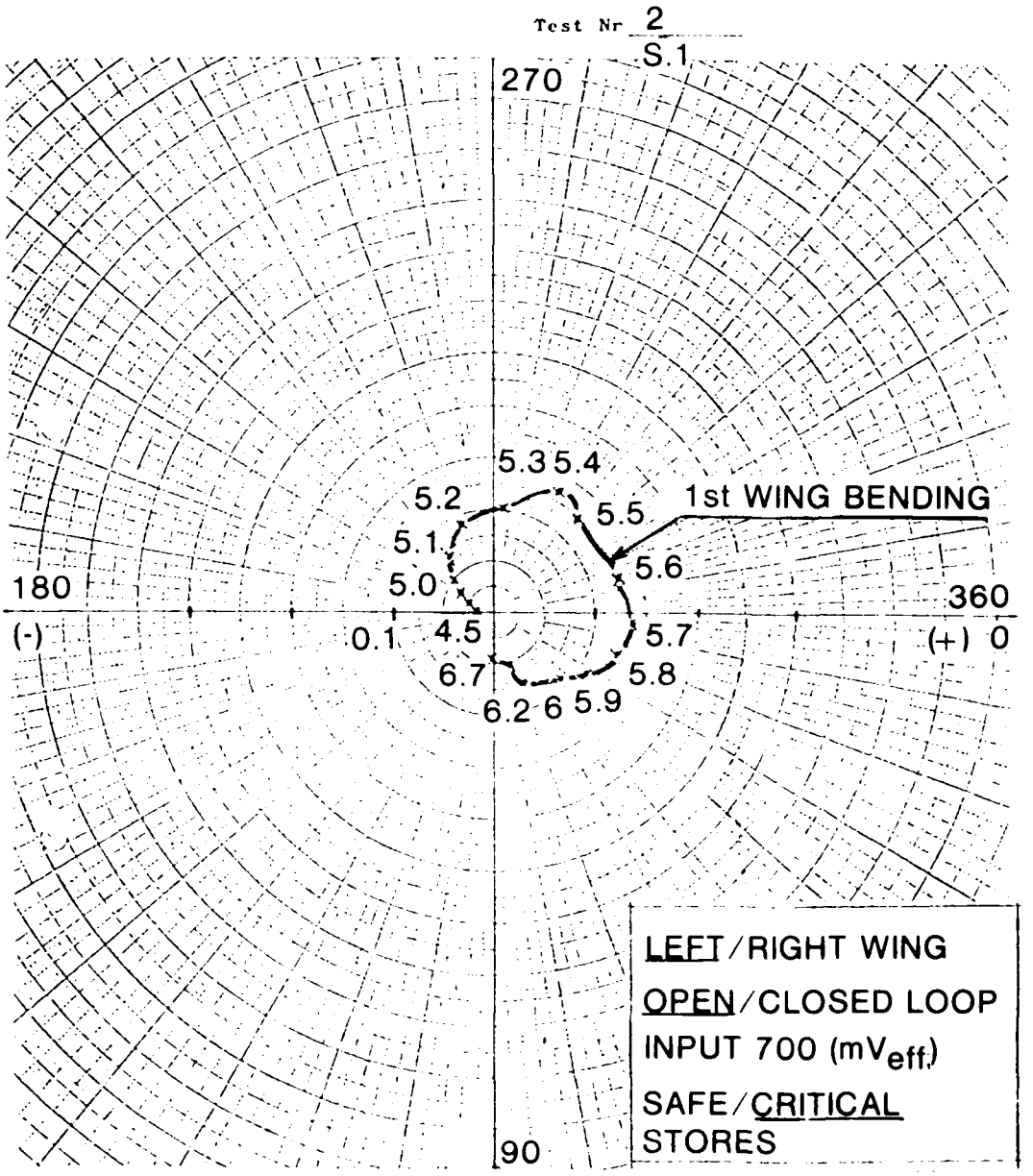


Figure 31. Nyquist Diagram, Structural Mode Coupling Test, Left Wing Bending

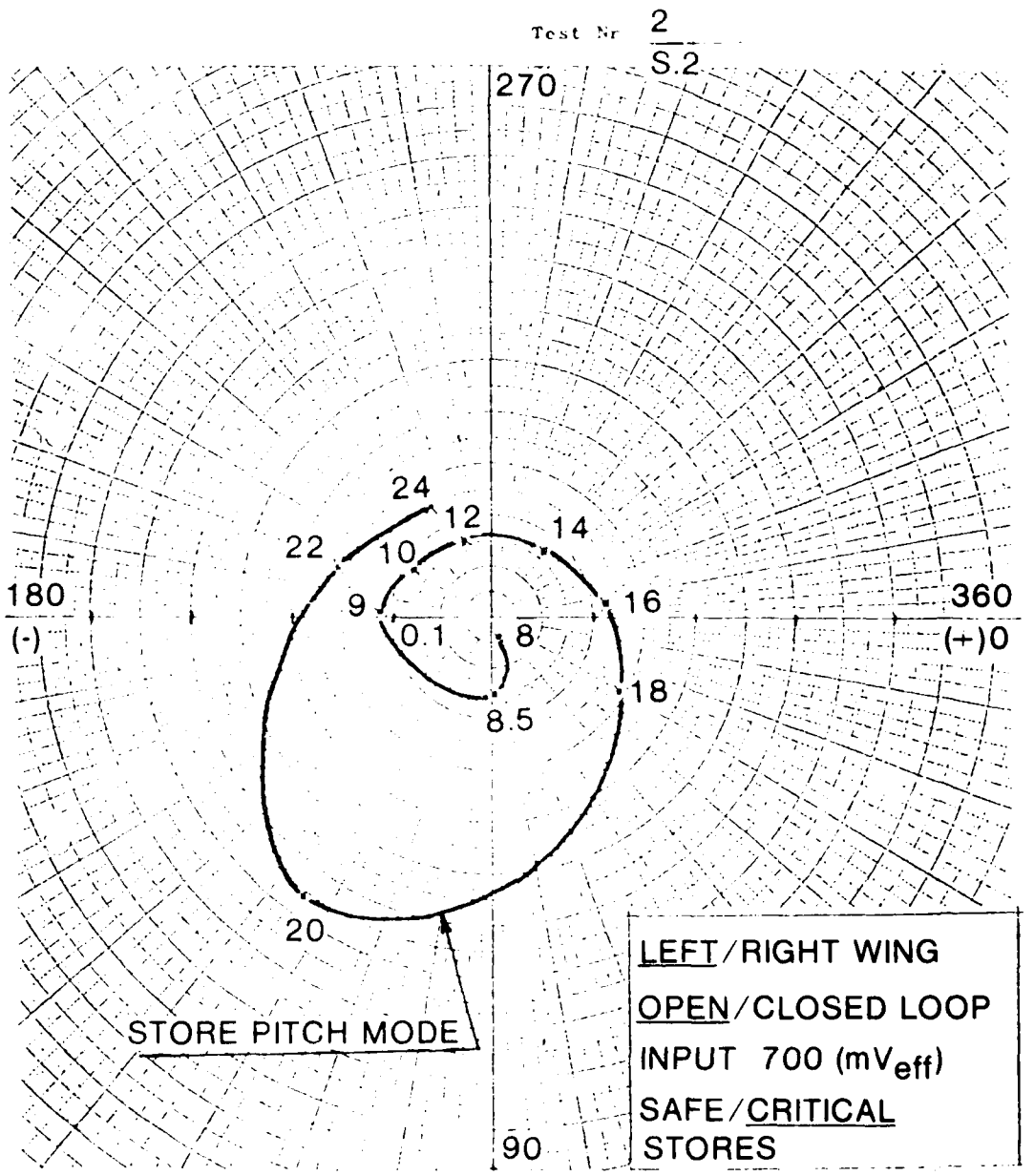


Figure 32. Nyquist Diagram, Structural M de Coupling Test, Left Wing Store Pitch

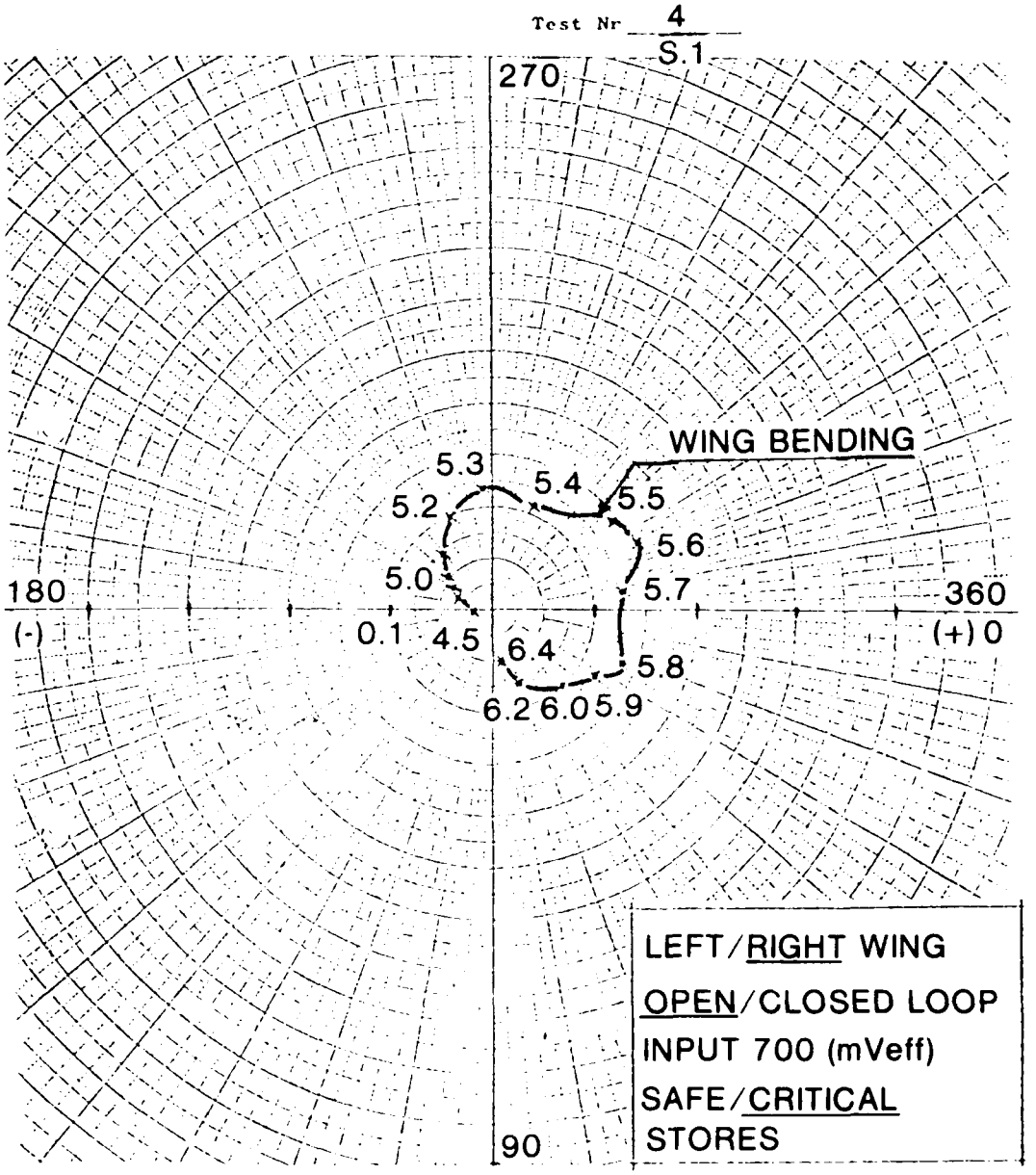


Figure 33. Nyquist Diagram, Structural Mode Coupling Test, Right Wing Bending

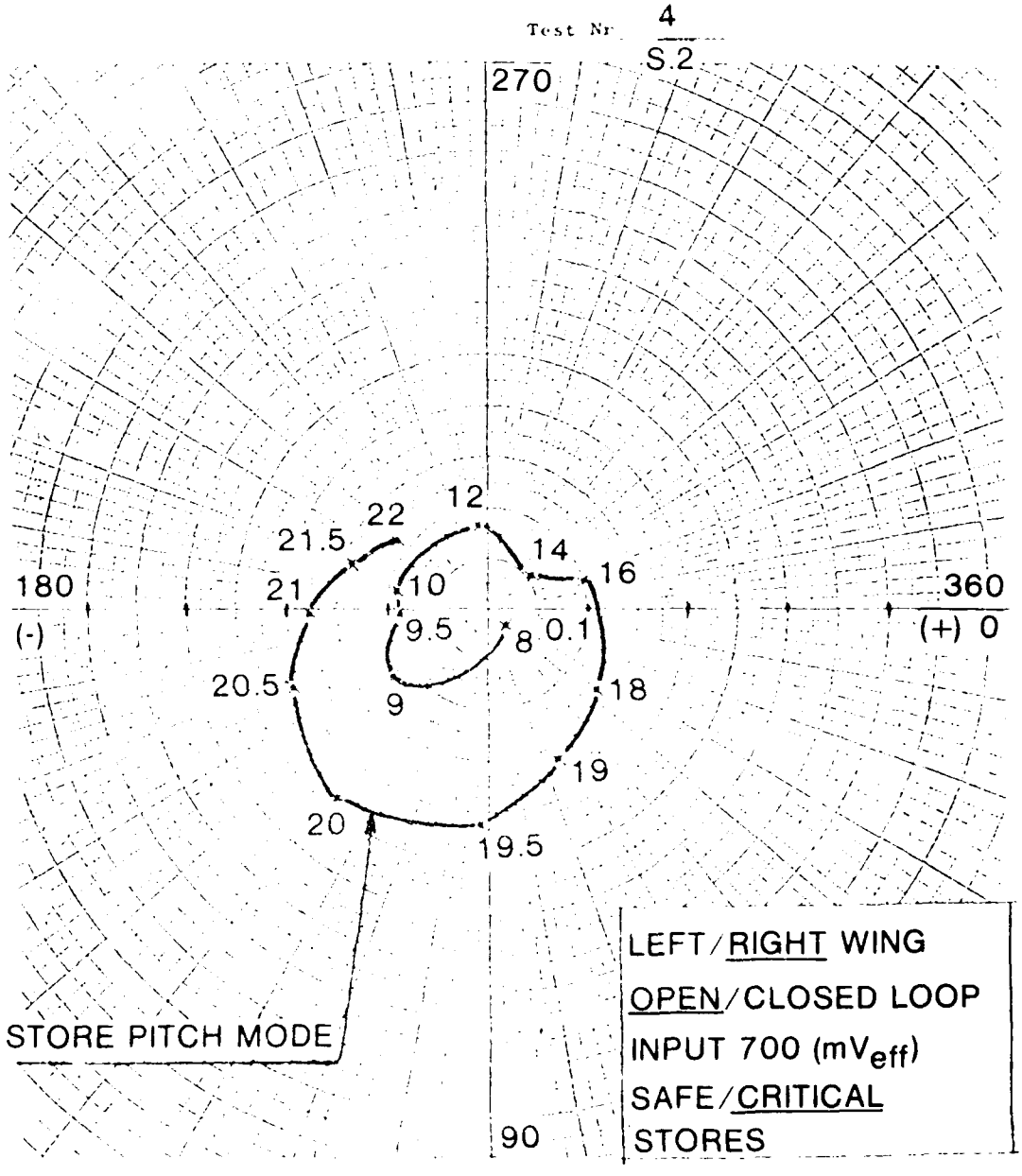


Figure 34. Nyquist Diagram, Structural Mode Coupling Test, Right Wing Store Pitch

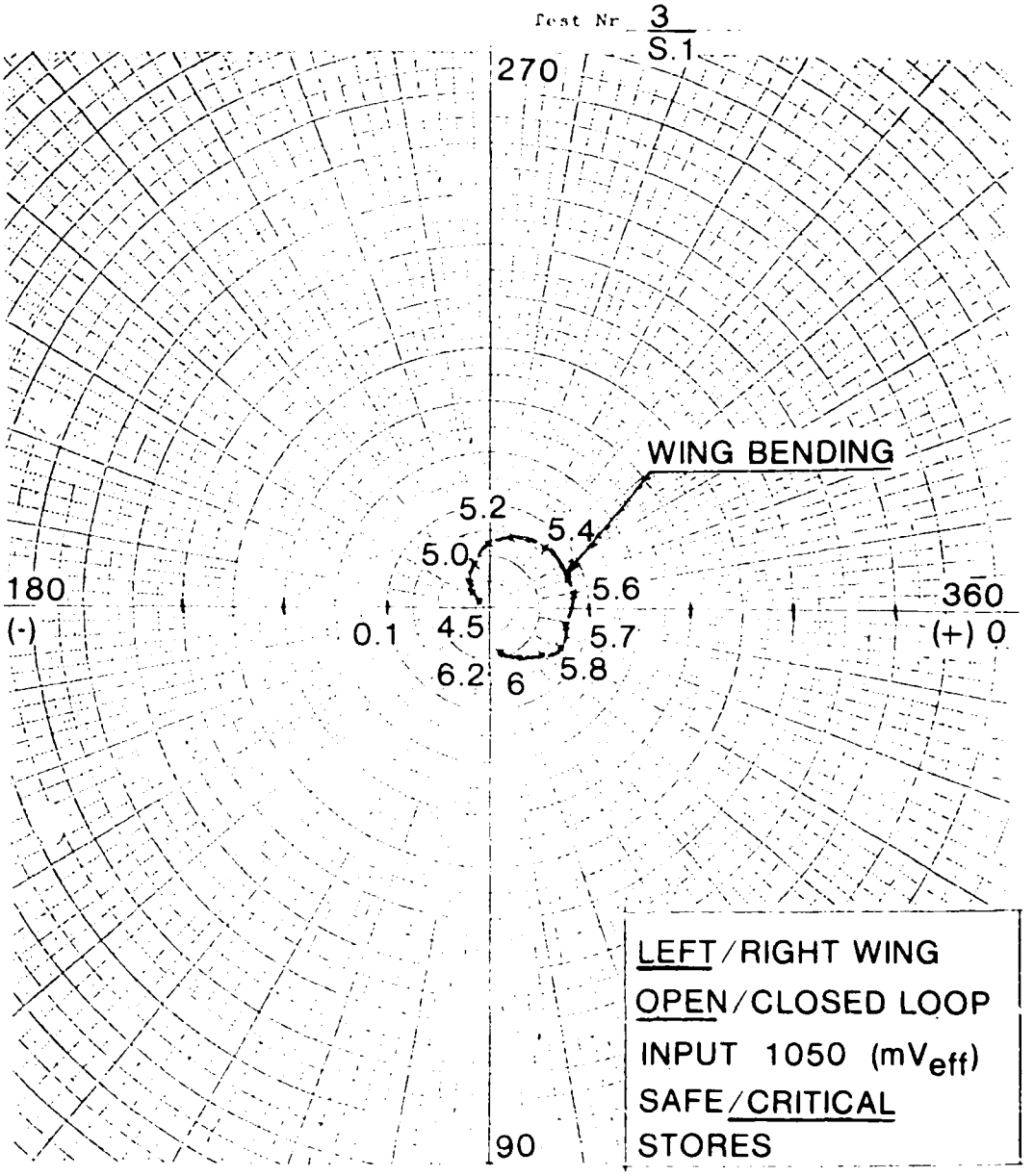


Figure 35. Nyquist Diagram, Structural Mode Coupling Test, Left Wing Bending

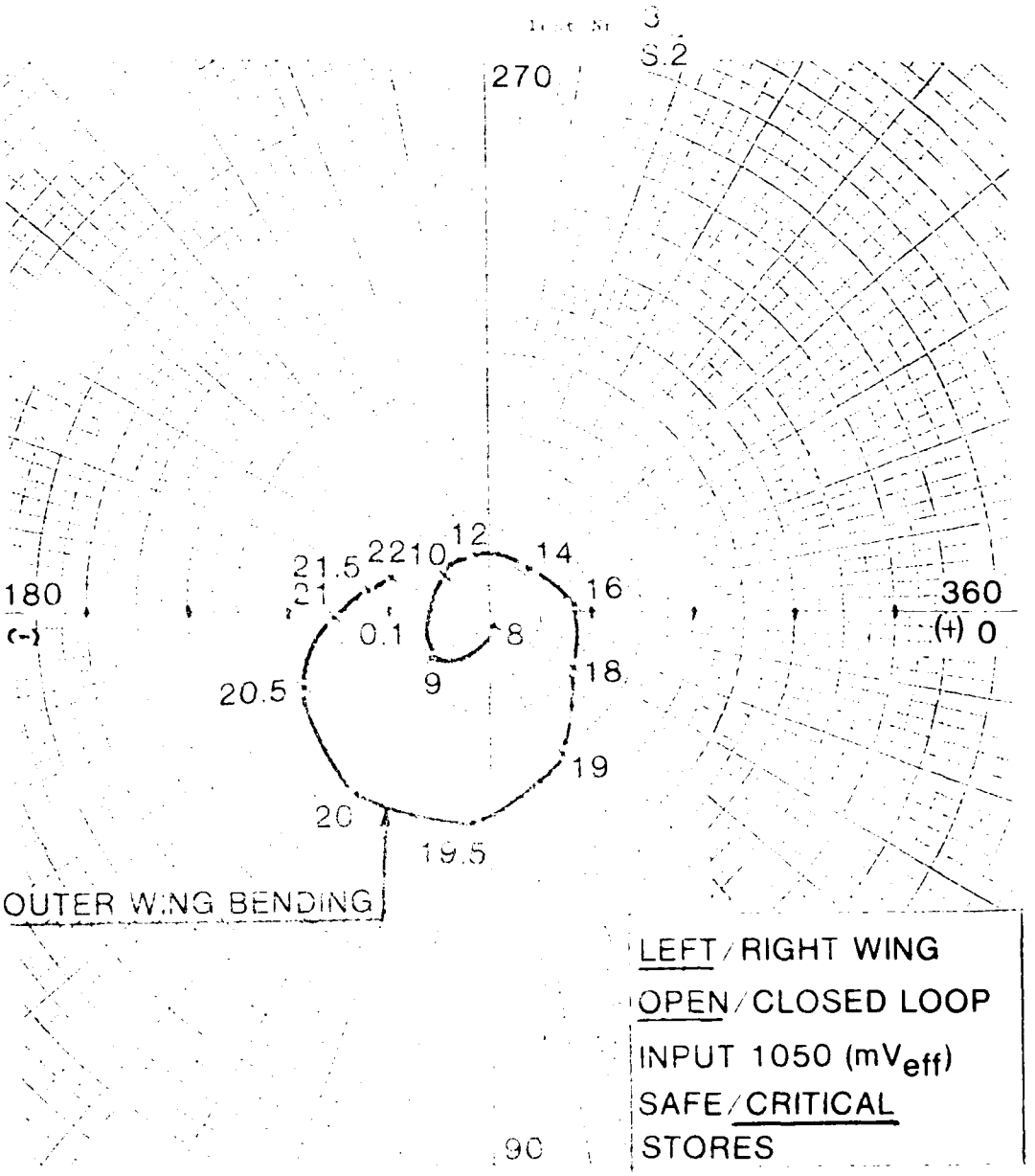


Figure 30. Typical Structural Mode Coupling Test, Outer Wing Bending [illegible]

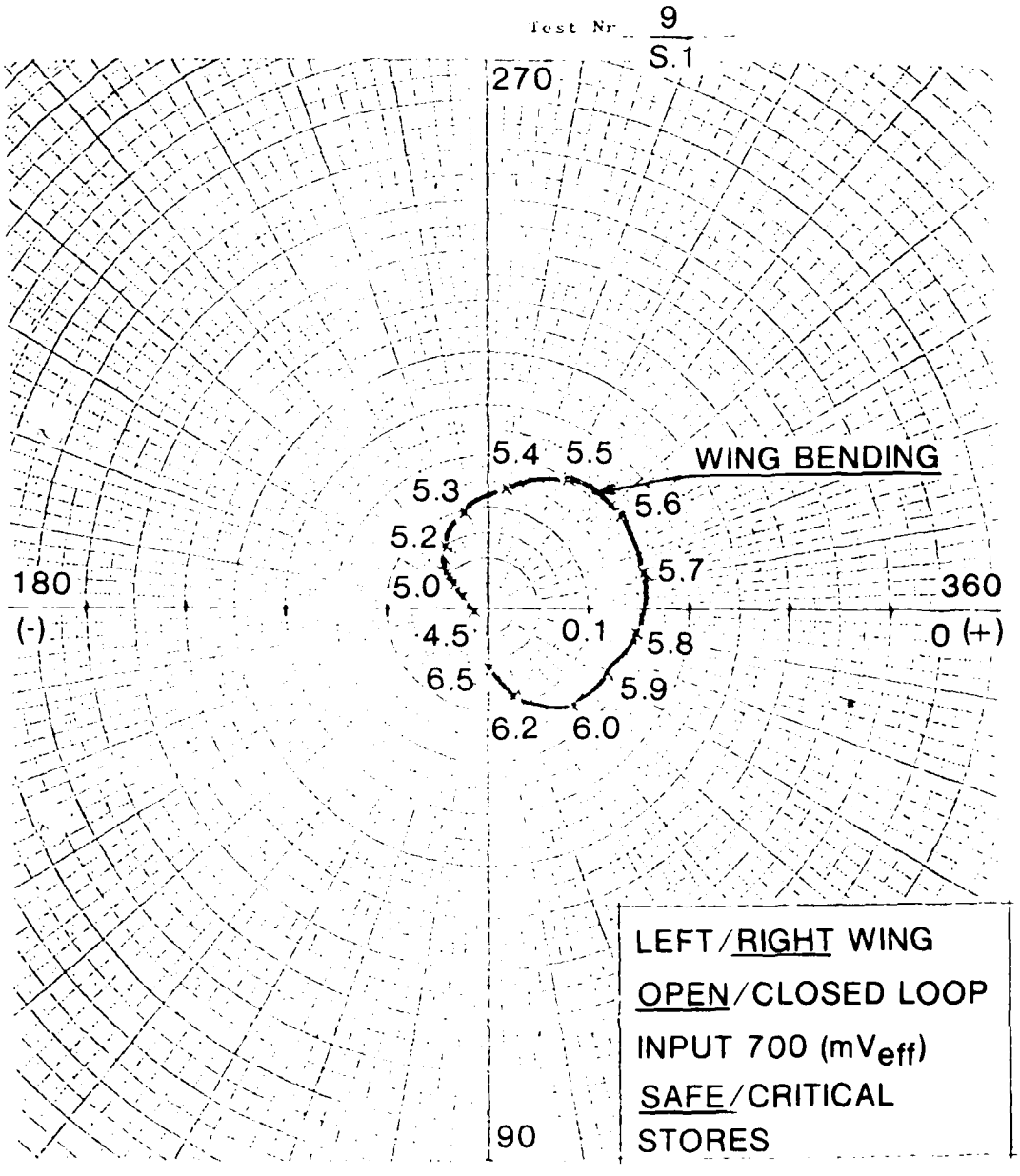


Figure 37. Nyquist Diagram, Structural Mode Coupling Test, Right Wing Bending

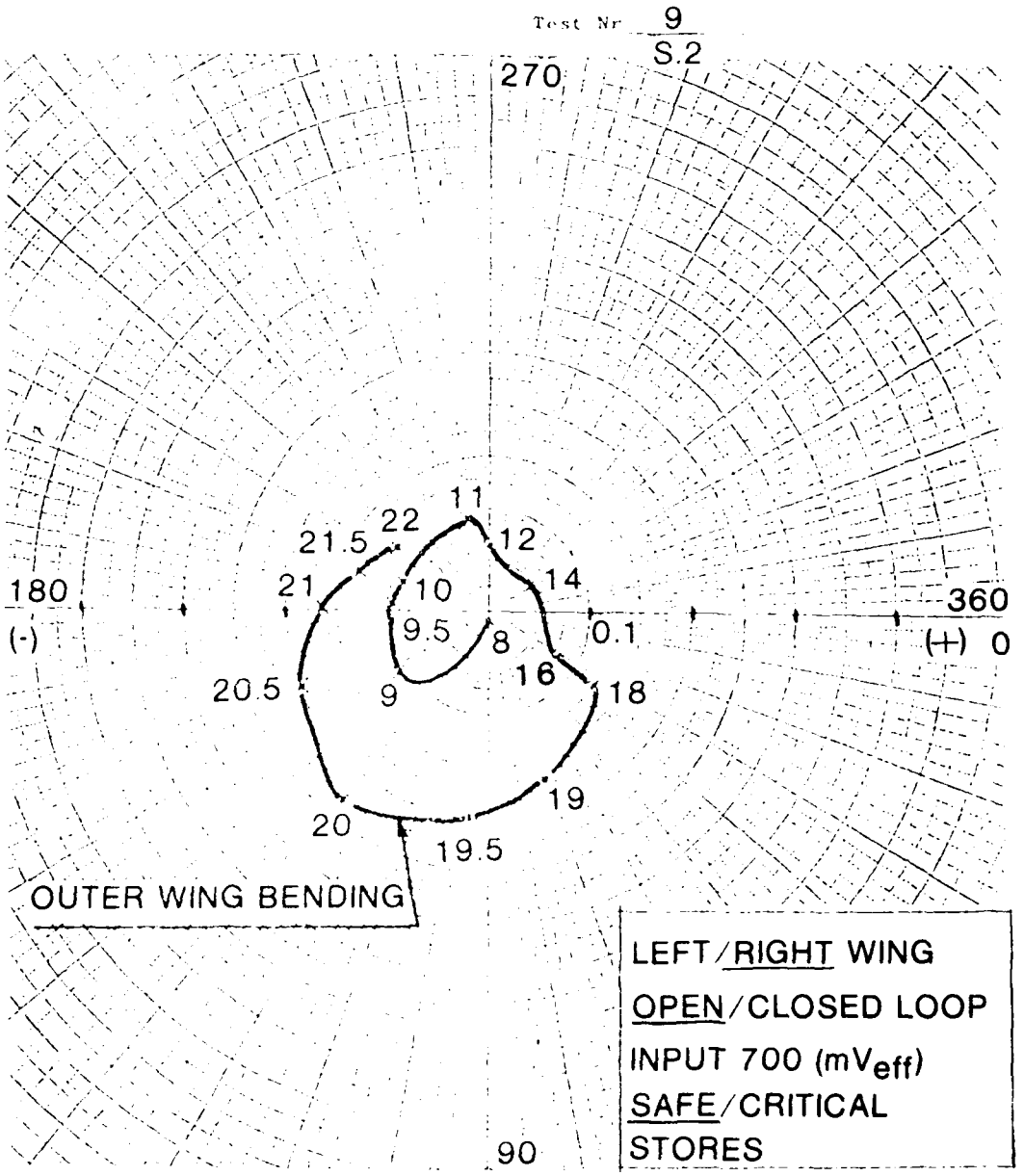


Figure 38. Nyquist Diagram, Structural Mode Coupling Test, Outer Wing Bending (Right)

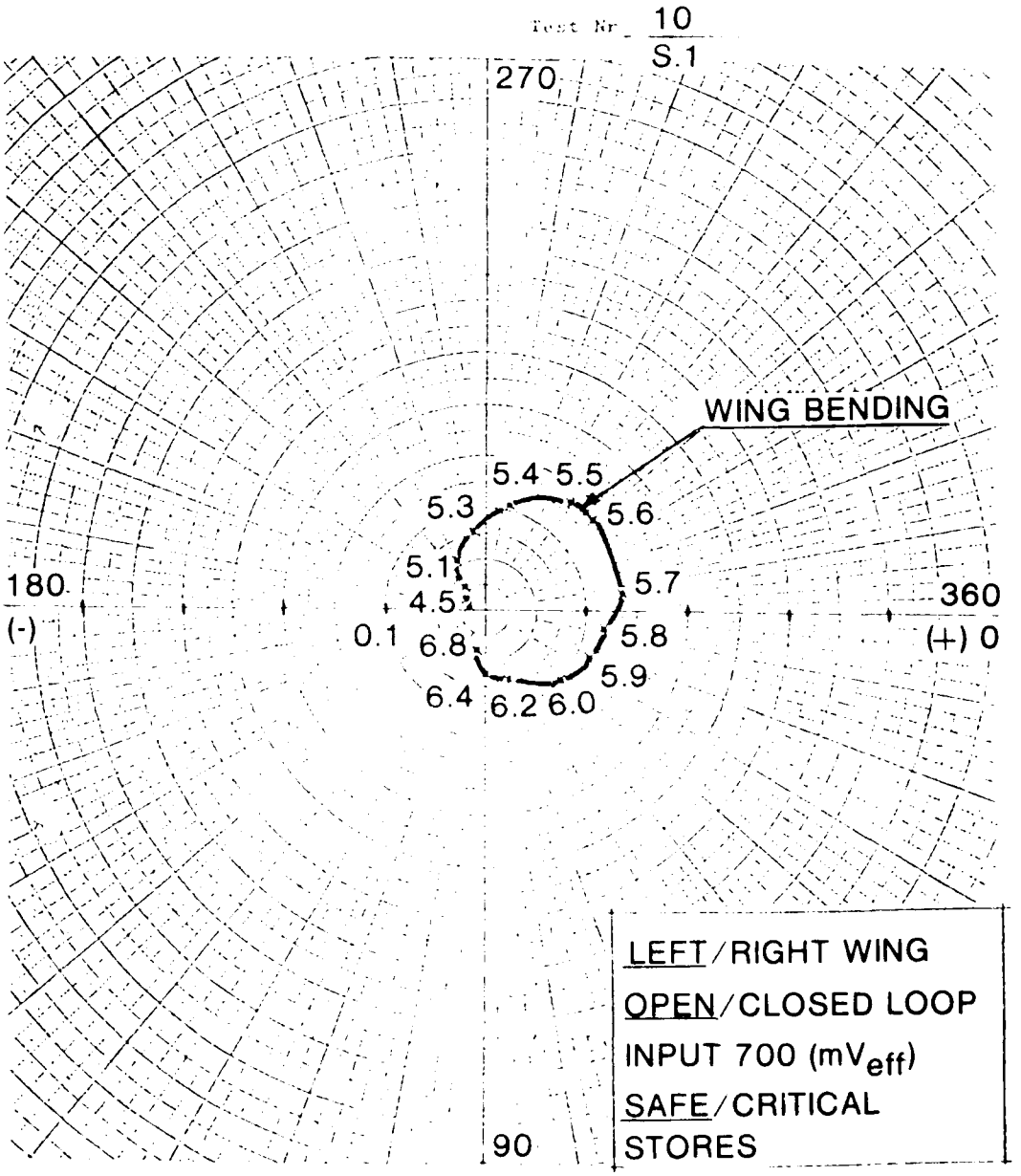


Figure 39. Nyquist Diagram, Structural Mode Coupling Test, Left Wing Bending

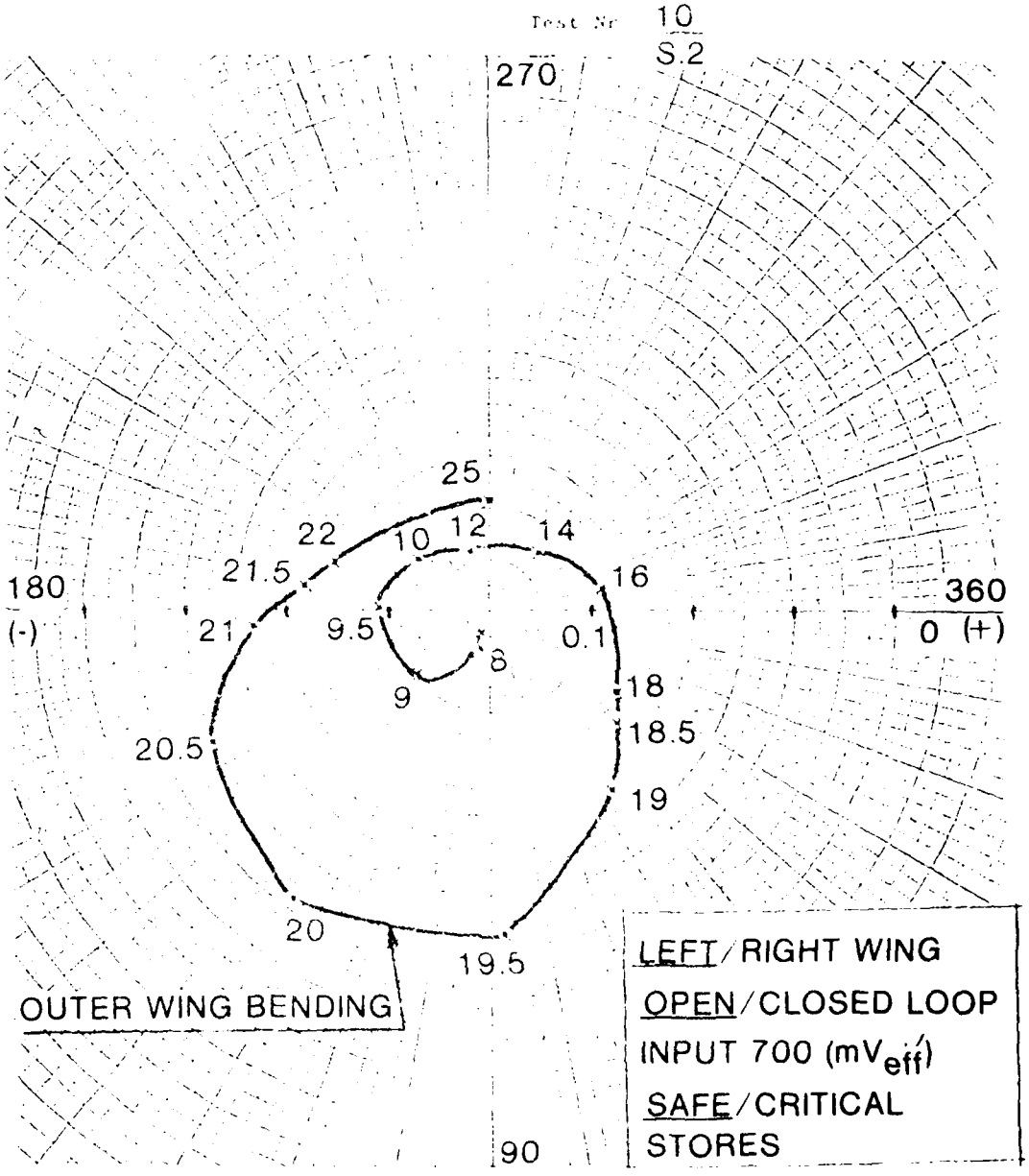


Figure 40. Nyquist Diagram, Structural Mode Coupling Test, Outer Wing Bending (Left)

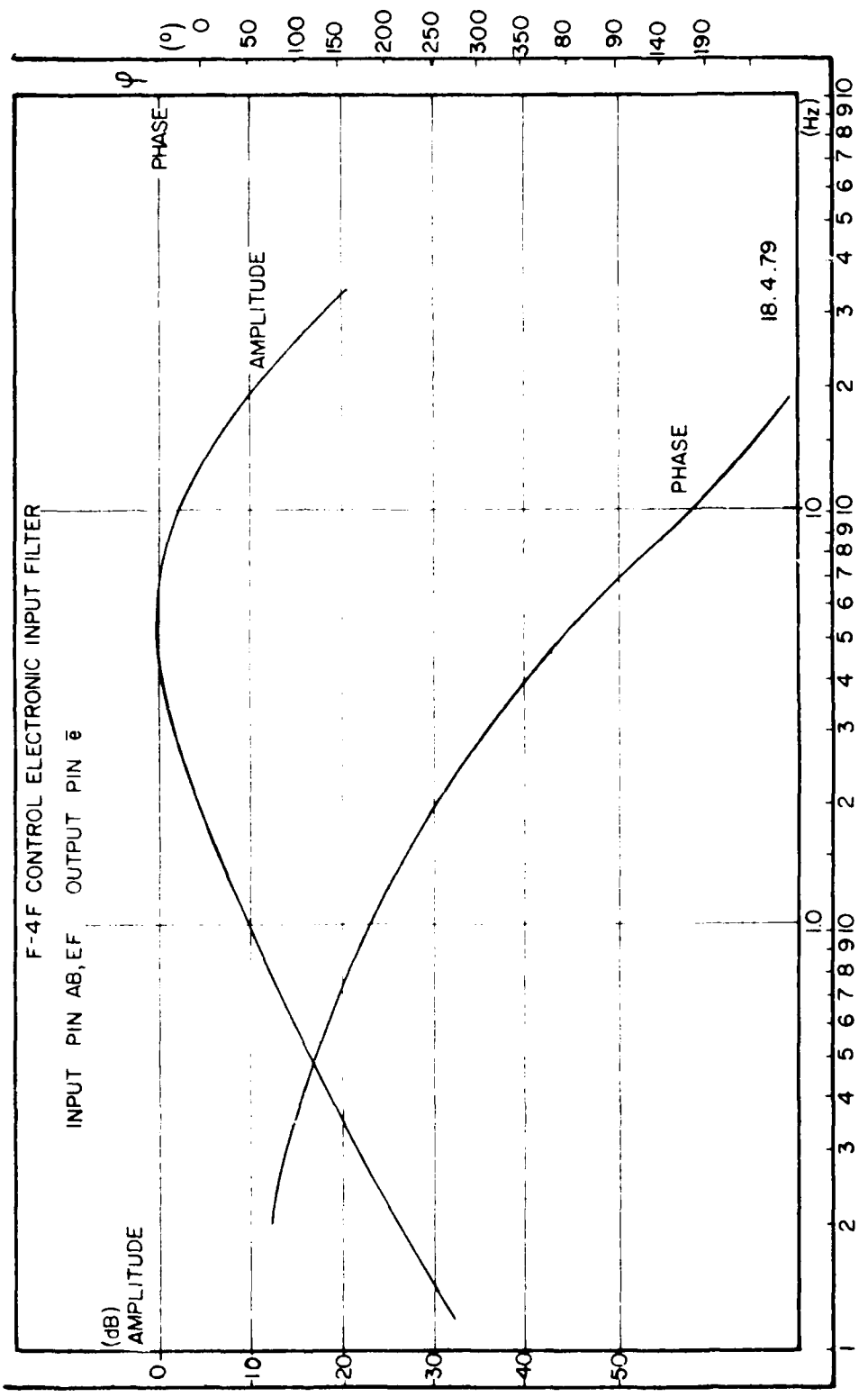


Figure 41. Transfer Function of the Control Electronics

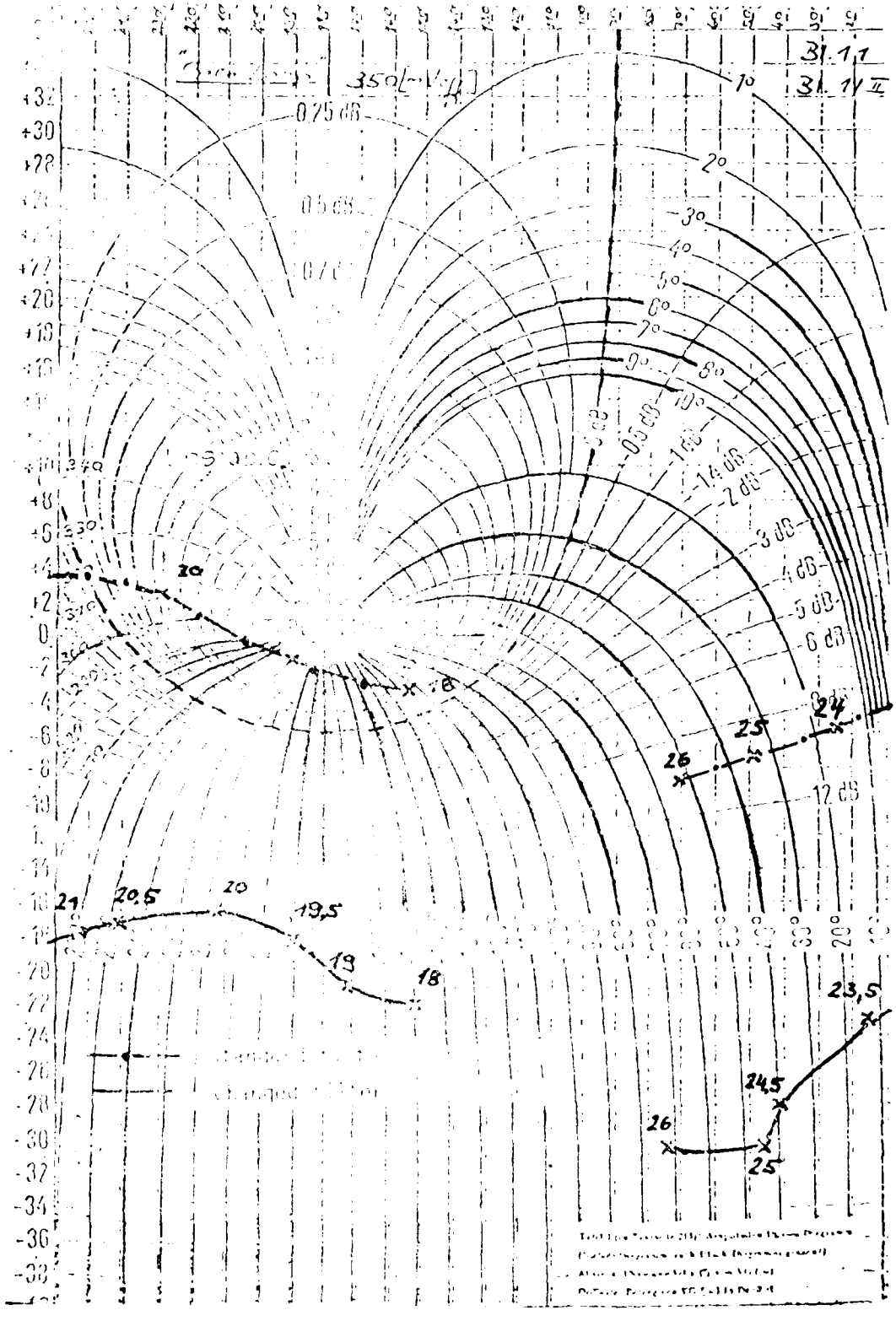


Figure 4-. Acoustic Scanner, Structural Mode Coupling Test, Store Pitch

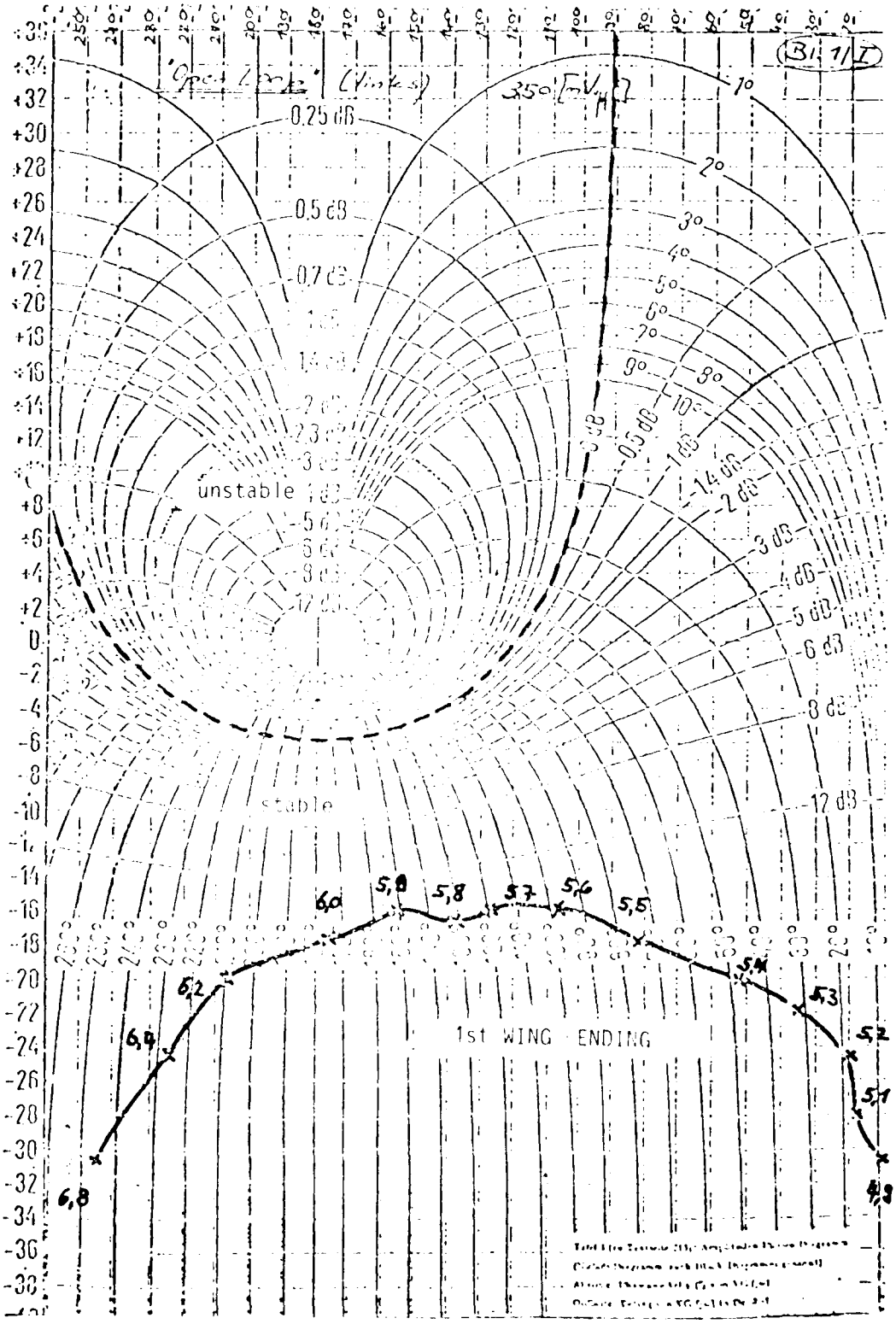


Figure 43. Nichols Diagram, Structural Coupling Test, First Wing Bending

AILERON WITH NW HIGH GAIN POWER ACTUATOR
LINEARITY CHECK AT 5.6 Hz

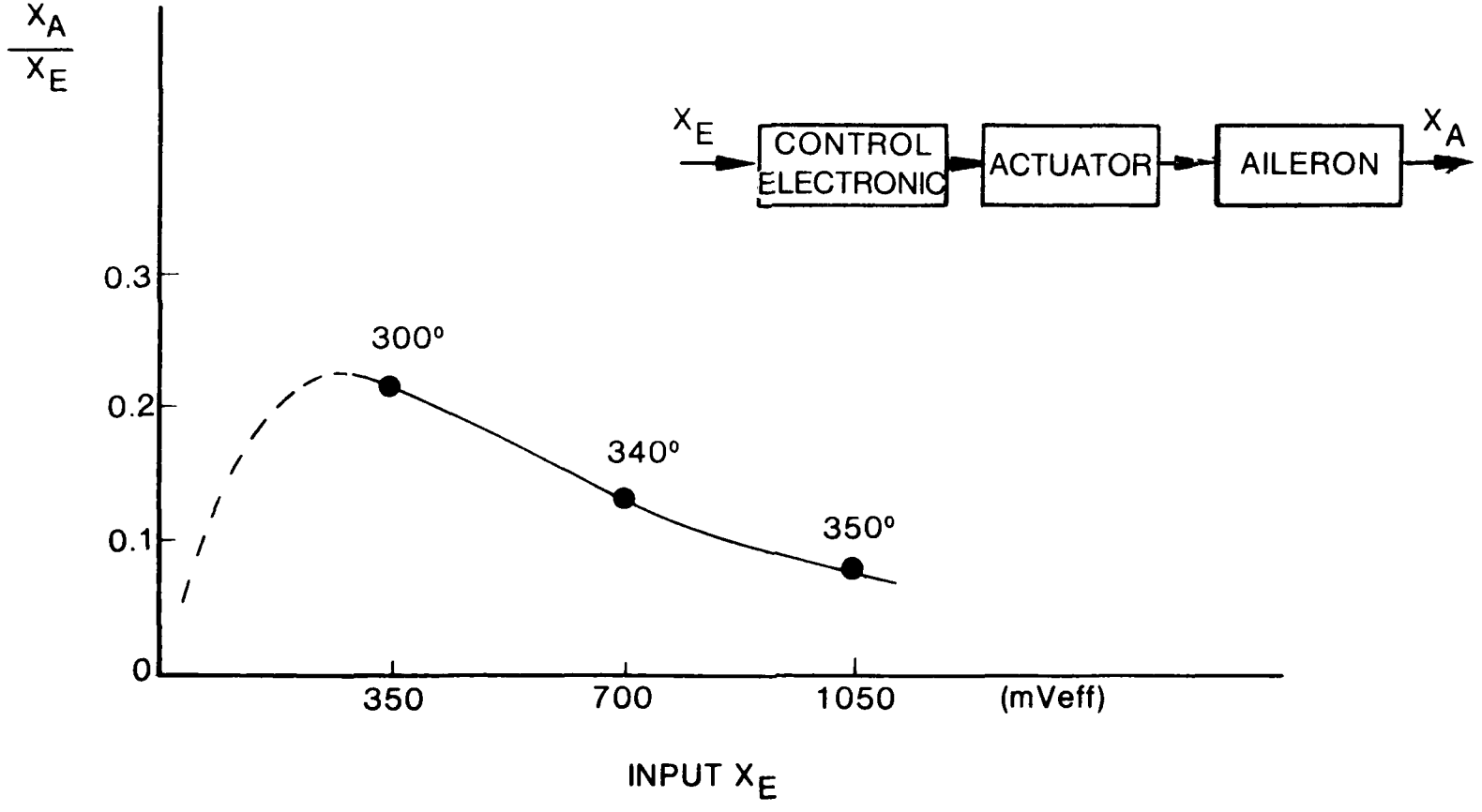


Figure 44. Effect of Non-Linearities in the Aileron Actuating System

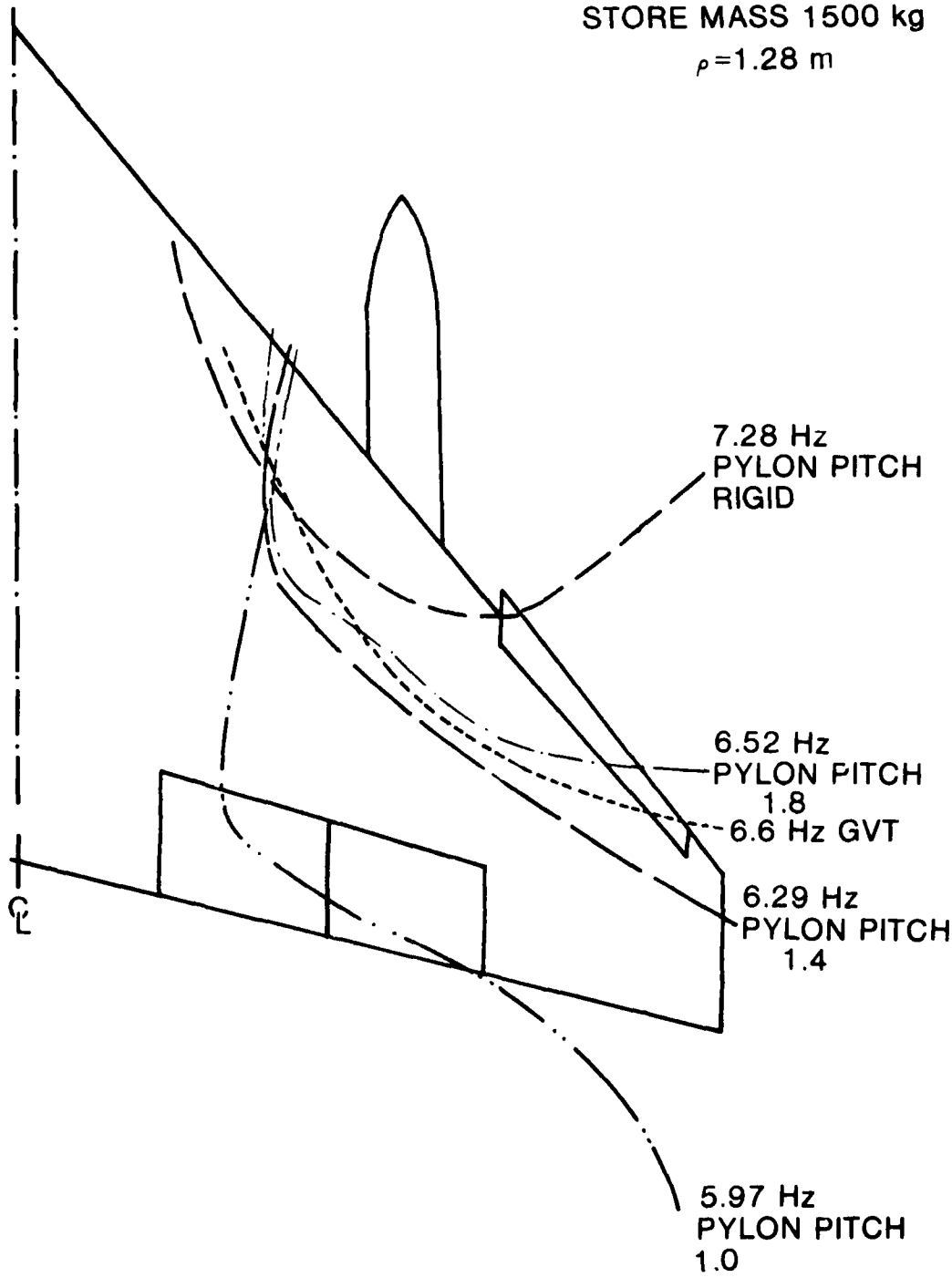


Figure 45. Shift of the Node Line for the Store Pitch Mode Due to Variations of the Pylon Pitch Stiffness

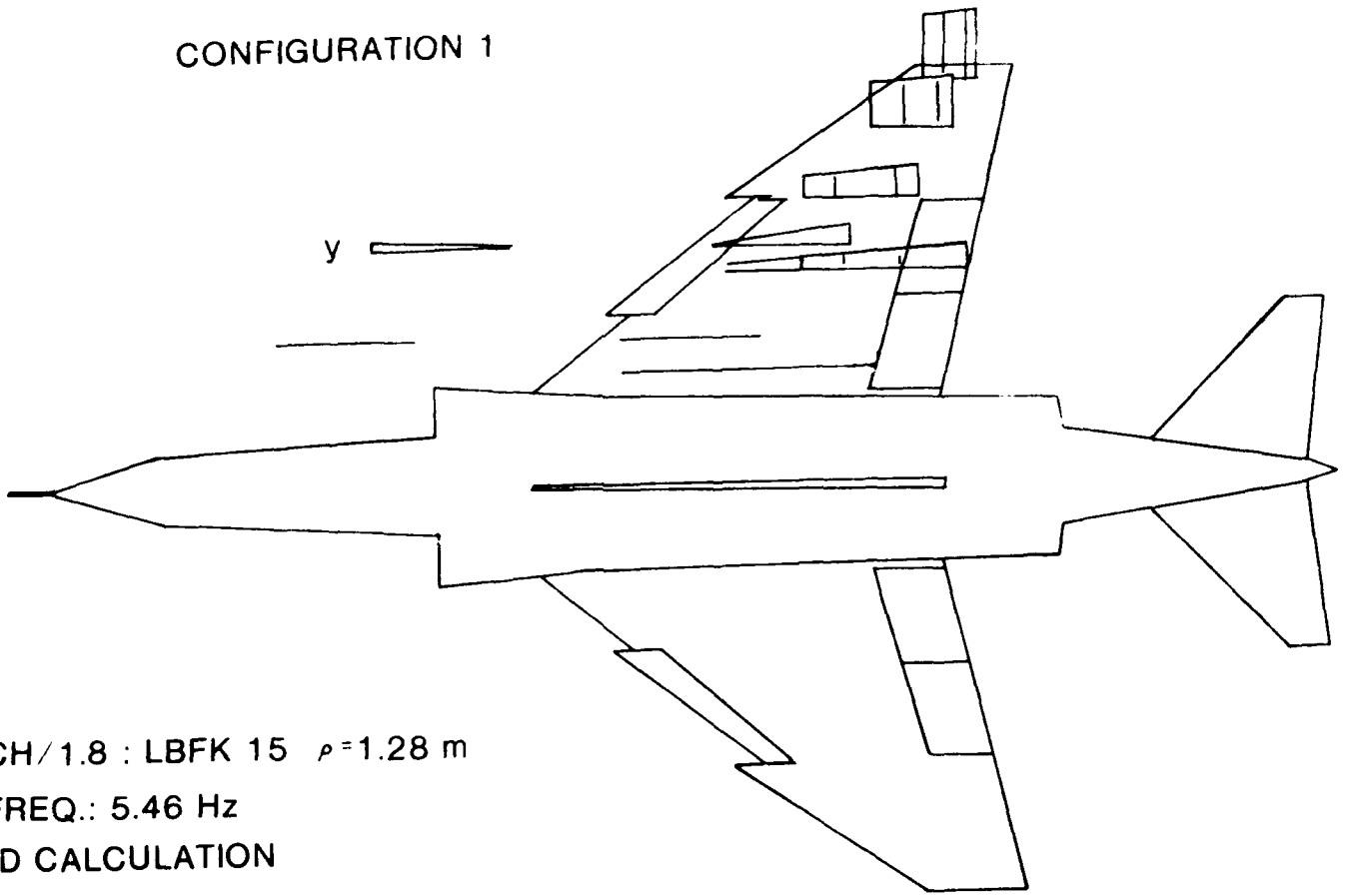


Figure 46. Calculated 1st Wing Bending with Adjusted Pylon Pitch Stiffness

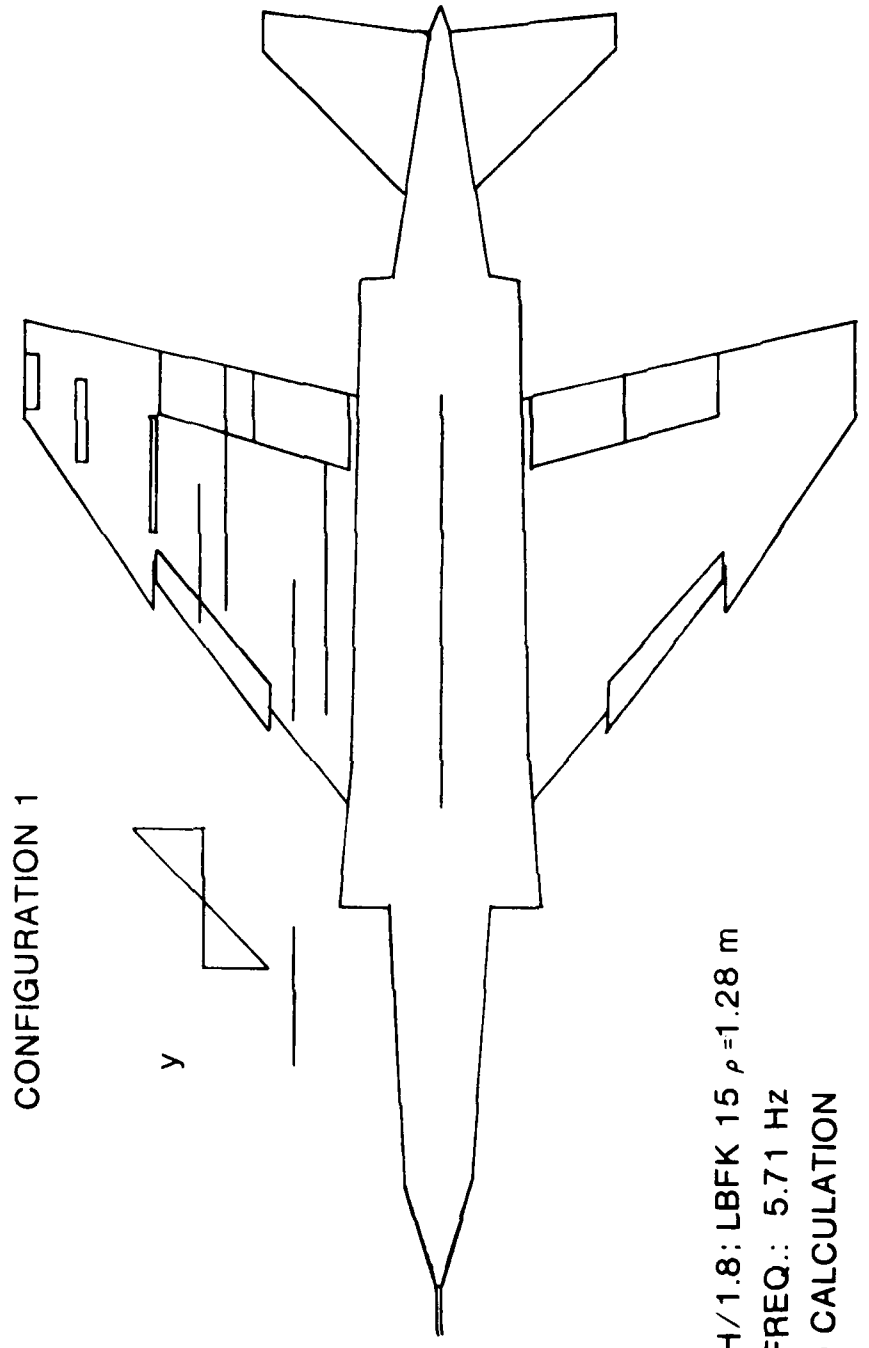


Figure 47. Calculated Store Yaw Mode with Adjusted Pylon Pitch Stiffness

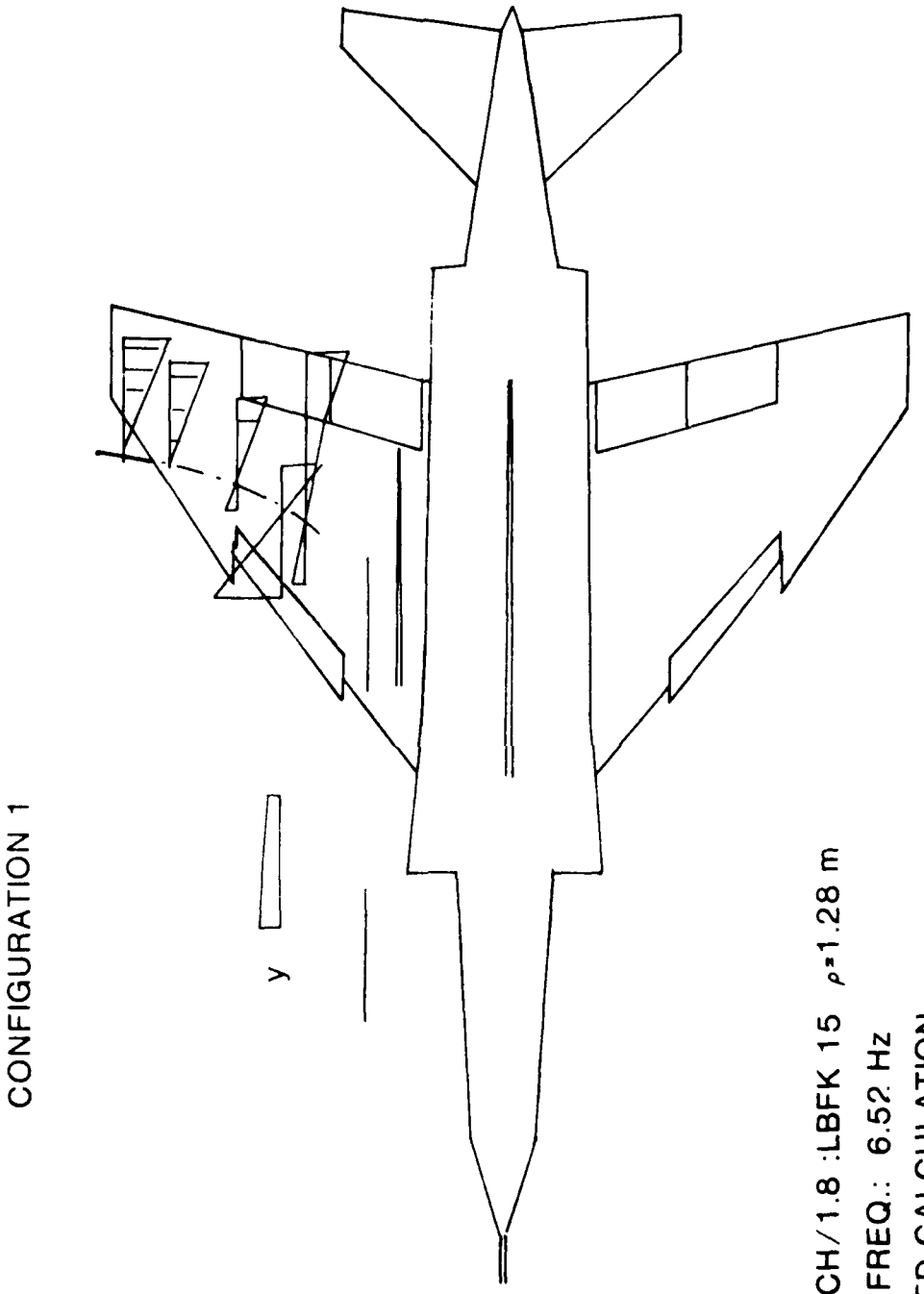


Figure 48. Calculated Store Pitch Mode with Adjusted Pylon Pitch Stiffness

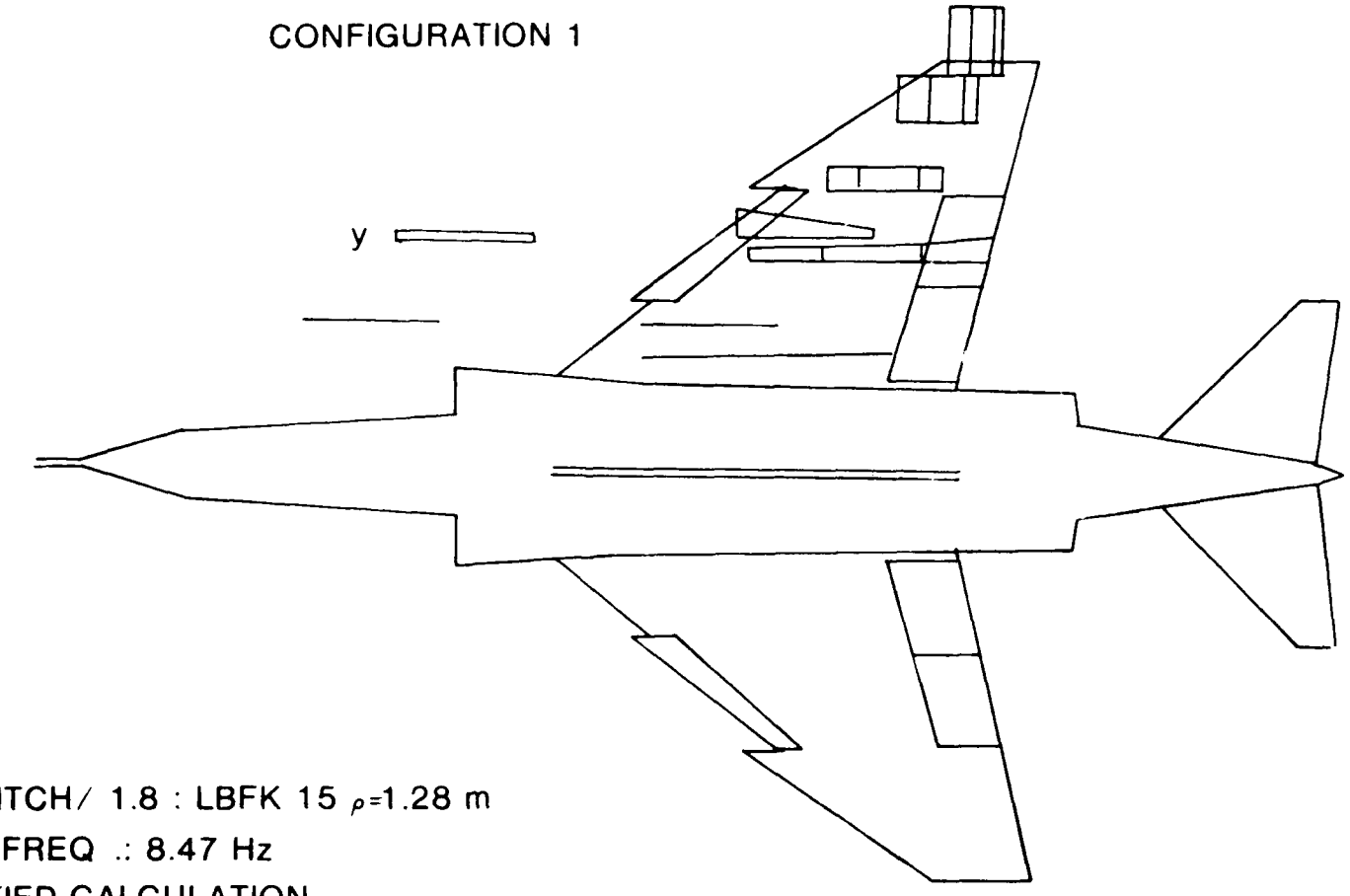


Figure 49. Calculated Store Roll Mode with Adjusted Pylon Pitch Stiffness

AD-A131 402 DEVELOPMENT AND FLIGHT TEST OF AN ACTIVE FLUTTER SUPPRESSION SYSTEM FOR T..(U) AIR FORCE WRIGHT AERONAUTICAL LABS WRIGHT-PATTERSON AFB OH

2/2

UNCLASSIFIED H HOENLINGER ET AL. APR 83 F/G 20/4 NL

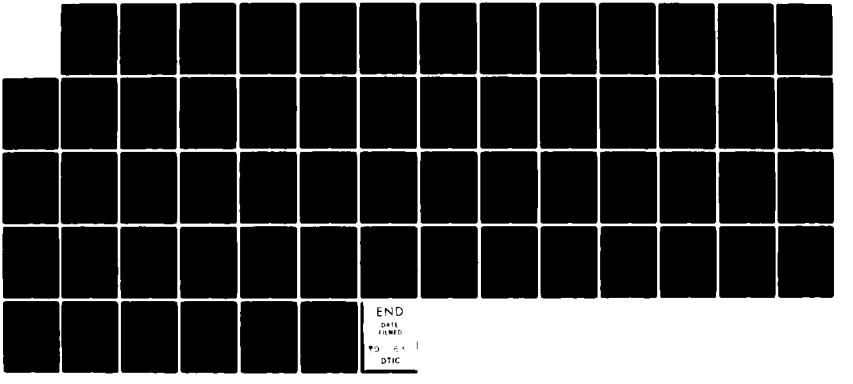

END

DATE FILMED

DTIC

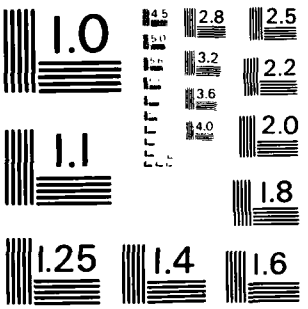

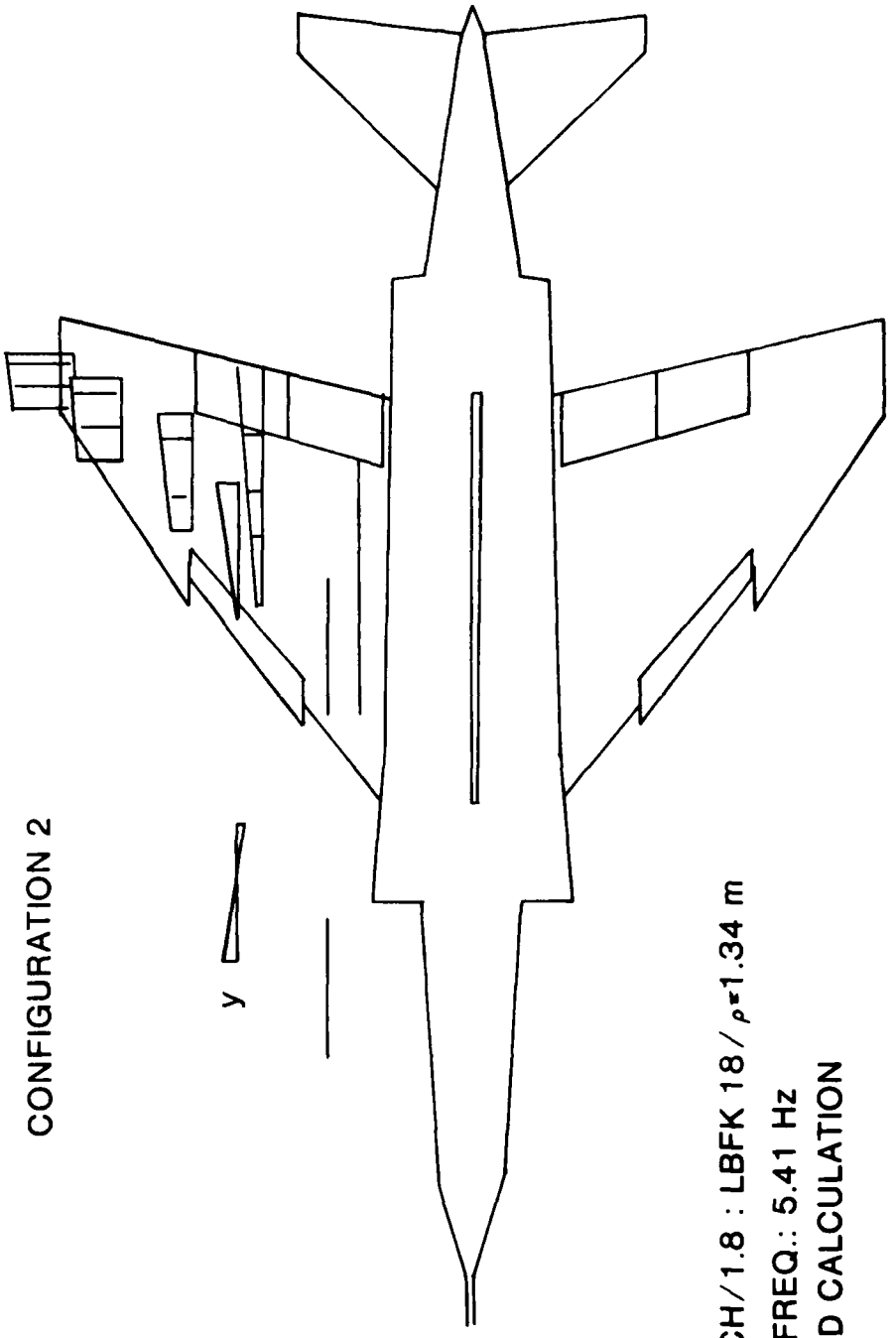


Figure 50. Calculated 1st Wing Bending with Adjusted Pylon Pitch Stiffness

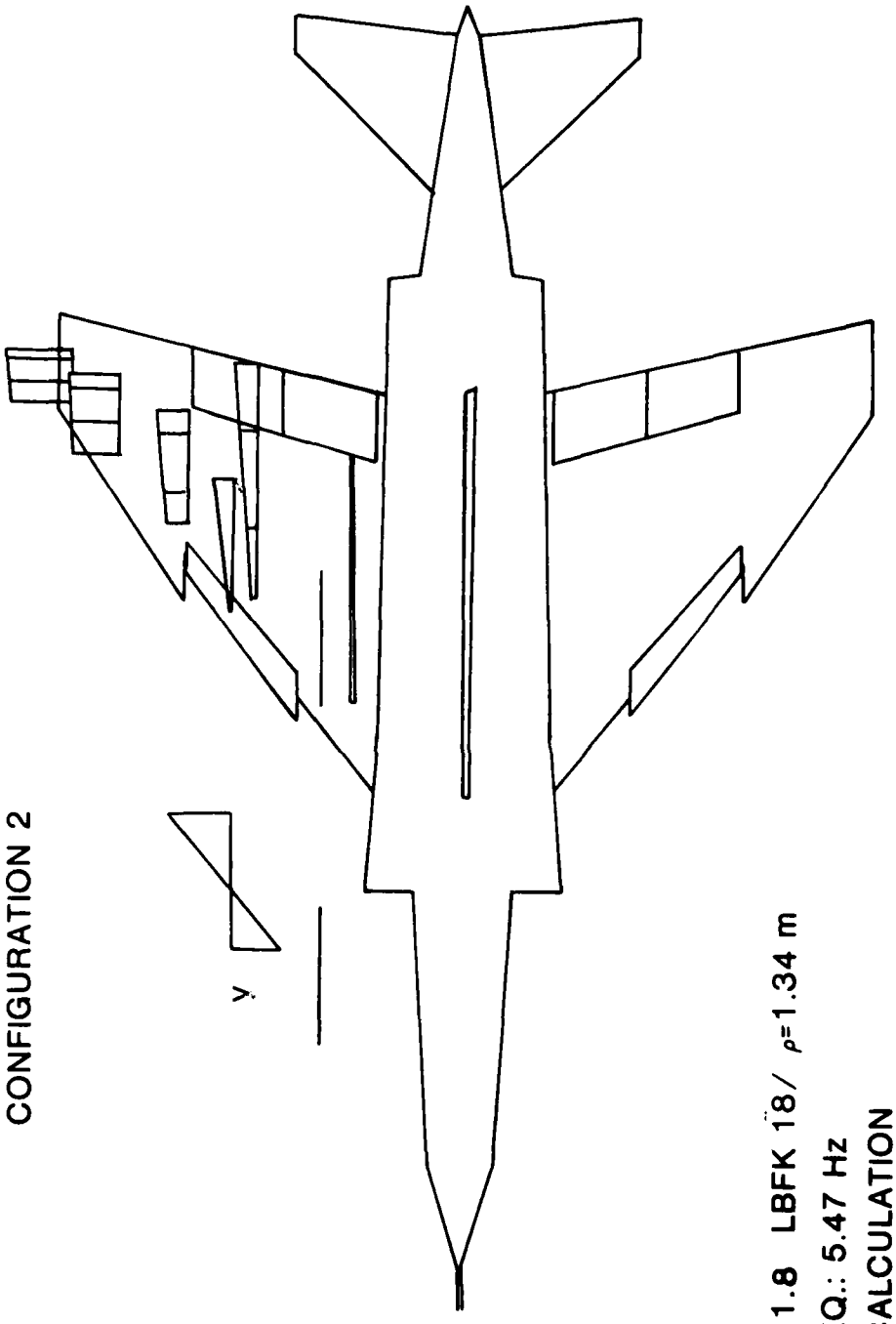


Figure 51. Calculated Store Yaw Mode with Adjusted Pylon Pitch Stiffness

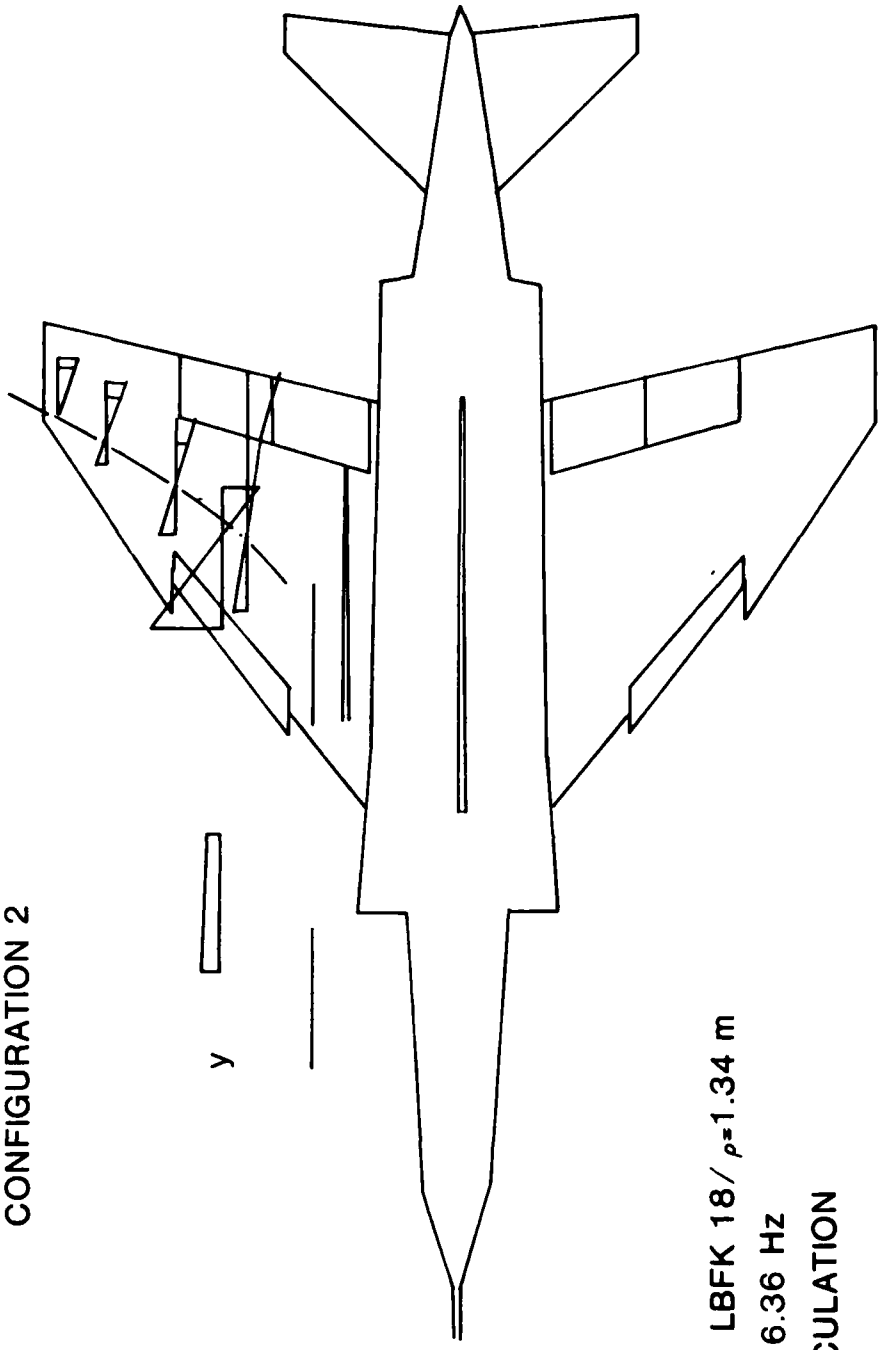


Figure 52. Calculated Store Pitch Mode with Adjusted Pylon Pitch Stiffness

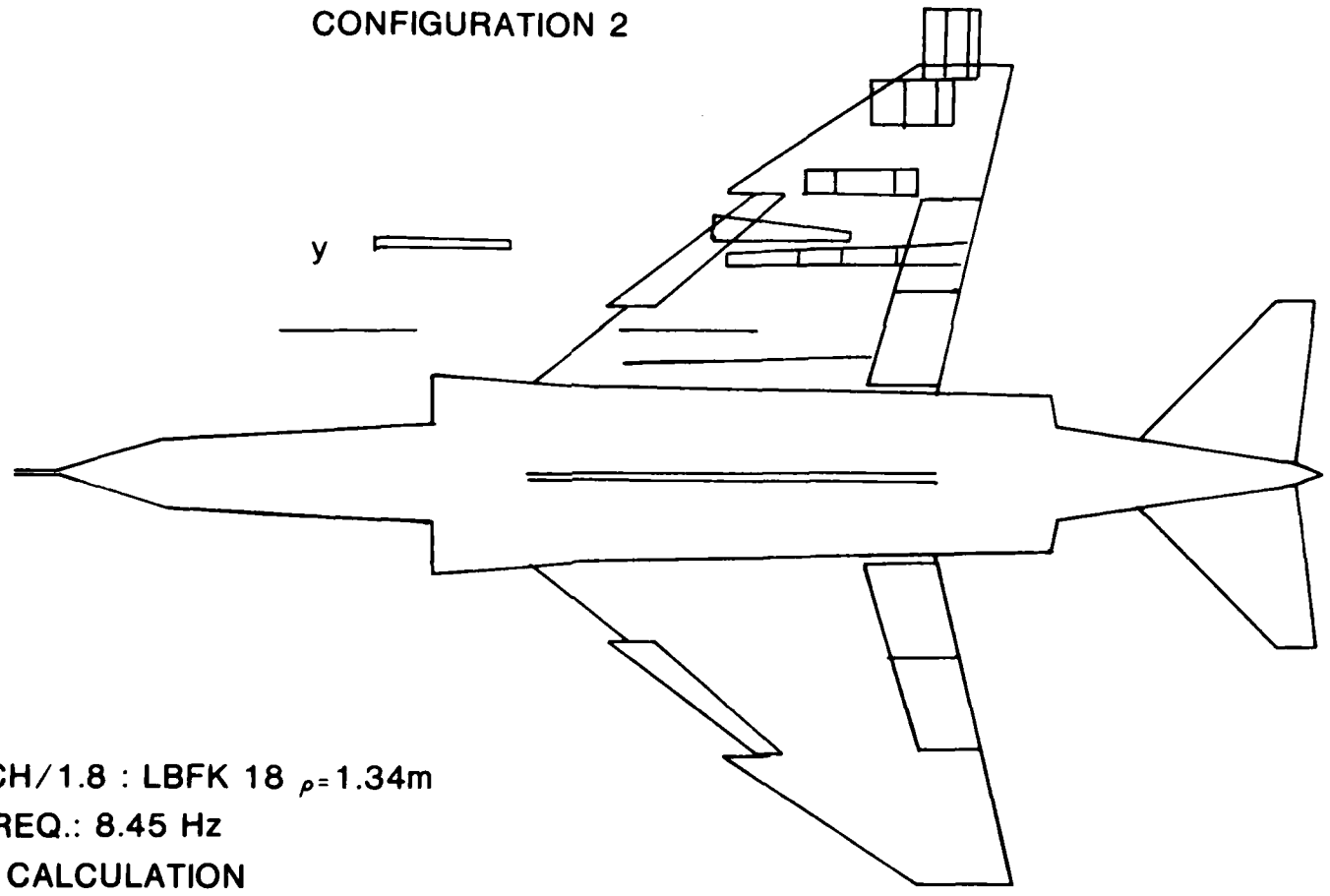


Figure 53. Calculated Store Roll Mode with Adjusted Pylon Pitch Stiffness

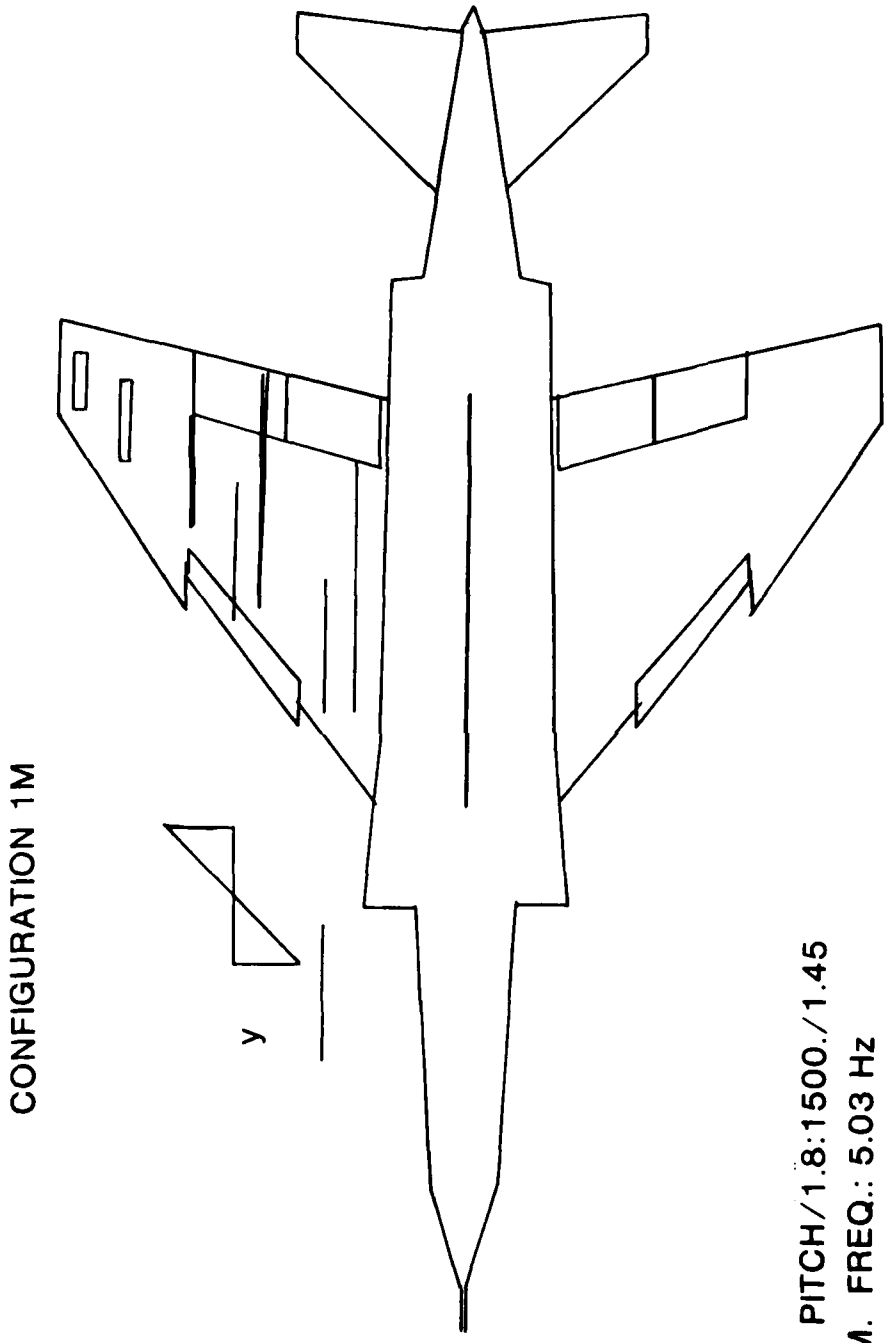


Figure 54. Calculated Store Yaw Mode with Modified Store Radius of Gyration and Adjusted Pylon Pitch Stiffness

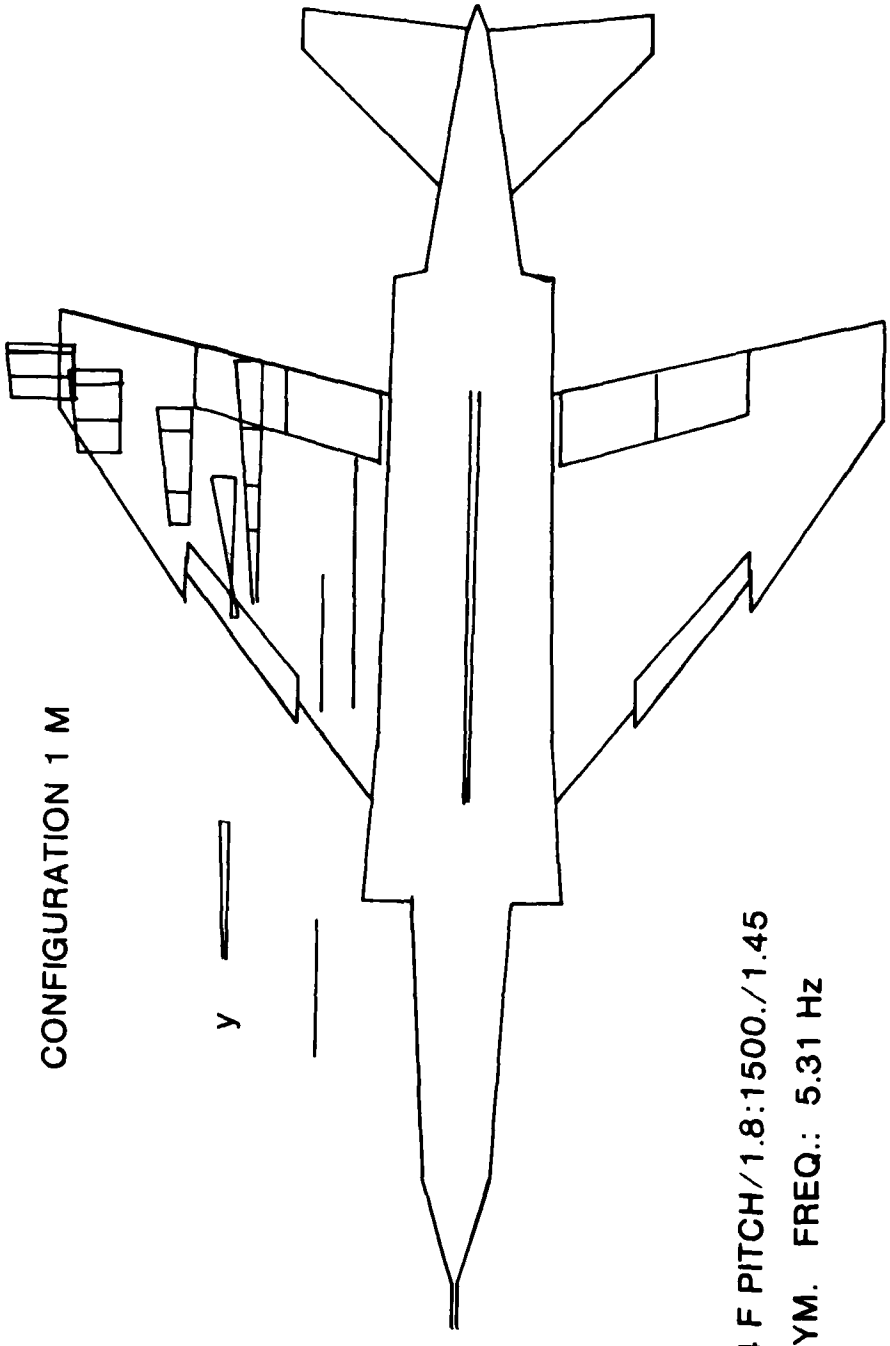


Figure 55. Calculated 1st Wing Bending Mode with Modified Store Radius of Gyration and Adjusted Pylon Pitch Stiffness

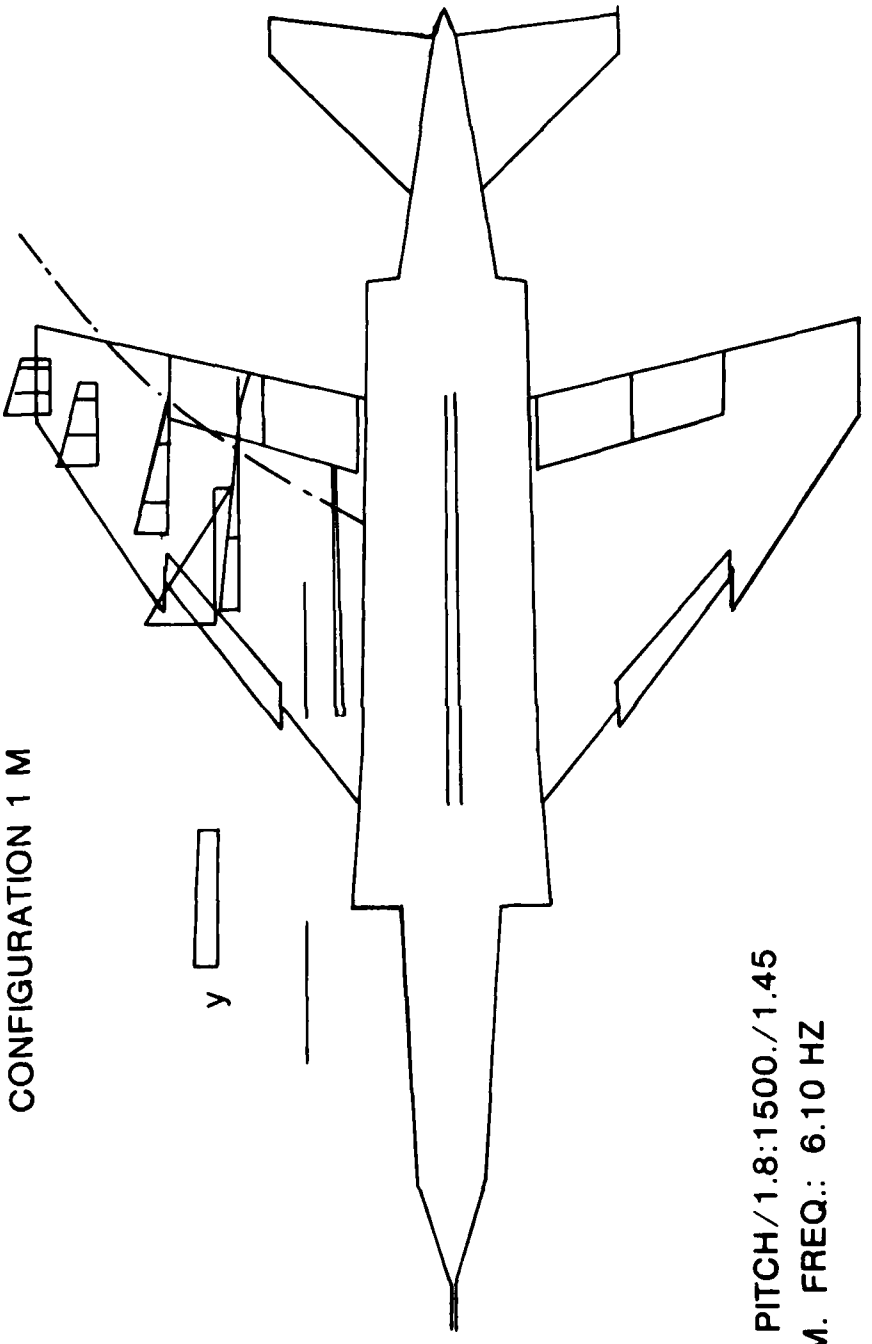


Figure 56. Calculated Store Pitch Mode with Modified Store Radius of Gyration and Adjusted Pylon Pitch Stiffness

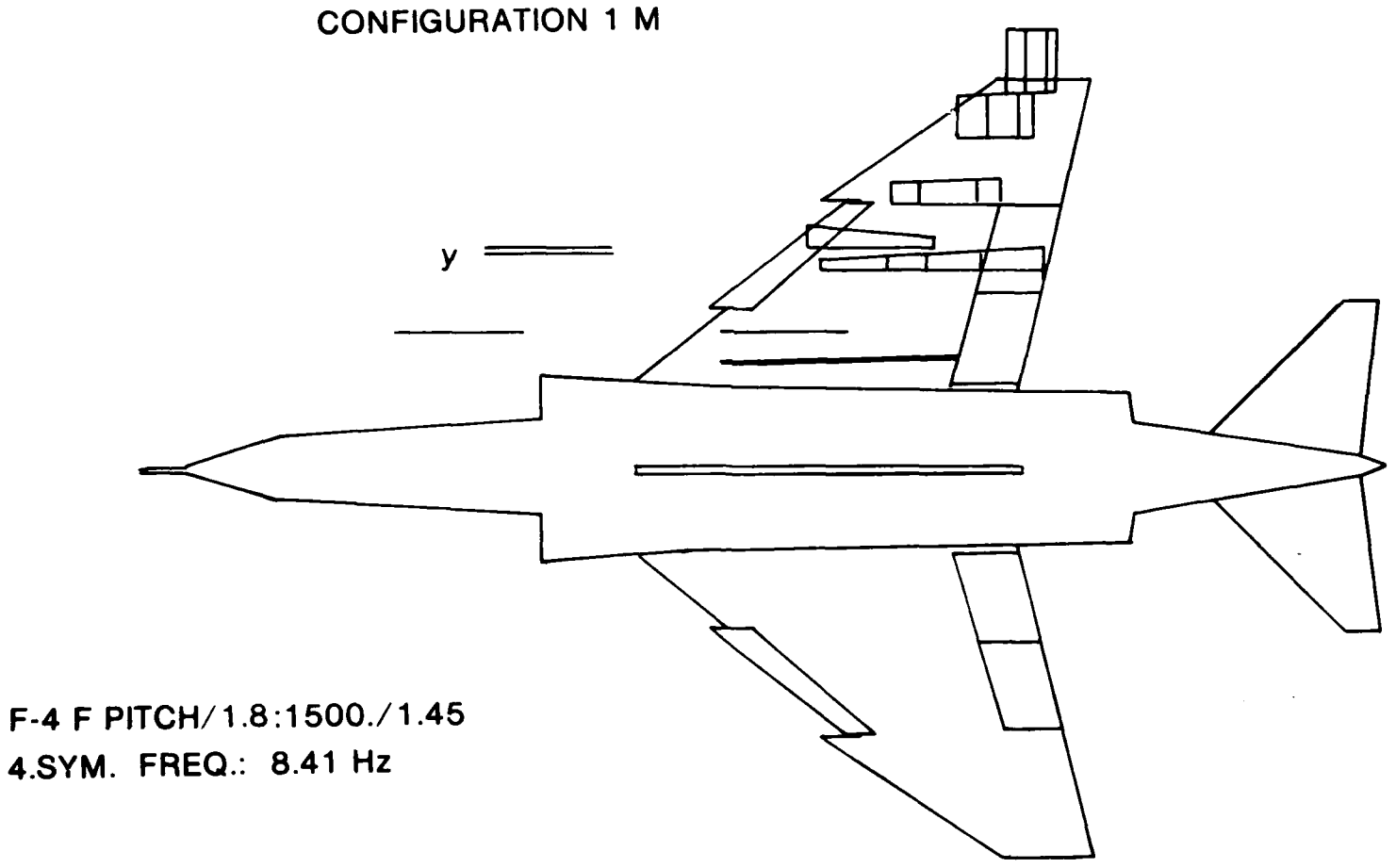


Figure 57. Calculated Store Roll Mode with Modified Store Radius of Gyration and Adjusted Pylon Pitch Stiffness

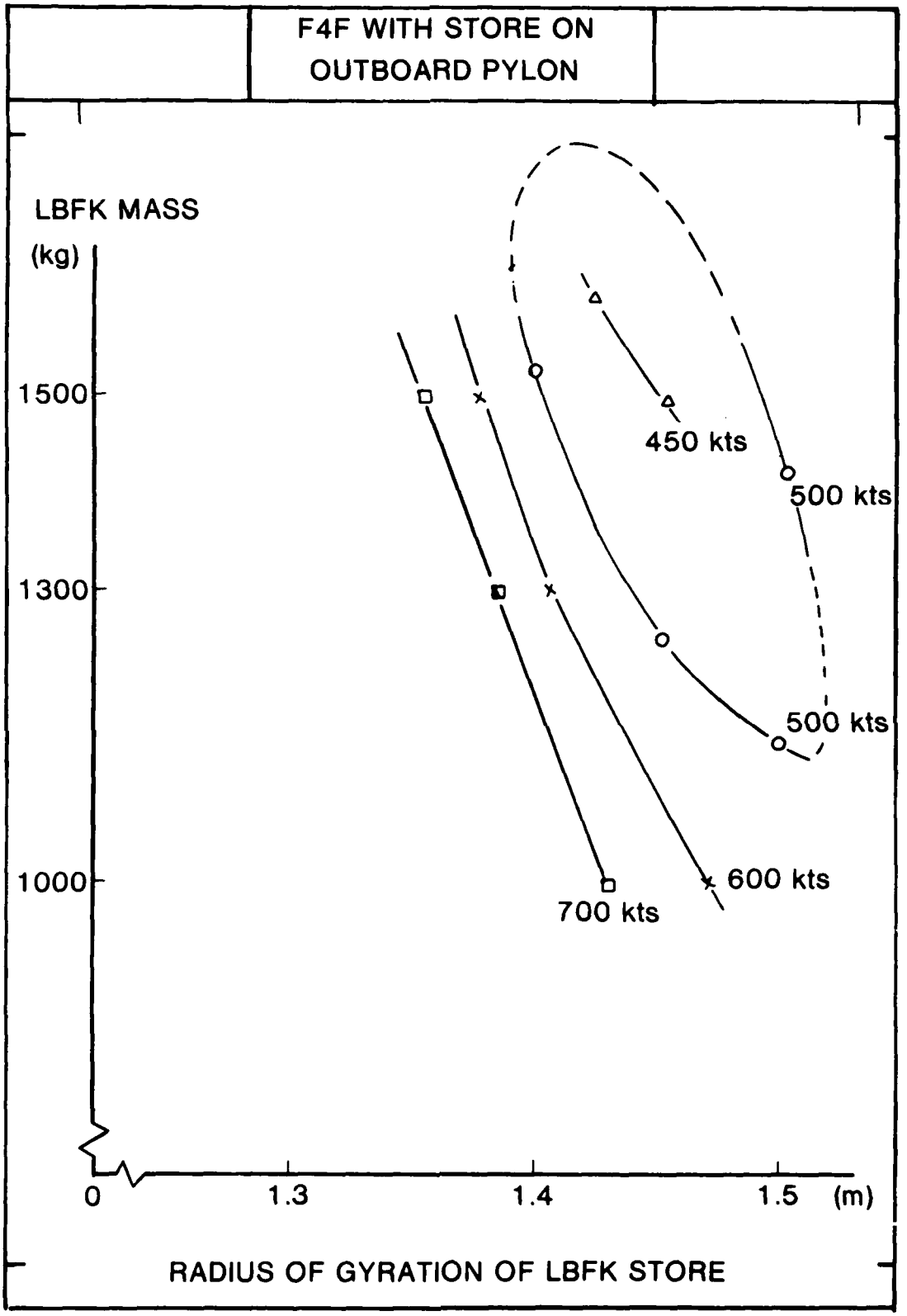


Figure 58. Flutter Speed vs Mass and Radius of Gyration of the LBFK-Store

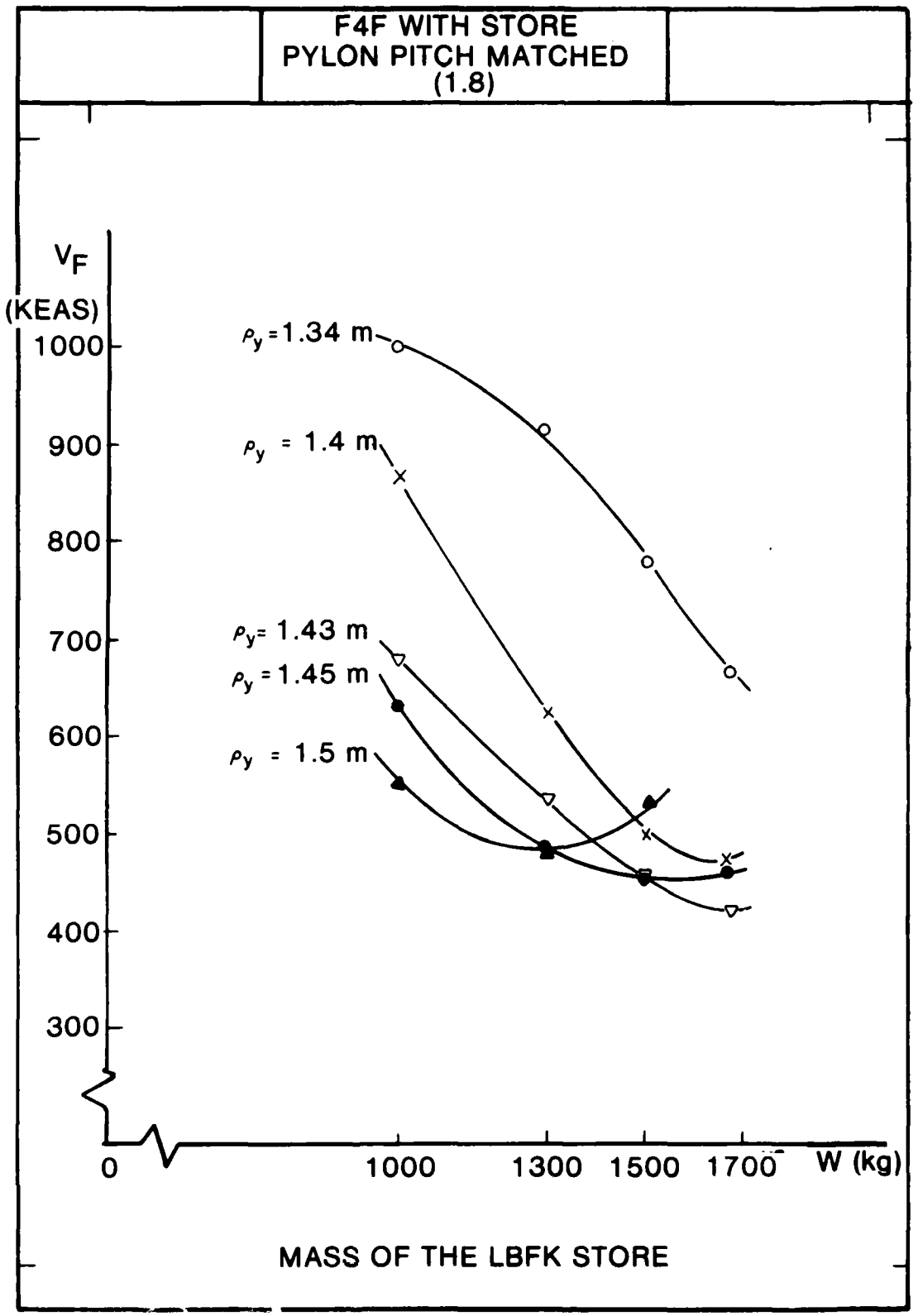


Figure 77. Flutter Speed vs Mass and Radius of Gyration of the LBFK-Store

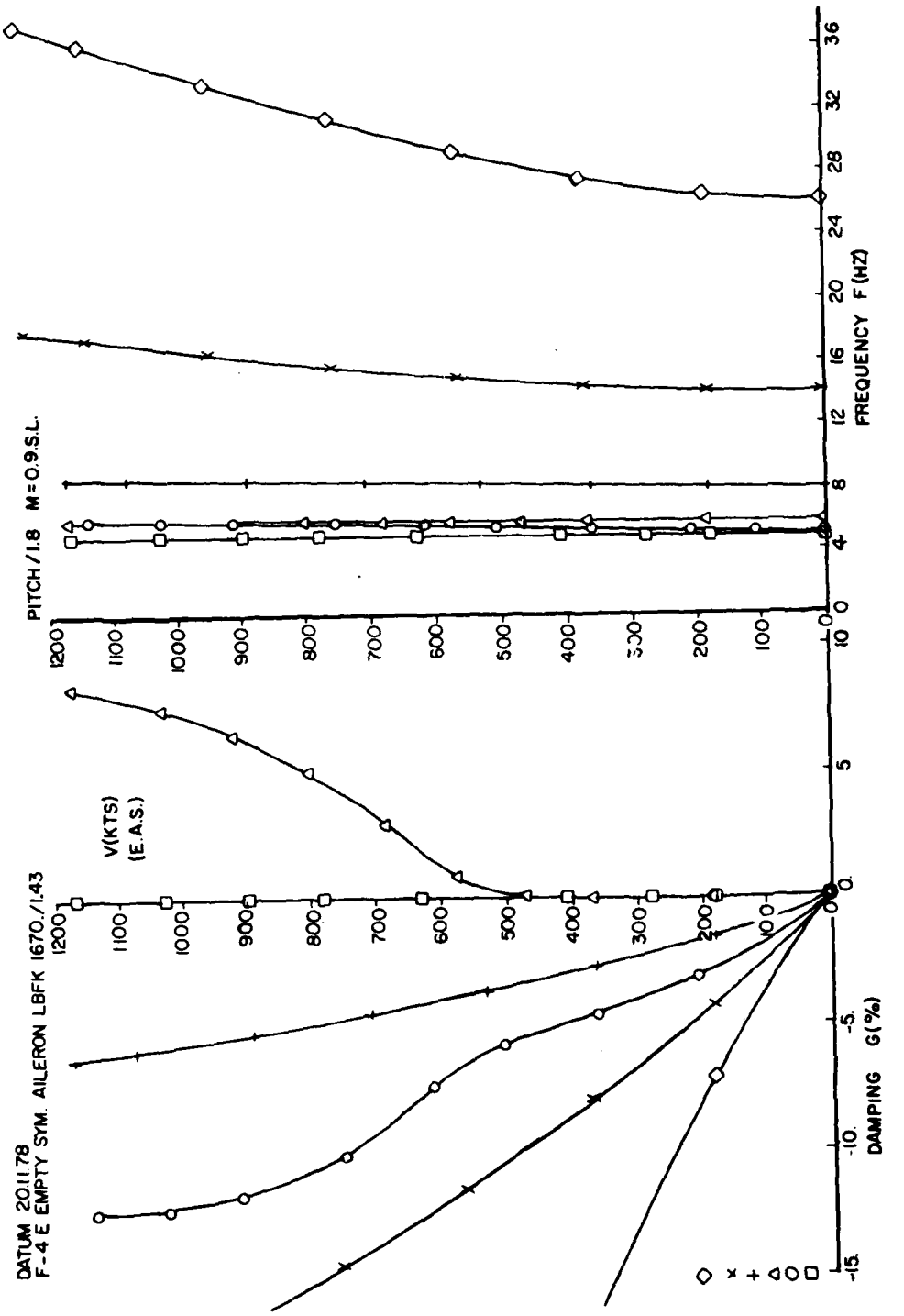


Figure 60. V-g Plot for $\rho$ = 1.43 m

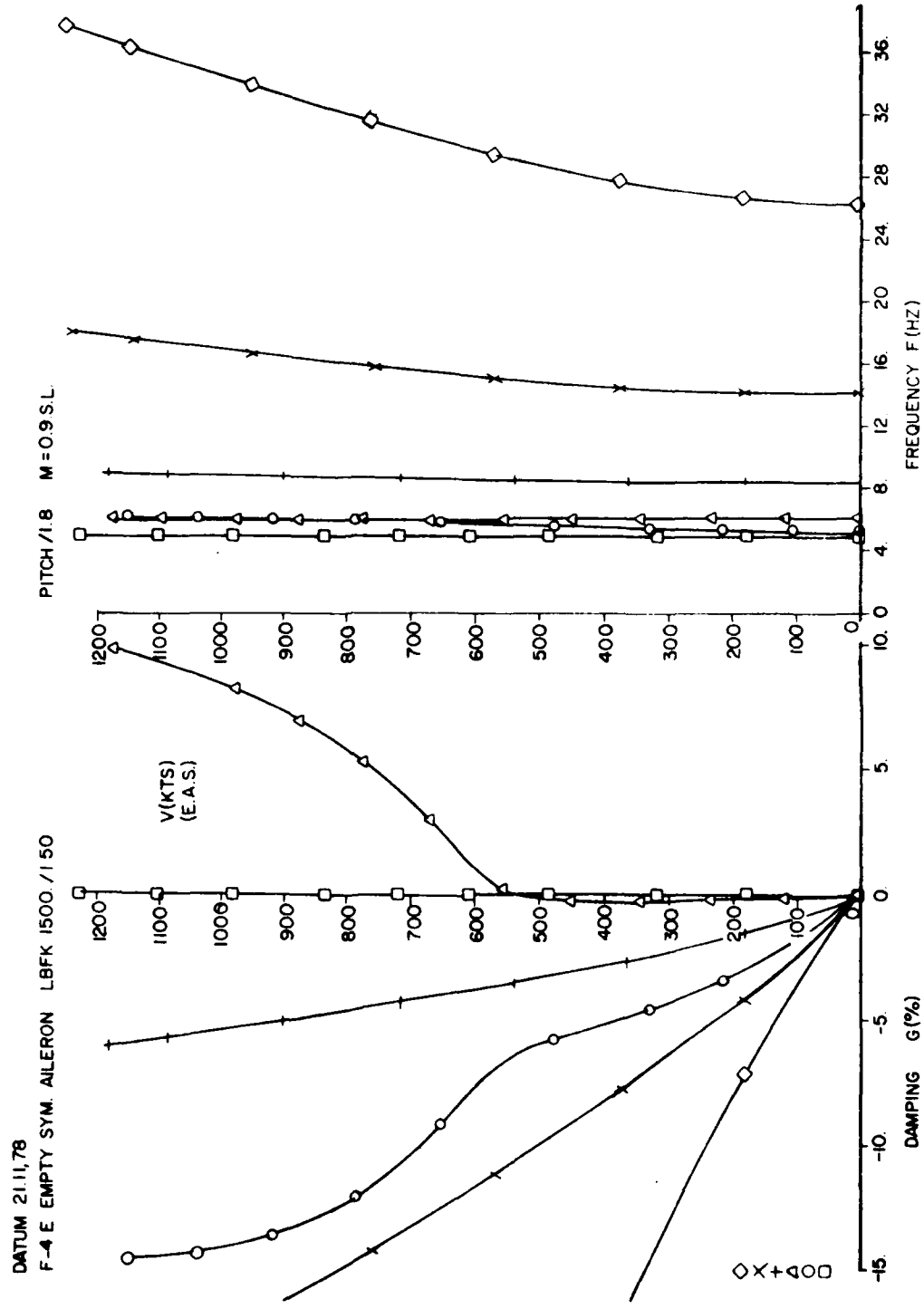


Figure 61. V-g Plot for $\rho$ = 1.50 m

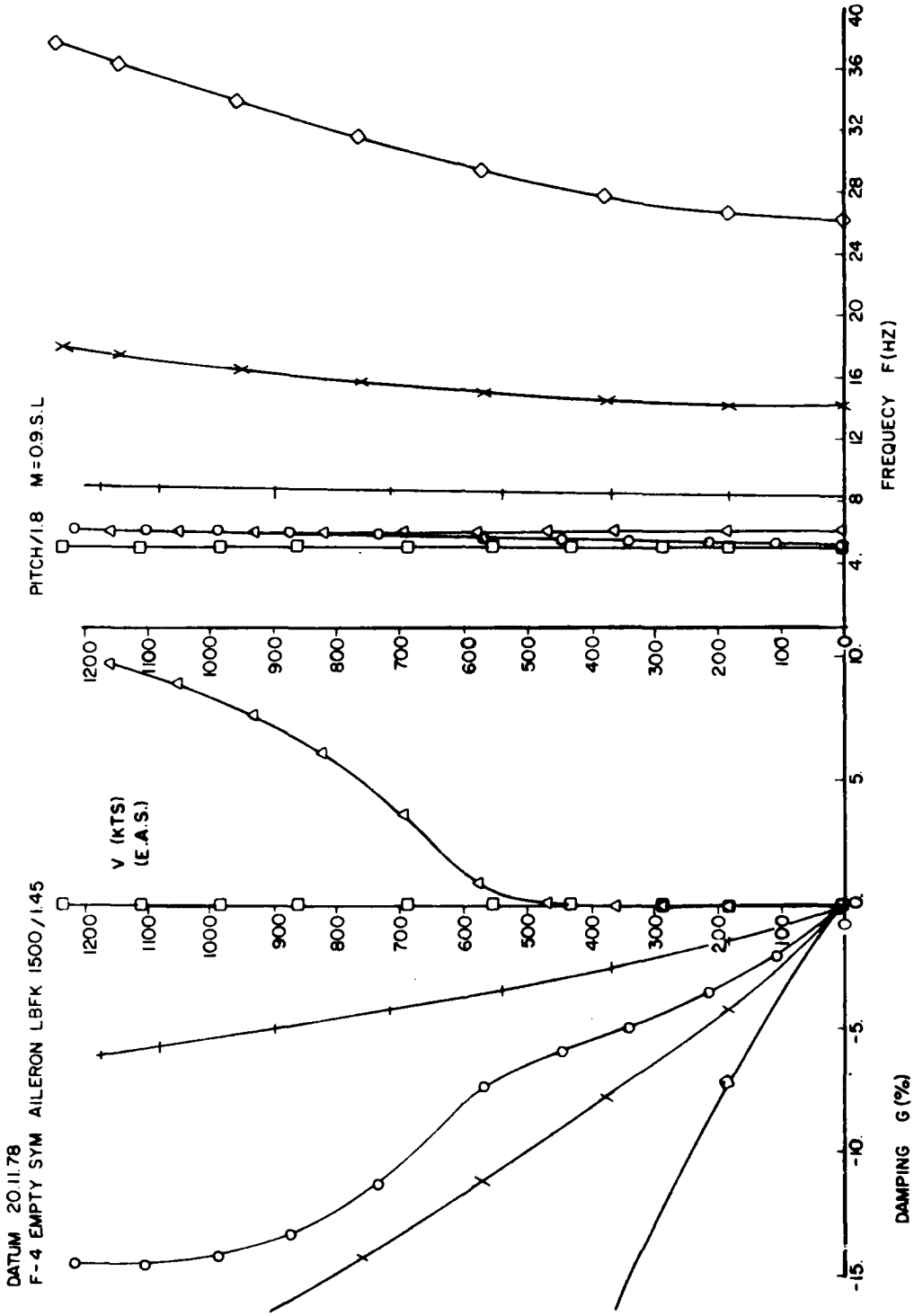


Figure 62. V-g Plot for $\rho$ = 1.45 m

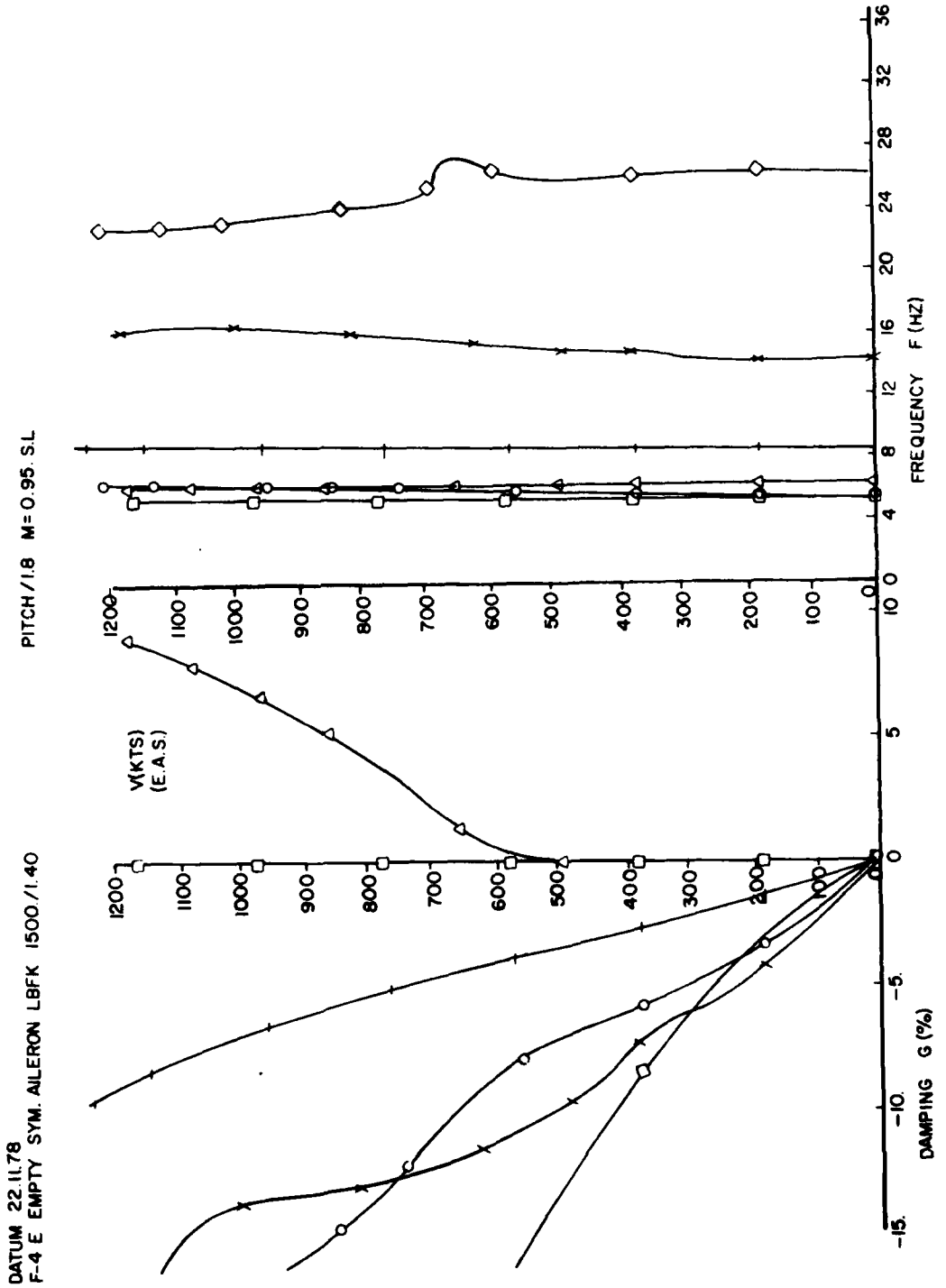


Figure 63. V-g Plot for [illegible] = 1.40 m

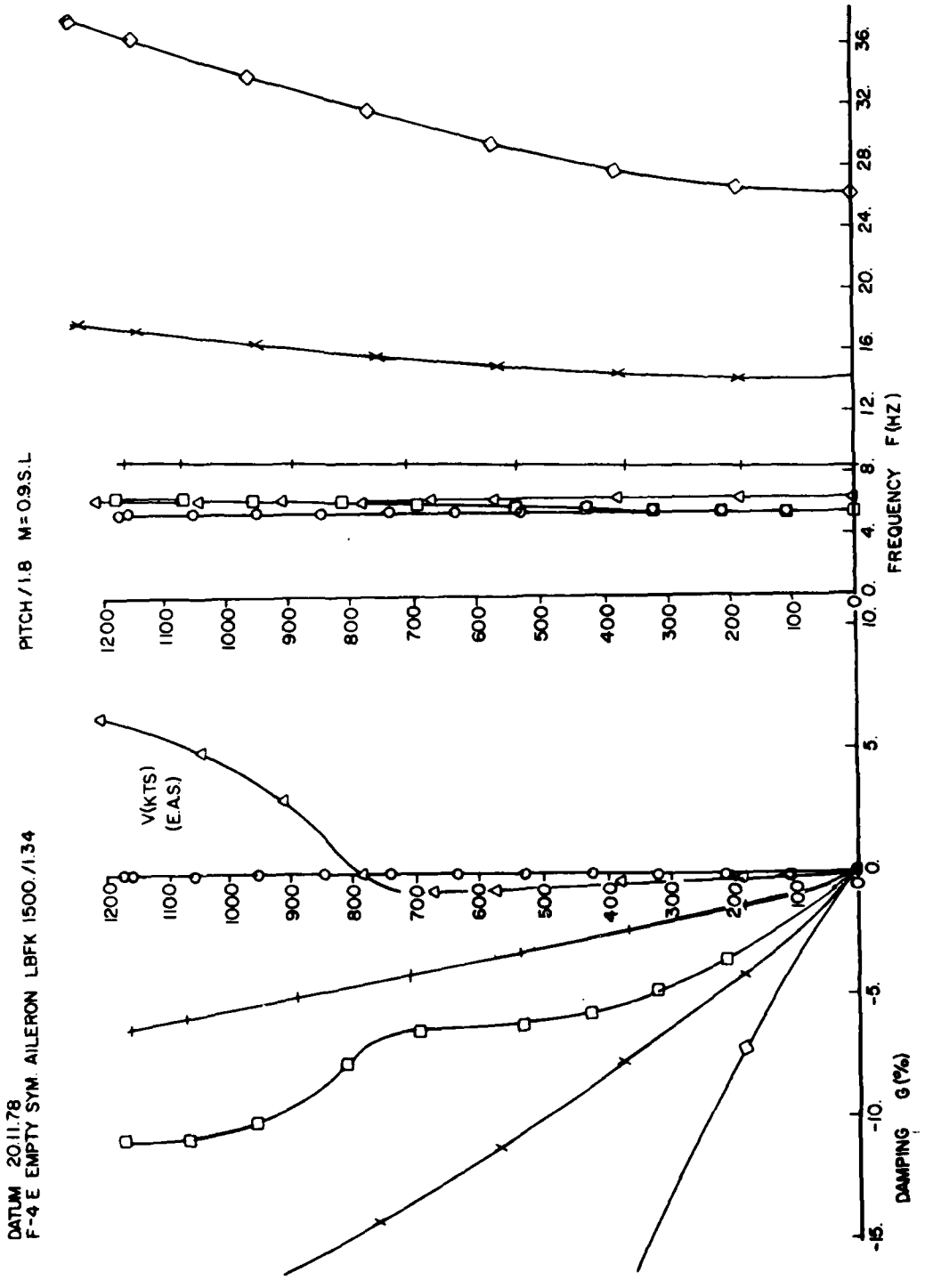


Figure 64. V-g Plot for $\rho$ = 1.34 m

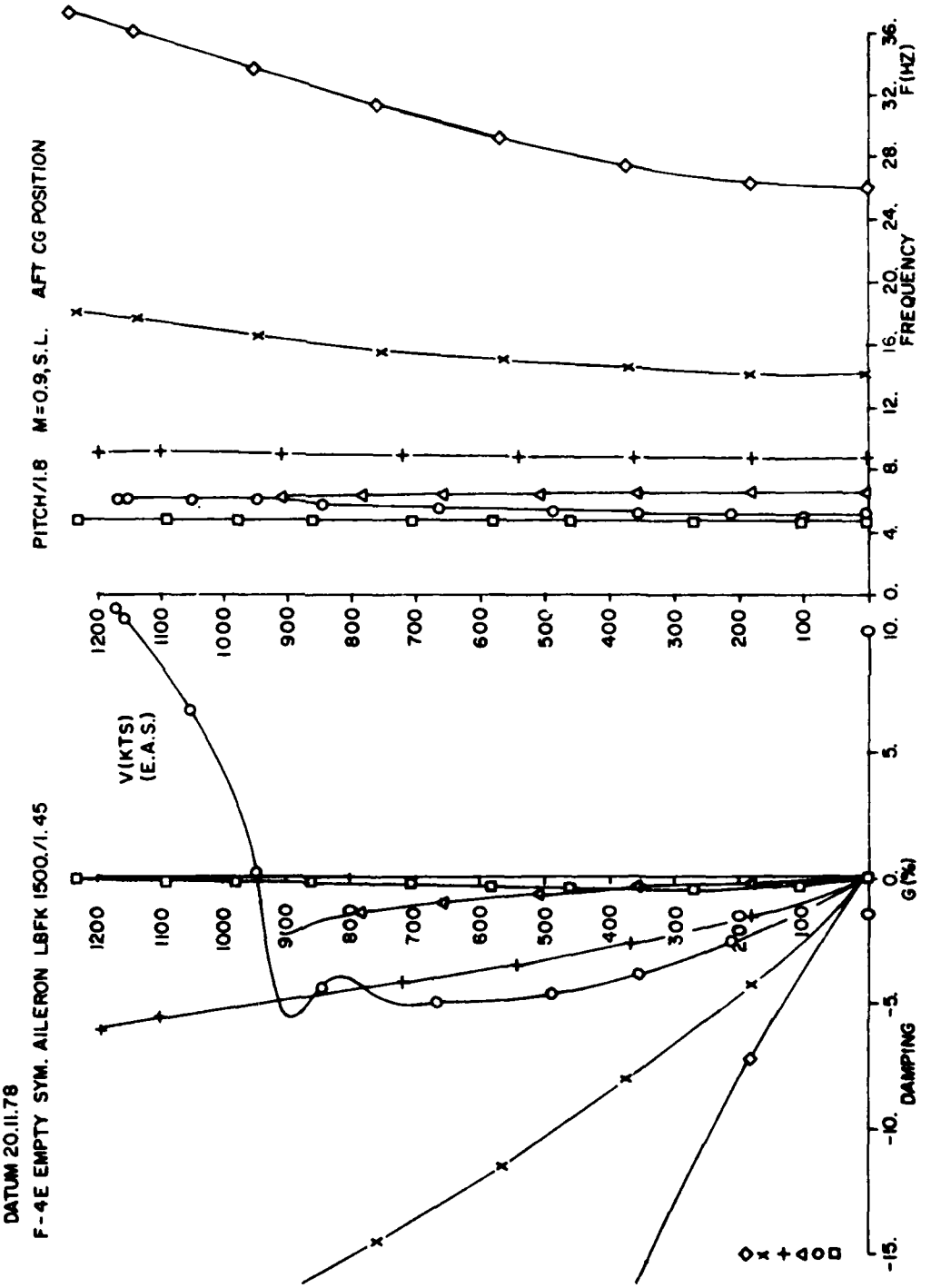


Figure 65. V-g Plot for c.g. in Aft Position

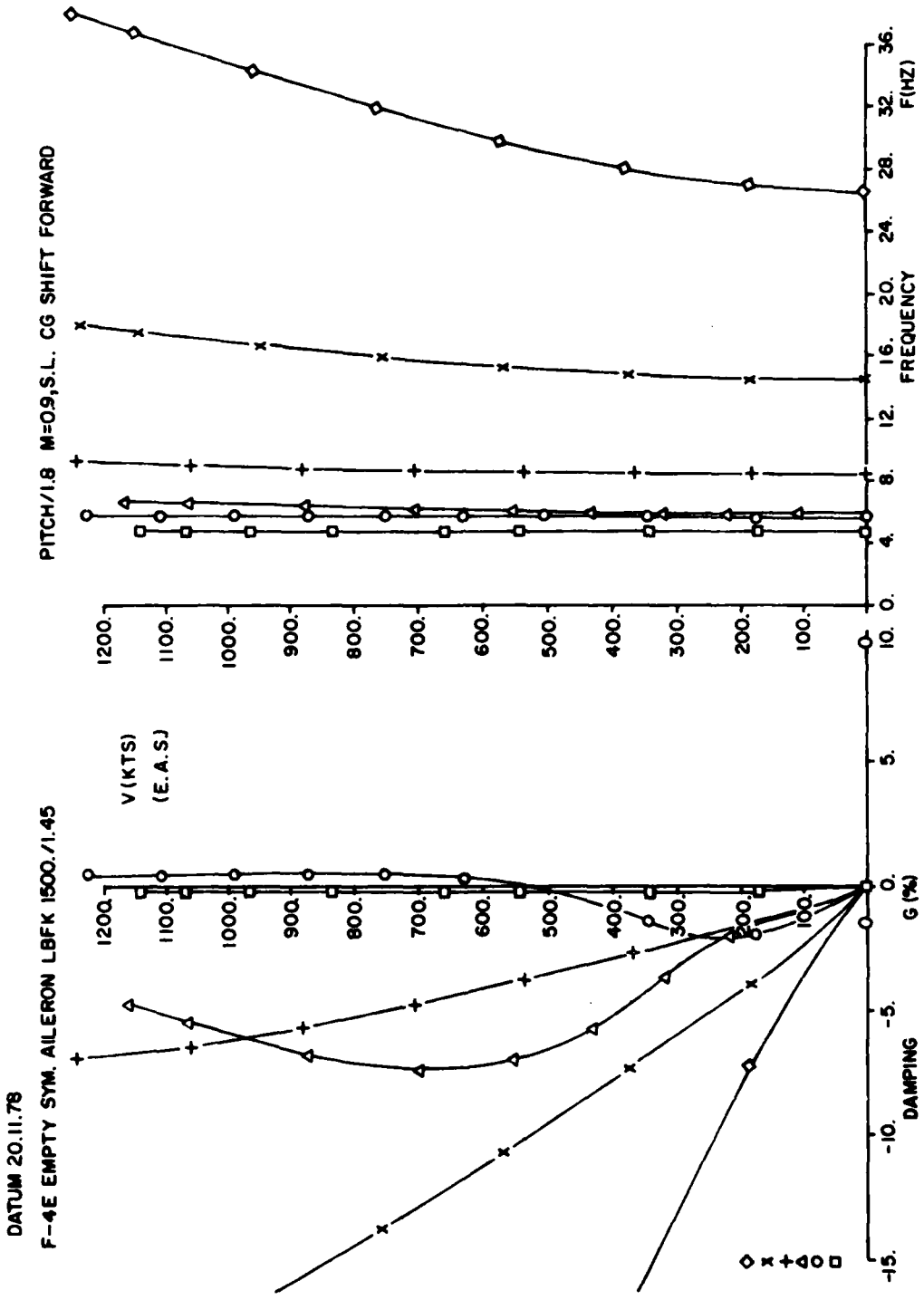


Figure 66. V-g Plot for c.g. in Forward Position

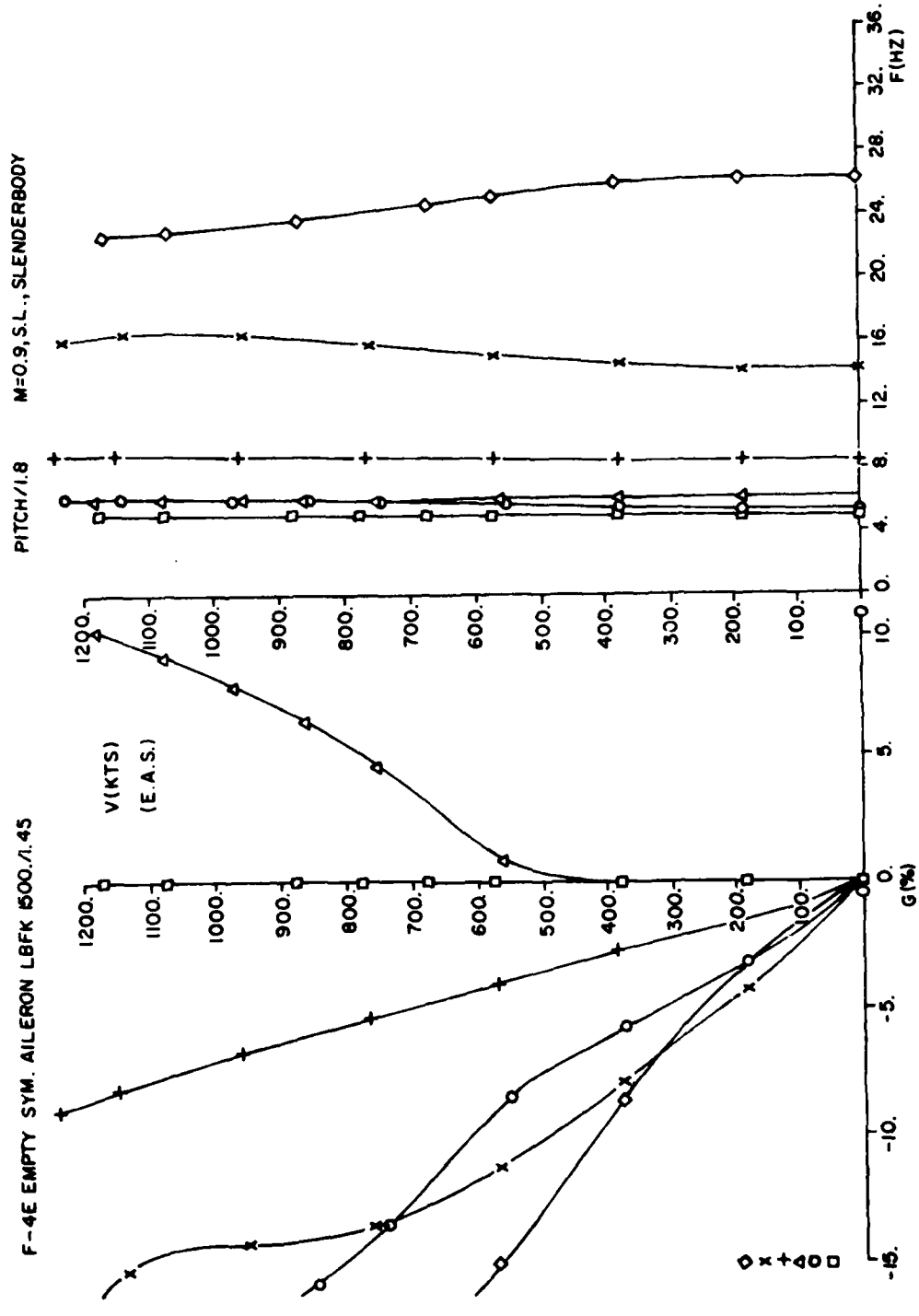


Figure 67. V-g Plot with Store Aerodynamics

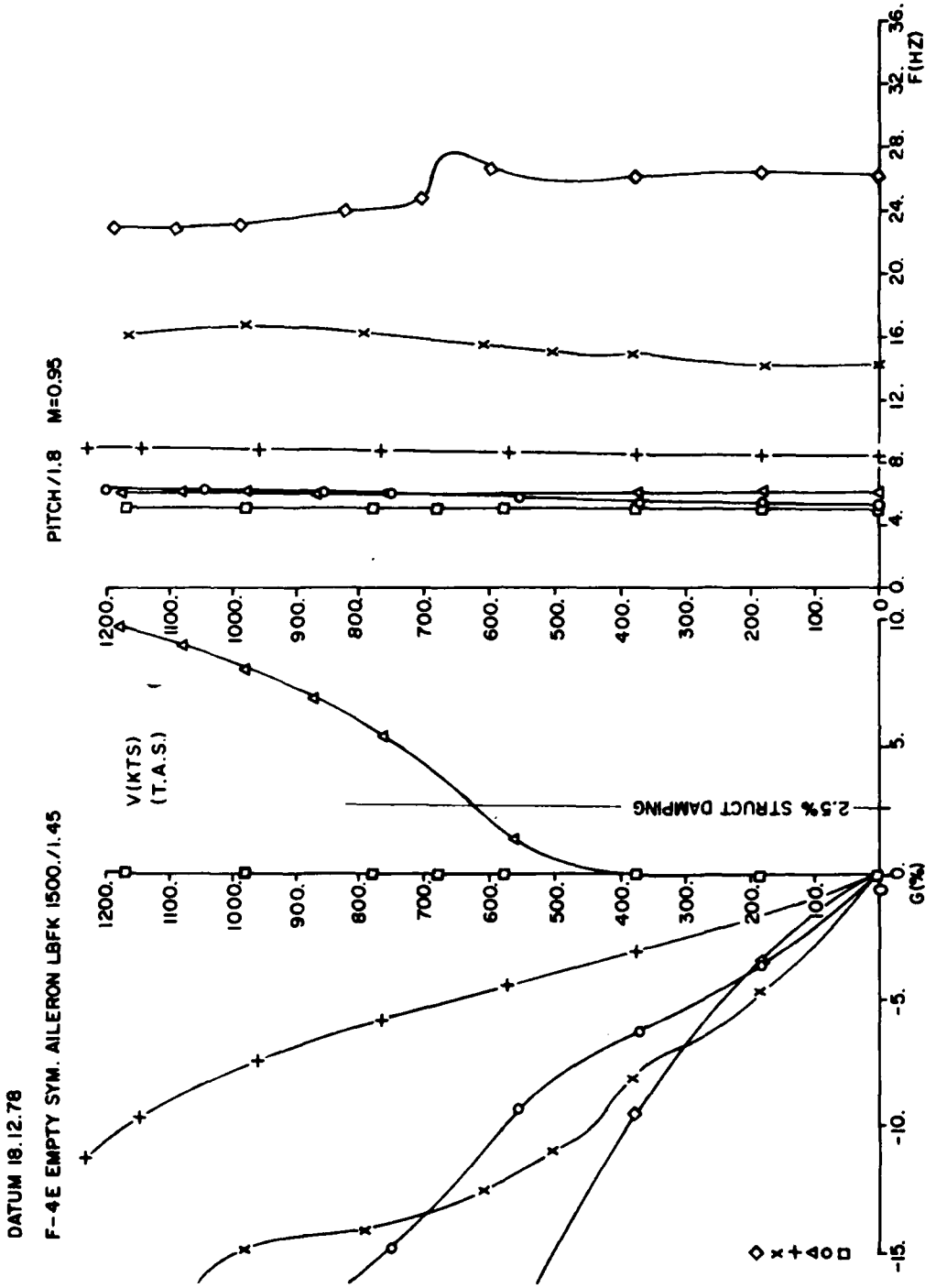


Figure 68. V-g Plot with Mach Number = 0.95

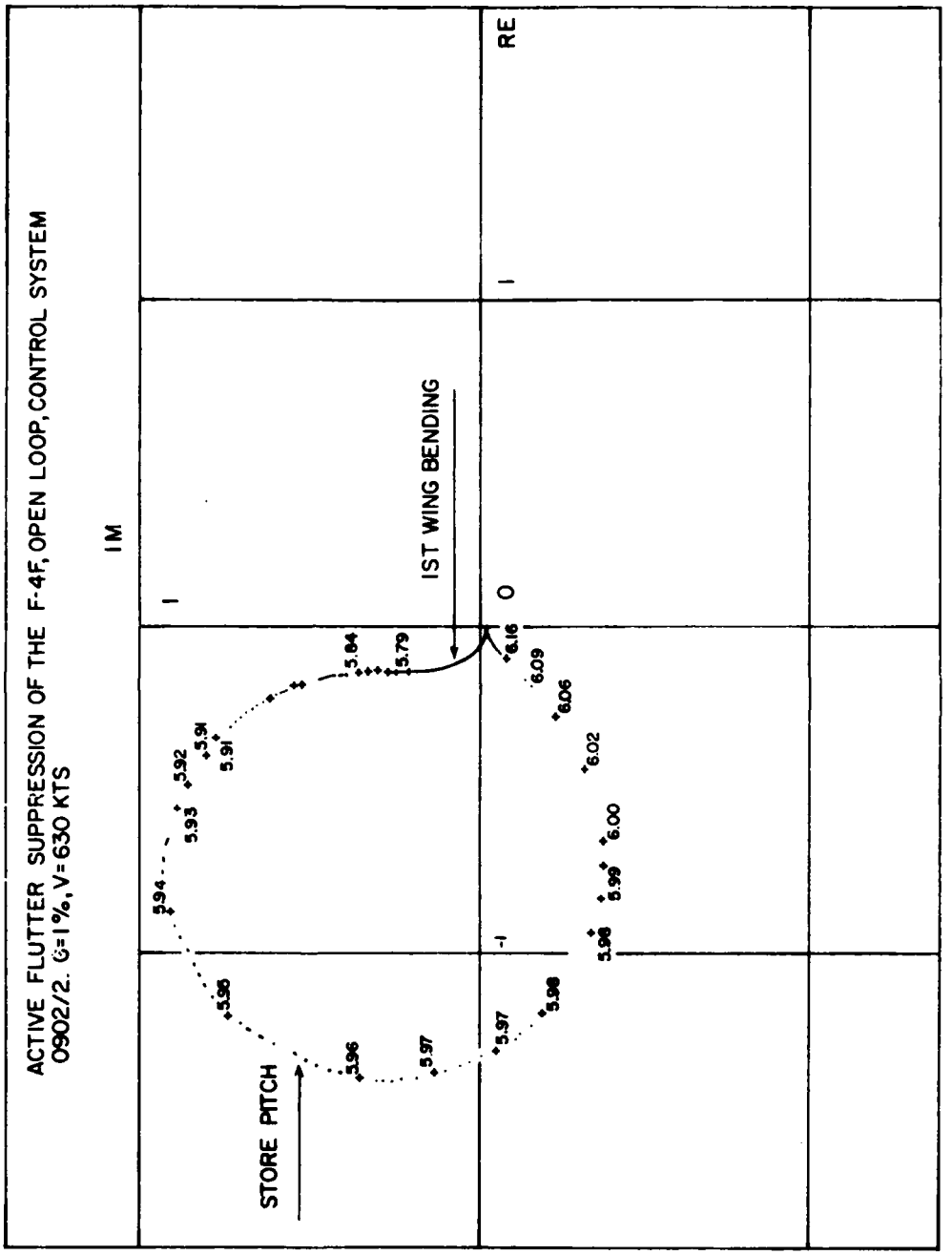


Figure 69. Nyquist Diagram for V = 630 kts

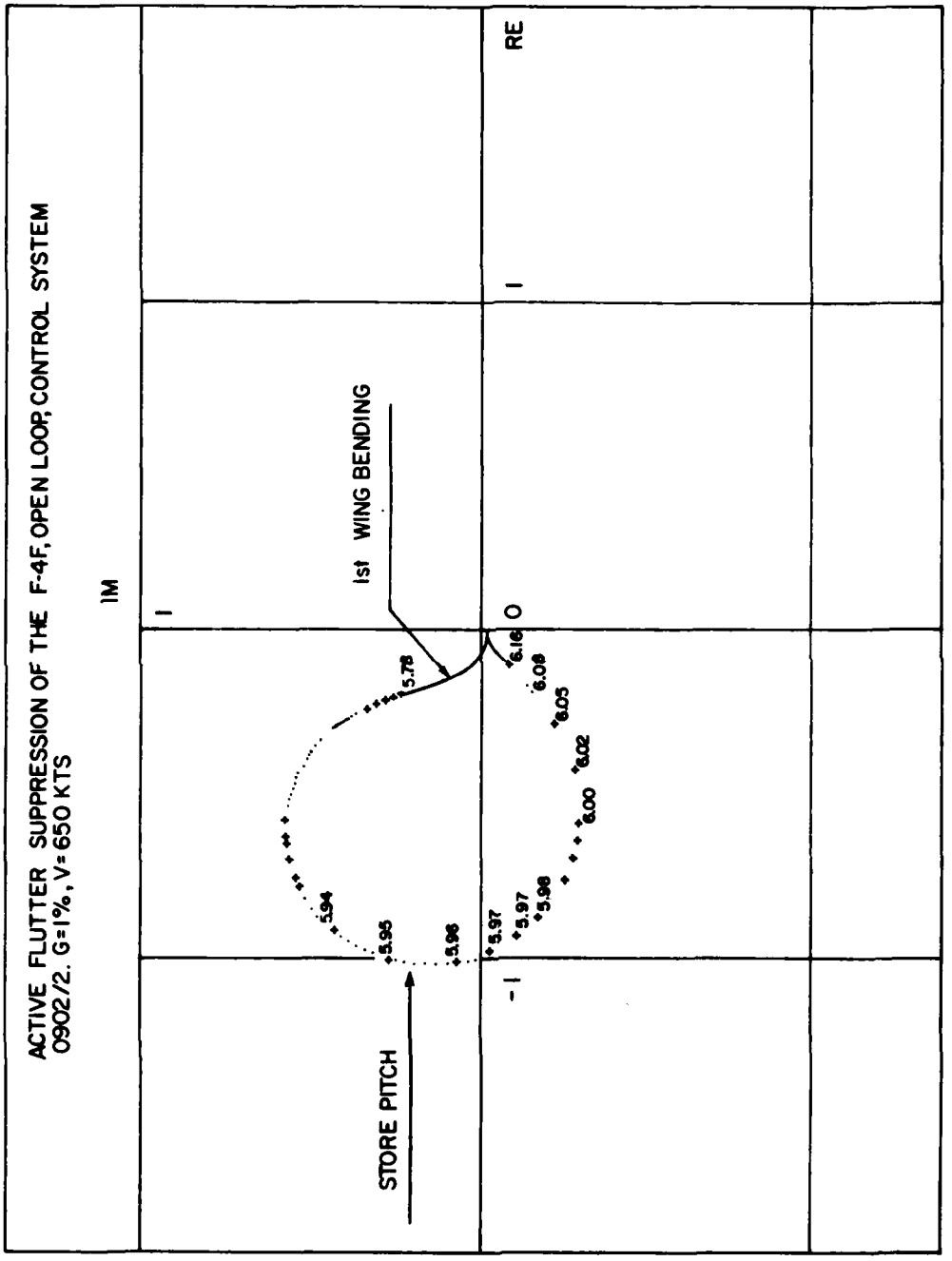


Figure 70. Nyquist Diagram for V = 650 kts

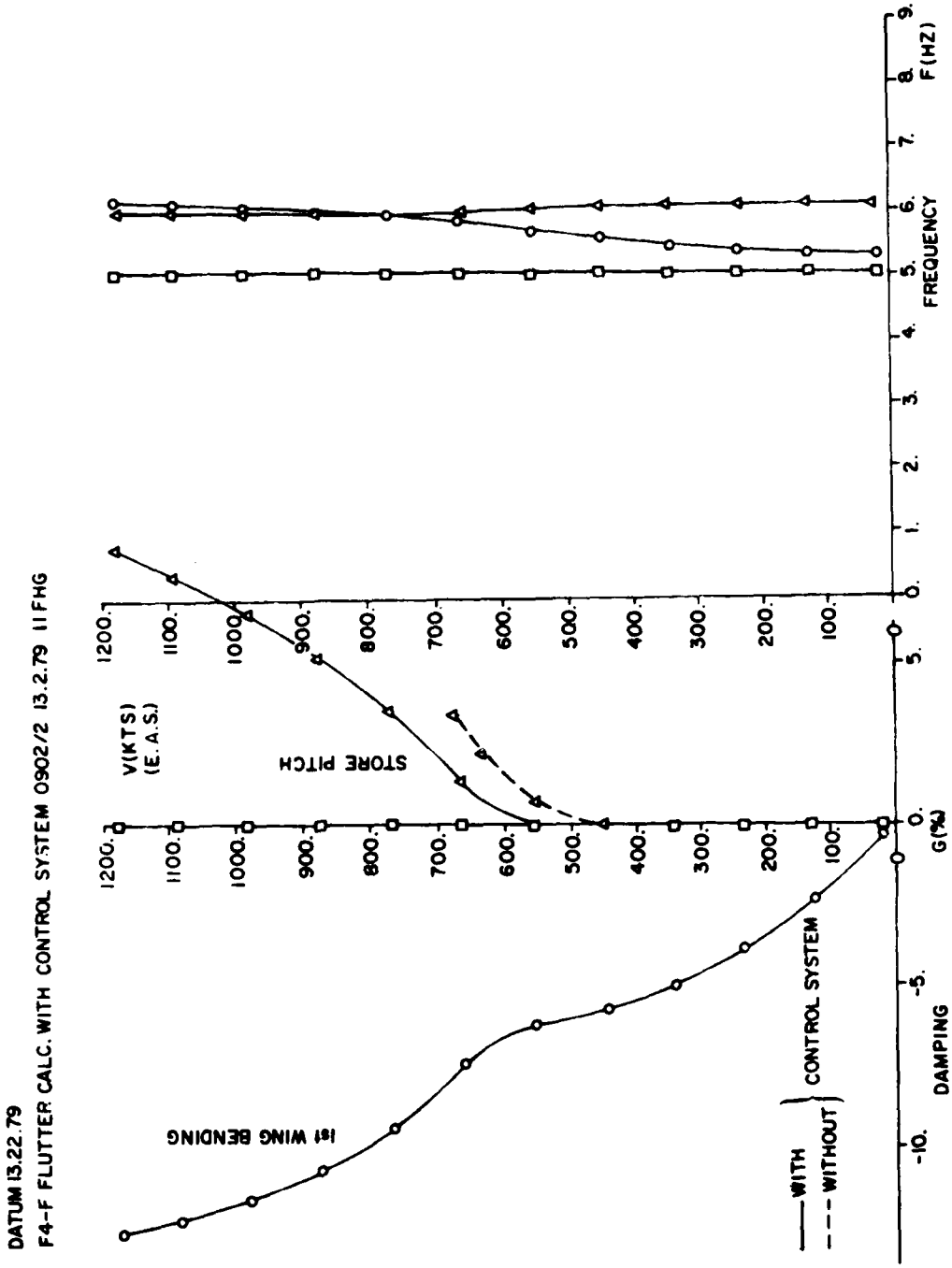


Figure 71. Flutter Calculation with Flutter Suppression System

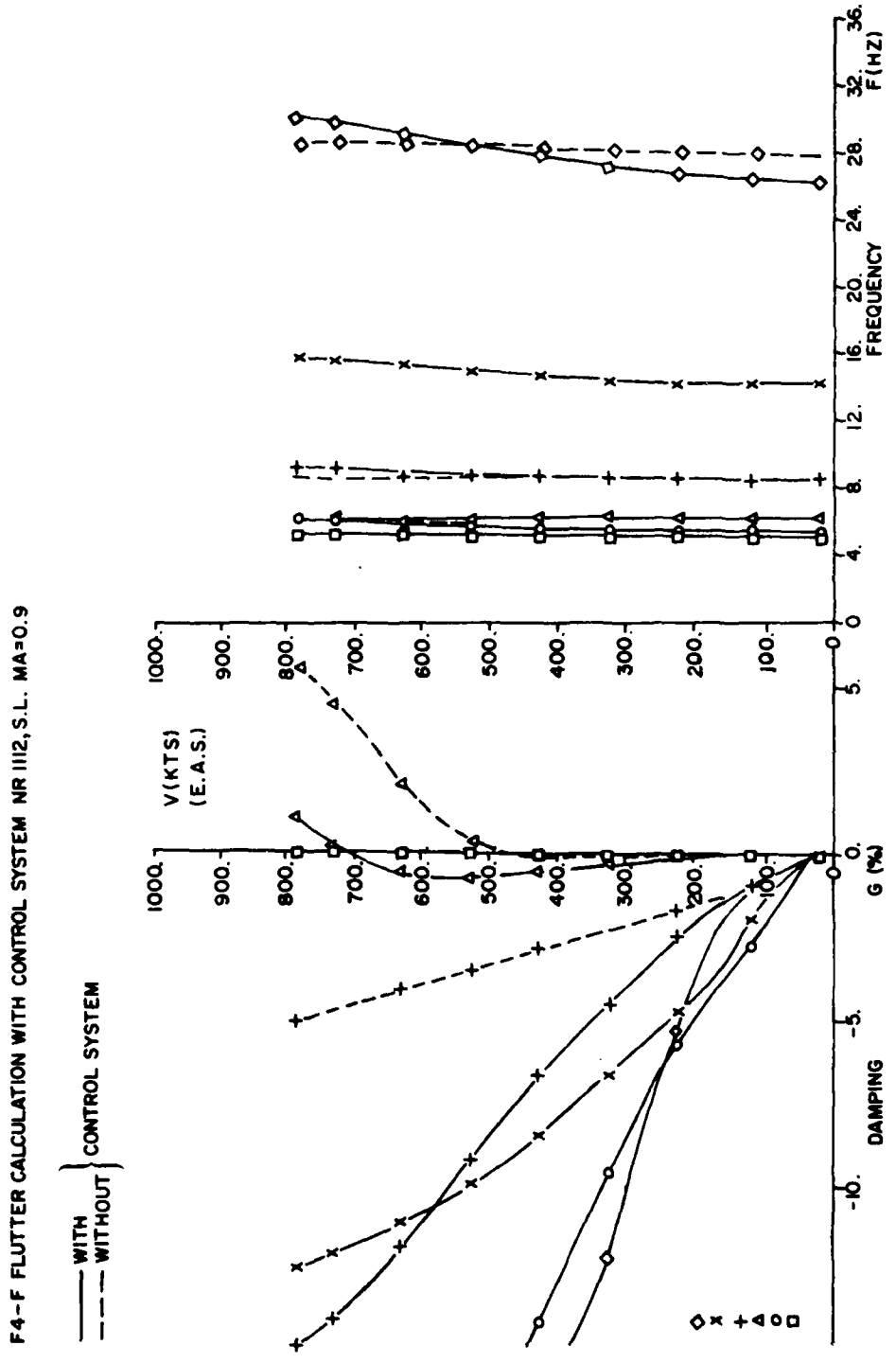


Figure 72. Flutter Calculation with Flutter Suppression System

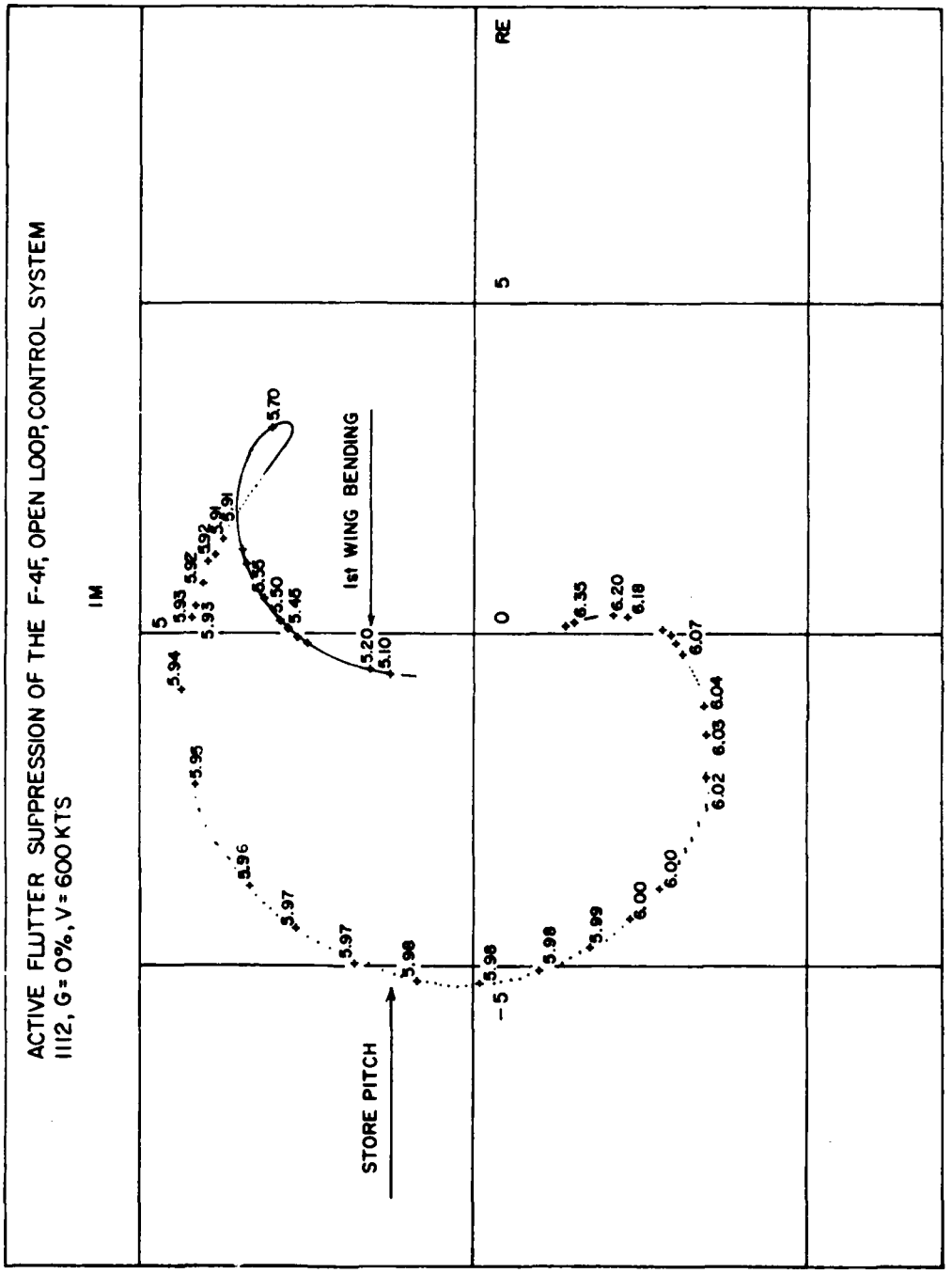


Figure 73. Nyquist Diagram for V = 600 kts

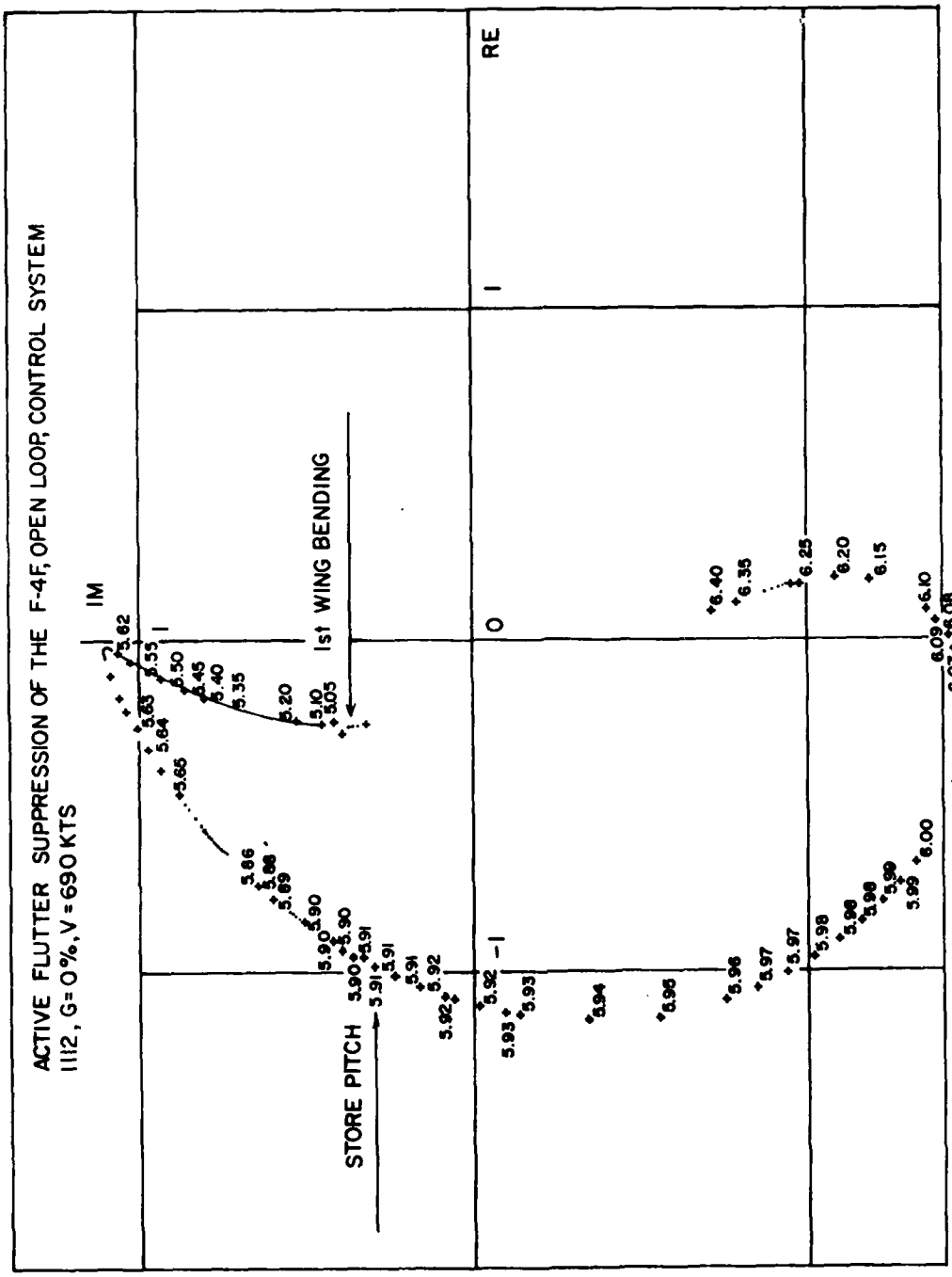


Figure 74. Nyquist Diagram for V = 690 kts

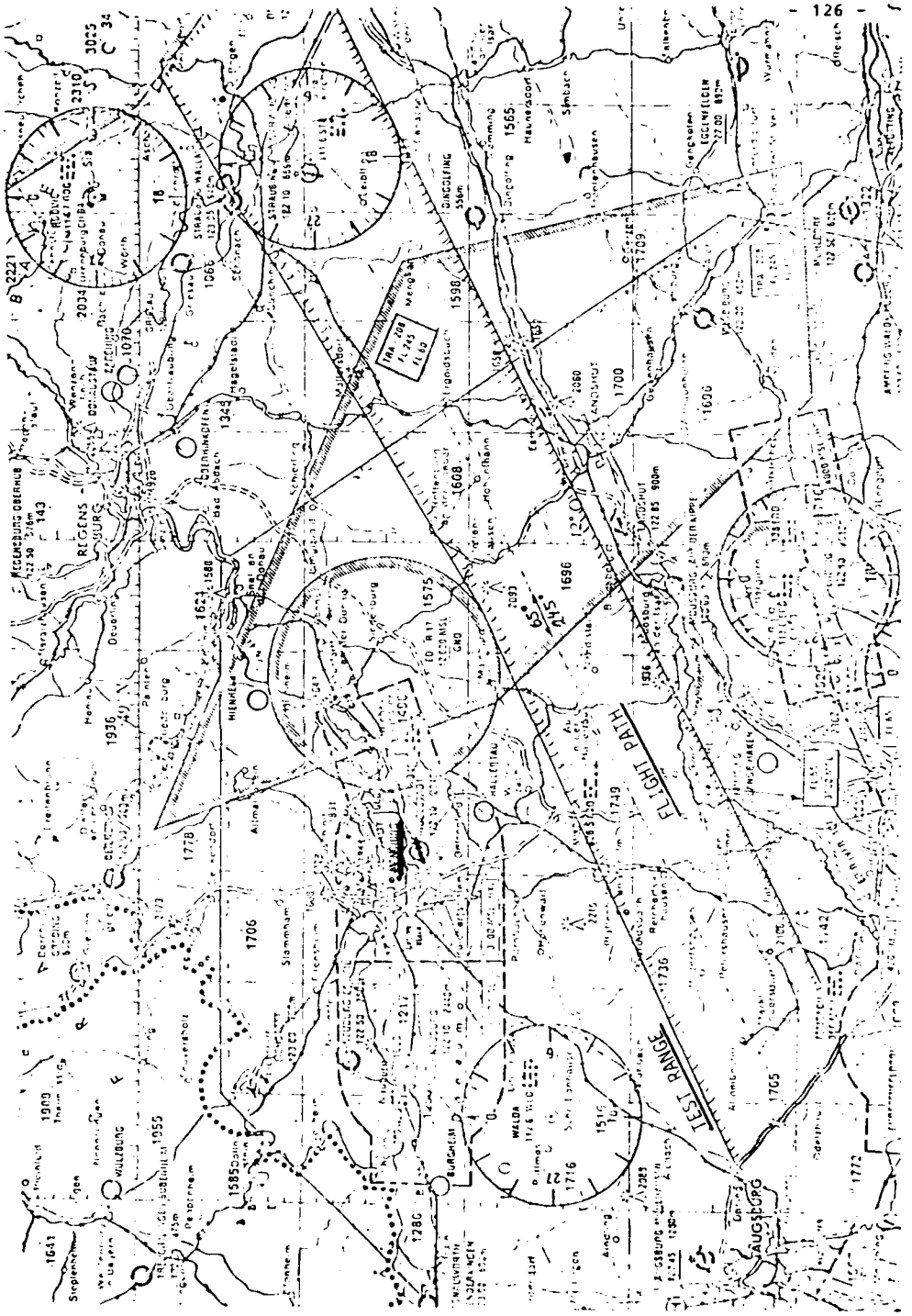


Figure 75. Test Range and Flight Path for the Flight Test at Manching

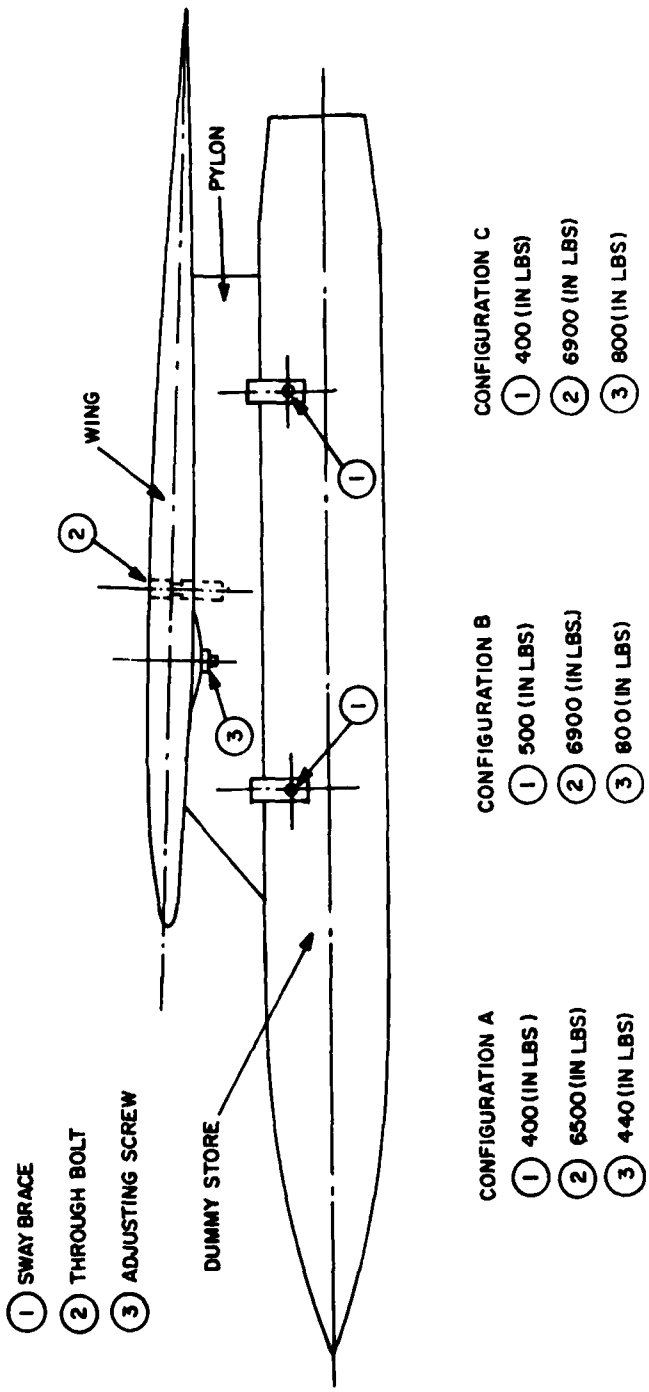


Figure 76. Torque Moments of Pylon and Store Attachment

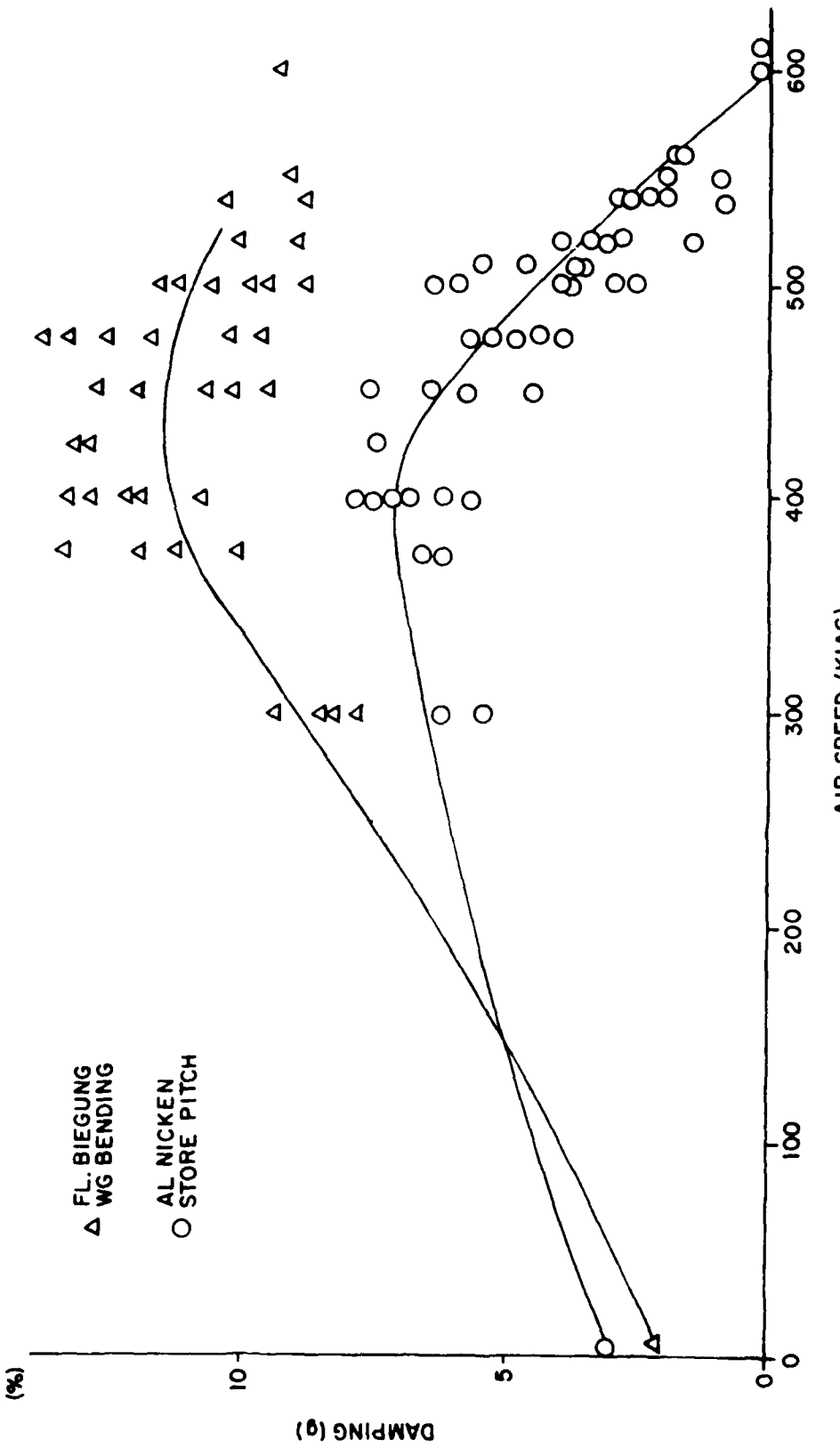


Figure 77. Damping Versus Airspeed of the Critical Store Configuration

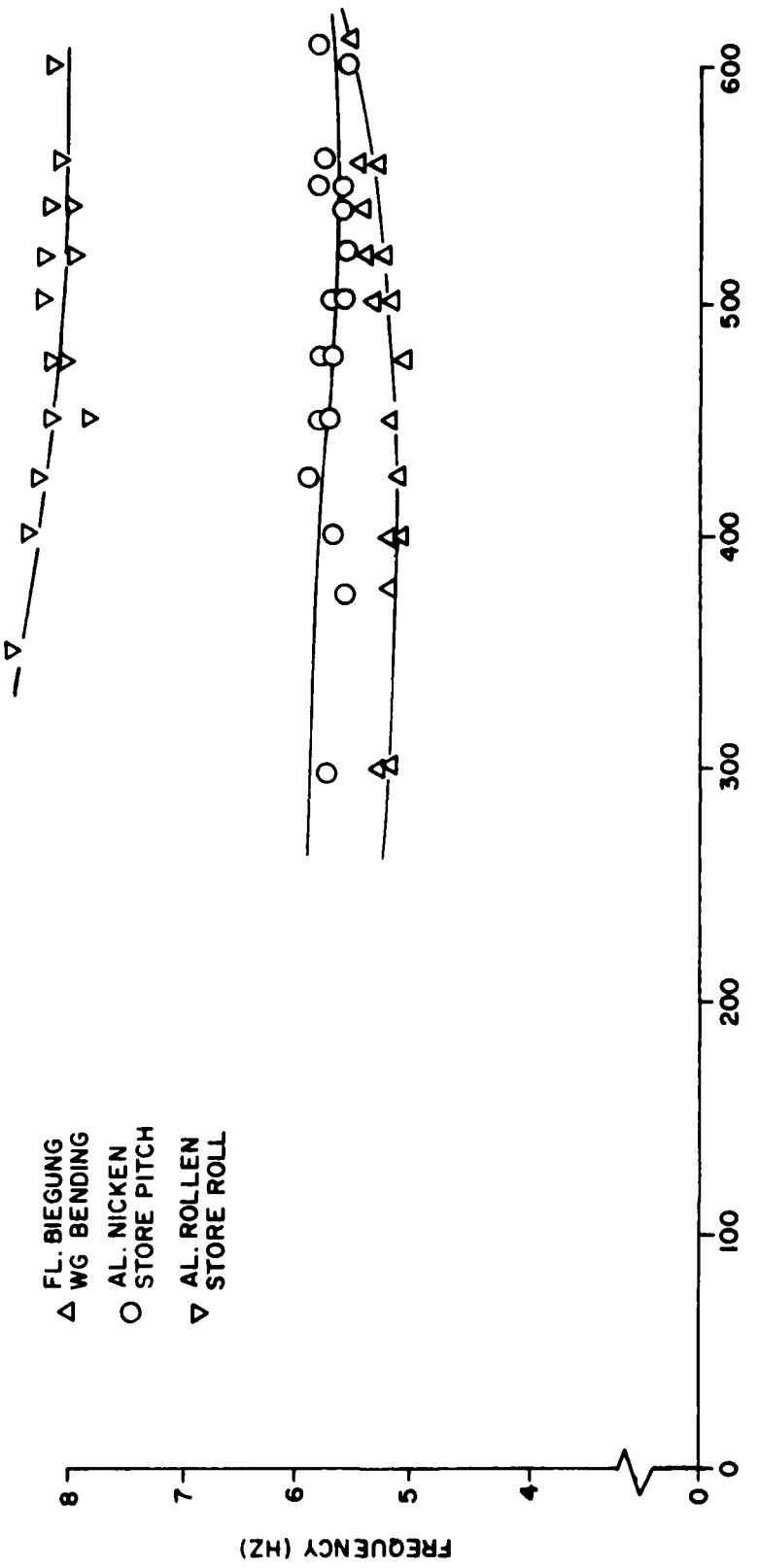


Figure 78. Frequency Versus Airspeed of the Critical Store Configuration

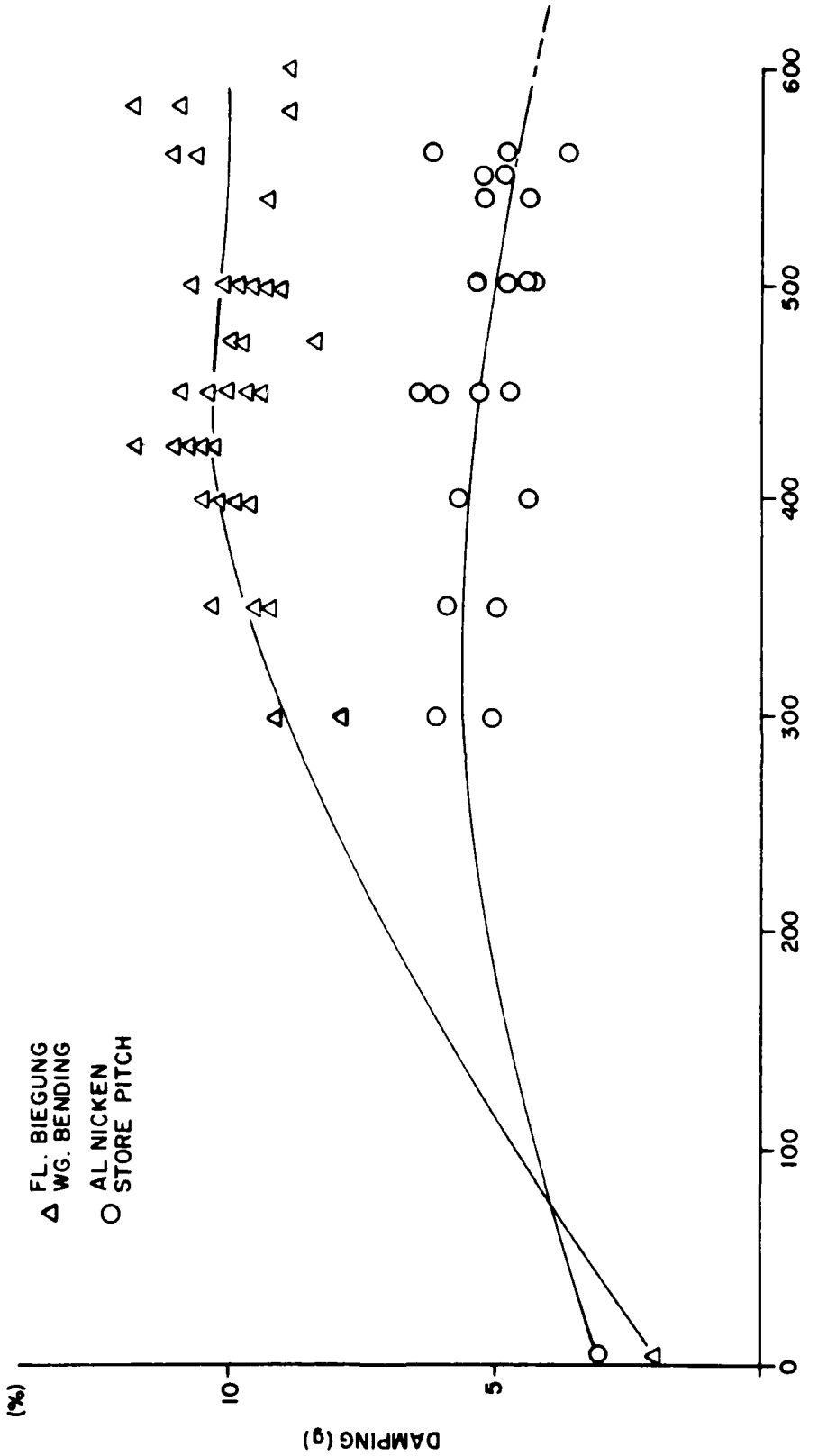


Figure 79. Damping Versus Airspeed of the Flutter Stopper

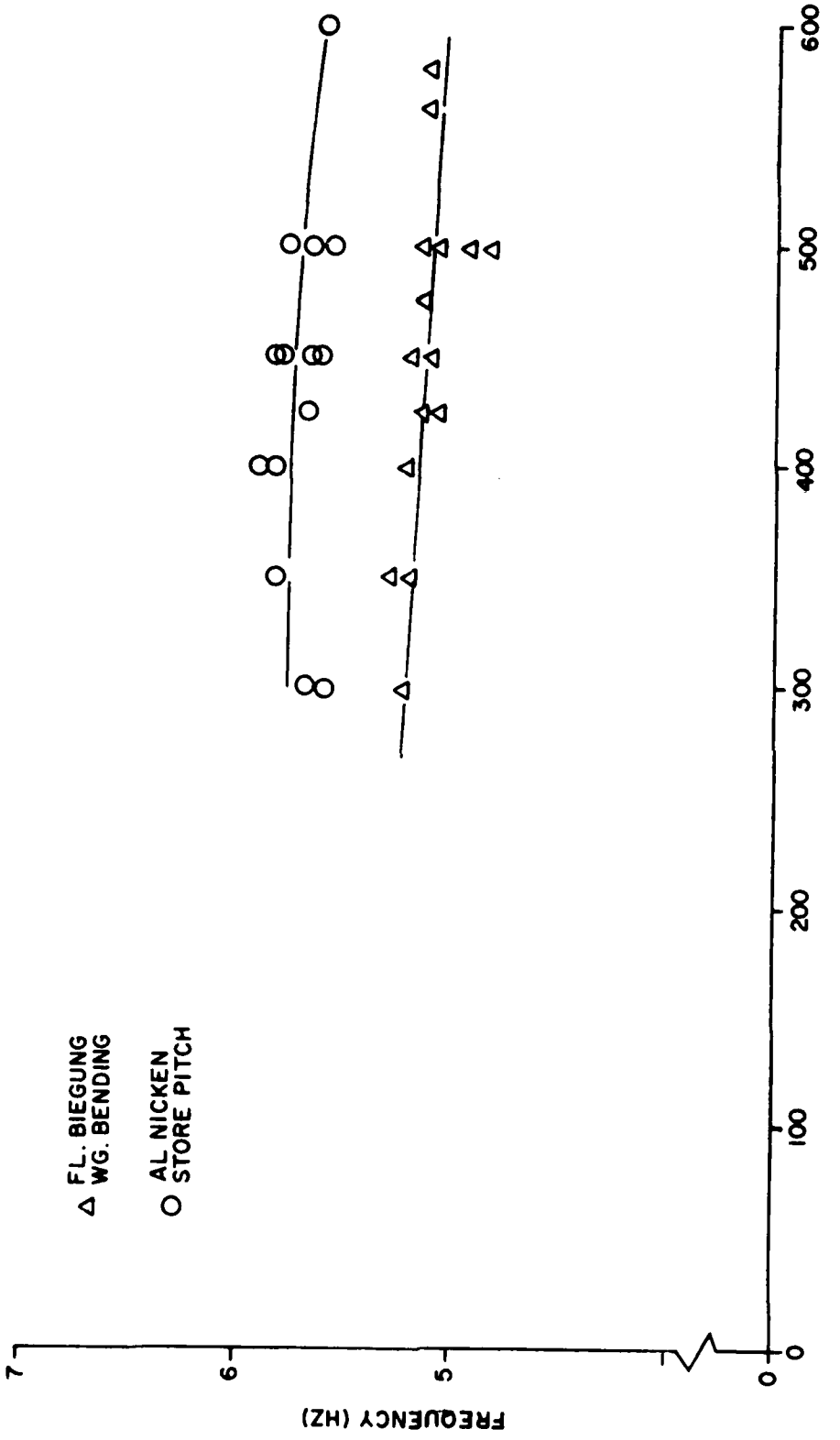


Figure 80. Frequency Versus Airspeed of the Flutter Stopper

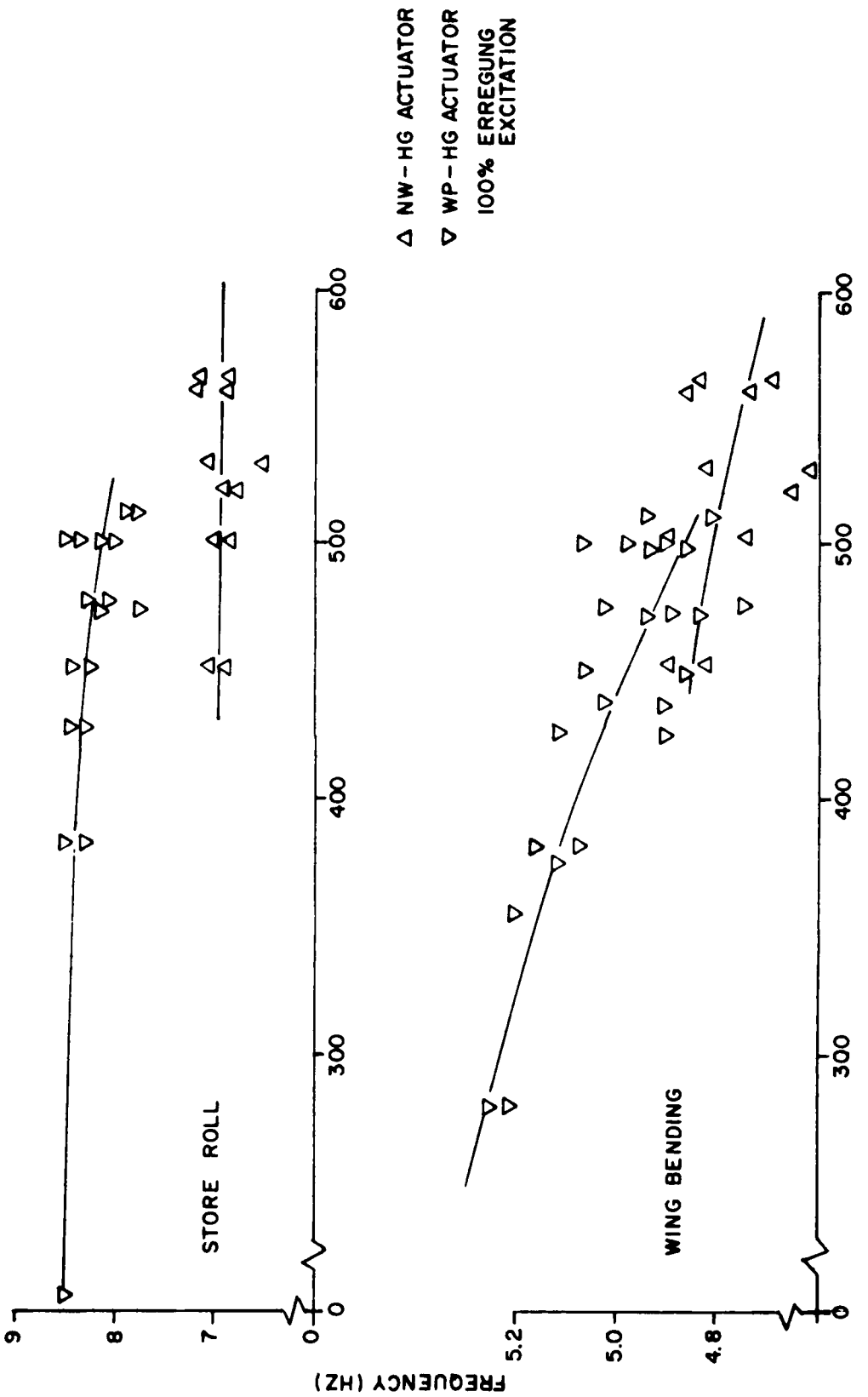


Figure 81. Frequency Shifts Due to Nonlinearities

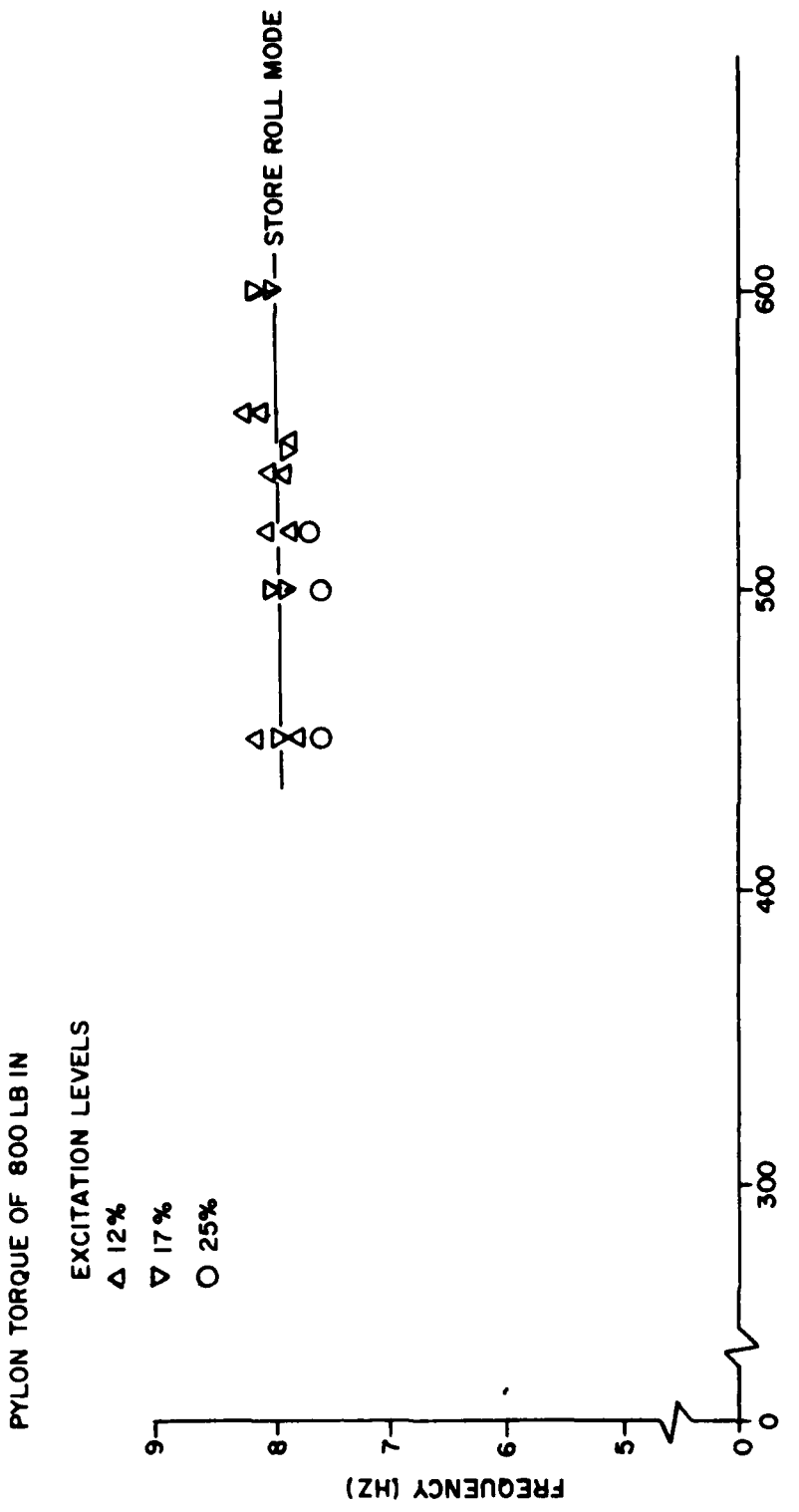


Figure 82. Frequency Shift of the Store Roll Mode Due to Various Excitation Levels

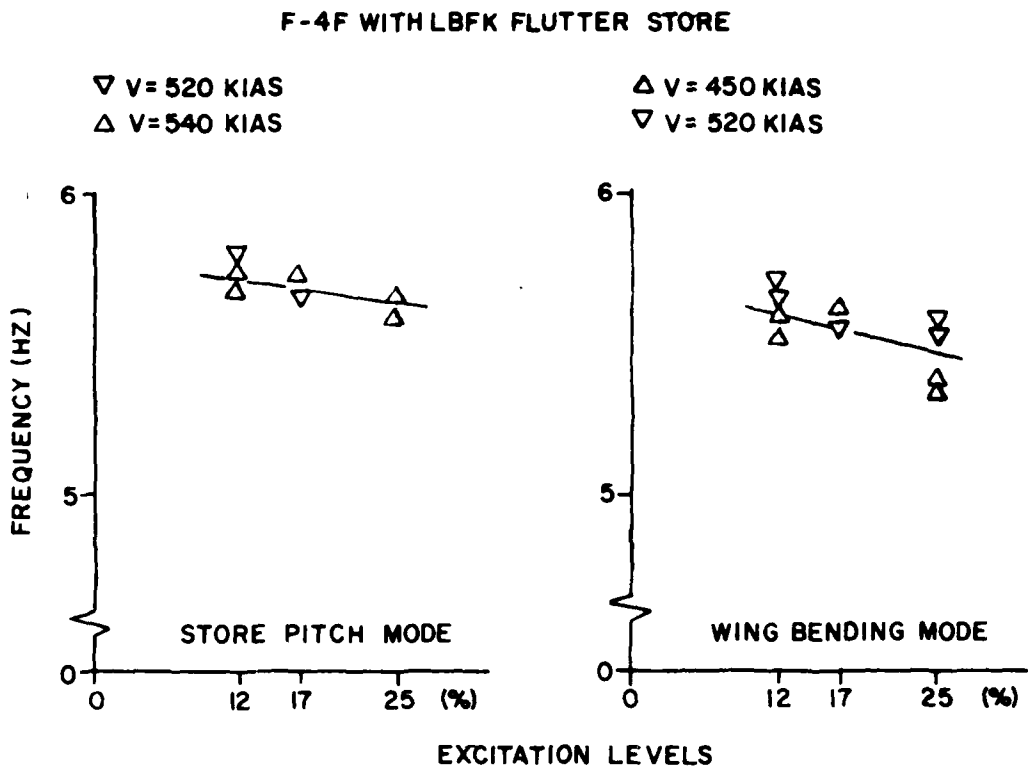


Figure 83. Frequency Shift Due to Nonlinear Effects Versus Excitation Levels

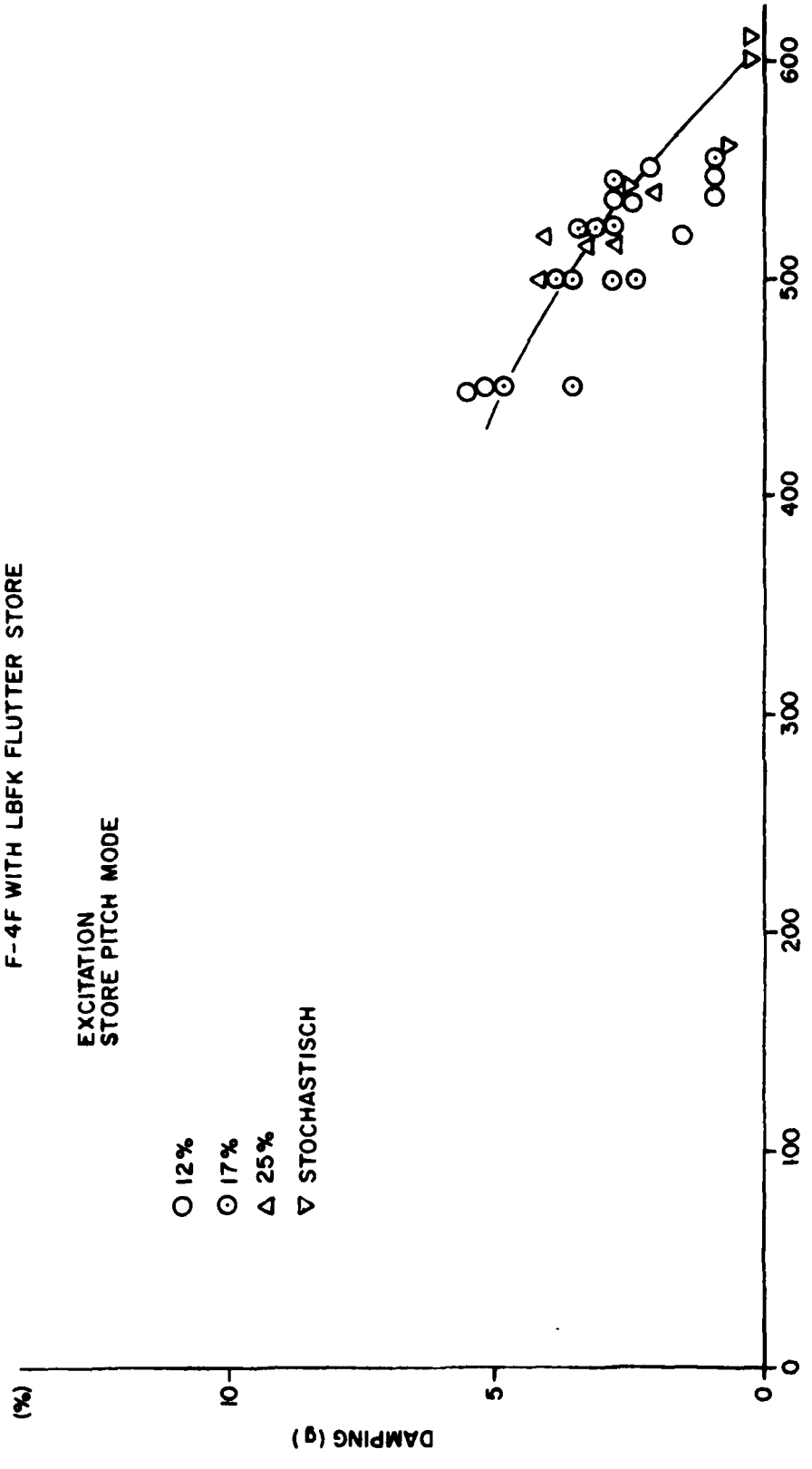


Figure 84. Damping Versus Airspeed for the Linear System

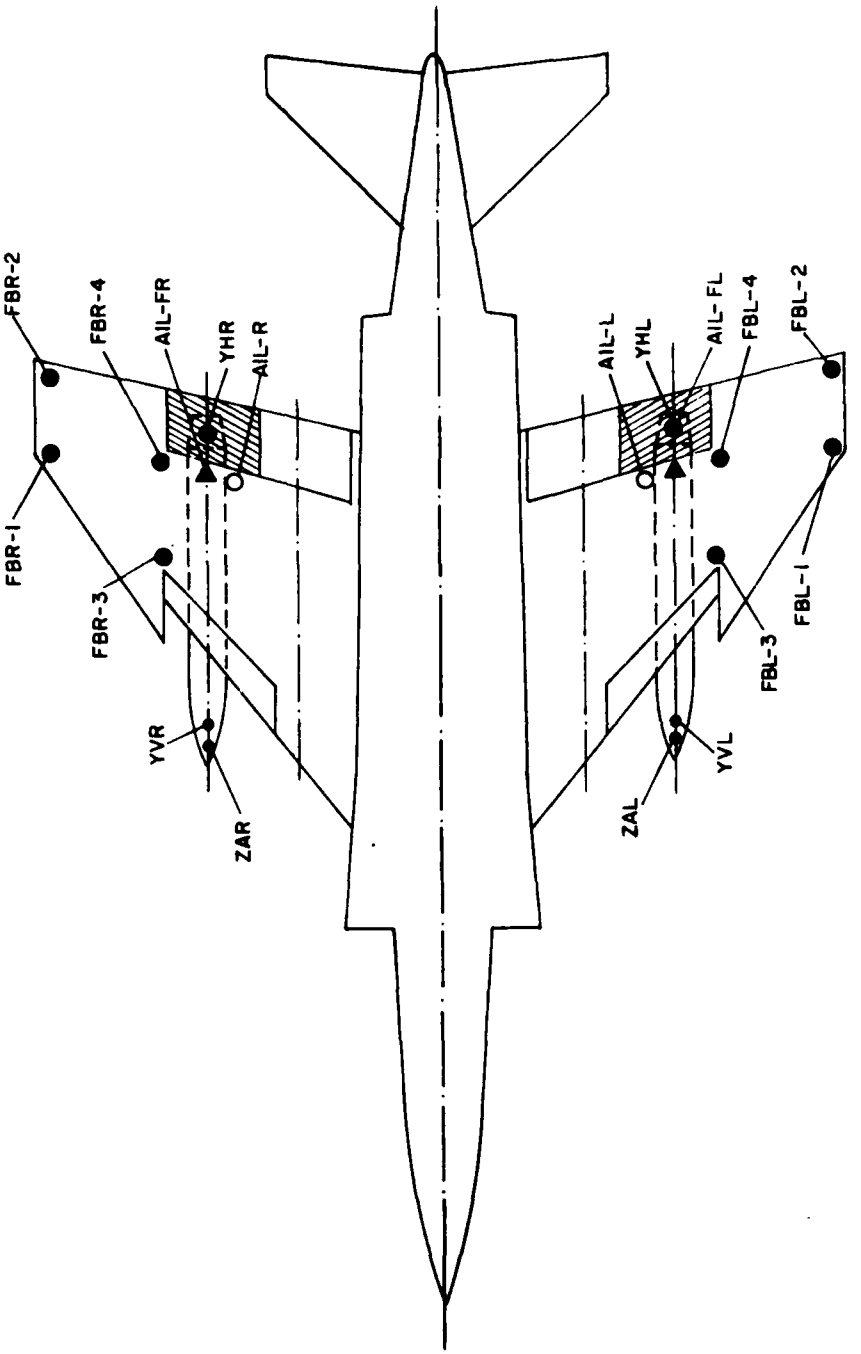


Figure 85. Locations of Sensors and Pick-ups

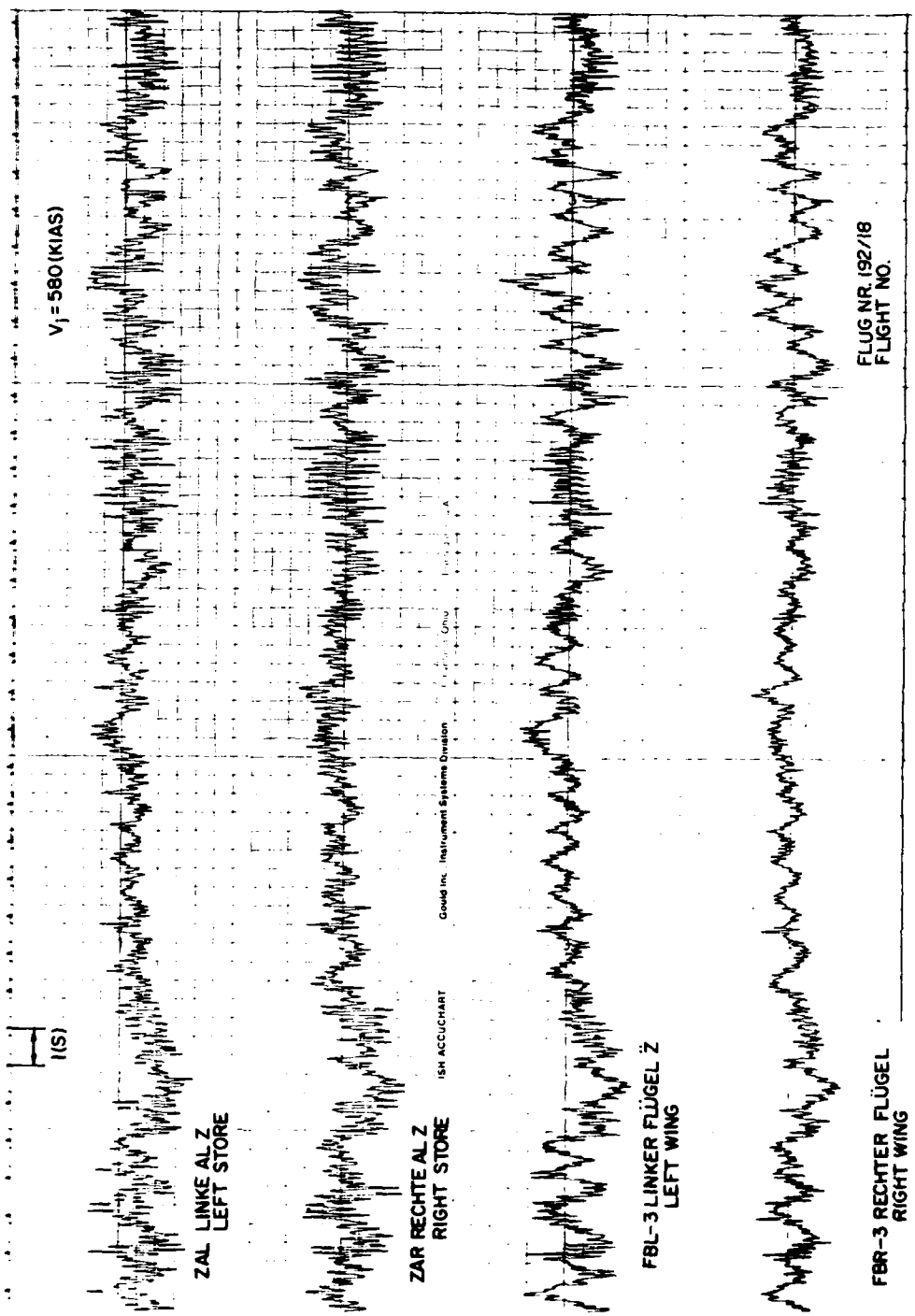


Figure 86. Time Histories of the Critical Store Configuration at 580 KIAS

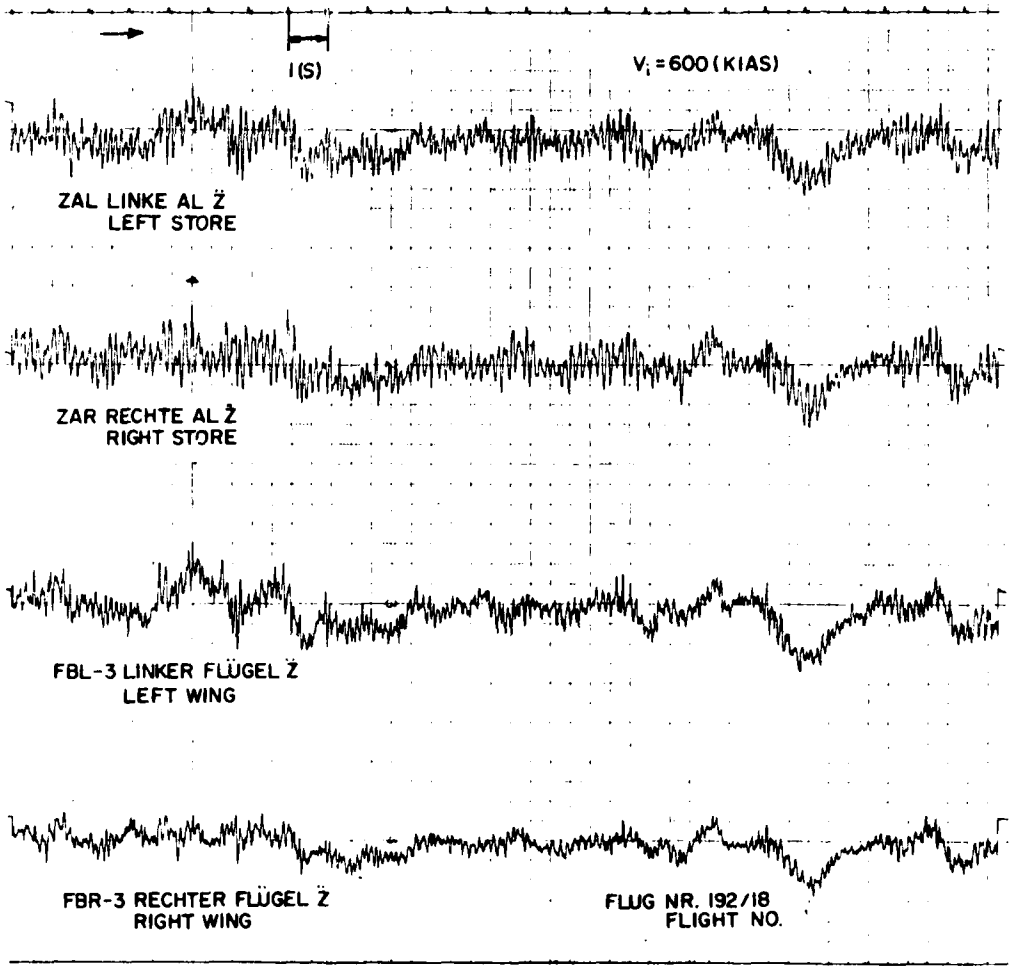


Figure 87. Time Histories of the Critical Store Configuration at 600 KIAS

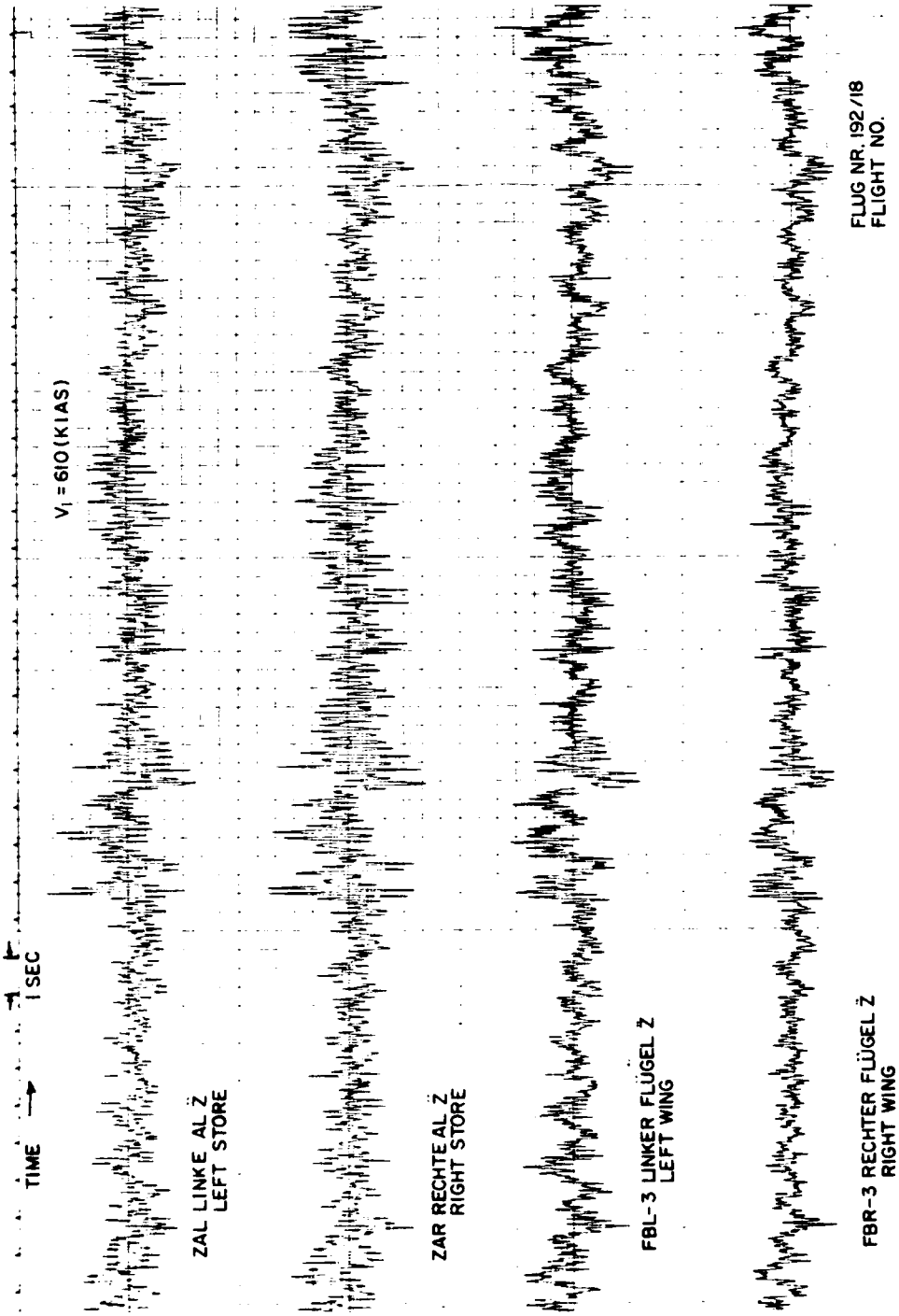


Figure 88. Time Histories of the Critical Store Configuration at 610 KIAS

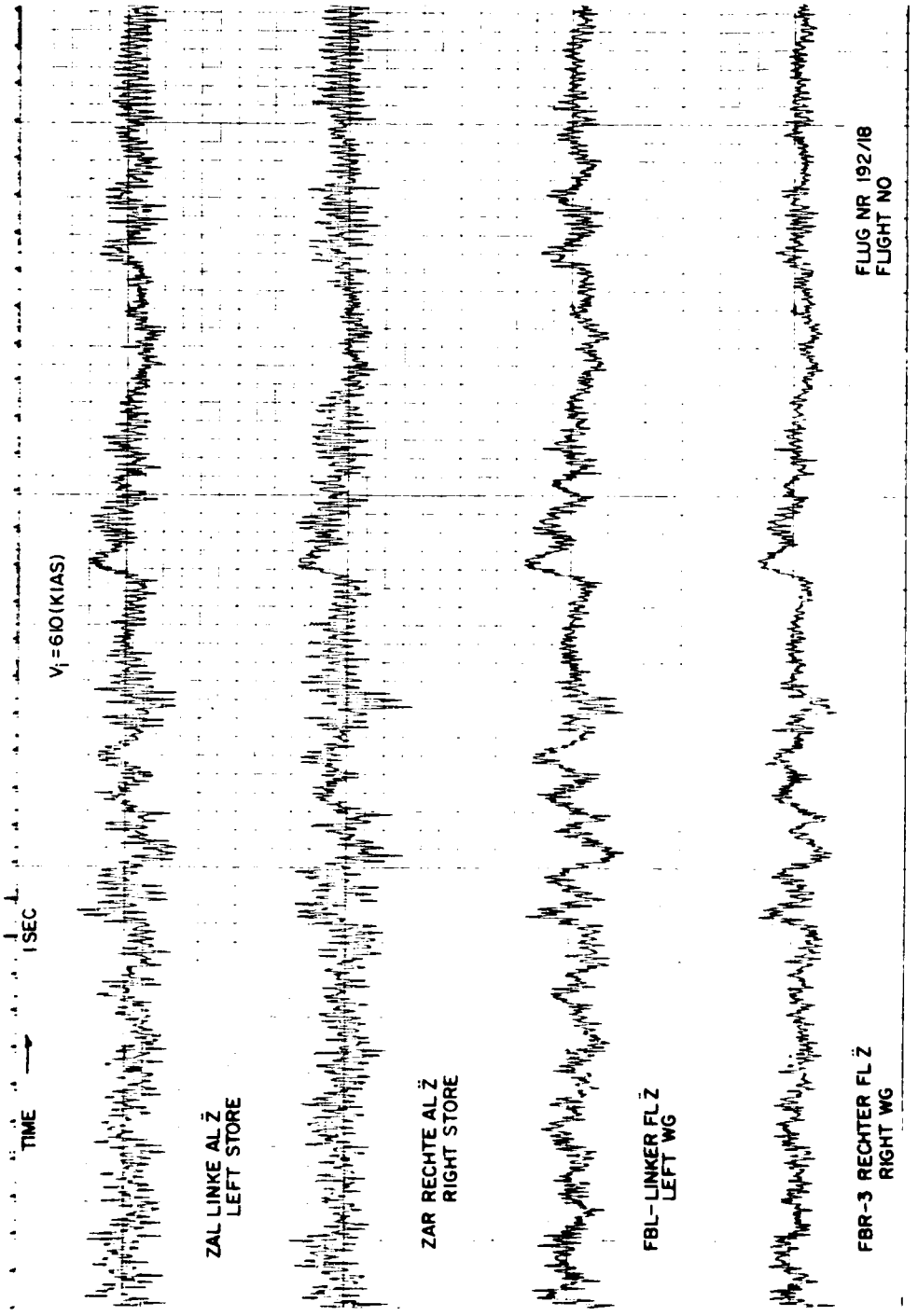


Figure 89. Time Histories of the Critical Store Configuration at 610 KIAS

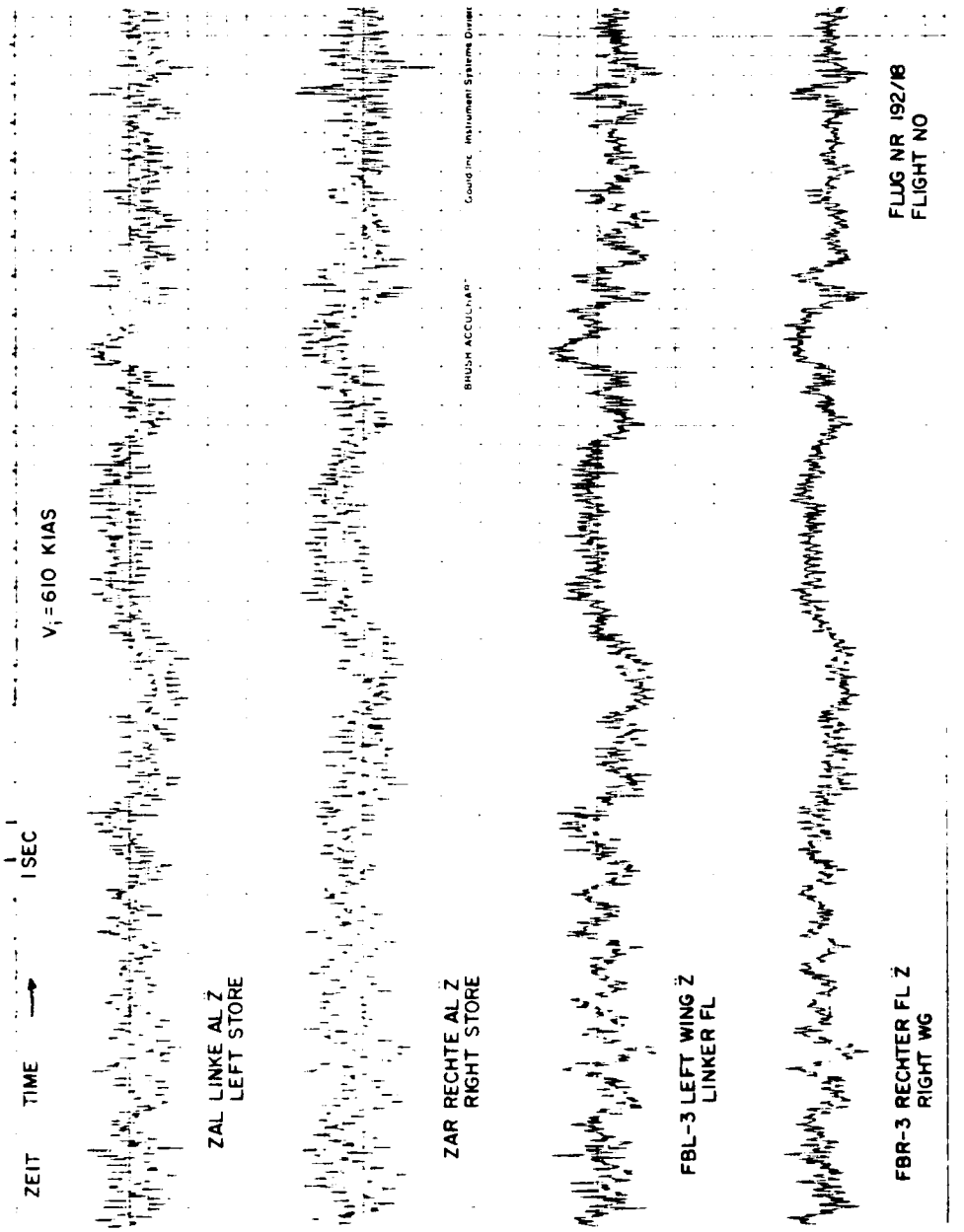


Figure 90. Time Histories of the Critical Store Configuration at 610 KIAS

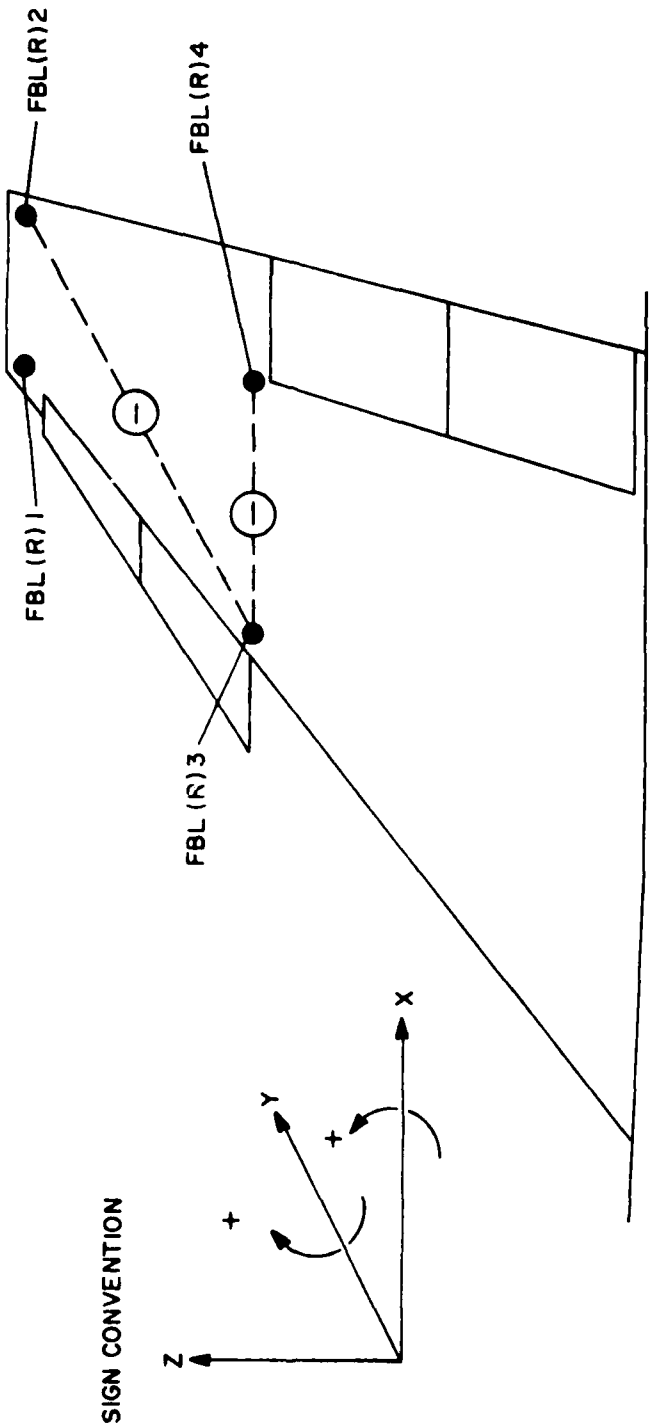


| WING BENDING | $\varphi$ | FBL(R)2 – FBL(R)3 |
|---|---|---|
| STORE PITCH | $\theta$ | FBL(R)3 – FBL(R)4 |
| VALID FOR FLIGHT 175/1-185/11 | | |

Figure 91. Sensor Combination I

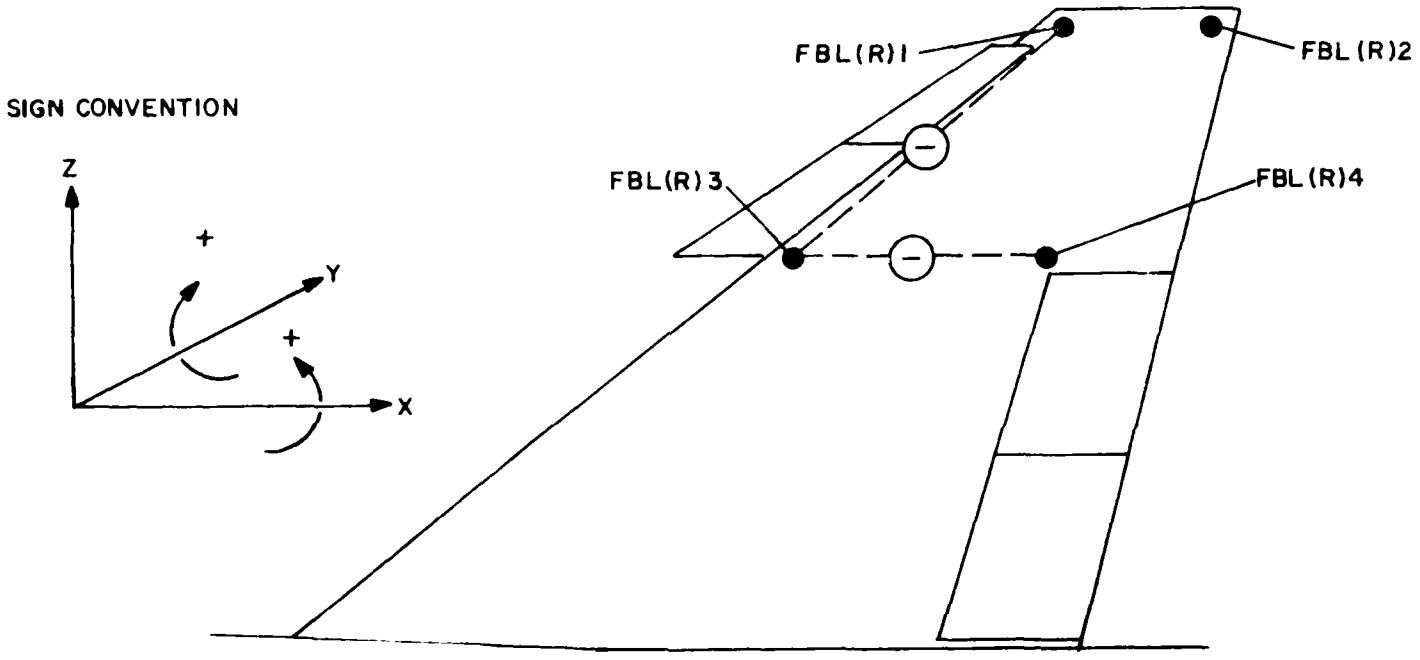


| | | |
|---|---|---|
| WING BENDING | $\varphi$ | FBL(R)1 − FBL(R)3 |
| STORE PITCH | $\theta$ | FBL(R)3 − FBL(R)4 |
| VALID FOR FLIGHT 187/13-192/18 | | |

Figure 92. Sensor Combination II

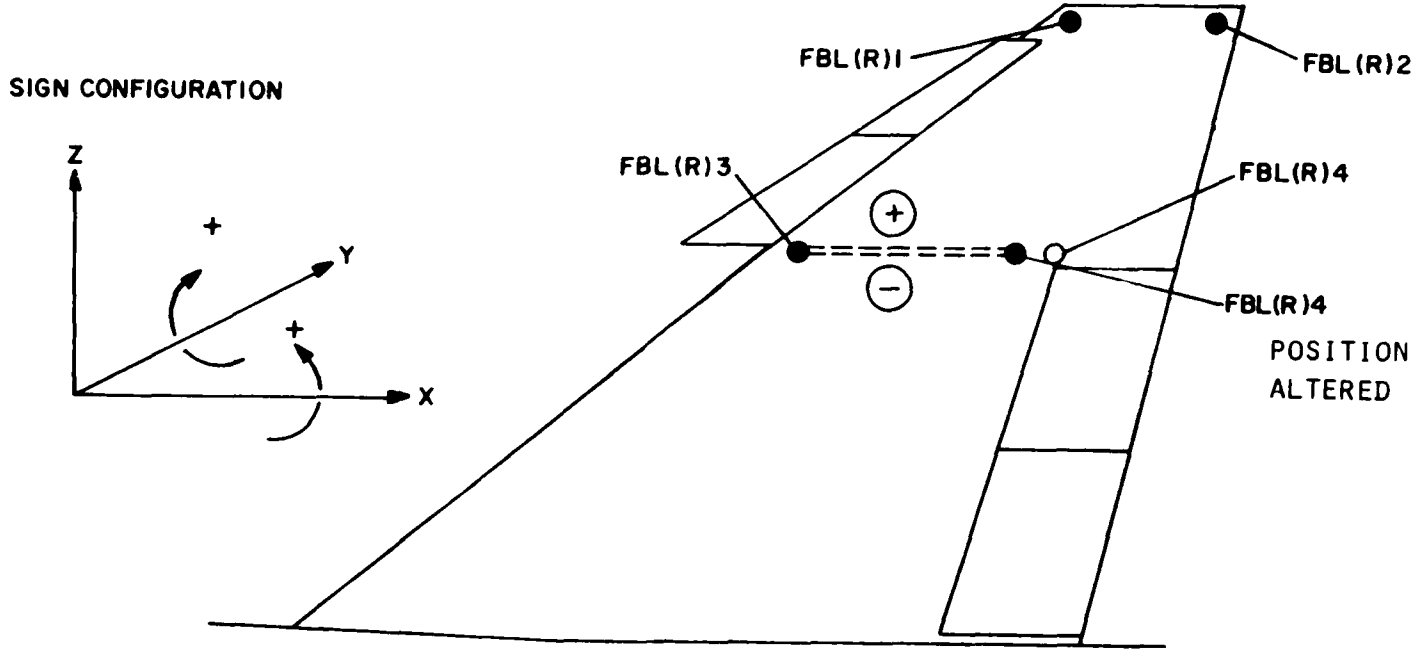


| | | |
|---|---|---|
| WING BENDING | $\gamma$ | FBL(R)3 + FBL(R)4 |
| STORE PITCH | $\theta$ | FBL(R)3 − FBL(R)4 |
| VALID FOR FLIGHT 193/19 | | |

Figure 93. Sensor Combination III

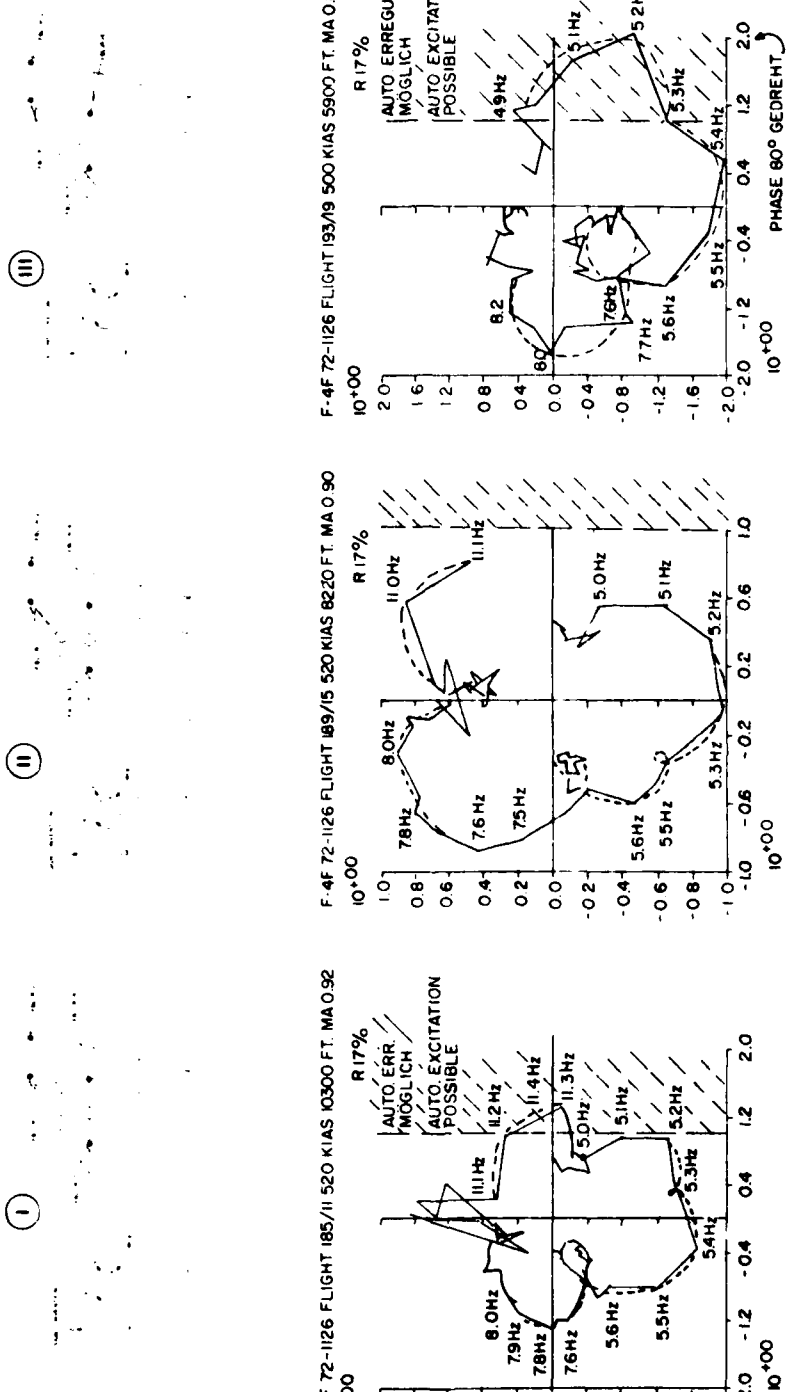


Figure 94. Nyquist Diagram for Various Sensor Combinations

F-4F 72-1126 FLIGHT 185/11 450 KIAS 10000 FT MA 0.84

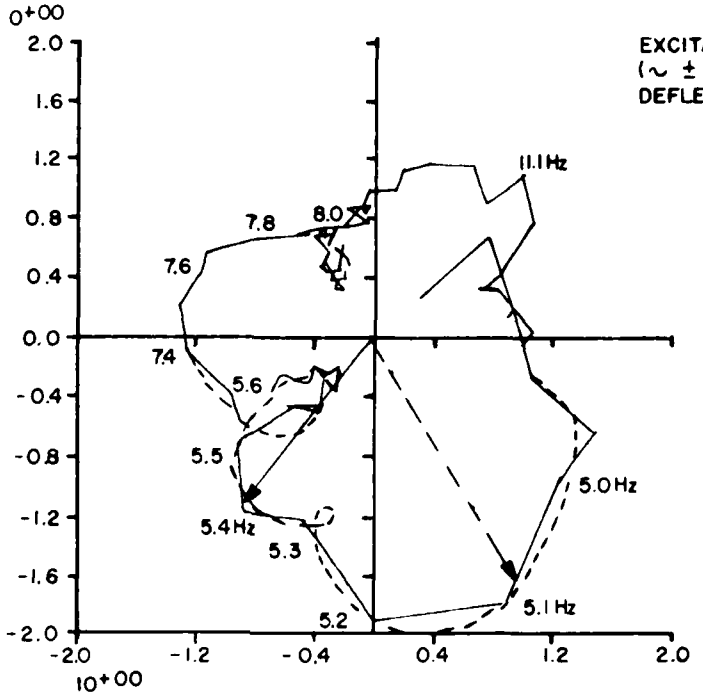


F-4F 72-1126 FLIGHT 185/11 520 KIAS 10300 FT MA 0.92

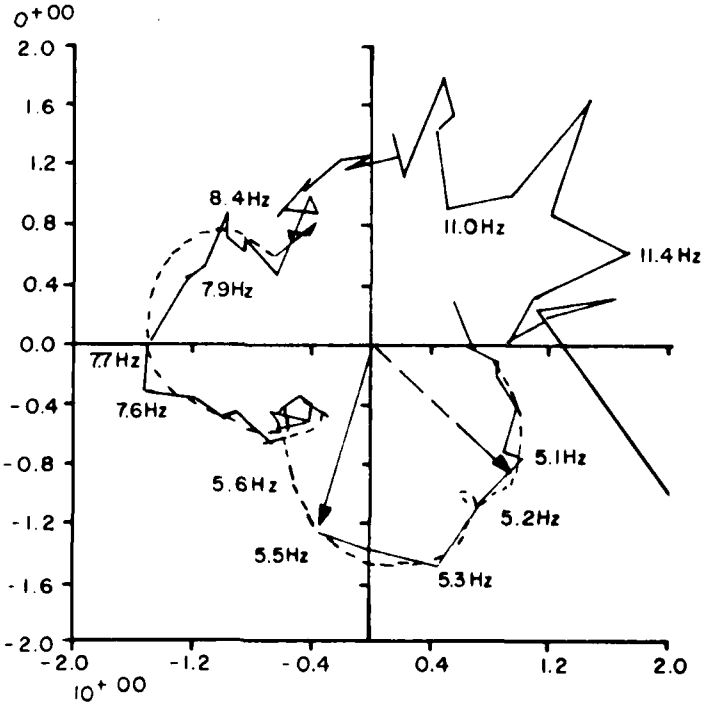


Figure 95. Nyquist Diagrams at Various Airspeeds

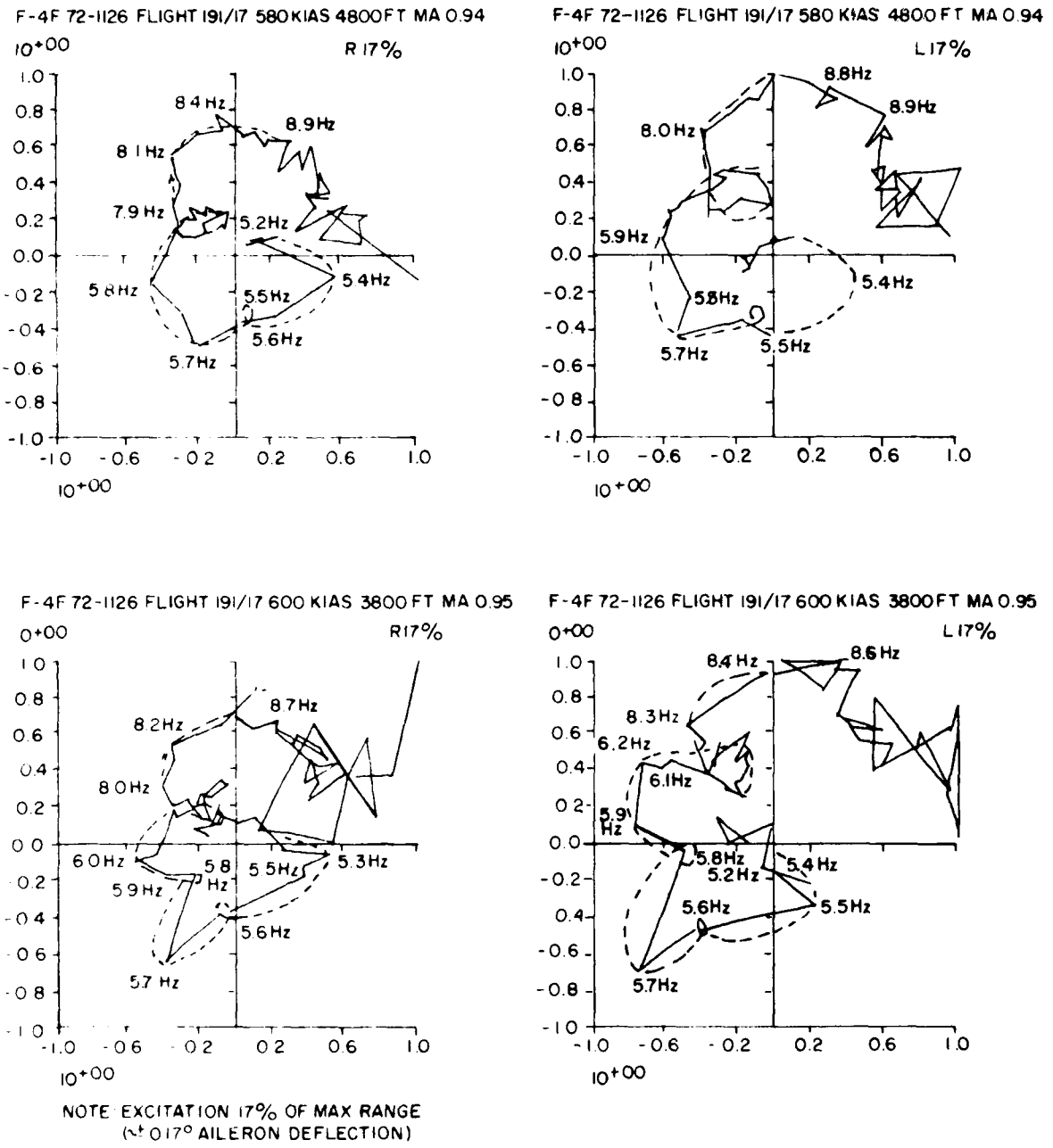


NOTE: EXCITATION 17% OF MAX RANGE
(± 0.17° AILERON DEFLECTION)

Figure 96. Nyquist Diagrams for High Stagnation Pressures

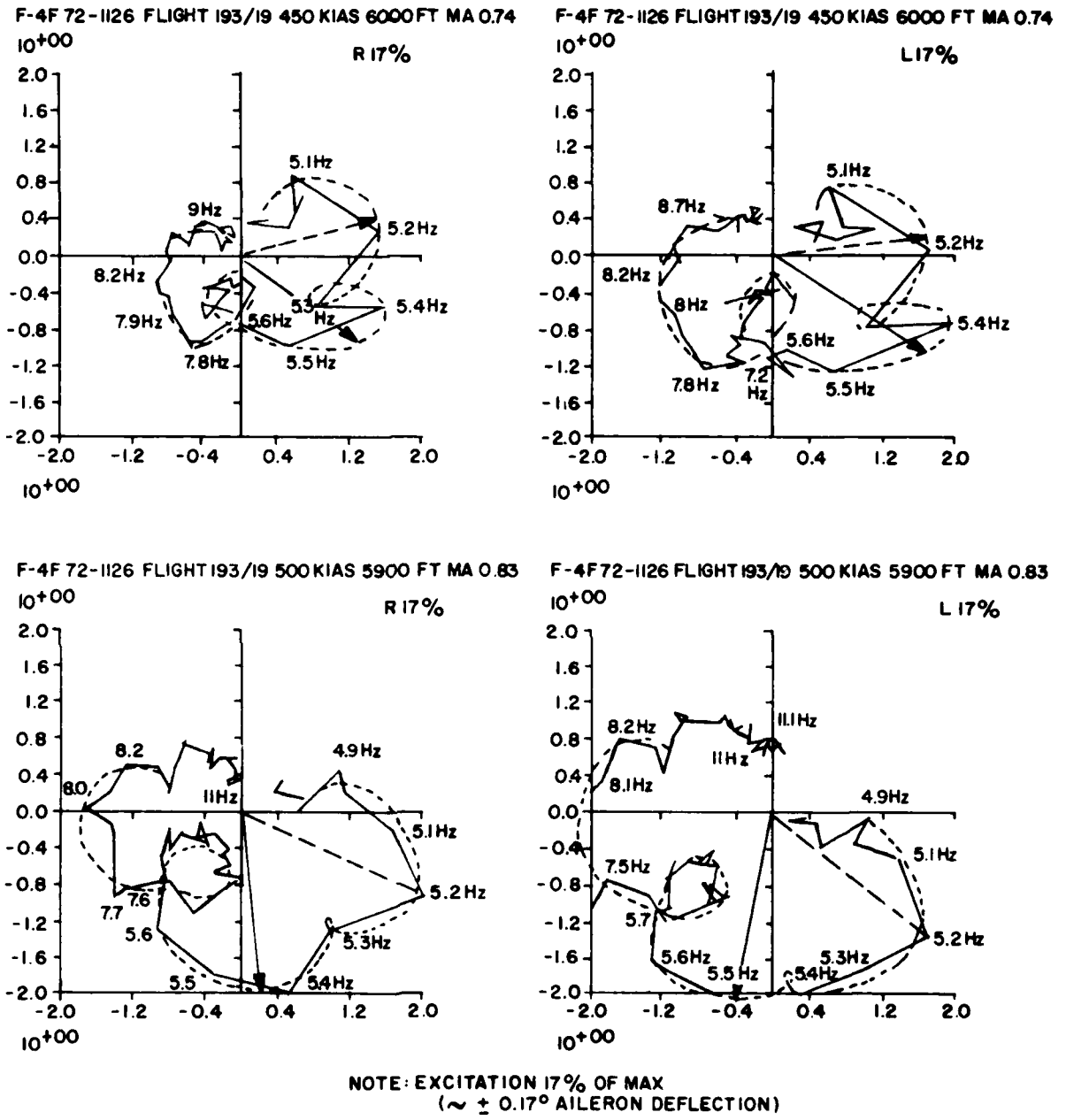


Figure 97. Nyquist Diagram of the Flutter Suppression System with Sensor Combination III, Mach Number of 0.74 and 0.83

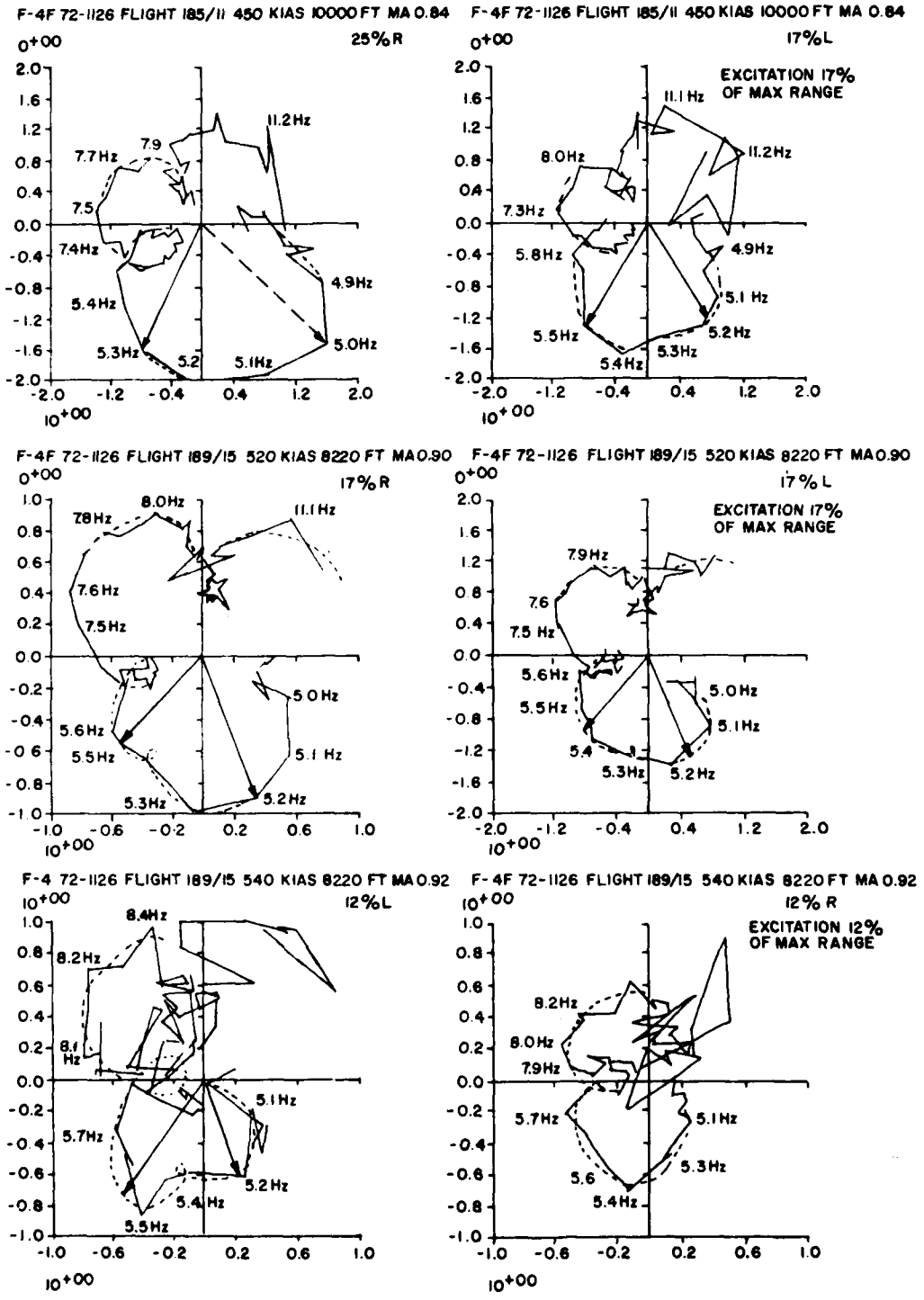


Figure 98. Nyquist Diagrams of Various Input Levels

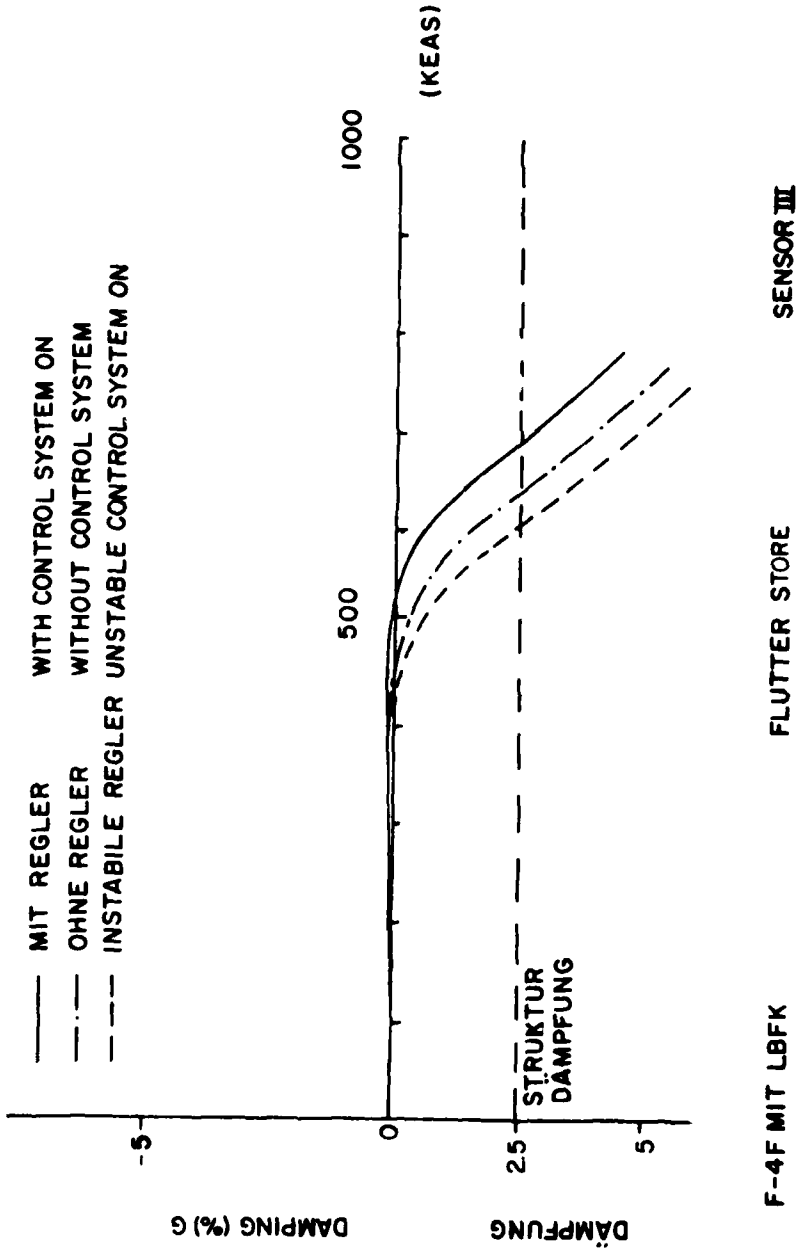


Figure 99. Comparison of the Calculated Damping of the Stable and Unstable Flutter Suppression System

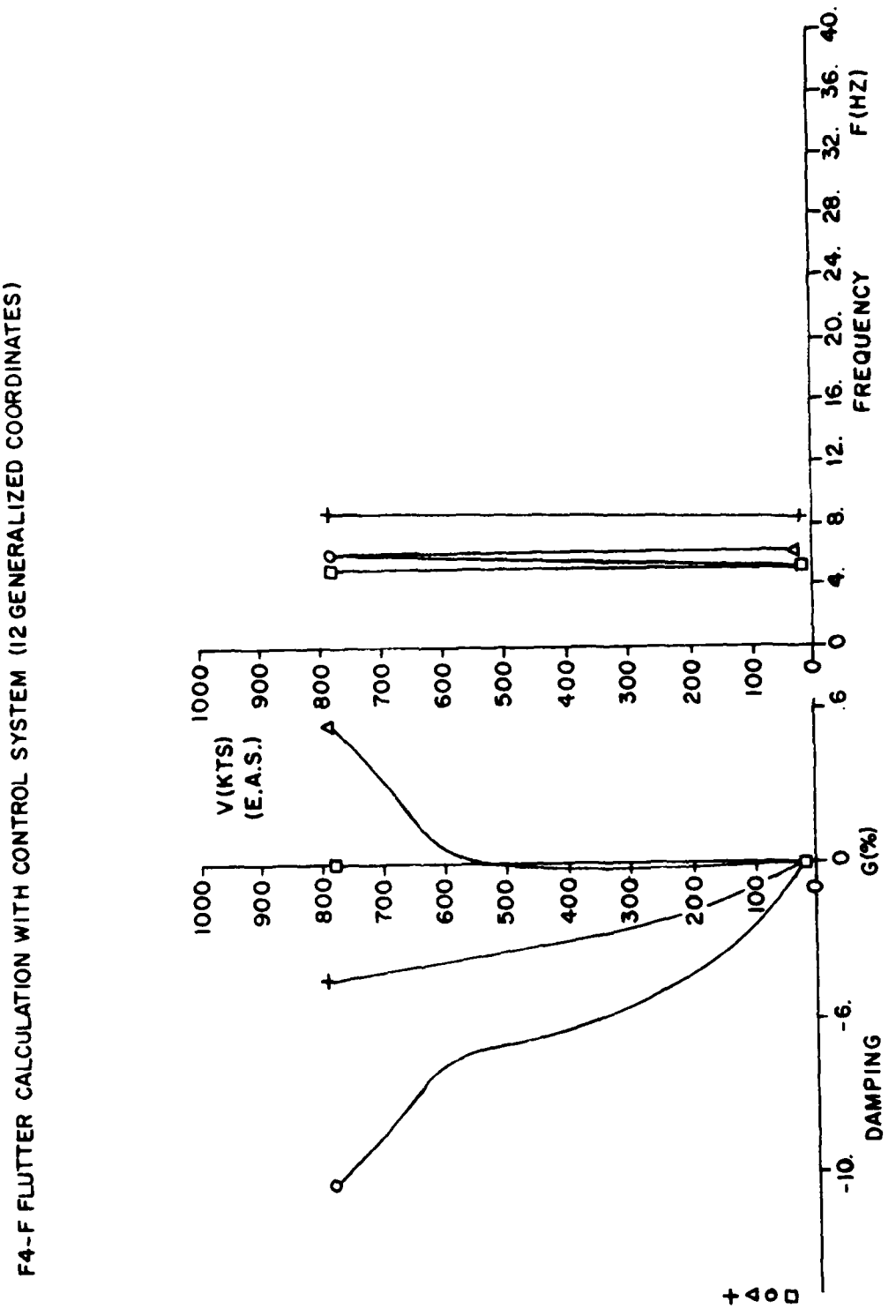


Figure 100. Flutter Calculation with FSS

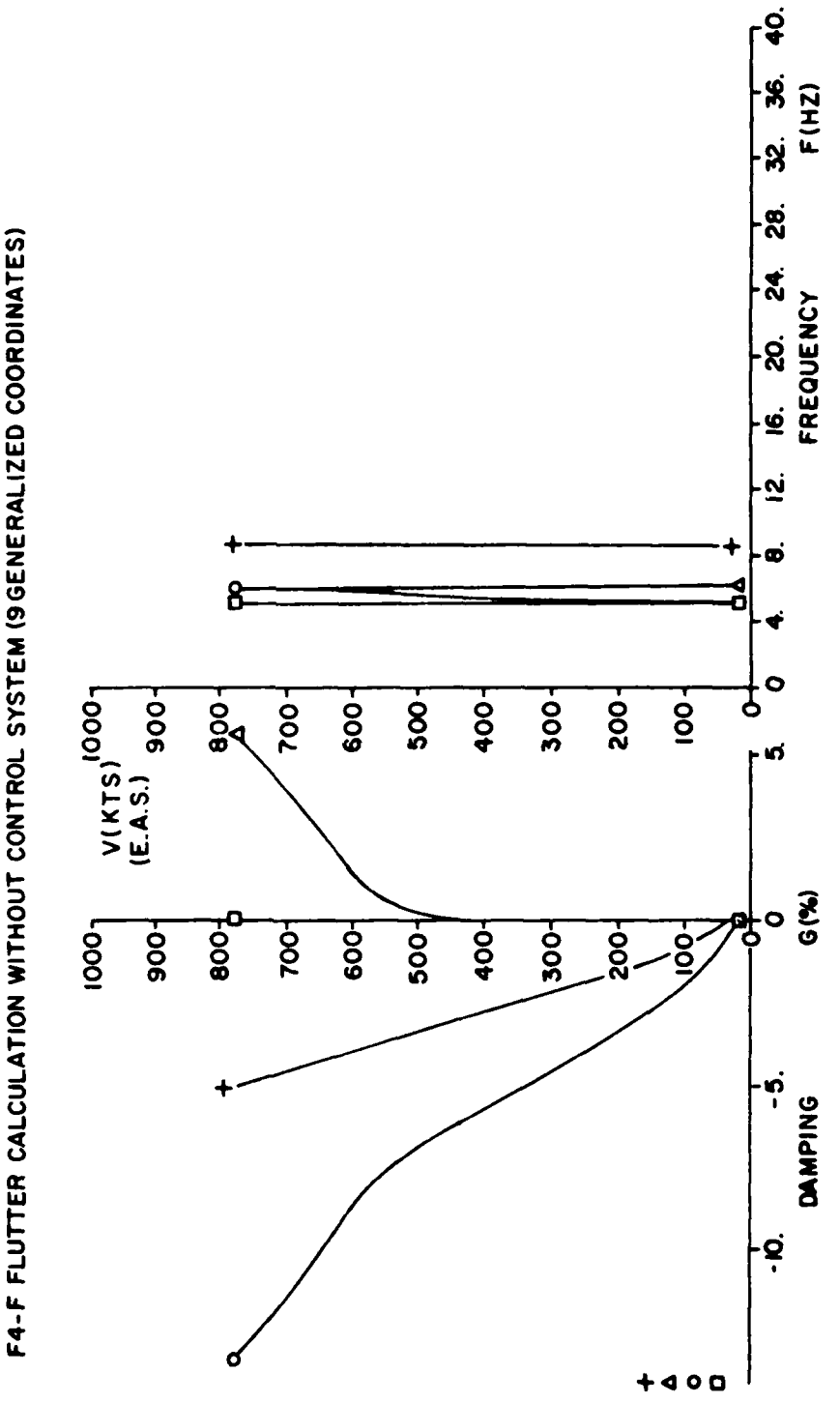


Figure 101. Flutter Calculation without FSS

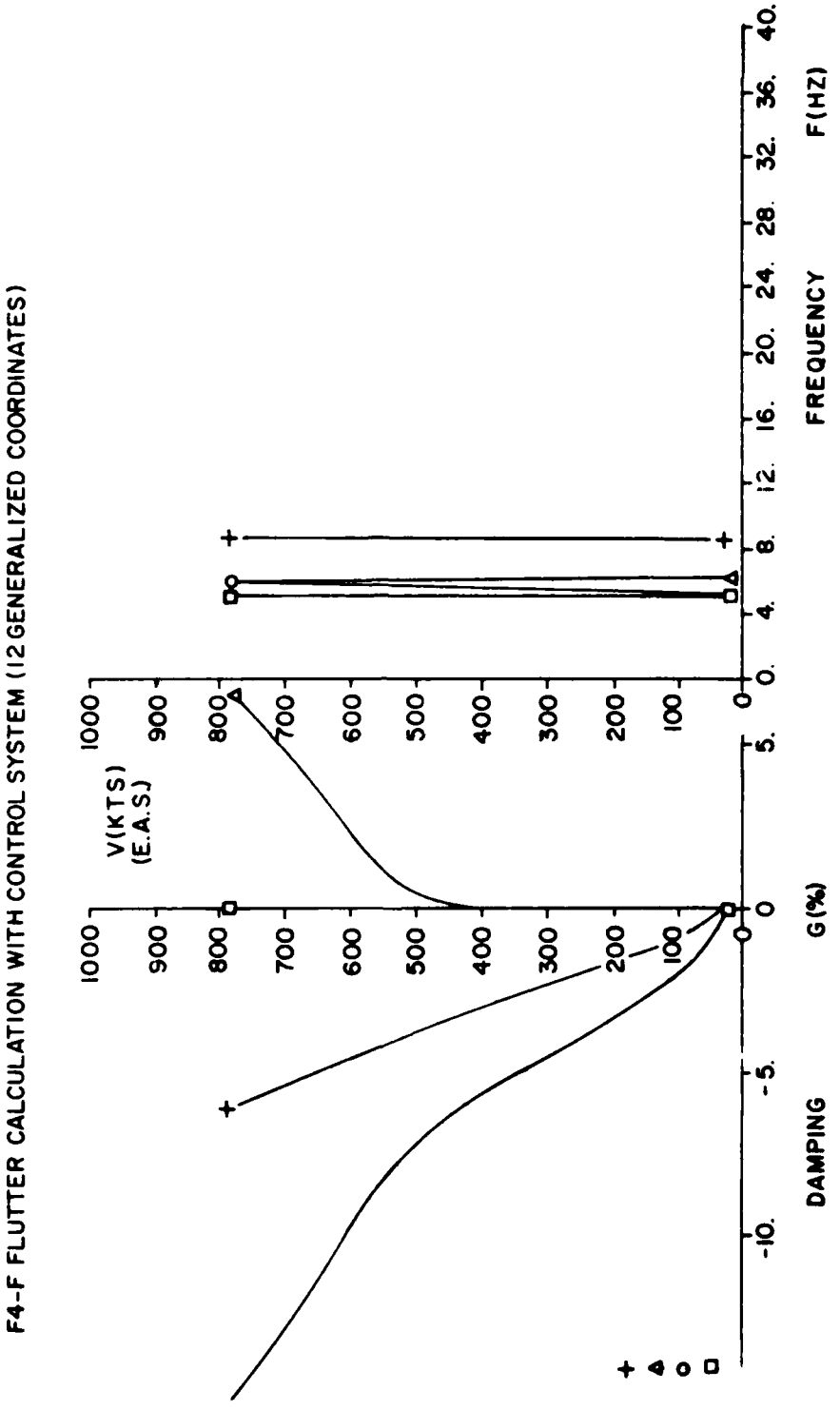


Figure 102. Flutter Calculation with Unstable FSS

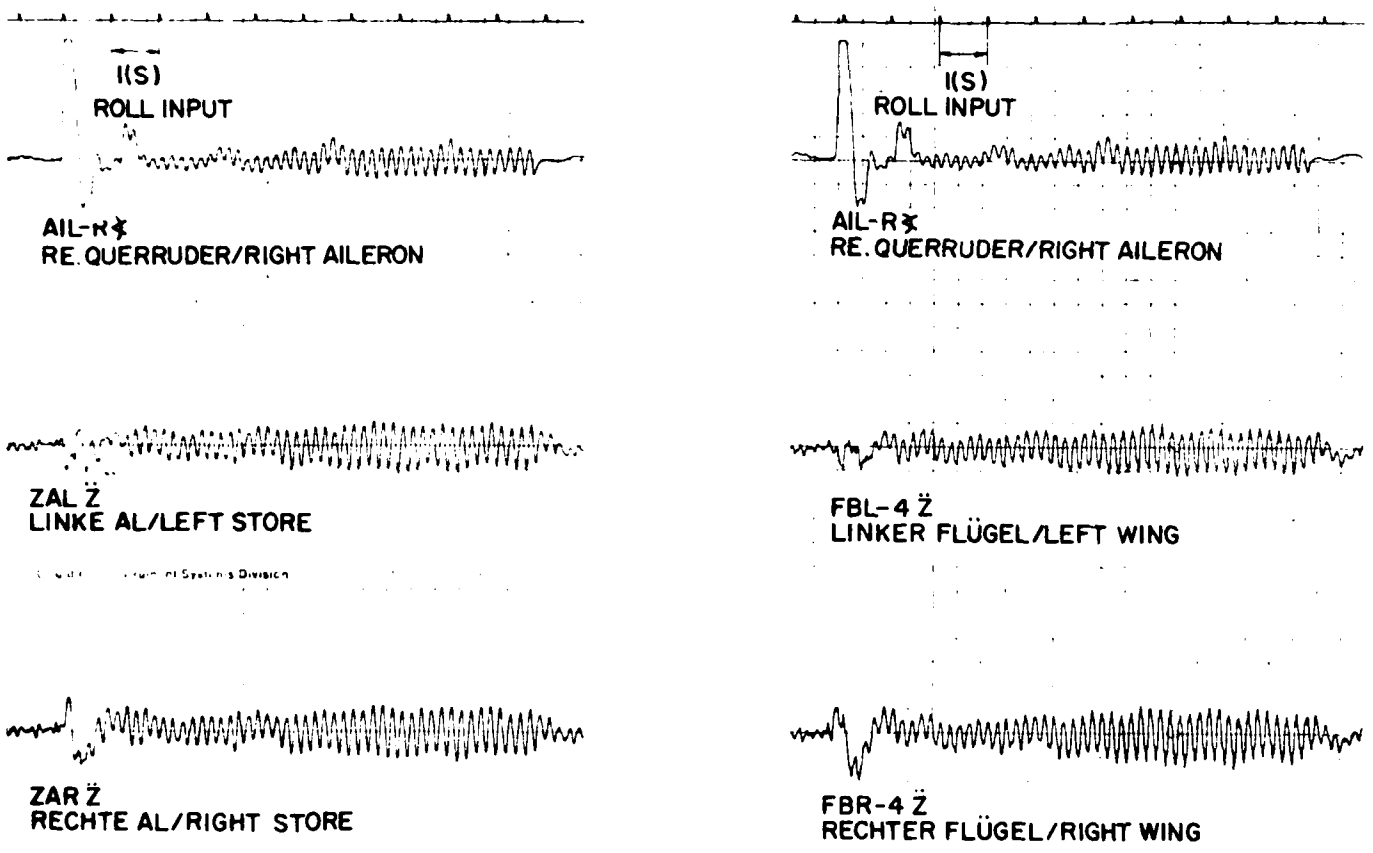


FLUG NR 193/19
FLIGHT NO.

PROGR 4

ERREGUNG: AUTOMATISCH
EXCITATION: AUTOMATIC

FLUG-GESCHW: 480 (KIAS)
AIR SPEED

FREQUENZ : 5.4 (HZ) FLÜGELBIEGUNG/WING BENDING
FREQUENCY

Figure 103. Time Histories with Automatic Excitation

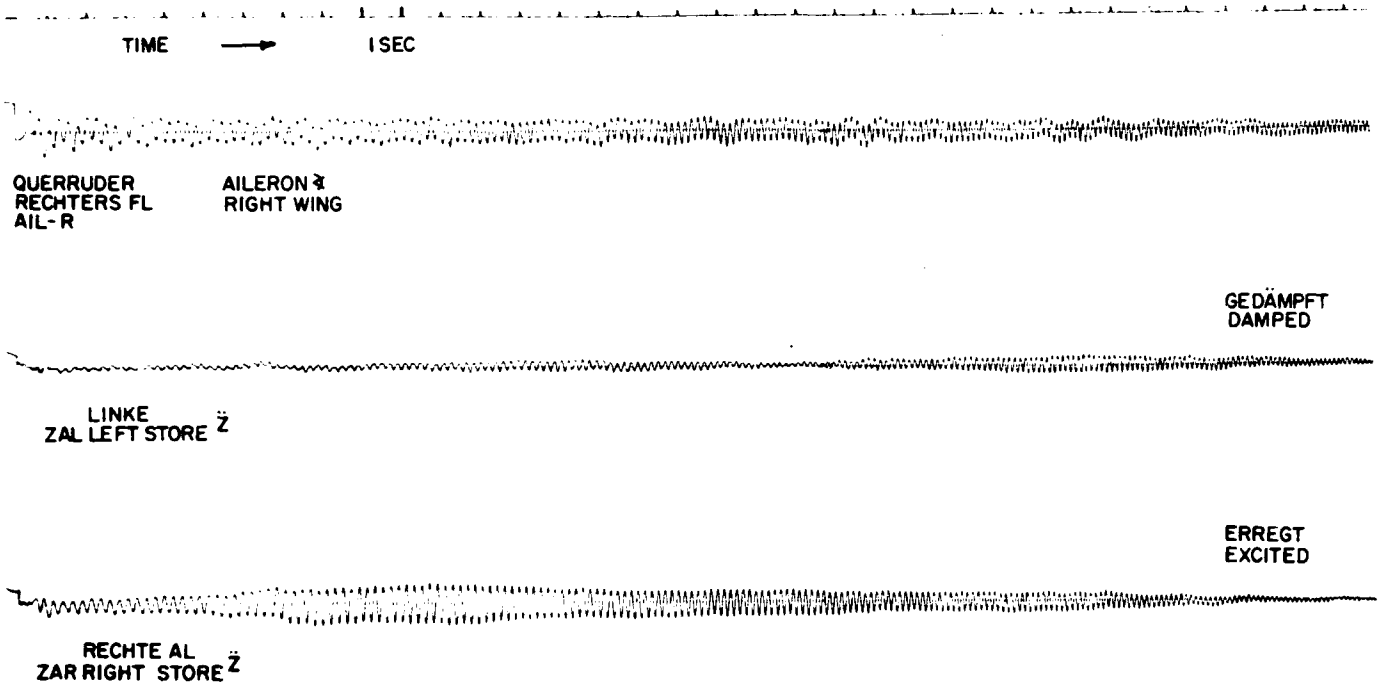


Figure 104. Tests of Vibration Suppression, 500 KIAS

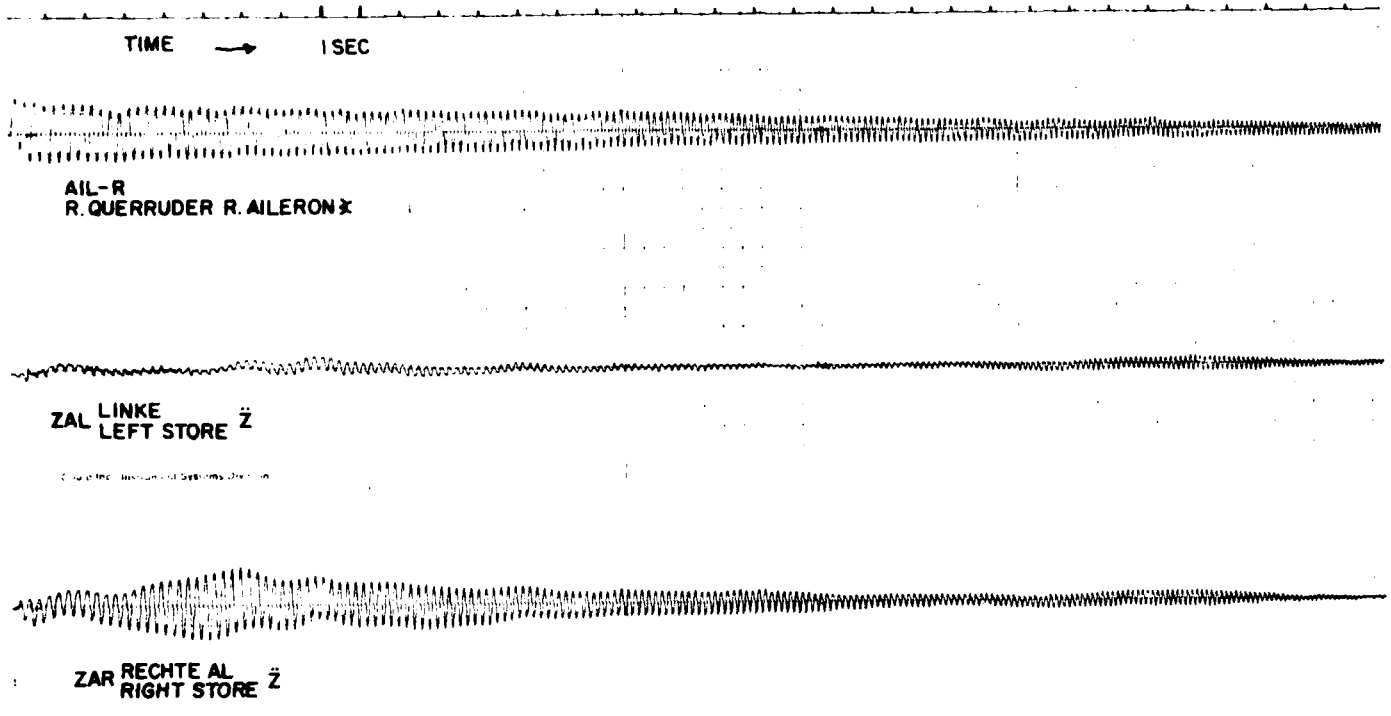


Figure 105. Tests of Vibration Suppression, 450 KIAS

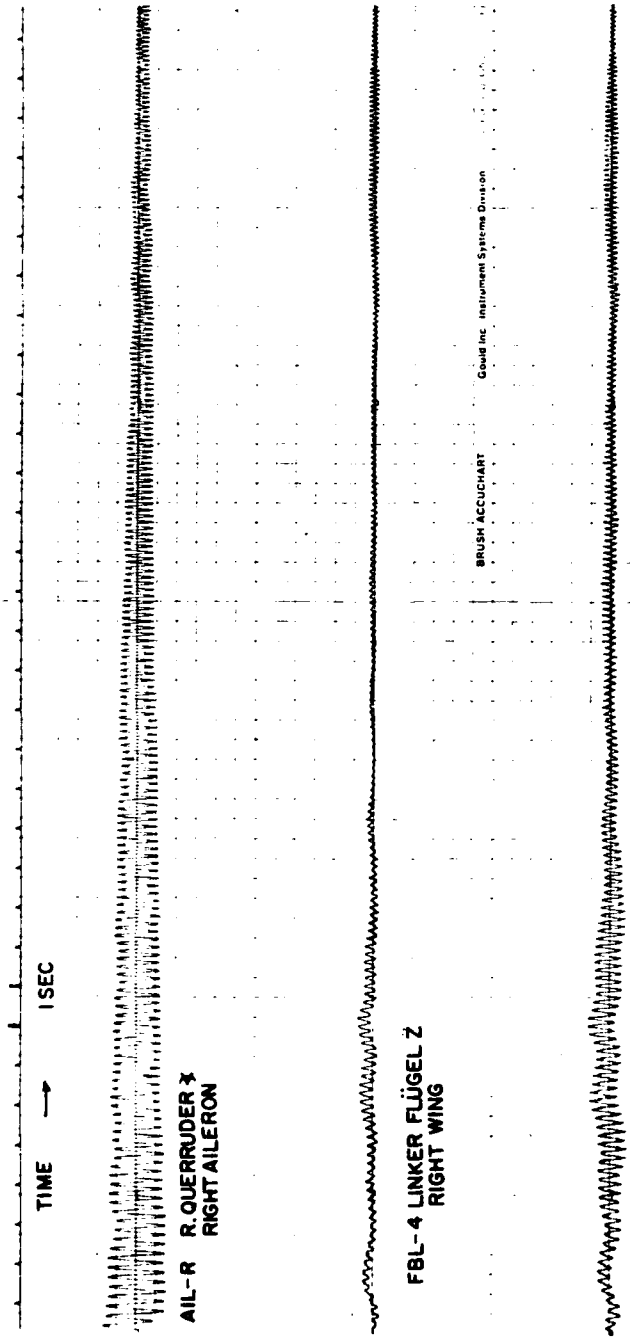


Figure 106. Tests of Vibration Suppression, 450 KIAS

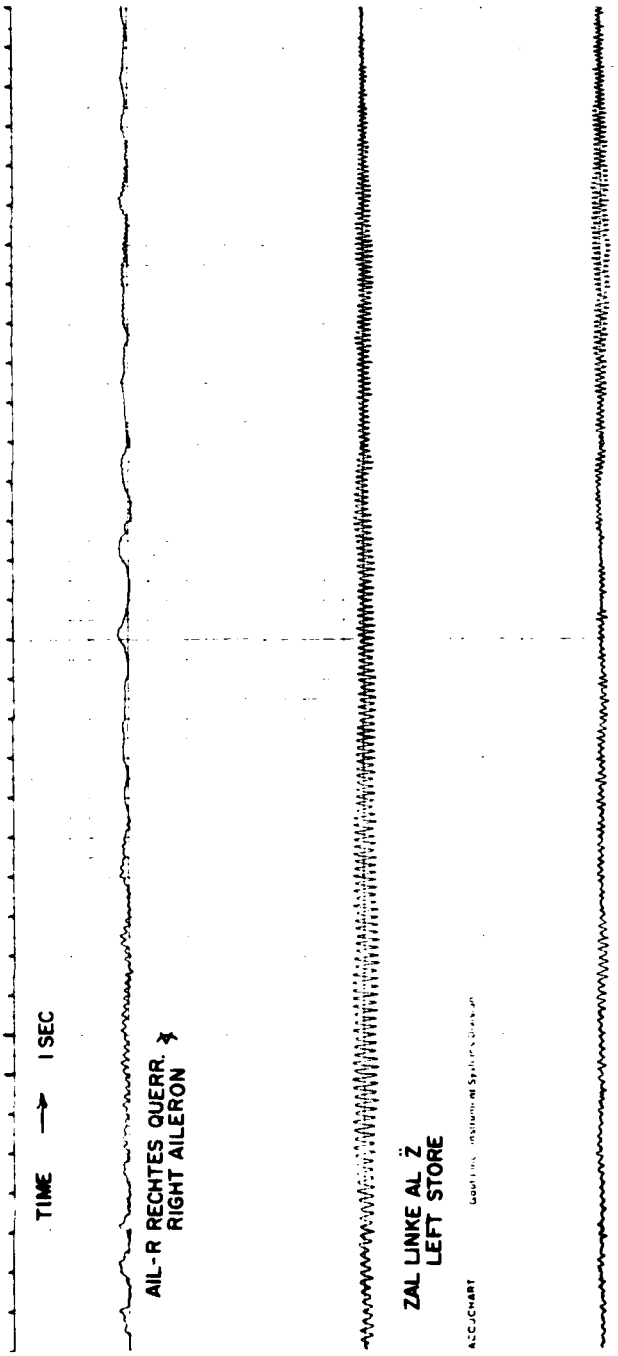


Figure 107. Tests of Vibration Suppression 450 KIAS

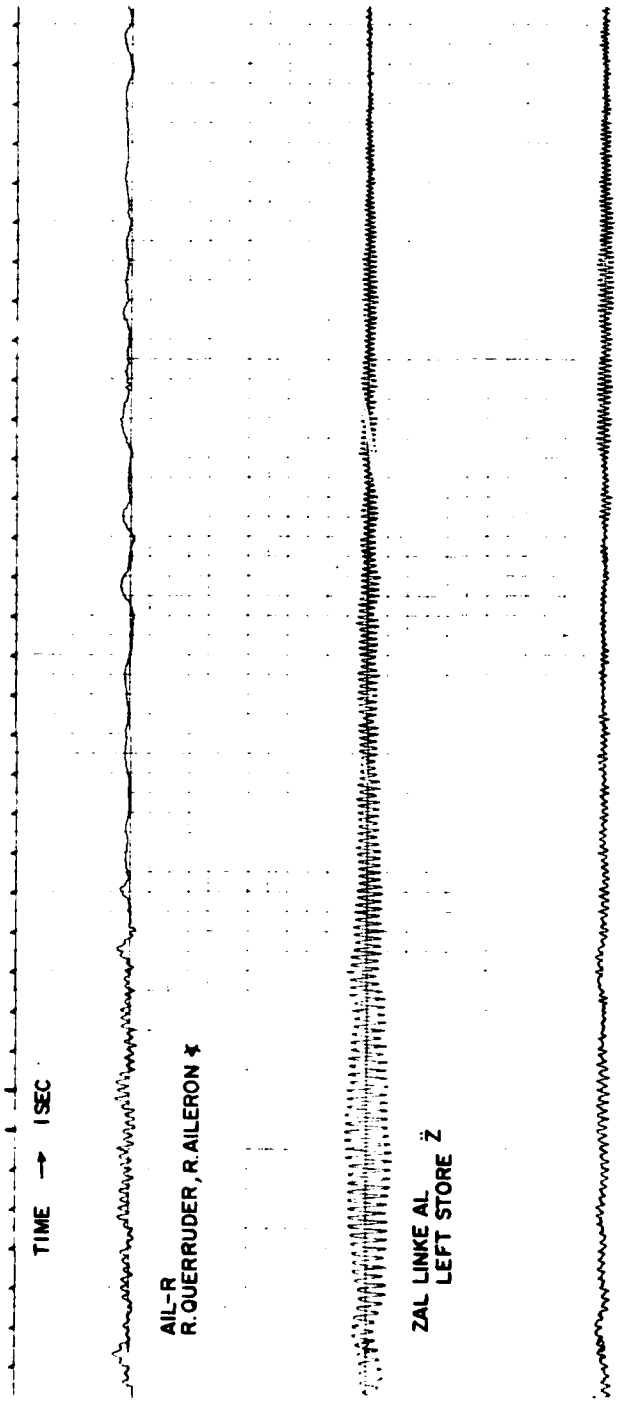


Figure 108. Tests of Vibration Suppression

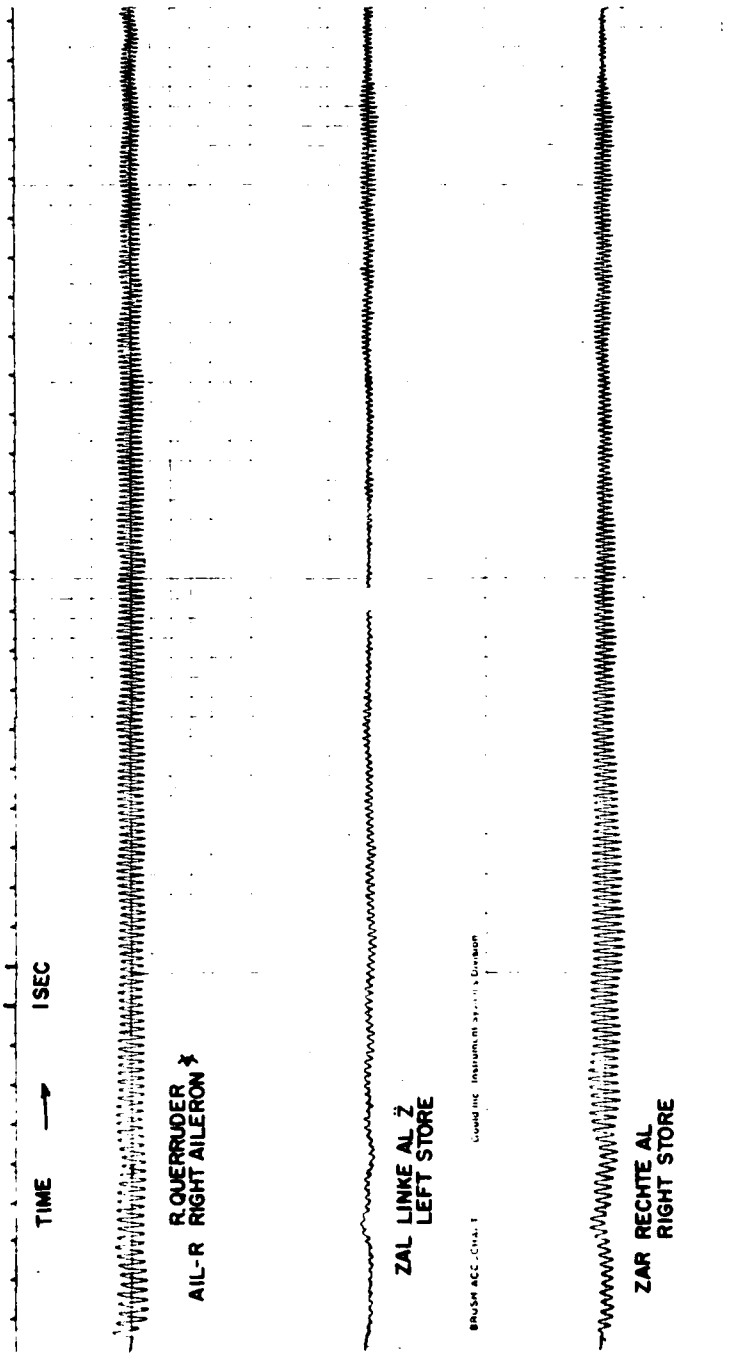


Figure 109. Tests of Vibration Suppression

END

DATE
FILMED

9 — 83

DTIC